INITIAL DEFORMATIONS OF PLAIN WOVEN FABRICS

A thesis submitted for the degree
of
Doctor of Philosophy

by

KHALED HUSSEIN ABDEL-RAZEK KANDIL

being an account of work carried out at
the Department of Textile Industries under
the direction of Mr. G.A.V. Leaf, M.Sc.,
F.S.S., F.T.I.

Department of Textile Industries
The University of Leeds
Leeds LS2 9JT.

October 1981

'To My Parents'

ABSTRACT

This work is an attempt to provide simple formulae that can predict the initial behaviour of the most commonly used fabric, namely the plain weave. To achieve this, a simple zigzag shape 'saw-tooth model' was adopted to describe the yarn configuration in the weave structure. An energy method, using Castigliano's theorem, was then employed to derive closed form solutions which relate the yarn parameters and the fabric moduli under either tensile or bending strains.

To examine the theory, series of tests were carried out on different plain weave structures and the theoretically calculated results were compared with the actual fabric behaviour.

The outcome of the study showed that, when the yarn and fabric parameters are accurately defined, it is possible to obtain a reasonable estimate of the above mentioned fabric properties using the formulae derived in the theoretical analysis.

The results and discussion also showed that the initial deformation of some plain weave constructions may produce extension and/or compression strain energies that cannot be ignored in estimating the fabric behaviour with reasonable accuracy.

ACKNOWLEDGEMENTS

I would like to express my deep gratitude to Mr. G.A.V. Leaf, for his guidance and sincere advice during the course of this work.

Thanks are also due to the various members and staff in the Department of Textile Industries, especially Professor P. Grosberg, Head of the Department, and Mrs. B. McClelland, for their help and assistance.

My appreciation goes to Mrs. S. McOwat for her efforts in typing this thesis.

The financial support of "El-NASR WOOL AND SELECTED TEXTILES CO., ALEXANDRIA", during a part of this research, is gratefully acknowledged.

CONTENTS

CHAPTER 1: INTRODUCTION

CHAPTER 1

INTRODUCTION

1.1 General Introduction

Textiles are now increasingly used for many purposes, from the traditional uses like garments and furniture to others such as conveyor belts, hovercraft skirts and aerospace applications. Probably, there are two reasons for this wide range of utilization, the first being that textile materials cover a wide range of different physical and mechanical properties, and the second is that textile technology is tending to become a science of well-established rules and predictable results, so that fabrics can be designed for specific purposes.

The end-uses of textiles decide the way they should be selected and constructed, suggesting that some properties should act in a certain way, while others remain of less relative importance. For example, outer-wear fabrics need to satisfy some aesthetic, physical and thermal properties as well as being required to be durable. On the other hand, fabrics used for industrial purposes are made for strength and flexibility, and possibly for certain electrical and thermal properties, and aesthetics are relatively unimportant.

Generally, for any end-use, the mechanical properties of fabrics are of special interest, and a theoretical study of how these properties are related to the fabric and yarn parameters could help in deciding how to produce a suitable fabric at a minimum cost when its likely range of use is known.

The actual use of fabrics involves complex deformations in multi-directions; however to study the problem, it is useful to begin by

considering the simplest forms of deformation and the corresponding fabric mechanical behaviour.

1.2 Mechanical Properties of Plain Woven Fabrics

The simple forms of fabric deformation are extension and shear in the fabric plane, bending perpendicular to the fabric plane and buckling out of the fabric plane. Investigations are more easily carried out when the structure does not have the added difficulties arising with the more intricate configurations, such as we may find in twill weaves which show skewness (1), and the usefulness of the plain weaves is obvious in this respect.

1.2.1 Tensile properties of plain weave

When a plain woven fabric is initially extended in one of the major directions, the yarns in the load direction are straightened. Accordingly, the crimp, c, crimp amplitude, h, and the weave angle, θ, decrease, while the thread spacing, p, increases. Because of the contact between warp and weft, at the cross over area, the fabric extension leads to a pressure build up in this area. This pressure leads to upcrimping of the yarns in the no-load direction, so that the crimp amplitude and weave angle will increase, while the thread spacing decreases. The latter effect will result in a widthwise contraction in the fabric. This fractional contraction, expressed as a fraction of the fractional extension in the load direction, gives the so called Poisson's ratio for this mode of deformation. The initial phase of extension is normally referred to as the crimp distribution phase because the yarns under such initial loads do not extend, or extend by very small amounts. It has been claimed that this phase is governed mainly by the yarn bending properties but further

work (2,3,4,5) has shown that the yarn compressional properties may also play an important role.

A typical load-extension curve, as shown in figure 1, reflects these effects. In the initial region, OA, the curve possesses a relatively high initial tensile modulus due to the high initial bending modulus of the yarns in which the fibres' frictional restraints have a great influence. Overcoming this frictional resistance, the curve shows a pure crimp interchange region, AB, dependent on both yarns' elastic rigidities and probably on their compressibilities. If the fabric is further extended, additional effects will take place. These will be yarn extension with fibre extension and slippage in the load direction, and more flattening for both the warp and weft at the cross over region. In this phase, BC, the yarn extensibility, compressibility and the coefficient of friction between fibres will play important roles. The above mentioned phases are affected by the magnitude of the forces existing between the two yarn systems before extension; hence the degree of fabric set or relaxation will be of appreciable importance.

On increasing the extension still further, the fabric tensile modulus rises progressively until the yield point is reached. Beyond this point, D in figure 1, comparatively small increases in load are enough to produce considerable increases in fabric extension. The behaviour, around and beyond the yield point, probably depends more on the yarn tensile properties than on the other yarn properties or the geometrical structure of the fabric. The point of rupture or break occurs at the end of the yield phase. This may happen instantaneously or after a self-hardening region.

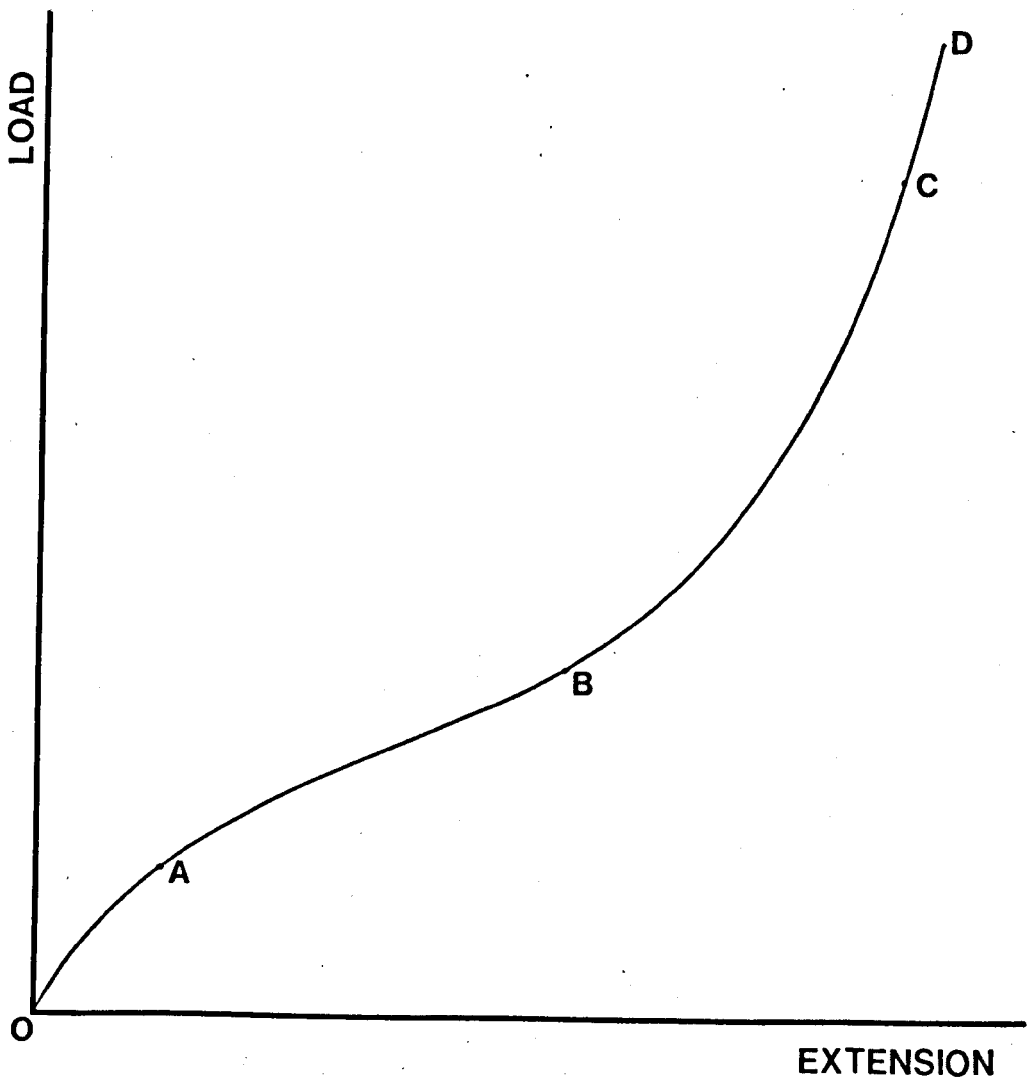

Fig. 1

1.2.2 Bending properties of plain weave

Bending is a very important property of fibres and yarns as well as of fabrics. Fibre bending is inherent in yarn bending and it can be shown that yarn bending takes place in almost all types of cloth deformations.

The most important among bending properties is the flexural rigidity. For simply defined bodies the flexural rigidity, B, can be defined as

$$B = EI,$$

where E is the Young's modulus of the material, and I is the moment of inertia of the cross-section of the body about a line perpendicular to the neutral axis.

In textiles, this equation is usually restricted to single fibre bending where I is reasonably accurately defined. The flexural rigidity for yarns and fabrics is better defined as the couple, M, necessary to produce a unit change in curvature, K, i.e.

$$B = M/K.$$

In the above equation, if B is independent of the value of K, the K-M relation would be linear, and in this case it is sufficient to find B by determining the value of M and the corresponding value of K at any moment. Actually, in both yarn and fabric bending, fibres are capable of independent movement within the structure. This causes the resultant moment-curvature relationship to be non-linear and in this case the need to take successive readings for M and K over a range of fabric curvatures is essential. A typical curve of M against K is shown in figure 2.

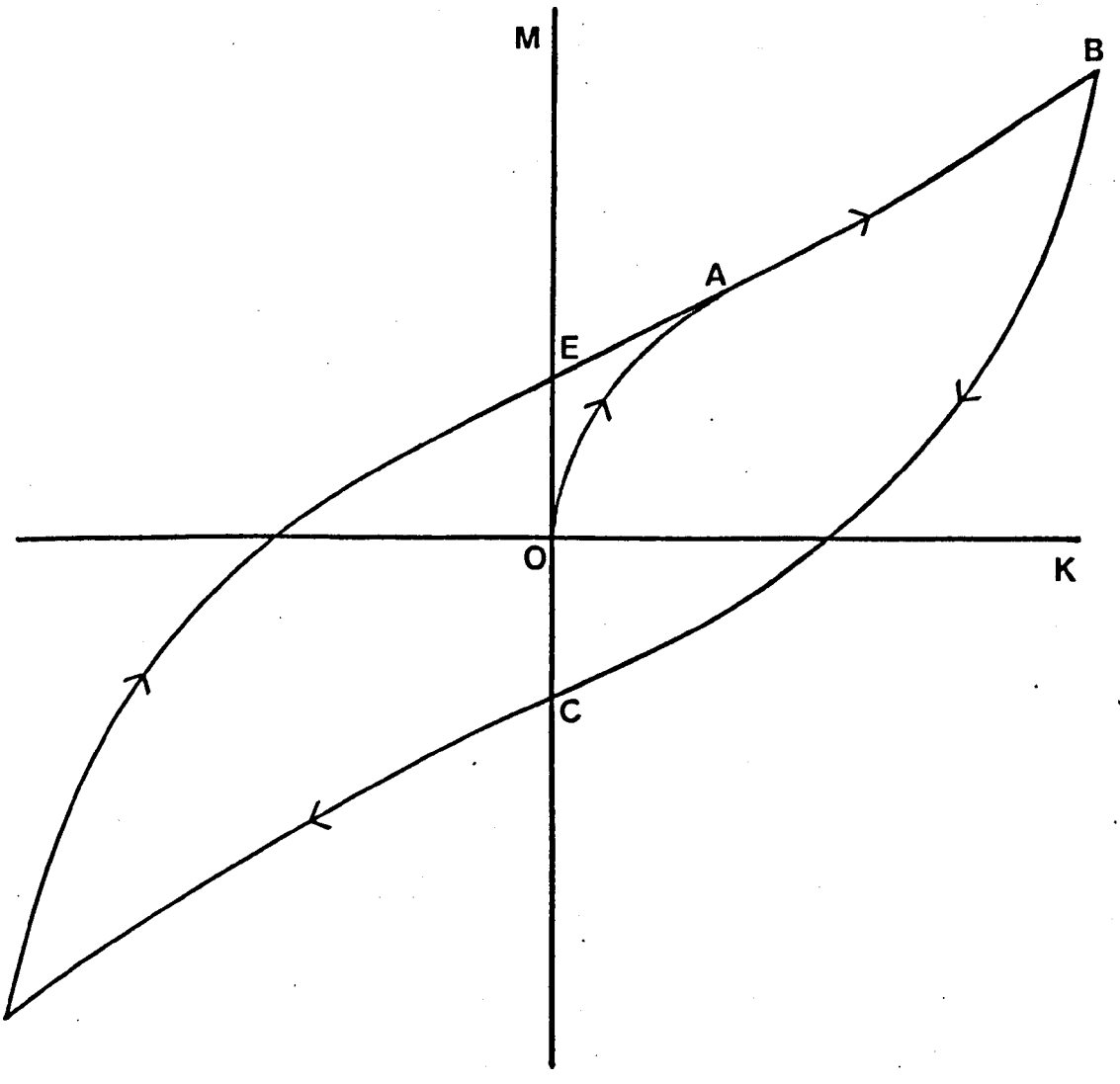

Fig. 2

It is now proposed to consider the fabric bending behaviour as shown by the bending hysteresis curve. The initial high modulus shown for the initial bending, OA, is probably due both to the resistance offered by the yarn rigidity (elastic component) and to an extra frictional resistance restricting the fibres' tendency to move relative to each other in the yarn (frictional component). The magnitude of the frictional resistance is governed, generally, by the coefficient of friction between fibres and by the interfibre pressure. Gradually overcoming these frictional restraints, the fabric is then more easily bent and the couple-curvature curve is, ideally, a linear relation, AB, representing the elastic component in bending.

If the fabric is allowed to recover from a certain imposed curvature (usually taken as 3 cm^{-1} in testing), the curve will show hysteresis. The difference between the magnitude of the couple at zero curvature, when loading and recovering, OC or OE in figure 2, represents that frictional couple, M_0, needed initially to overcome the frictional restraints. The elastic component in bending, therefore, obeys a law of the type

$$B = (M-M_0)/K .$$

The fabric elastic rigidity, B, is influenced by both geometrical and mechanical factors. Geometrical parameters such as the fabric cover factor, ratio of the number of warp threads to weft, type of weave and fabric relaxation will affect the magnitude of the interyarn forces which have to be overcome in bending the fabric. The mechanical factors would be mainly the yarn's rigidity and, probably, the yarn's compressional properties. The former depends on the yarn twist factor, fibre density,

and tensile and torsional properties of fibres. A summary of the main factors contributing to fabric bending is given by Owen (6).

Mechanism of fabric bending

When the fabric is bent, the applied couple will induce internal forces between the two yarn systems which will lead to several changes in the warp and weft configurations. In the bending plane, the yarns will increase their length of contact with the cross yarns on the outside of the bend and will unwrap from the cross-yarns on the inside of the bend, as shown in figure 3. Between these contact regions, the yarns are free to bend. Denby (7) assumed that large scale bending of woven fabrics involves the imposition of additional constant curvature to the individual yarns. Considering the crossing yarns Abbott (8), in a theoretical study, showed that fabric bending involves an increase in the crimp of the crossing threads. Skelton and Schoppee (9), using Denby's assumption and considering a simple model of fabric crimp, reached the same conclusion as Abbott. They stated that the bending of idealized plain woven fabric (figure 3) will always result in an increased amplitude of fabric crimp which for certain fabrics reduces the restraining forces on the crossing yarns.

1.2.3 Shear of plain weave

Because of the different treatments and terminology used to study shear as mechanical behaviour, it is useful to consider first the general definitions.

Pure shear is defined as the deformation of a body caused by uniform extension in one direction and contraction in the perpendicular direction, so that its area remains constant. As demonstrated by Hearle (10), if such a definition is applied to shear the square abcd (figure 4a),

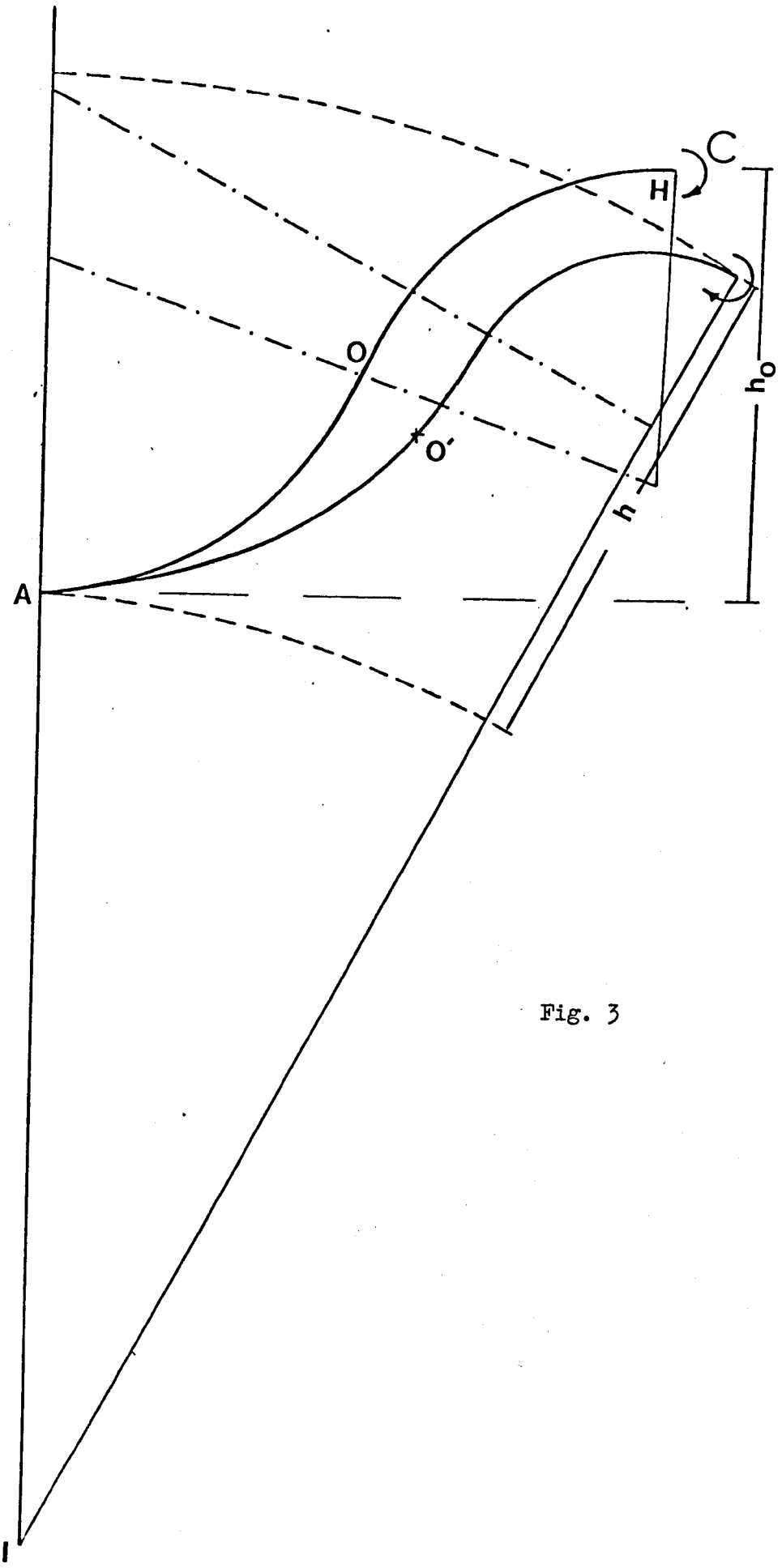

Fig. 3

the resultant shape will be a′b′c′d′. Rotating this parallelogram so that one pair of its sides becomes parallel to its original direction, we get what is known as a simple shear strain in the direction aa′, bb′, cc′ and dd′ (figure 4b). A simple shear of a square initially constructed with one side in the direction, ab or cd, will result in the shape shown in figure 4c, where tanθ is taken as the shear strain.

When testing textile fabrics under pure shear, a problem arises. This is because fabrics are thin sheets, they tend to buckle easily under compressive forces. The problem is overcome by introducing a tensile force much higher than the compressive force. Practically this is achieved by hanging a weight W, uniformly distributed, over LK as shown in figure 4c. It follows that the effective shear force, S, is

$$S = F - W \tan\theta .$$

The shear stress-strain diagram represents the relation between the shear force, S, and the shear angle θ. A typical curve is shown in figure 4d where it can be seen that a considerable hysteresis is involved in shear deformations.

The effect of weave construction and material, as well as the mechanism of shear, have been studied by a considerable number of workers (11-17).

Cusick (12,13) gave results for a variety of fabrics, and the curves were often found to be asymmetrical. Lindberg and his colleagues (14) gave a detailed study of different commercial fabrics. They pointed to the relation between bending rigidity, buckling and shear angle. Also, they showed that the formability of a fabric, defined as the maximum compression a fabric can take up before it buckles, is related to the product of buckling load and shear angle.

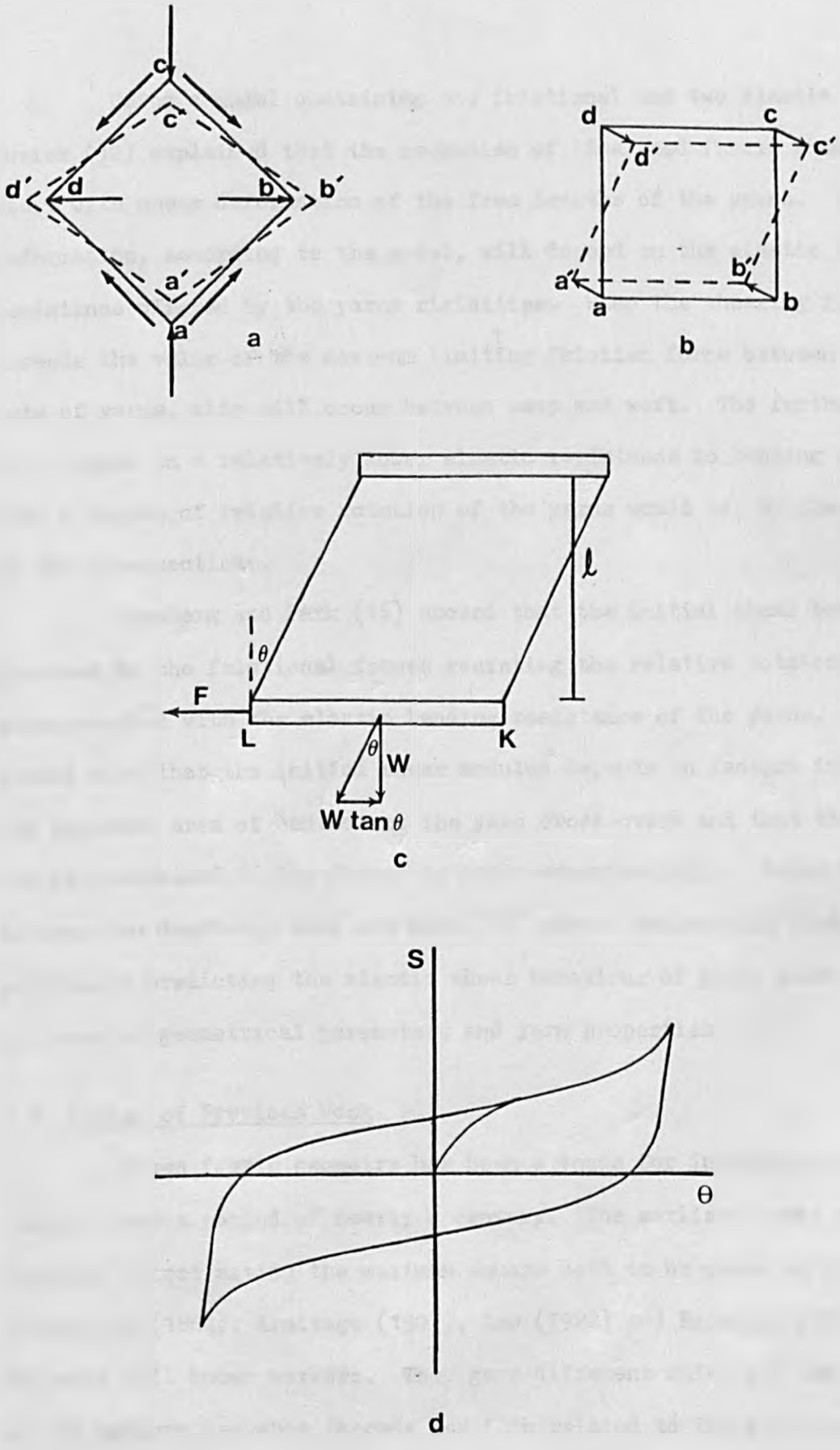

Fig. 4

Using a model containing one frictional and two elastic elements, Cusick (12) explained that the mechanism of idealized fabric shear will start with shear deformation of the free lengths of the yarns. Such deformation, according to the model, will depend on the elastic bending resistance offered by the yarns rigidities. When the shearing force exceeds the value of the maximum limiting friction force between the two sets of yarns, slip will occur between warp and weft. The further shear will depend on a relatively lower elastic resistance to bending provided that a degree of relative rotation of the yarns would be, by then, allowed at the intersections.

Grosberg and Park (16) showed that the initial shear behaviour is governed by the frictional forces resisting the relative rotation of the yarns coupled with the elastic bending resistance of the yarns. They showed also that the initial shear modulus depends on factors including the apparent area of contact at the yarn cross-overs and that the latter can be determined if the former is known experimentally. Using this information Grosberg, Leaf and Park (17) gave a theoretical study of the problem of predicting the elastic shear behaviour of plain woven fabrics in terms of geometrical parameters and yarn properties.

1.3 Review of Previous Work

Woven fabric geometry has been a topic for investigation by many workers over a period of nearly a century. The earliest works were directed to estimating the maximum square sett to be woven on the loom. Ashenhurst (1884), Armitage (1907), Law (1922) and Brierley (1931) were the most well known workers. They gave different rules for the problem of the maximum weavable threads per inch related to the yarn count. Empirical data and assumptions which express the diameter as a function

of the yarn count were used in their cloth geometry (18-19). Their four rules give slightly different answers to stable fabric problems, Brierley's being the most accurate for general purposes.

Peirce's work (20) can be considered as a watershed, as he thoroughly investigated the plain weave structure and gave both a flexible-thread geometry and an elastic-thread model. However, the first was primarily used for the same purpose as the earlier works, i.e. to investigate the jammed condition. Recently, the theoretical study of fabric mechanical properties has received much attention by many, and in this respect Peirce's rigid-thread model is considered an important contribution.

In this section, both of the plain fabric models and some different approaches to the theoretical calculation of fabric properties in extension and bending are reviewed.

1.3.1 Plain fabric models

The different models of the plain woven fabric can be classified as geometrical (descriptive) and mechanistic (21). In the geometrical models no account of internal forces produced by the yarn rigidities is taken into consideration. In the mechanistic models it is assumed that the two systems of yarns are balanced in a way determined by their relative rigidities and the weave construction. The advantage of using the descriptive model is its comparative simplicity; on the other hand, the information that may be obtained about mechanical behaviour is rather limited. A mechanistic model is likely to be more capable of supplying such information, provided that its idealization is sufficiently realistic, but at the expense of greater complexity (22).

a. Descriptive geometrical models

Peirce (20) was the first to describe the plain fabric geometry using flexible, circular bars set into the shape shown in figure 5. Taking a normal section to the plane of the cloth through one of the thread axes, Peirce defined the geometrical parameters of the fabric using the following symbols:

p - Thread spacing. The distance between two planes, normal to the fabric, containing two successive cross yarns.

ℓ - Modular length. The length, measured along the yarn axis, of half a crimp wave.

c - Yarn crimp, expressed as the fraction $(\frac{\ell-p}{p})$.

h - Modular height. The amplitude of the crimp wave.

θ - Weave angle. The maximum angle of the thread axis with the fabric central plane.

d - Yarn diameter.

D - Scale factor, equal to the sum of warp and weft diameters.

The subscript '1' is used to refer to warp parameters, while '2' refers to weft. In this thesis the same symbols and subscripts are used.

The geometry shown in figure 5 leads to the following equations:

$$p_2 = (\ell_1 - D\theta_1)\cos\theta_1 + D\sin\theta_1, \qquad (1.1)$$

and

$$h_1 = (\ell_1 - D\theta_1)\sin\theta_1 + D(1-\cos\theta_1). \qquad (1.2)$$

Similar euqations could be obtained for the weft with an appropriate interchange of subscripts.

Also, $$h_1 + h_2 = d_1 + d_2 = D. \qquad (1.3)$$

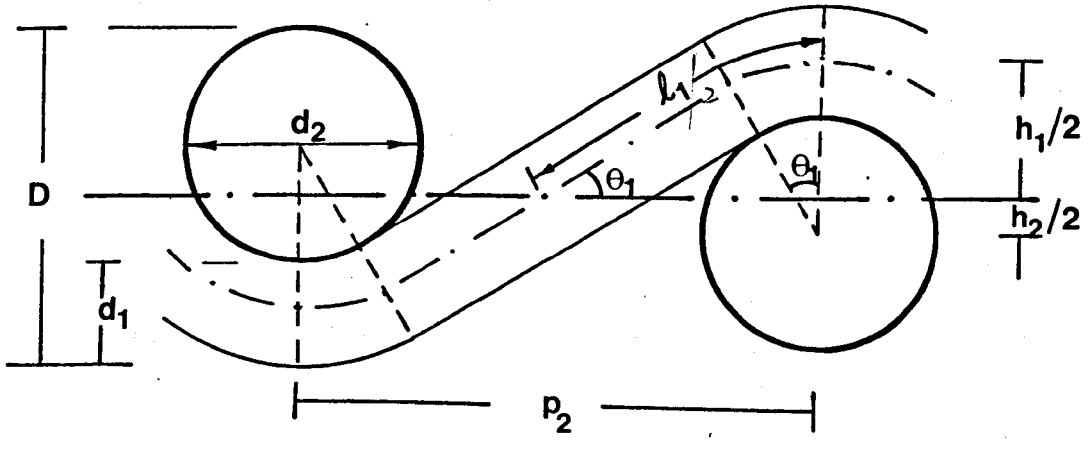

Fig. 5

This provides a system of 5 simultaneous equations with 9 unknowns ($p_1, p_2, \ell_1, \ell_2, h_1, h_2, \theta_1, \theta_2$ and D). Therefore the model is completely defined when 4 parameters are known. The easiest and most measurable quantities are possibly the thread spacings and the modular lengths.

Due to the difficulties encountered in solving these simultaneous equations, a set of curves was produced by Peirce (20) and Love (23) to assist in the calculations. For practical uses, Peirce derived a simplified formulae. This is found by expanding the trigonometrical functions in equations (1.1) and (1.2) in terms of ascending powers of θ to give

$$p_2 = (\ell_1 - D\theta_1)\left(1 - \frac{\theta_1^2}{2!} + \frac{\theta_1^4}{4!} - \ldots\right) + D\left(\theta_1 - \frac{\theta_1^3}{3!} + \frac{\theta_1^5}{5!} - \ldots\right), \qquad (1.4)$$

and

$$h_1 = (\ell_1 - D\theta_1)\left(\theta_1 - \frac{\theta_1^3}{3!} + \frac{\theta_1^5}{5!} - \ldots\right) + D\left[1 - \left(1 - \frac{\theta_1^2}{2!} + \frac{\theta_1^4}{4!} - \ldots\right)\right]. \qquad (1.5)$$

When θ_1 is small, θ_1^3 and higher terms can be ignored to give (from 1.4)

$$\theta_1 = (2)^{\frac{1}{2}}(c_1)^{\frac{1}{2}}.$$

Also, when θ_1 is small, $h_1 \simeq \ell_1\theta_1$ (from equation 1.5) and $p_2 \simeq \ell_1$, which gives

$$h_1 = (2)^{\frac{1}{2}} p_2 (c_1)^{\frac{1}{2}}.$$

Peirce modified the latter equation to:

$$h_1 = \frac{4}{3} p_2 (c_1)^{\frac{1}{2}} = \frac{4}{3} p_2 \left(\frac{\ell_1}{p_2} - 1\right)^{\frac{1}{2}}. \qquad (1.6)$$

He stated that this formula reproduces the exact values well enough for many purposes and only in extreme structures does the error amount to 5%. The equation relating p_2, ℓ_1 and θ_1 was later modified by Peirce when he considered his rigid-thread model and was given as

$$(c_1)^{\frac{1}{2}} = 0.55\ \theta_1,$$

when θ_1 is measured in radians, or

$$\theta_1(\text{degrees}) = 104(c_1)^{\frac{1}{2}}.$$

For the normal range of weave angles a better approximation is obtained by writing

$$\theta_1(\text{degrees}) = 106(c_1)^{\frac{1}{2}} = 106\left(\frac{\ell_1}{p_2} - 1\right)^{\frac{1}{2}}. \qquad (1.7)$$

Equations (1.3),(1.6) and (1.7), in addition to the equations provided for h_2 and θ_2 in the weft direction, define a simplified model for the plain woven fabrics which is completely determinate if 4 parameters are already known.

Grosberg (24) pointed out that applying the original or the simplified equations of Peirce's flexible-thread model, knowing only 3 geometrical parameters, leads to an infinity of possibilities for the fabric geometry, whereas in fact any relaxed fabric with these 3 parameters fixed has only one geometry. As will be seen later, the mechanistic models yield another condition in the relaxed fabrics (equation 1.11), and hence only 3 geometrical parameters are needed to define a mechanistic model, providing that the rigidities of the yarns are known.

Dealing with the geometrical models, two separate lines of work have been followed since Peirce. The first is to modify Peirce's flexible-

thread model to accommodate more realistic shapes of yarn cross-section. The second is to approximate the crimped shape of the yarn path by a relatively simple function, such as a sine wave.

Modifying the circular cross-sectional shape of the yarn was, in fact, considered by Peirce (20). He suggested that when flattened, the specific volume of the yarn remains constant and the area of cross-section may be taken as

$$\frac{\Pi ab}{4} = \frac{\Pi d^2}{4} ,$$

where a and b are the major and minor axes of an elliptical cross-section, see figure 6a. From this, Peirce obtained a distortion factor $e = \sqrt{b/a}$ with which the original yarn diameter, d, can be modified. Peirce showed that in order to make such an elliptical geometry determinate, it is necessary to know further data about the relative ellipticity, α, of the two threads. He suggested that e_1 may then be found by applying the following relation:

$$\frac{4}{3}(p_2\sqrt{c_1} + p_1\sqrt{c_2}) = b_1+b_2$$

$$= 36\ e_1\left(\frac{1}{\sqrt{N_1}} + \frac{\alpha}{\sqrt{N_2}}\right) ,$$

where N_1 and N_2 are the thread cotton counts and $\alpha = \frac{e_2}{e_1}$. However, Peirce pointed out that it would be rather laborious to develop and use a model based on the formal relations of an elliptic section.

Kemp (25) provided a reasonable alternative cross-sectional yarn shape to the ellipse. He suggested a 'Race-track' section consisting of a rectangle with semi-circular ends as shown in figure 6b. The ratio (b/a)

was made the distortion factor instead of Peirce's $\sqrt{b/a}$. Kemp related the initial parameters given by Peirce and the parameters resulting from the race-track shape and he used Peirce's equations, thus modified, to provide more accurate solutions for the jammed condition.

Recently, Hearle and Shanahan (26) modified Peirce's flexible model assuming a 'Lenticular Geometry' in which the yarn cross-section is represented by two intersecting arcs as shown in figure 6c. The yarn path is assumed linear except where it wraps over the crossing yarn. For such a model, the need to define the major and minor diameters of the yarns is essential and the flattening coefficient was presented as $F = a/b$. The other parameters of the yarn cross-section can then be calculated in the following way

$$\sin \Phi = \frac{a}{2r} , \qquad \text{and} \qquad \cos \Phi = 1 - \frac{b}{2r} .$$

This gives

$$r = \frac{a^2+b^2}{4b} .$$

Substituting in the above relation gives

$$\Phi = \sin^{-1}\left(\frac{2ab}{a^2+b^2}\right) = \cos^{-1}\left(\frac{a^2-b^2}{a^2+b^2}\right).$$

Also, if $D_1 = 2r_2+b_1$ and $D_2 = 2r_1+b_2$,

the modified equations for this model are

$$p_2 = (\ell_1 - D_1\theta_1)\cos\theta_1 + D_1\sin\theta_1$$

and

$$h_1 = (\ell_1 - D_1\theta_1)\sin\theta_1 + D_1(1-\cos\theta_1) .$$

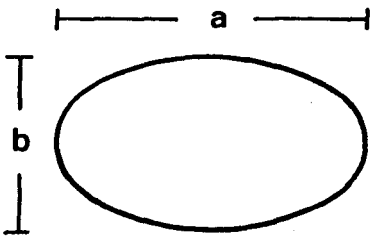

Fig. 6a

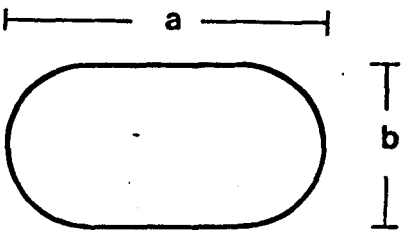

Fig. 6b

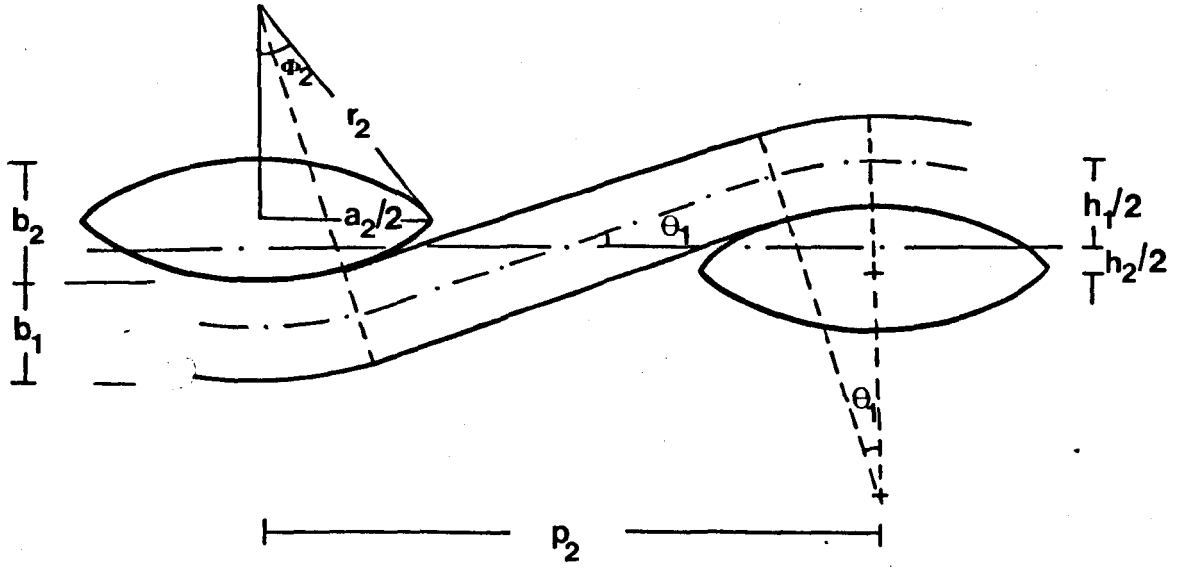

Fig. 6c

Similar equations are provided for weft parameters and, in addition,

$$h_1+h_2 = b_1+b_2 \ .$$

Providing that the cross-section parameters are already defined, the model is completely determinate when 3 other parameters of the fabric are known.

The 'Lenticular-Geometry' was developed with the aim of providing a realistic interaction between the yarn rigidity and yarn flattening, when the fabric deforms under tensile forces. With this objective, the original equations for the model were presented, by the authors, in a different form, including the flattening coefficients F_1 and F_2.

The crimp-wave shape of the yarn path has been approximated in different ways and for this purpose the yarn cross-section was not always taken into consideration. A twin arc model has been used by Olofsson (27) and Wilson (28). In this model, it is proposed that the crimp-wave of the yarn consists of two arcs, one above and one below the central plane of the cloth. The geometry of such a model leads to the relations

$$\ell_1 = p_2 \frac{\theta_1}{\sin\theta_1} \qquad \text{and} \qquad h_1 = p_2 \frac{(1-\cos\theta_1)}{\sin\theta_1} \ .$$

A sinusoidal shape of the yarn was assumed by Lord and Mohamed (29). Mathematically the yarn shape may be expressed by

$$y = \frac{h_1}{2} \sin(\pi x/p_2),$$

and the yarn modular length is given approximately by

$$\ell_1 \simeq p_2\left[1+(\pi h_1/4p_2)^2\right].$$

A straight line model has been used by Kawabata et al. (3) and Leaf and Kandil (5), and further details of this will be given later. This model is, probably, the simplest and leads to

$$p_2 = \ell_1 \cos\theta_1 \ , \qquad \text{and} \qquad h_1 = \ell_1 \sin\theta_1 .$$

b. Mechanistic models

In the mechanistic model, the shape of the yarn path is assumed to be determined by the yarn flexural rigidity, B, and by the vertical force, v, and the external tension, f, acting as point loads at the apex, as shown in figure 7. This gives

$$B.\frac{d\psi}{ds} = -v.x + f.y \ , \tag{1.8}$$

referred to axes shown.

If the external tension on the fabric is zero, the equation is reduced to

$$B\,\frac{d\psi}{ds} = -v.x \tag{1.9}$$

Peirce (20) was interested in this case and he showed that integrating the last equation gives

$$x = \left(\frac{2B}{v}\right)^{\frac{1}{2}}(\sin\theta - \sin\psi)^{\frac{1}{2}}. \tag{1.10}$$

At the apex $x = p/2$ and $\psi = 0$; substituting in the above equation in the warp and weft directions then gives

$$p_2^2 = \frac{8B_1\sin\theta_1}{v_1} \qquad \text{and} \qquad p_1^2 = \frac{8B_2\sin\theta_2}{v_2} .$$

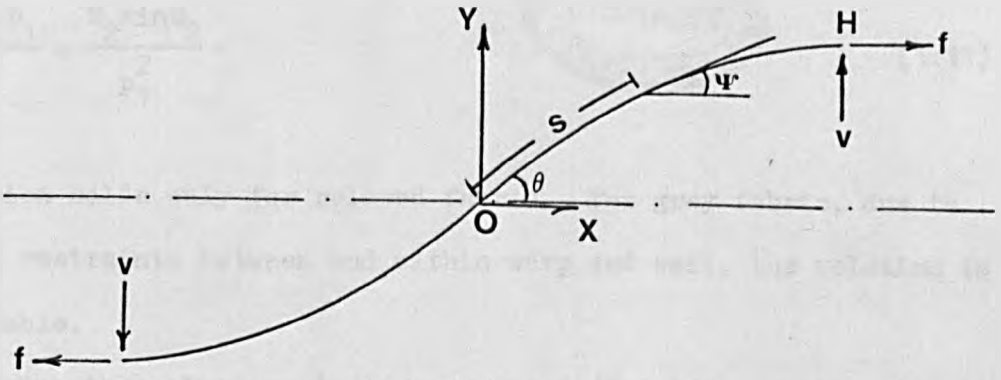

Fig. 7

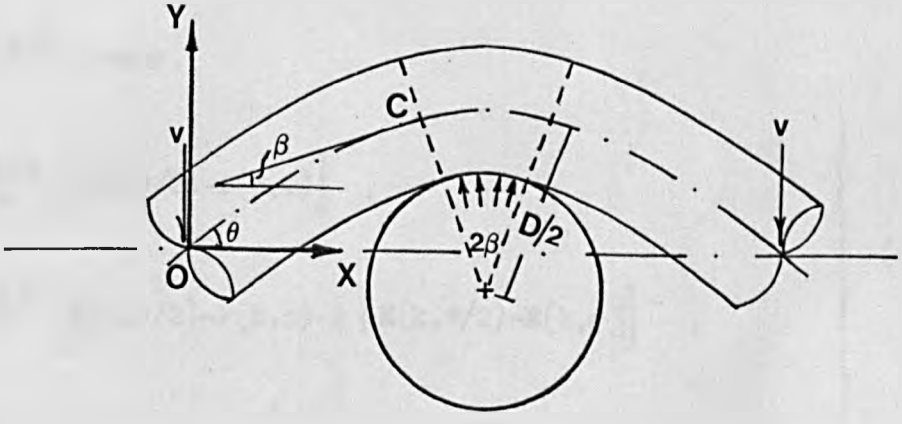

Fig. 8

The equilibrium condition between warp and weft is attained when $v_1=v_2$, which leads to

$$\frac{B_1 \sin\theta_1}{p_2^2} = \frac{B_2 \sin\theta_2}{p_1^2} . \qquad (1.11)$$

This relation holds only for relaxed fabric. For grey fabric, due to frictional restraints between and within warp and weft, the relation is not applicable.

Using the relations $dx/ds=\cos\psi$ and $dy/ds=\sin\psi$, equations (1.9) and (1.10) can be converted to give the relation between ds and $d\psi$ or between dy and $d\psi$, and hence integrated. The parameters at any point of the yarn axis can be expressed in the form of standard elliptic integrals as follows:

$$\left.\begin{aligned} x &= 2\left(\frac{B}{v}\right)^{\frac{1}{2}} k \cos\Phi , \\ s &= \left(\frac{B}{v}\right)^{\frac{1}{2}} \left[F(k,\pi/2)-F(k,\Phi)\right] , \\ y &= \left(\frac{B}{v}\right)^{\frac{1}{2}} \left[F(k,\pi/2)-F(k,\Phi)-2\left\{E(k,\pi/2)-E(k,\Phi)\right\}\right] , \end{aligned}\right\} \qquad (1.12)$$

and

$$\cos\psi = 2k\sin\Phi\,(1-k^2\sin^2\Phi)^{\frac{1}{2}} ,$$

where $F(k,\pi/2)$ and $F(k,\Phi)$ are the complete and incomplete elliptic integrals of the first kind, and $E(k,\pi/2)$ and $E(k,\Phi)$ are the complete and incomplete integrals of the second kind. The modulus, k, and amplitude, Φ, of these integrals are given by

$$k = \sin(\theta/2+\pi/4) \qquad \text{and} \qquad \sin\Phi = \frac{1}{k}\sin(\psi/2+\pi/4).$$

At the apex, denoted by point H in the figure, $\psi=0$; hence $\Phi_H = \sin^{-1}(1/2^{\frac{1}{2}}k)$. The values of $p/2$, $\ell/2$ and $h/2$ can be expressed in the form of elliptic integrals by substituting $\Phi = \Phi_H$ in the above equations.

Olofsson (30) dealt with the general case of elastic yarns formed to the shape in the fabric by the action of both external tension, f, and vertical force, v, (equation 1.8). Using this assumption and the relations $dx = \cos\psi ds$ and $dy = \sin\psi ds$, he derived new expressions for p and h related to ℓ. However, the final expressions are clumsy and laborious to use. Olofsson showed that the shape of the elastica is nearly independent of the ratio v/f, that the parameters at the apex could be obtained by simpler equations if we consider $v/f = 0$. This gave

$$p_2/\ell_1 = \frac{2E(k', \pi/2)-F(k', \pi/2)}{F(k', \pi/2)},$$

and

$$h_1/\ell_1 = \frac{2\sin(\theta_1/2)}{F(k', \pi/2)},$$

where $F(k', \pi/2)$ and $E(k', \pi/2)$ are the complete elliptic integrals of the first and second kind with modulus $k' = \sin(\theta_1/2)$.
These values of p_2/ℓ_1 and h_1/ℓ_1, for a fixed value of θ_1 can be taken to be the same for different ratios of v/f. The same conclusion was reached by Grosberg and Kedia (31). Grosberg (24) stated that it becomes possible, therefore, to use the approximate relationships

$$h/p = \frac{4}{3}(c)^{\frac{1}{2}} \qquad \text{and} \qquad \theta = 106(c)^{\frac{1}{2}},$$

with considerable confidence since they give values close to the rigid-

thread model and have already been proved to be independent of the ratio v/f.

Nordby (2) gave a comparison between the different models and showed that there is some, but not complete, agreement between the results obtained from Olofsson's relations assuming v=0 and Peirce's relations assuming f=0.

Apart from considering the yarn rigidity, a realistic fabric geometry may also take into account two other aspects namely, the rigid-thread shape with finite contact, and the degree of yarn set. The first of these is important when investigating a fabric deformation which is highly dependent on the contact length between the two yarns, while the second aspect is important when investigating the deformations of partially set fabrics.

Peirce (20) considered a model in which the rigid yarn has a finite contact with the crossing thread. This case, in a sense, constitutes an intermediate state between his completely flexible-thread model and the highly rigid-thread model with point contact. The model with finite contact is shown in figure 8 where the contact starts at the point denoted by C,(x_c,y_c) referred to the axes shown; the inclination of the yarn axis to the fabric plane at this point is β. Equation (1.12) of the rigid-thread model with point contact gives the parameters x,y and s in the region $\theta \geq \psi \geq \beta$, while the following relations hold in the region $\beta \geq \psi \geq 0$

$$x = \frac{D}{2}(\sin\beta-\sin\psi)+2\left(\frac{B}{v}\right)^{\frac{1}{2}}k \cos \Phi_c \ ,$$

$$y = \frac{D}{2}(\cos\psi-\cos\beta)+\left(\frac{B}{v}\right)^{\frac{1}{2}}\left[F(k,\pi/2)-F(k,\Phi_c)-2\left\{E(k,\pi/2)-E(k,\Phi_c)\right\}\right] \ ,$$

and

$$s = \frac{D}{2}(\beta-\psi)+(\frac{B}{v})^{\frac{1}{2}}\left[F(k,\pi/2)-F(k,\Phi_c)\right] ,$$

where $k = \sin(\theta/2+\pi/4)$, $\sin\Phi_c = \frac{1}{k}\sin(\beta/2+\pi/4)$,

and the parameters at the apex ($p/2$, $h/2$ and $\ell/2$) are given by the above equations after substituting $\psi=0$.

Thus

$$\ell = D\beta+2(\frac{B}{v})^{\frac{1}{2}}\left[F(k,\pi/2)-F(k,\Phi_c)\right] ,$$

and

$$h = D(1-\cos\beta)+2(\frac{B}{v})^{\frac{1}{2}}\left[F(k,\pi/2)-F(k,\Phi_c)-2\{E(k,\pi/2)-E(k,\Phi_c)\}\right] .$$

To make this model available for use, v and β are also defined in terms of the other parameters. It can be shown that

$$v = \frac{2B}{pD-D^2\sin\theta} \qquad \text{and} \qquad \sin\beta = 2\sin\theta-(p/D) .$$

The model can now be defined by the 4 equations giving ℓ and h in both directions, together with the following two relations

$$h_1+h_2 = D ,$$

and

$$v_1 = v_2 ,$$

or

$$\frac{B_1}{p_2D-D^2\sin\theta_1} = \frac{B_2}{p_1D-D^2\sin\theta_2} .$$

This gives a total of 6 independent relations between 11 unknowns $(p_1, p_2, \ell_1, \ell_2, h_1, h_2, \theta_1, \theta_2, B_1, B_2, D)$; therefore it is enough to define 3 parameters and the yarn rigidities, B_1 and B_2, to define the geometry.

In order to differentiate between the two rigid-thread models given by Peirce, the curvature, $1/\rho$, can be calculated at the apex from the relation $1/\rho = vp/2B$, then

(a) if $1/\rho \leqslant 2/D$, the rigid-thread model with point contact applies;

(b) if $1/\rho > 2/D$, a finite contact with the crossing yarn occurs, starting at the point $x_c = \frac{2B}{vD}$.

It is commonplace in many analyses of fabric deformations, which use a rigid-thread model as a starting point, to assume that the interyarn forces in the structure before deformation take one of the two following extremes:

1. they remain with the same value needed initially to form the fabric at the intersections in which case the fabric is said to be completely unset;
2. they gradually vanish and the yarn keeps its curvature inside the fabric structure due to permanent bending deformations; the fabric is then considered to be completely set.

Fabrics, in fact, take an intermediate state (partially set) which can be demonstrated by unravelling a yarn from the fabric and observing how it undergoes a limited change in crimp. Olofsson (30) assumed that in a partially set fabric, the yarn curvature at any point is proportional to its curvature in the released state outside the fabric. The constant of proportionality was termed the 'form factor'; thus

$$\frac{d\psi_r}{ds_r} = \text{'form factor'} \times \frac{d\psi_0}{ds_0} .$$

where suffix 'r' refers to the released state and '0' refers to yarns inside the fabric. This assumption proved to be useful (2,8,32) in calculating the degree of fabric set experimentally, as it can be shown to lead to 'set' as a function of the crimps inside the fabric, c_0, and in the released state, c_r, namely

$$\text{'set'} = (c_r/c_0)^{\frac{1}{2}}. \qquad (1.13)$$

1.3.2 Different approaches to the theoretical calculation of fabric properties

This subject has been handled under two different categories. The first, which has been more generally used, considers the fabric as a complex geometrical combination of fibres and yarns, while the second category treats the fabric as a planar sheet. The choice of which method to use depends on the final requirements of the study. For instance, if we are analysing the fabric to discover rather complicated mechanical behaviour, such as its ability to take up complex double curvatures or drape, it is probably better that the fabric should be modelled as a two dimensional uniform sheet, irrespective of its constituent fibres or yarns, except in so far as they are responsible for the particular properties of the sheet. The planar stress-strain analysis involves many complications and it is, up to now, limited in its use.

Theoretical approaches considering the fabric as geometrical combinations of fibres and yarns can be further classified into energy approaches and force approaches.

1.3.3 Theoretical calculations of fabric tensile properties

(a) Energy approaches

Grosberg and Kedia (31) considered the initial extension as a result of only bending energy changes. The force, f, needed to extend a warp thread in the fabric was regarded as divided into two parts, f' to decrimp the warp thread and f'' to upcrimp the crossing thread. The force f'' is related to the force v needed at the intersection to increase the crimp of the weft. If the fabric elongation is δp_2 and δh_2 is the change in the crossing thread height, then energy considerations demand that

$$f''.\delta p_2 = v.\delta h_2$$

Therefore

$$f = f' + f'' = f' \left[1 + \frac{v}{f'} \frac{\delta h_2}{\delta p_2}\right]$$

$$= f' \left[1 + \frac{v}{\delta h_2} \frac{\delta p_2}{f'} \left(\frac{\delta h_1}{\delta p_2}\right)^2\right].$$

The ratio $\delta h_1/\delta p_2$ was obtained using purely geometrical relations. The term $\delta p_2/f'$ was calculated by defining the strain energy, in the warp thread, due to the bending deformations caused by f' alone, then differentiating the energy expression according to Castigliano's rule. Using a similar procedure $v/\delta h_2$ was calculated after finding the strain energy in the weft thread caused by 'v' alone. The final expression for the fabric modulus was given by

$$E_1 = \frac{8B_1}{p_1 h_1^2}\left[1 + \frac{B_2 p_2^3}{B_1 p_1^3} F_1(\theta_1, \theta_2)\right], \qquad (1.14)$$

where

$$F_1(\theta_1,\theta_2) = \frac{\sin^{3/2}(\theta_2)\left[1-0.56(h_1/p_2)^2\right]^2}{F_2(\theta_2).2\sqrt{2}\ (1.12)^2} \quad ,$$

and

$$F_2(\theta_2) = E(k,\pi/2)-E(k,\Phi_H)+(k^2-1)\left\{F(k,\pi/2)-F(k,\Phi_H)\right\}.$$

The modulus $k = \sin(\theta_2/2+\pi/4)$ and $\Phi_H = \sin^{-1}\frac{1}{\sqrt{2}\,k}$

Hearle and Shanahan (22) have recently described a uniform energy approach that can be applied to various types of fabric deformations. For the general treatment, they assumed that the fabric geometry gives one or more relations equivalent to:

$$f(x_1,x_2,\ldots,x_\ell,y_1,y_2,\ldots,y_n) = 0 \quad , \tag{1.15}$$

where $(x_1,x_2,\ldots,x_\ell)$ are the generalized dimensions or displacements or both associated with the external deformations, and $(y_1,y_2,\ldots,y_n)$ are a set of independent geometrical parameters.

Due to deformation by the external forces F_i acting on x_i, the total energy in the system, E, is

$$E = \sum_{i=1}^{\ell} -(F_i x_i)+U(y_1,y_2,\ldots,y_n,\alpha_1,\alpha_2,\ldots,\alpha_m) \quad , \tag{1.16}$$

where $(\alpha_1,\alpha_2,\ldots,\alpha_m)$ are the dependent geometric parameters, and U is the strain energy.

The principle of minimum energy was then applied with any one of the displacements (say x_1) chosen as the dependent mode of deformation. This gives

$$F_k + F_1 \frac{\partial x_1}{\partial x_k} = \sum_{j=1}^{m} \frac{\partial U}{\partial \alpha_j} \frac{\partial \alpha_j}{\partial x_k}, \quad k = 2,3,\ldots,\ell$$

$$\text{and} \quad F_1 \frac{\partial x_1}{\partial y_i} = \frac{\partial E}{\partial y_i} + \sum_{j=1}^{m} \frac{\partial U}{\partial \alpha_j} \frac{\partial \alpha_j}{\partial y_i} \quad i = 1,2,\ldots,n \qquad (1.17)$$

These conditions give a total of $(\ell+n-1)$ equations. In conjunction with the geometrical relation given by equation (1.15), there will be a system of $(\ell+n)$ equations describing the behaviour of the structure under the specified types of loads. If $\alpha_1, \alpha_2, \ldots, \alpha_m$, which may be eliminated, are ignored, there will be $(2\ell+n)$ unknowns (F_i, x_i and $y_1 \ldots, y_n$). The system is then completely defined when ℓ of these quantities are given. According to the authors, the following limitations are imposed:

1. The approach is restricted to materials in which there is a well defined strain energy.
2. Frictional effects can not be included because the frictional forces can act in any direction.

(b) Force approaches

Basically, the force approach generally uses a numerical approximation method to solve a set of equations resulting from both the geometrical relations of the yarn shape and the stress analysis of the forces acting on the yarn. The procedure is carried out for each fabric direction separately, bearing in mind that for equilibrium $v_1 = v_2$. An additional necessary condition can be obtained by considering the displacement of the point of contact between warp and weft.

When investigating the fabric behaviour under high strains, it is necessary to consider both the initial configuration of the yarns and their

stressed shape. In the following, the notation is the same as in the previous section but an additional suffix '0' will be used to denote quantities in the undeformed state.

Nordby (2) used a force approach to study the load-elongation properties of plain fabrics. He considered the crimped shape of the yarn as divided into consecutive arcs, where the geometrical relations between the parameters of each arc are as shown in figure 9. When the fabric is deformed, the forces acting on the yarn will be as shown in figure 10. The bending moment, M, and the tension force, T, at the middle of a general arc PQ are

$$M = f(y+\Delta y/2)-v(x+\Delta x/2) \quad ,$$

and

$$T = f.\cos(\psi-\Delta\psi/2)-v.\sin(\psi-\Delta\psi/2) \quad .$$

If the bending property of the yarn is defined in such a way that

$$M = B\left(\frac{1}{\rho_0} - \frac{1}{\rho}\right) \quad ,$$

a solution of the stressed shape is possible, provided that the undeformed shape of each arc is known. The solution is then checked against

a - boundary conditions (ψ=0 at the apex);

b - continuity of contact stresses and displacements between warp and weft.

When a consistent solution is obtained, the co-ordinates at the apex are obtained by summing the increments Δy_i, and Δx_i for all the arcs.

In Nordby's analysis it was possible to include the following:

1. Effect of yarn extensibility. This was done by assuming $ds/ds_0 = 1+mT^n$, where m and n are constants.

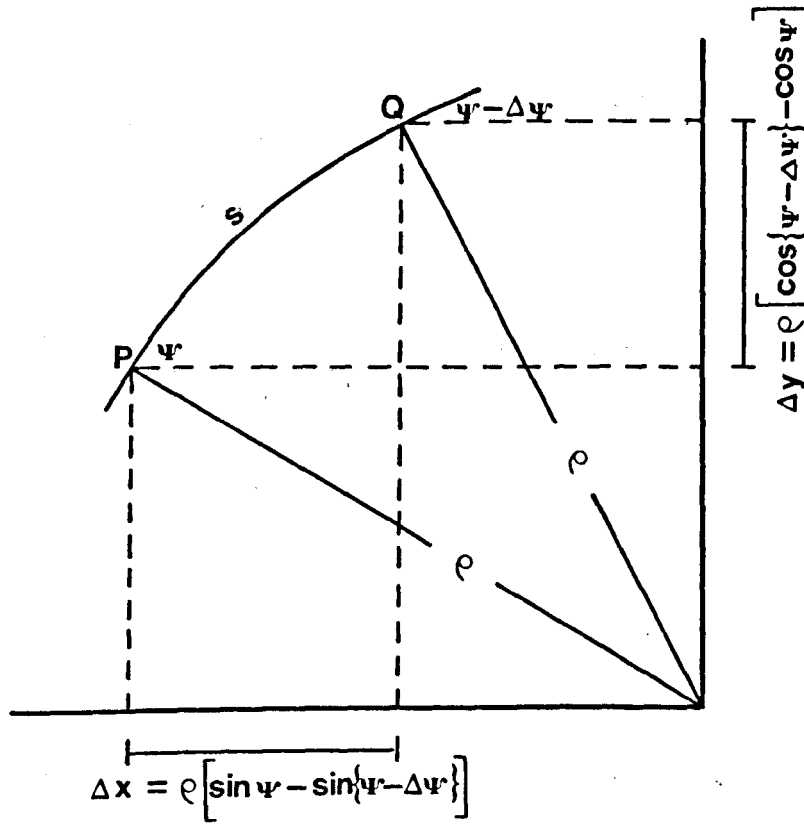

Fig. 9

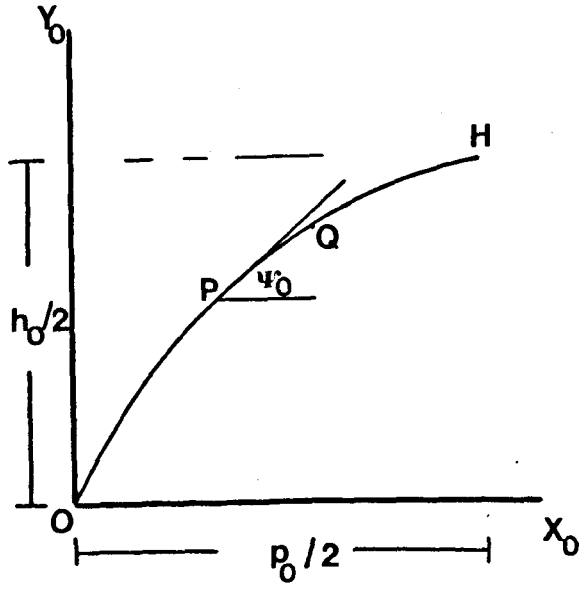

Fig. 10a

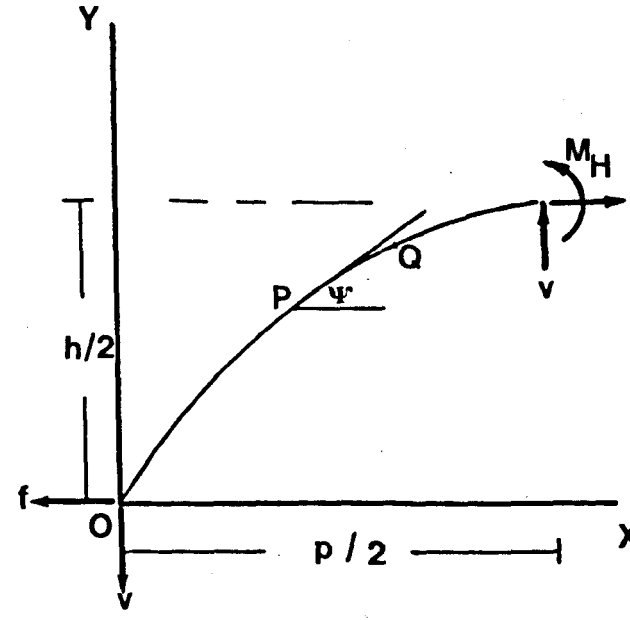

Fig. 10b

2. Effect of yarn compressibility. The compression strains were also assumed to be a power function of the load v.

3. Effect of frictional restraints. This was included by assuming the yarn to bend according to a law such as

$$M-M_0 = B\left(\frac{1}{\rho_0} - \frac{1}{\rho}\right) ,$$

where $M_0 = M_{0y}$, $\quad 0 \leqslant s \leqslant \ell_f/2$

and $M_0 = M_{0y}+M_{0f}$. $\quad \ell_f/2 \leqslant s \leqslant \ell/2$

M_{0y} is the coercive couple of the yarn, ℓ_f is the yarn length free of contact with the crossing yarn and M_{0f} is an additional frictional couple due to fibre slippage.

4. Deformation of partially set fabrics. For this purpose, the factor 'set' was evaluated experimentally, thus enabling the remaining interyarn forces, v_r, to be calculated from the equation $v_r = v_0(1-\text{set})$. The general bending equation for this case becomes

$$f(y+\Delta y/2)-(v+v_r)(x+\Delta x/2) = B\left(\frac{1}{\rho_0} - \frac{1}{\rho}\right) ,$$

which obviously gives higher values of 'f' compared to the case of set fabrics (v_r=0).

Mashaly (33) solved the mechanism of fabric extension for the case when twistless yarns are used for warp and weft. An assumption was made to suit this case, that the yarn cross-sections occupy the cavity shaped by the other crimped yarn in the cross-wise direction. The reaction from the weft when the warp is extended was assumed uniformly distributed over the warp crimp-wave length. It follows that the bending moment, M, at the general point P, shown in figure 11, is

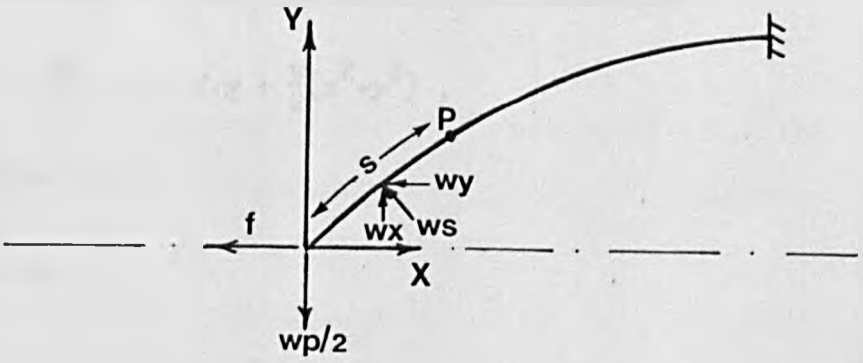
Y
P
s
wy
wx
ws
f
X
wp/2

Fig. 11

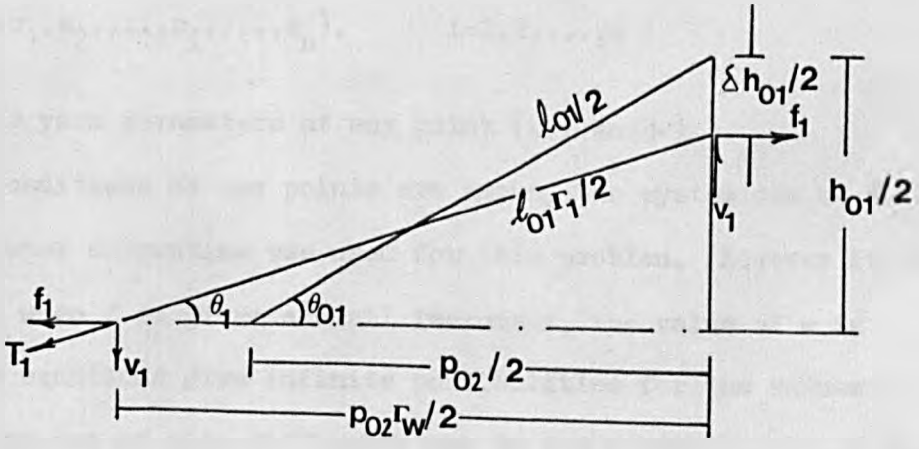
$\delta h_{01}/2$
$l_{01}/2$
f_1
$l_{01}r_1/2$
v_1
$h_{01}/2$
f_1
θ_1
θ_{01}
T_1
v_1
$p_{02}/2$
$p_{02}r_w/2$

Fig. 12

$$M = \frac{-wp}{2}.x + f.y + \frac{w}{2}(x^2+y^2),$$

where w is the interyarn force, expressed as intensity of load.
The main governing equation in this case is therefore

$$B\frac{d\Psi}{ds} = -\frac{wp}{2} \cdot x + f.y + \frac{w}{2}(x^2+y^2) ,$$

which, together with

$$\frac{dx}{ds} = \cos\Psi ,$$

and

$$\frac{dy}{ds} = \sin\Psi ,$$

represent a system of differential equations which can be put in the general form

$$\frac{d\alpha_i}{ds} = f(s,\alpha_1,\alpha_2,\ldots,\alpha_i,\ldots,\alpha_n), \qquad i=1,2,\ldots,n$$

where α_i are the yarn parameters at any point (x,y and Ψ).
If n boundary conditions at two points are known, the system can be solved. A standard computer subroutine was used for this problem. However it will be noticed that when f is given a small increment, the value of w is unknown and the equations give infinite possibilities for the values of p and h. The way out of this difficulty was to fix a value of f and then solve the system of equations for several values of w. In the cross-wise direction f=0 and the system of equations for the cross-thread were solved for the same values of w. Only one value of w will give the exact solution which should satisfy the condition

$$h_1+h_2 = \text{constant},$$

assuming incompressible yarns. The constant is determined when the system is solved at f=0 in both directions.

The results were used to investigate the effect of the inter-yarn forces, developed during extension, in sustaining this twistless yarn structure.

In both of the above force treatments a criticism may be made concerning the way the yarn is assumed to bend. In Nordby's analysis, an idealized law of yarn bending was chosen and the bending property is not defined in the region $(0 \leqslant M \leqslant M_0)$, while in the Mashaly treatment, the general bending equation is applied as if the yarn is initially straight i.e. $\frac{d\Psi_0}{ds_0} = 0$.

A more rigorous version of the force approach has been given by Huang.[4] For the biaxial extension of completely set plain fabrics, he used Peirce's rigid-thread model to define the fabric initial parameters. These will be labelled by the additional suffix '0' while in the stressed state the parameters are only labelled by '1' or '2' to indicate the warp and weft directions.

Peirce's formulae yields the following expressions for the yarn curvature and its inclination at a general point $P(x_0,y_0)$

$$\frac{d\psi_0}{ds_0} = -4k \left[F(k,\pi/2)-F(k,\Phi_H)\right] X \cos\Phi / \ell_0 \ , \qquad (1.18)$$

and

$$\cos\psi_0 = 2k \cos\Phi (1-k^2\sin^2\Phi)^{\frac{1}{2}} \ , \qquad (1.19)$$

where the modulus, k, and amplitudes, Φ and Φ_H, of the above elliptic integrals can be defined in terms of θ_0 and x_0, as follows:

$$k = \sin(\theta_0/2+\pi/4),$$

$$\Phi = \cos^{-1}\left[\frac{x_0}{k\ell_0}\left\{F(k,\pi/2)-F(k,\Phi_H)\right\}\right], \qquad (1.20)$$

and

$$\Phi_H = \Phi(p_0/2) = \sin^{-1}(2^{-\frac{1}{2}}k^{-1}).$$

In addition, the values of x_0 and y_0 at the apex are given by

$$h_0 = \ell_0\left[1-2\left\{\frac{E(k,\pi/2)-E(k,\Phi_H)}{F(k,\pi/2)-F(k,\Phi_H)}\right\}\right],$$

and

$$p_0 = 2k\ell_0\cos\Phi_H/\left\{F(k,\pi/2)-F(k,\Phi_H)\right\}.$$

When the fabric is deformed by forces f_1 and f_2 per thread in the warp and weft directions respectively, O remains a point of inflection (figure 10b) and forces 2v are generated at the intersections. The tension and bending moment at P are then given by

$$T = f\cos\psi+v\sin\psi \qquad \text{and} \qquad M = f.y - v.x$$

If λ and B are the yarn tensile and bending moduli, and yarn bending has the bilinear behaviour shown in figure 13, it can be shown that

$$\frac{ds}{ds_0} = 1 + \frac{1}{\lambda}(f\cos\psi+v\sin\psi),$$

and

$$\frac{d\psi}{ds} = \frac{d\psi_0}{ds_0} + \begin{cases} M/B^* & M\leq M_0 \\ (M_0/B^*)+(M-M_0)/B\ . & M>M_0 \end{cases}$$

Huang's analysis then proceeds to formulate the finite deformation of the fabric as a non-linear boundary value problem which can be represented by

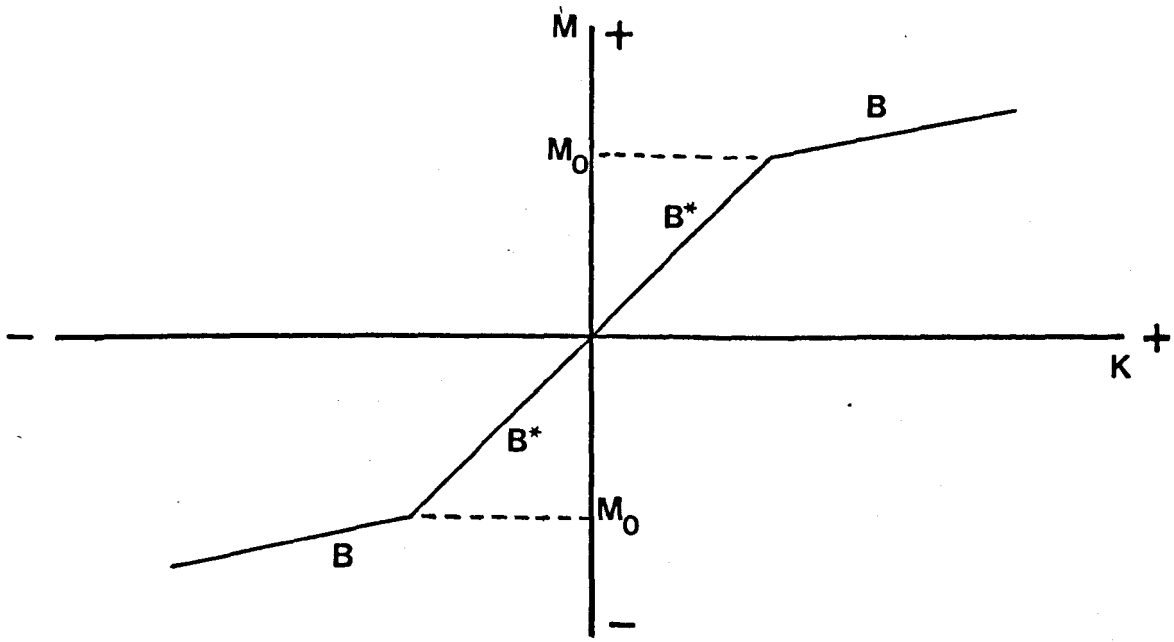

Fig. 13

a set of differential equations. Regarding x_0 as the independent variable and the parameters ψ, x and y, of the deformed state as the dependent variables, the main governing equations are

$$\frac{d\psi}{dx_0} = \frac{d\psi}{ds}\,\frac{ds}{ds_0}\,\frac{ds_0}{dx_0} ,$$

$$\frac{dx}{dx_0} = \frac{dx}{ds}\,\frac{ds}{ds_0}\,\frac{ds_0}{dx_0} ,$$

and

$$\frac{dy}{dx_0} = \frac{dy}{ds}\,\frac{ds}{ds_0}\,\frac{ds_0}{dx_0} .$$

The value of $dx_0/ds_0 (=\cos\psi_0)$ can be obtained from equation (1.19); hence

$$\frac{ds}{ds_0}\,\frac{ds_0}{dx_0} = \frac{\lambda+(f\cos\psi+v\sin\psi)}{2\lambda k\cos\Phi(1-k^2\sin^2\Phi)^{\frac{1}{2}}} = Z, \text{ say.}$$

The above governing equations, then, yield

$$\frac{d\psi}{dx_0} = \begin{cases} Z\left[\dfrac{f.y-v.x}{B^*} + \dfrac{d\psi_0}{ds_0}\right], & M \leqslant M_0 \\ Z\left[\dfrac{M_0}{B^*} - \dfrac{M_0}{B} + \dfrac{f.y-v.x}{B} + \dfrac{d\psi_0}{ds_0}\right], & M > M_0 \end{cases} \qquad (1.21)$$

$$\frac{dx}{dx_0} = Z\cos\psi , \qquad (1.22)$$

and

$$\frac{dy}{dx_0} = Z\sin\psi . \qquad (1.23)$$

Provided that the initial parameters of the undeformed state have already been defined, either by measurements (such as p and ℓ) or by calculation (such as k, Φ and $\dfrac{d\psi_0}{ds_0}$, calculated from equations (1.20) and (1.18) respectively); the above equations (1.21) to (1.23) can be

regarded as

$$\frac{dJ_i}{dx_0} = F(x_0, J_1, J_2, \ldots, J_i, f, v), \qquad (i=1,2 \text{ and } 3)$$

where J_i are the dependent parameters of the yarn in the deformed state (ψ,x,y) and x_0 is the independent parameter.

The boundary conditions for the problem are

$$x(0) = y(0) = \psi(p/2) = 0.$$

The numerical computation was carried out using an approach similar to that described by Mashaly (33), yet different in detail. Again the idea is to set a value for f, and by trial and error, several values for v are to be examined. The correct value of v must fulfil an additional condition based on the yarn compatability.

Due to the fact that warp and weft must remain in contact during deformation, the following condition is imposed:

$$\delta\{\tfrac{1}{2}(h_1-d_1)\} + \delta\{\tfrac{1}{2}(h_2-d_2)\} = 0, \qquad (1.24)$$

where $\delta\{x\}$ denotes the change in $\{x\}$ during the deformation.

The decrease in the yarn parameter, $\delta\{d\}$, was assumed by Huang to be the result of two factors:

(a) A yarn Poisson's effect, for which

$$\delta\{d\}/d = -\alpha_y(\tfrac{f}{\lambda}) ,$$

where α_y is the yarn Poisson's ratio and (f/λ) gives the yarn fractional extension at the apex.

(b) A yarn compressive effect, for which

$$\delta\{d\}/d = \mu v ,$$

where μ is the yarn compression modulus.

Superimposing the two effects and subscripting the changes by the appropriate suffices for warp and weft, equation (1.24) gives

$$\left[(h_{01}-h_1)+d_{01}(\sigma_{y1}\frac{f_1}{\lambda_1}+\mu_1 v)\right]+\left[(h_{02}-h_2)+d_{02}(\sigma_{y2}\frac{f_2}{\lambda_2}+\mu_2 v)\right] = 0.$$

When the correct value of v is found, the solution of the deformed shape is determined, from which the values of p in both directions can be obtained.

The numerical results provided by Huang for the load-extension behaviour (f vs. $p-p_0$) show a marked resemblance to the real behaviour of fabrics; also some features of the load-contraction, under uniaxial conditions, show similarity to the behaviour of some fabrics tested in the present work. However, further work on this subject is needed.

Kawabata et al. (3) introduced a finite deformation theory, based on force approach, to solve the same problem, i.e. the biaxial tensile deformation of plain fabrics. They used the straight line model to describe the yarn's configuration initially and after deformation. While the rigidity of the yarns was ignored in their earliest theory (3), yarn extension and compression were taken into consideration.

In contrast to the previous approaches, the fabric stretch in this analysis was assumed to be the independent variable for the stress-strain relation. For this purpose stretch ratios for the fabric, Γ_W and Γ_T, and for the yarns, Γ_1 and Γ_2, were defined in the following way:

$$\Gamma_W = p_2/p_{02} \quad , \quad \Gamma_T = p_1/p_{01},$$

$$\Gamma_1 = \ell_1/\ell_{01} \quad \text{and} \quad \Gamma_2 = \ell_2/\ell_{02}.$$

where the suffix '0' refers to the initial state (see figure 12).

The tension, T, in the yarn developed due to fabric stretch can be resolved to give both the tensile force acting on the fabric, f, and the compressive force acting on the crossing yarn, v, so that

$$f_1 = T_1\cos\theta_1 \qquad \text{and} \qquad f_2 = T_2\cos\theta_2 \tag{1.25}$$

$$v = T_1\sin\theta_1 = T_2\sin\theta_2. \tag{1.26}$$

From purely geometrical considerations (figure 12), they showed that

$$\Gamma_1 = \frac{\left[(h_{01}-\delta h_1)^2+(p_{02}\,\Gamma_W)^2\right]^{\frac{1}{2}}}{\left[h_{01}^2 + p_{02}^2\right]^{\frac{1}{2}}}, \tag{1.27}$$

and

$$\theta_1 = \sin^{-1}\frac{h_{01}-\delta h_1}{\left[(h_{01}-\delta h_1)^2+(p_{02}\,\Gamma_W)^2\right]^{\frac{1}{2}}}. \tag{1.28}$$

Similarly, Γ_2 and θ_2 were defined in the weft direction by using the appropriate suffices.

The load-extension relations for the yarns were defined by

$$T_1 = g_1(\Gamma_1) \qquad \text{and} \qquad T_2 = g_2(\Gamma_2), \tag{1.29}$$

where $g_1(\Gamma_1)$ and $g_2(\Gamma_2)$ are functions.

From equations (1.26-1.29), the equilibrium between warp and weft is attained when the following relation is satisfied:

$$g_1(\Gamma_1)\frac{h_{01}-\delta h_1}{\left[(h_{01}-\delta h_1)^2+(p_{02}\,\Gamma_W)^2\right]^{\frac{1}{2}}} = g_2(\Gamma_2)\frac{h_{02}+\delta h_2}{\left[(h_{02}+\delta h_2)^2+(p_{01}\,\Gamma_T)^2\right]^{\frac{1}{2}}}.$$

For the case of incompressible yarns, $\delta h_1=\delta h_2=\delta h$ (say) and the above equation, for a particular set of (Γ_W and Γ_T), can be solved for δh;

hence θ_1, θ_2, f_1 and f_2 are found from equations (1.28) and (1.25). A graphical solution was adopted and the extension-load curve was obtained up to high strains for biaxial deformations.

The yarn compression was included later by substituting

$$\delta h_1 = \delta h_2 - \phi(v) ,$$

where $\phi(v)$ is a function depending on the interyarn force, v, and both warp and weft compressional properties.

Kawabata et al. also treated other fabric deformations using the same principle and model (34,35).

1.3.4 Theoretical calculations of the fabric bending properties

Very few published works have tried to tackle the problem of predicting the fabric bending properties when the fabric parameters are known. Most of the other works on the subject provide qualitative analyses of the effect of fabric and yarn construction on bending behaviour.

Peirce (36) suggested that a theoretical warp-way stiffness of a fabric may be calculated by summing the flexural rigidities of the fibres composing the warp or weft yarns. If in a fabric strip there are N yarns per unit width and each yarn cross-section contains n fibres of an average flexural rigidity B_f, the simple estimate of the minimum cloth flexural rigidity, B_{min}, is then given by

$$B_{min} = n.N.B_f .$$

It is obvious that any friction or binding between fibres causes the observed stiffness to exceed this limit. Due to the possible interactions between fibres and between yarns, when the fabric is bent, N.J.Abbott et al. (37) suggested that the bending rigidity of fabric, B, is related to the

bending rigidity of single fibre by the following relationship,

$$B/B_f = n.N.(C.T.R),$$

where C is a clustering modifying factor,

T is a twist modifying factor,

and R is a geometrical modifying factor which is related to the yarn contact in the fabric.

Two of the above factors, C and T, are in fact related to the yarn geometry, while the third, R, depends on the fabric structure. Modifying the yarn rigidity by a 'clustering factor', results from the fact that in yarn bending there is a restriction on the individual fibre's free movement due to friction, and the fibres tend to move in groups. Platt, Klein and Humburger (38) suggested that this effect may be defined as

$$C = \frac{(B_y) \text{ with clustering}}{(B_y) \text{ with no clustering}} = n_c/P \ ,$$

where B_y is the yarn flexural rigidity, n_c is the average number of fibres per cluster and P is the packing factor within the cluster.

It is obvious that if the yarn bends as one cluster, i.e. as a solid beam, then $n_c=n$; also if the fibre diameter is very small compared to yarn diameter, P=1. This gives the above factor 'C' equal to n and the maximum limit of yarn rigidity reaches a value n^2B_f. The above analysis shows the large effect produced by fibres being prevented from bending independently; however, it does not explain how in yarn bending the flexural rigidity yields lower values after the transient phase of initial bending.

More analyses (39,40) have been carried out on these lines and a model of parallel plates was used to demonstrate the effect of interfibre friction. G.M. Abbott et al. (40), on theoretical grounds, gave the

following law for yarn bending .

$$B_y K = M^2/4M_0 , \qquad 0 \leqslant M \leqslant 2M_0$$

and

$$B_y K = M - M_0 . \qquad M > 2M_0$$

The 'twist modifying factor' is needed since the fibres in a yarn tend to lie in helical paths with different radii and they undergo both bending and torsional strains when the yarn is bent. An analysis by Livesey and Owen (41) showed that this factor may be taken as

$$T = \frac{(B_y)\text{twisted yarn}}{(B_y)\text{twistless yarn}} = \left[\frac{2}{\alpha^2 a^2 (1+B_f/r_f)}\right] \ln \left[1+ \frac{\alpha^2 a^2 (1+B_f/r_f)}{2}\right],$$

where a is the yarn radius, α is the twist in radians per unit length, and r_f is the torsional rigidity of a single fibre.

This analysis applies only for small bending deformations since the derived relations were found by analysing the forces and couples acting on the undeformed shape of the fibres. Leaf (42), in a recent publication, examined the geometry of a bent helix under large deflections, and he was able to show that the equation developed by Livesey and Owen was accurate to within 2% for even the largest strains considered. However, he also showed that the neutral axes of the helices moved by an amount depending on the helix radius. Hence independence of filament behaviour is unobtainable at large deformations.

Modifying the rigidity of the interlaced yarn inside the fabric by a "geometrical factor", R, assumes that the yarns at the cross-over region are prevented from bending by being in contact with the cross-yarns. This assumption was first pointed out by N.J. Abbott, Coplan and Platt (37).

The lengths of yarn that can not bend, ℓ_c, and that can bend, $\ell-\ell_c$, were defined by the above workers as projections of the crimped yarn on the fabric plane. Accordingly, they gave the factor 'R' as

$$R = \frac{(B_y)\text{interlaced yarn}}{(B_y)\text{straight yarn}} = \frac{\ell}{\ell-\ell_c} \quad .$$

The ratio 'R' according to the above relation is never less than unity, a fact which fails to explain some results obtained by other workers (6,8) for some open fabric structures. Following a similar argument to that given by N.J. Abbott et al. and accounting for the yarn crimp, c, it can be shown that

$$R = \frac{\ell}{(\ell-\ell_c)(1+c)} \quad , \qquad (1.30)$$

which can take values less than 1.

The interaction between yarns in fabric bending is probably more complicated than to be expressed by the mentioned geometrical factor. The relation between the weave construction and fabric flexural rigidity was examined by Eeg-Olofsson (43,44), who made an extensive study of a set of different commercial fabrics. In his study, the type of weave was regarded as of limiting effect, except in so far as it affects the length of yarns in the unit fabric cell. From his experimental results, the following conclusions were reached:

(a) The stiffness of fabric is proportional to a function of the number of threads per cm, which function increases faster than the number of threads per cm.

(b) The stiffness is inversely proportional to a function of the length of the bent threads between two consecutive points, where the threads pass from one side to the other of the fabric.

These relations can be represented as follows:

$$B_W \alpha \frac{1}{p_1^2 p_2 n_2} \quad \text{and} \quad B_T \alpha \frac{1}{p_2^2 p_1 n_1}, \tag{1.31}$$

where B_W and B_T are the warp-way and weft-way fabric stiffness per unit width, n_1 is the number of warp threads which a weft crosses between two consecutive points of passing through the fabric, and n_2 is the corresponding number for the weft. It seems reasonable to suppose that the influence from the crossing system of yarns is less than that from the bent system. To include the effect of the crossing system the former relations were, thus, modified to

$$B_W \alpha \frac{\sqrt{n_1}}{p_1^2 p_2 n_2} \quad \text{and} \quad B_T \alpha \frac{\sqrt{n_2}}{p_2^2 p_1 n_1}.$$

G. Abbott, Grosberg and Leaf (45) calculated the whole hysteresis bending curve using both energy and force approaches. A similar force approach to that used by Nordby was used for the case of set fabrics. For unset fabric defined by the parameters p, ℓ and B in both directions, the undeformed yarn configuration was completely defined using Peirce's rigid-thread model with finite contact. When the fabric plane deforms by an angle Φ, the deformed configuration of the yarn was determined using the following assumptions:

1. The yarn length does not change in bending the fabric.

2. The modular height of the yarn, in the bending plane, say the warp, will change by a small amount proportional to the inter-yarn pressures, V. The spring modulus, $\frac{dV}{dh}$, for this deformation can then be derived using small deformation theory (31) as

$$\frac{dV}{dh} = \frac{2.36\ B_2}{p_1^3} .$$

Knowing the deformed and the undeformed configurations of the yarn, in the bending plane, the sum of the energy changes can be found and is made up of three terms:

1. Energy changes in the contact regions due to the yarn in the bending plane increasing the length of contact with the cross yarns on the outside of the bend and decreasing it on the inside of the bend.
2. Energy changes in the free section of the yarn due to changes in curvature.
3. The energy increase or decrease due to the change in crimp of the cross yarn.

The fabric flexural rigidity was then calculated by equating the sum of the energy changes in the system with the work done by the external couple bending the fabric. The final calculated results gave lower values than the observed fabric bending rigidity. Abbott et al. suggested that this discrepancy was mainly due to possible errors in estimating equivalent yarn diameters which require a detailed knowledge of the load-compression of the yarns.

A suggested model and energy approach were also given by Hearle and Shanahan (22,26). In order to apply their method, a general geometry of the fabric had to be defined, in which the fabric bending angle, Φ, was

introduced. This angle was used in the energy equations as the generalized displacement associated with the deforming external couple, M. The general mechanism of fabric bending, described by G. Abbott et al. (45), had to be preserved when defining the bent shape of the fabric, i.e. in the bending plane an increase of the angle of contact on the outside of the bend and a decrease of this angle on the inside of the bend should be achieved in such a way that the difference between the two contact angles is Φ.

Figure 14 shows this geometry, described by the authors as a modified Peirce's flexible-thread model. According to the bent geometry, the yarn contact length in the cell unit will be reduced from $D\theta_{01}$ to $\frac{D}{2}(2\theta_1-\Phi)$. Referring to axes XZ in the bending plane and YZ perpendicular to this plane, the generalized dimensions and displacements are defined as follows:

$$x = D\sin\theta_1 + \left\{\ell_1 - \frac{D}{2}(2\theta_1-\Phi)\right\}\cos\theta_1, \qquad (a)$$

$$Z = \frac{D}{2}(1-2\cos\theta_1) + \left\{\ell_1 - \frac{D}{2}(2\theta_1-\Phi)\right\}\sin\theta_1,$$

$$r_1 = (x/\tan\Phi)+Z\ ,\ r_2 = (x/\sin\Phi)-D/2,\ R = (r_1+r_2)/2$$

$$h_1 = r_1-r_2 = Z + \frac{D}{2} - x\tan\frac{\Phi}{2}\ , \qquad (b)$$

$$h_2 = (\ell_2-D\theta_2)\sin\theta_2+D(1-\cos\theta_2)\ , \qquad (c)$$

and $$h_1+h_2 = D\ . \qquad (d)$$

It can be shown that the above relations may be reduced (from b, c and d via a) to only one single relation in the form

$$Z+\frac{D}{2}-\left[D\sin\theta_1+\left\{\ell_1-\frac{D}{2}(2\theta_1-\Phi)\right\}\cos\theta_1\right]\tan\frac{\Phi}{2}+(\ell_2-D\theta_2)\sin\theta_2-D\cos\theta_2 = 0\ , \qquad (1.32)$$

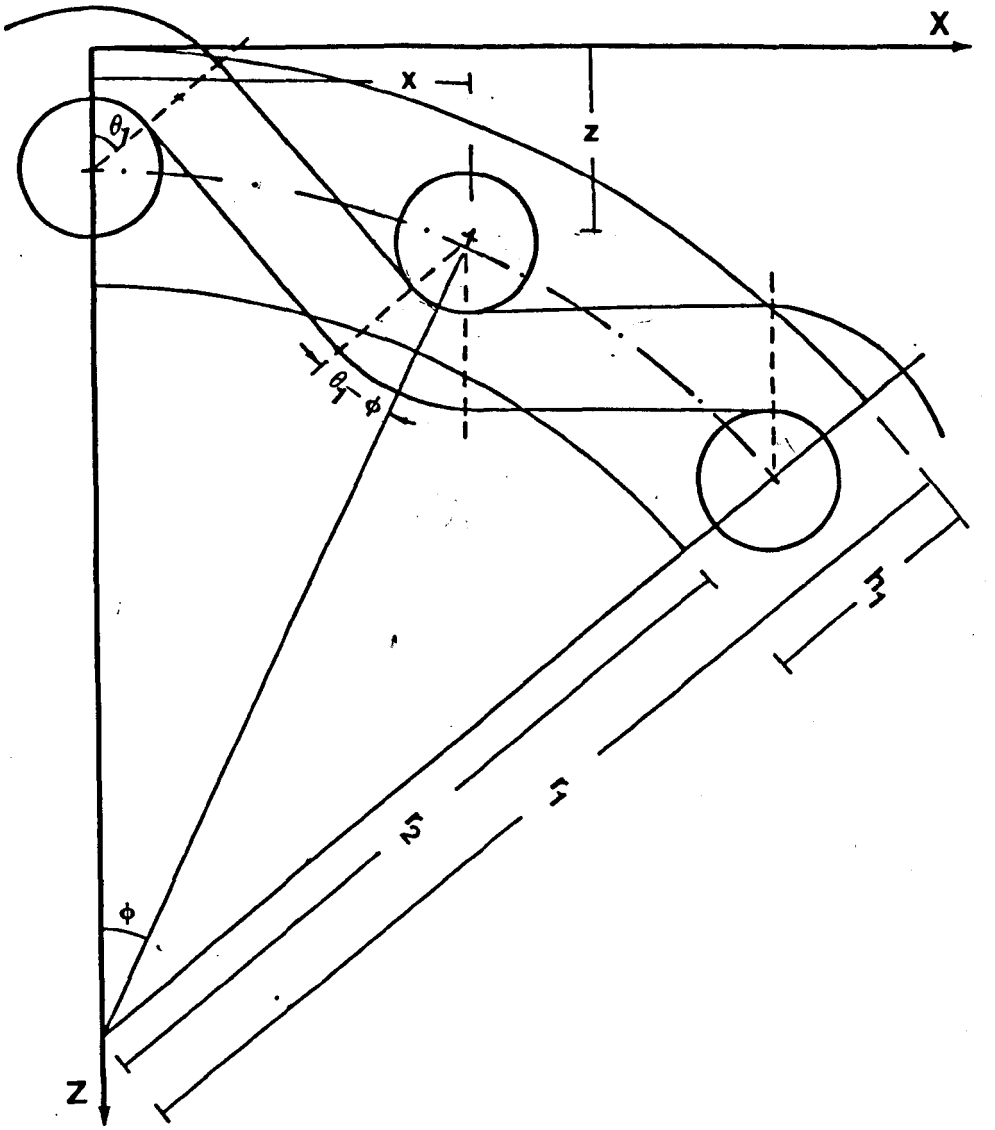

Fig. 14

which may be regarded as $\Phi = f(\theta_1, \theta_2)$, provided that ℓ_1 and ℓ_2 are constants initially defined and D is calculated for the undeformed configuration (D is also constant for incompressible yarns). In order to define the deformed shape and the M-Φ relation, we need two more relations relating the external couple M to Φ, θ_1 and θ_2. These relations are provided by the minimum energy method. The energy equation is given by

$$E = -M\Phi + U ,$$

where U is the strain energy due to the yarn bending only, and is defined as

$$U = \frac{1}{D}\left\{B_1(2\theta_1 - \Phi) + 2B_2\theta_2\right\}. \qquad (1.33)$$

Regarding θ_1 and θ_2 as the independent parameters, the minimum energy conditions (equation 1.17) give

$$M\frac{\partial\Phi}{\partial\theta_1} = \frac{\partial U}{\partial\theta_1} + \frac{\partial U}{\partial\Phi}\frac{\partial\Phi}{\partial\theta_1} , \qquad (1.34)$$

and

$$M\frac{\partial\Phi}{\partial\theta_2} = \frac{\partial U}{\partial\theta_2} + \frac{\partial U}{\partial\Phi}\frac{\partial\Phi}{\partial\theta_2} , \qquad (1.35)$$

where the derivatives are found from equations (1.32) and (1.33). The problem is reduced to 3 simultaneous equations, (1.32) and (1.34-1.35), in 3 unknowns (θ_1, θ_2 and either Φ or M) which can be solved by iterative techniques.

1.4 Scope of the Present Work

This thesis is an attempt at a theoretical study of the initial extension and bending of fabrics. The study is limited to dealing with the simplest and most commonly used weave, namely the plain fabric. The final aim of the work is to provide a closed form solution, for the above-

mentioned initial fabric deformations, that directly relates the fabric modulus and fabric parameters.

In section 1.3 it was shown that a computer was a common feature used by all workers, in order to obtain numerical results that can be compared with experimental data. When large deformations are to be considered, it seems that this recourse to powerful computing techniques is most probably unavoidable. The need to know the fabric mechanical behaviour, at higher strains, is of considerable interest in industry in order to check the quality of the fabric and the effect of various methods of fabric treatment. However, in the practical uses of commercial fabrics, these high strains are rarely met with and in many applications only small deformations are expected to take place. For such cases, it would be useful if a closed form solution could be found, that gives a reasonable prediction of real fabric behaviour without the need for a computer.

A clear disadvantage of a computer-based solution is that only a specific solution, for the specific fabric in hand is obtained, and even with some approaches if a graphical method or dimensionless representation is used, a general solution can not be obtained which covers all the possibilities arising from the endless combinations of fabric parameters. On the other hand, a closed form solution can provide such a general solution. Obviously, for practical purposes, the latter is recommended. In addition, the closed form solution is more capable of showing the inter-relation between the fabric parameters. A quick glance provides an idea about the interaction, magnitude and importance of the parameter when a fabric is required to have certain given properties.

Apart from investigating higher strains, another reason why most of the analyses mentioned previously require the use of a computer is

their employment of relatively sophisticated fabric models. Using Peirce's flexible-thread model or the modified models, involving non-circular shapes of cross-section, necessitates the solution of a system of usually non-linear simultaneous equations. Another alternative is to find an exact solution, considering Peirce's rigid-thread model as a starting point. This will involve the use of elliptic integrals and so the resulting equations of equilibrium are highly non-linear. A simple way out of the difficulty is to use a much simpler model, and this has been the approach adopted in the present work. For this purpose, a simplified shape of the plain woven fabric was considered where the yarns, warp and weft, were assumed to be modelled as elastic, straight thin rods forming a saw-tooth shape.

CHAPTER 2: THEORETICAL

CHAPTER 2

THEORETICAL

2.1 The Straight-line Model

It has been suggested in the preceding chapter that, in order to obtain closed form solutions for the initial tensile and bending moduli, a simple model for the plain weave geometry is necessary. A straight line model was thought to be most suitable for this purpose.

Different representations for the yarn axis, in one of the major directions, of a plain weave structure have been given in figures (5-8); these representations have been shown to be dependent on the assumed yarn properties, namely their rigidity and compressibility. Two possible simplified models, using straight lines, are shown as EFGI and AOH in figure 15. Of these, the first is in some respects a better representation, as it can be thought of as simulating the flattening which occurs in the yarn cross-section during fabric formation. On the other hand, adopting such a model in the present analysis, will be at the expense of additional difficulties in defining the properties of the horizontal bits EF and GI, in the shape. The second model, AOH, which may be termed the "Saw tooth" model, was considered preferable, at least at the outset of the investigation.

We may now consider the geometrical characteristics of the model, and the mechanical properties of the constituent yarns, that have been assumed.

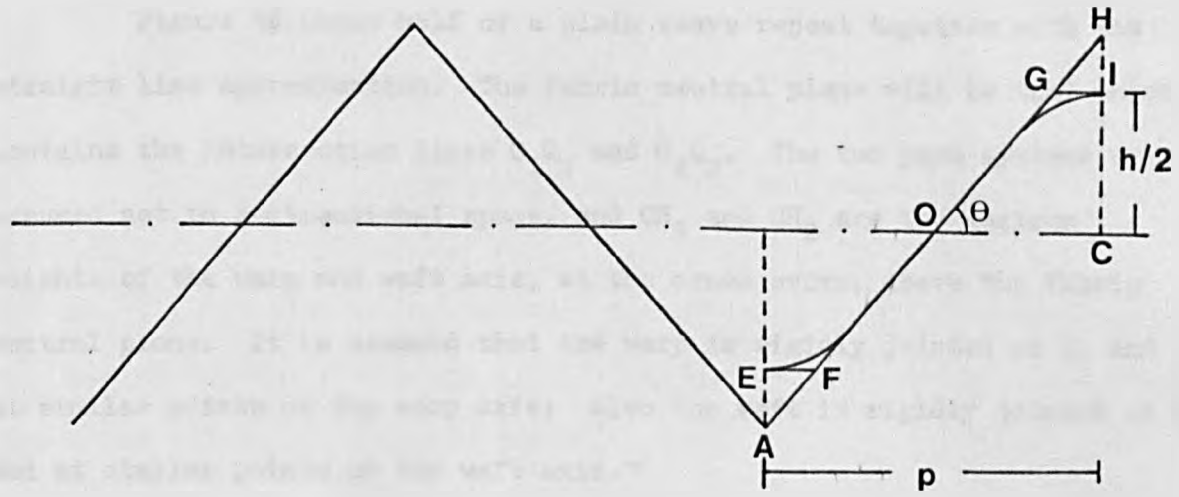

Fig. 15

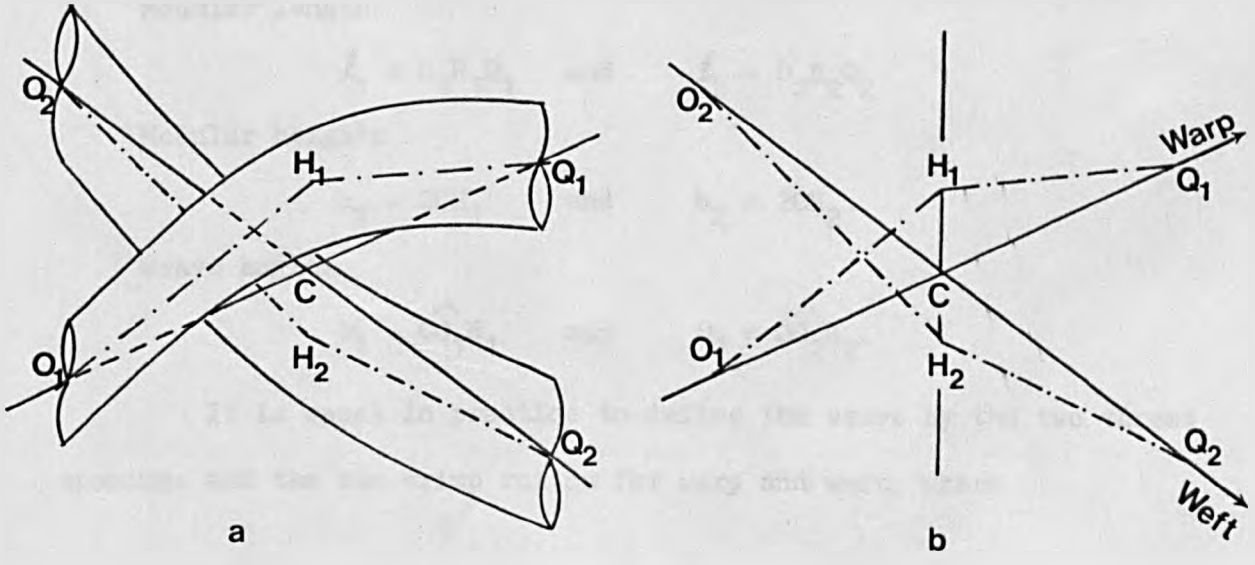

Fig. 16

Geometrical characteristics of the 'Saw-tooth' model

Figure 16 shows half of a plain weave repeat together with the straight line approximation. The fabric neutral plane will be that which contains the intersecting lines O_1Q_1 and O_2Q_2. The two yarn systems are assumed set in 3-dimensional space, and CH_1 and CH_2 are the maximum heights of the warp and weft axis, at the cross overs, above the fabric neutral plane. It is assumed that the warp is rigidly jointed at H_1 and at similar points on the warp axis; also the weft is rigidly jointed at H_2 and at similar points on the weft axis.

Using the notations given by Peirce, the fabric parameters related to figure 16b are as follows:

Thread spacings

$$p_1 = O_2Q_2 \quad \text{and} \quad p_2 = O_1Q_1.$$

Modular lengths

$$\ell_1 = O_1H_1Q_1 \quad \text{and} \quad \ell_2 = O_2H_2Q_2.$$

Modular heights

$$h_1 = 2CH_1 \quad \text{and} \quad h_2 = 2CH_2.$$

Weave angles

$$\theta_1 = \widehat{CO_1H_1} \quad \text{and} \quad \theta_2 = \widehat{CO_2H_2}.$$

It is usual in practice to define the weave by the two thread spacings and the two crimp ratios for warp and weft, where

$$c_1 = \frac{\ell_1}{p_2} - 1 \quad \text{and} \quad c_2 = \frac{\ell_2}{p_1} - 1 .$$

The triangles formed by a quarter of the plain weave repeat then yield the following relations:

$$\theta_1 = \cos^{-1} p_2/\ell_1 \quad , \quad \theta_2 = \cos^{-1} p_1/\ell_2$$

and

$$h_1 = \ell_1 \sin\theta_1 \quad , \quad h_2 = \ell_2 \sin\theta_2 .$$

The geometry is completely defined if the measurable quantities p_2, p_1, ℓ_1 and ℓ_2 are given.

Because the fabric deformation depends on both the weave construction and the constituent yarn properties, it is necessary to define the mechanical properties of the yarns in the system.

The yarn mechanical properties

(a) Yarn bending

The yarns are assumed to have constant rigidities, B, along their lengths. The relation between the change in curvature, K, and the applied bending moment, M, is assumed linear for initial deformations, i.e. the yarn rigidity does not change with the change in curvature. Using the notation of section 1.3.3, the assumed bending behaviour gives

$$\frac{M}{B} = K = \frac{d\Psi}{ds} - \frac{d\Psi_0}{ds_0}$$

$$= \frac{d\Psi}{ds} \quad \text{if the yarn is naturally straight.}$$

The strain energy, dU_B, due to bending of an element of length ds is (46)

$$dU_B = \frac{B}{2} \left(\frac{d\Psi}{ds}\right)^2 ds = \frac{M^2}{2B} ds .$$

(b) Yarn compression

Because of the forces generated between the yarns when the fabric deforms, the yarns will be compressed, so that their dimension in the plane of the fabric is much greater than that out of the plane of the fabric.

In a real fabric, the compressive forces will be distributed over the region of yarn contact, but in the model they are represented as point forces. If the inter-yarn force is T_c and the original diameter of the yarn is d, the compression modulus of the yarns, μ, will be assumed given by

$$\mu = \frac{T_c}{\mathcal{E}_c} ,$$

where $\mathcal{E}_c = \Delta d/d$ is the fractional change in diameter.
The strain energy of compression, U_c, is then

$$U_c = \tfrac{1}{2} \Delta d \, (T_c) = T_c^2 d/2\mu .$$

(c) Yarn extension

The forces acting on the system when the fabric is deformed will usually have a tension component, T_T, acting axially on the yarns. If $\mathcal{E}_T$ is the fractional extension produced, the tensile modulus of the yarns, λ, is

$$\lambda = \frac{T_T}{\mathcal{E}_T} .$$

The strain energy, dU_T, due to extension of an element of length ds is

$$dU_T = (T_T)^2 \, ds/2\lambda .$$

2.2 Solution for the Initial Tensile Properties of Plain Fabrics

It is now proposed to find the relation between the initial load-extension of plain woven fabrics, when the constituent warp and weft yarns have the shape and properties defined in section 2.1. Before we proceed to consider the solution for the general case, it may be useful to demonstrate the adopted approach by considering a simple case. In this case, the yarns

are assumed incompressible and inextensible. The strain energy in the system, when it is deformed, is thus due only to bending deformations.

2.2.1 Simple case: Incompressible and inextensible yarns

Suppose the fabric is deformed, biaxially, by forces F_1 and F_2 per unit width along the warp and weft directions respectively. If the number of ends per cm and picks per cm are $1/p_1$ and $1/p_2$ respectively, the forces f_1 and f_2 acting on the individual warps and wefts are

$$f_1 = F_1 p_1 \qquad \text{and} \qquad f_2 = F_2 p_2.$$

Fabric extension will cause forces $2v_1$ and $2v_2$ to be generated along the line H_1H_2 between the threads (figure 17a). From statical considerations $v_1 = v_2$, but it is convenient to retain the separate notations for the moment.

The forces f and v can be resolved as in figure 17c, to give an axial tension, transverse shear and bending moment, at any point on the yarn axis. In general, for such deformations it is usually assumed that the yarn cross-cross section is undeformed by shear. The tension and bending moment at a point P(x,y), a distance 's' from O', is (see figures 17b-c)

$$T_T = f \cos\Psi + v \sin\Psi ,$$

and

$$M = fy - vx .$$

If the deformations $\Delta p/2$ in the fabric plane and $\Delta h/2$ perpendicular to the fabric plane are small, then approximately $\Psi = \theta$

and $x = s \cos\theta$, $y = s \sin\theta$,

i.e. the small deformations have no significant effect on the system geometry and the forces can be calculated on the basis of the undeformed

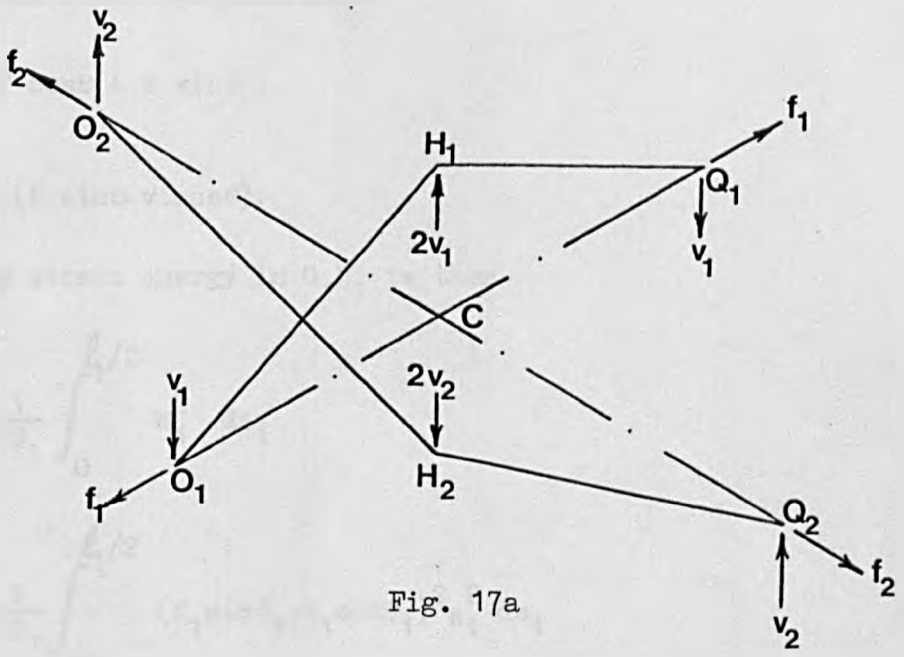

Fig. 17a

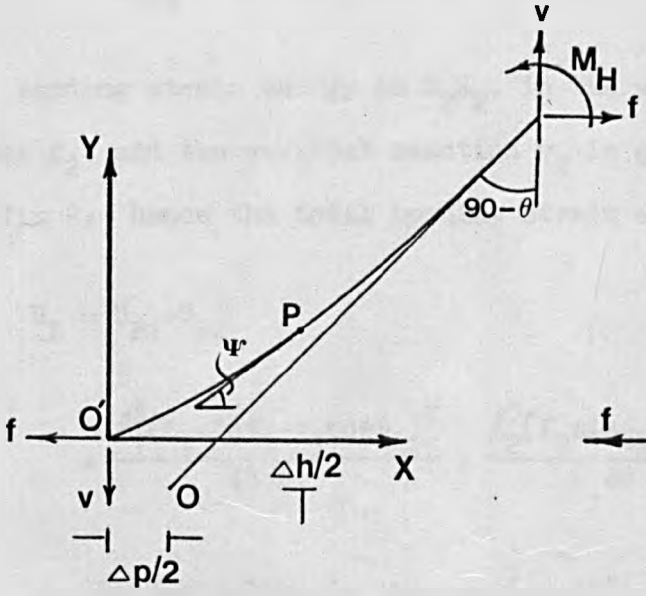

Fig. 17b

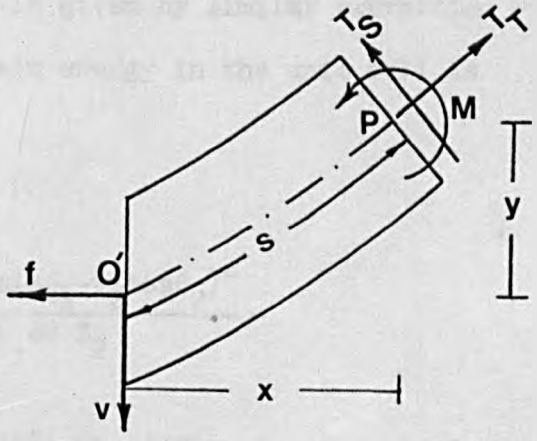

Fig. 17c

configuration (46). We then have

$$T_T = f\cos\theta + v\sin\theta ,$$

and

$$M = s(f.\sin\theta - v.\cos\theta).$$

The bending strain energy in O_1H_1 is then

$$U_{B1} = \frac{1}{2B_1}\int_0^{\ell_1/2} M_1^2 \, ds_1$$

$$= \frac{1}{2B_1}\int_0^{\ell_1/2} (f_1\sin\theta_1 - v_1\cos\theta_1)^2 s_1^2 \, ds_1$$

$$= \frac{\ell_1^3}{48B_1}(f_1\sin\theta_1 - v_1\cos\theta_1)^2.$$

The bending strain energy in O_2H_2, in the weft direction, due to the tensile force f_2, and the vertical reaction v_2 is given by similar expression with suffix 2; hence the total bending strain energy in the unit cell is

$$U_B = U_{B1} + U_{B2}$$

$$= \frac{\ell_1^3(f_1\sin\theta_1 - v_1\cos\theta_1)^2}{48\,B_1} + \frac{\ell_2^3(f_2\sin\theta_2 - v_2\cos\theta_2)^2}{48\,B_2}.$$

By Castigliano's theorem (46,47), the deflection in a load direction is given by the partial derivative of the strain energy in the body with respect to this particular load. Applying Castigliano's rule gives

$$\Delta p_2/2 = \frac{\partial U_B}{\partial f_1} = \frac{\ell_1^3 \sin\theta_1}{24\ B_1}\ (f_1\sin\theta_1 - v_1\cos\theta_1)\ , \tag{2.1}$$

$$\Delta p_1/2 = \frac{\partial U_B}{\partial f_2} = \frac{\ell_2^3 \sin\theta_2}{24\ B_2}\ (f_2\sin\theta_2 - v_2\cos\theta_2)\ , \tag{2.2}$$

$$\Delta h_1/2 = \frac{\partial U_B}{\partial v_1} = \frac{-\ell_1^3 \cos\theta_1}{24\ B_1}\ (f_1\sin\theta_1 - v_1\cos\theta_1), \tag{2.3}$$

and

$$\Delta h_2/2 = \frac{\partial U_B}{\partial v_2} = \frac{-\ell_2^3 \cos\theta_2}{24\ B_2}\ (f_2\sin\theta_2 - v_2\cos\theta_2). \tag{2.4}$$

Another condition that must be satisfied is provided by the compatability condition of the point of contact between warp and weft. Assuming incompressible yarns we know that h_1+h_2 = constant and hence

$$\Delta h_1 + \Delta h_2 = 0$$

Substituting in the above equation from (2.3) and (2.4) gives

$$\frac{\ell_1^3 \cos\theta_1}{B_1}\ (f_1\sin\theta_1 - v_1\cos\theta_1) + \frac{\ell_2^3 \cos\theta_2}{B_2}\ (f_2\sin\theta_2 - v_2\cos\theta_2) = 0. \tag{2.5}$$

Furthermore, at any moment of deflection, the vertical force acting from the weft on the warp, v_1, must be equal to the force acting from the warp on weft, v_2, i.e.

$$v_1 = v_2 = v \text{ (say)}.$$

Equation (2.5) can be solved for v, giving

$$v = \frac{f_1 B_2 \ell_1^3 \sin\theta_1\cos\theta_1 + f_2 B_1 \ell_2^3 \sin\theta_2\cos\theta_2}{B_2\ell_1^3\cos^2\theta_1 + B_1\ell_2^3\cos^2\theta_2}\ .$$

We shall define here a force ratio $Q = f_2/f_1$; the above equation is then

$$v = \frac{f_1(B_2\ell_1^3\sin\theta_1\cos\theta_1+QB_1\ell_2^3\sin\theta_2\cos\theta_2)}{B_2\ell_1^3\cos^2\theta_1 + B_1\ell_2^3\cos^2\theta_2} . \qquad (2.6)$$

Equations (2.1) and (2.6) give

$$\Delta p_2 = f_1 \frac{\ell_1^3\sin\theta_1}{12B_1}\left[\sin\theta_1 - \frac{\cos\theta_1(B_2\ell_1^3\sin\theta_1\cos\theta_1+QB_1\ell_2^3\sin\theta_2\cos\theta_2)}{B_2\ell_1^3\cos^2\theta_1 + B_1\ell_2^3\cos^2\theta_2}\right].$$

The above equation gives the fabric warp-way extension under the biaxial loads f_1 and f_2. If only a uniaxial load is applied, arbitrarily taken in the warp direction, i.e. Q=0, the equation reduces to

$$\Delta p_2 = \frac{f_1\,\ell_1^3\ell_2^3\sin^2\theta_1\cos^2\theta_2}{12(B_2\ell_1^3\cos^2\theta_1 + B_1\ell_2^3\cos^2\theta_2)} .$$

If we let $\mathcal{E}_1$ be the fabric fractional extension in the warp direction, then

$$\mathcal{E}_1 = \Delta p_2/p_2 ,$$

and we can define a fabric initial modulus E_1 by

$$E_1 = F_1/\mathcal{E}_1$$

$$= \frac{f_1\,p_2}{p_1\Delta p_2}$$

$$= \frac{12p_2(B_2\ell_1^3\cos^2\theta_1 + B_1\ell_2^3\cos^2\theta_2)}{p_1\ell_1^3\ell_2^3\sin^2\theta_1\cos^2\theta_2}$$

$$= \frac{12B_1p_2}{p_1\ell_1^3\sin^2\theta_1}\left[1 + \frac{B_2\ell_1^3\cos^2\theta_1}{B_1\ell_2^3\cos^2\theta_2}\right] , \qquad (2.7)$$

which is similar to the result derived by Grosberg and Kedia (31), equation (1.14).

2.2.2 General case: Compressible and extensible yarns

It is well known that the actual deformation of fabrics involves both yarn flattening and yarn extension as well as bending, and the errors which may result from ignoring these effects could be crucial. Therefore, the above approach is extended to the general case of extensible and compressible yarns.

The strain energy in the system

In the general case,it is slightly easier to consider the strain energy in half a repeat of the weave, i.e. the whole unit shown in figure 17a. The total strain energy will be the sum of the following 3 terms:

(a) Strain energy due to yarn bending

The bending strain energy in O_1H_1 and O_2H_2 is as before; hence the bending strain energy in the unit cell shown is

$$U_B = \frac{\ell_1^3(f_1\sin\theta_1 - v_1\cos\theta_1)^2}{24B_1} + \frac{\ell_2^3(f_2\sin\theta_2 - v_2\cos\theta_2)^2}{24B_2} .$$

(b) Strain energy due to yarn extension

The tensile force in O_1H_1 is $(f_1\cos\theta_1 + v_1\sin\theta_1)$, and from the definition given earlier for the yarn properties, the extension strain energy in the whole unit is

$$U_E = \frac{\ell_1(f_1\cos\theta_1 + v_1\sin\theta_1)^2}{2\lambda_1} + \frac{\ell_2(f_2\cos\theta_2 + v_2\sin\theta_2)^2}{2\lambda_2} .$$

(c) Strain energy due to yarn compression

If d_1 and d_2 are the original yarn diameters of the warp and weft threads, the compression strain energy in the unit cell is given by

$$U_C = \tfrac{1}{2}\frac{(2v_1)^2 d_1}{\mu_1} + \tfrac{1}{2}\frac{(2v_2)^2 d_2}{\mu_2}$$

$$= \frac{2v_1^2 d_1}{\mu_1} + \frac{2v_2^2 d_2}{\mu_2}.$$

The total strain energy in the cell unit is

$$U_T = U_B + U_E + U_C$$

$$= \sum_{i=1,2}\left\{\frac{\ell_i^3(f_i\sin\theta_i - v_i\cos\theta_i)^2}{24B_i} + \frac{\ell_i(f_i\cos\theta_i + v_i\sin\theta_i)^2}{2\lambda_i} + \frac{2v_i^2 d_i}{\mu_i}\right\}. \quad (2.8)$$

Calculation of fabric extension

The points of application of the forces $2v_1$ on the warp thread and $2v_2$ on the weft thread coincide with the point of contact of the two yarns. These points are initially at a height $(h_1-d_1)/2$ when regarded as a point on the warp thread, as shown in figure 18. Obviously,

$$\tfrac{1}{2}(h_1-d_1) = \tfrac{1}{2}(d_2-h_2).$$

When the fabric deforms, the height of this point will change by virtue of a decrease or an increase with respect to the fabric plane. If the yarns are to remain in contact, the above argument leads to

$$\Delta(h_1-d_1)/2 = \Delta(d_2-h_2)/2 ,$$

or

$$\Delta(h_1-d_1) + \Delta(h_2-d_2) = 0. \quad (2.9)$$

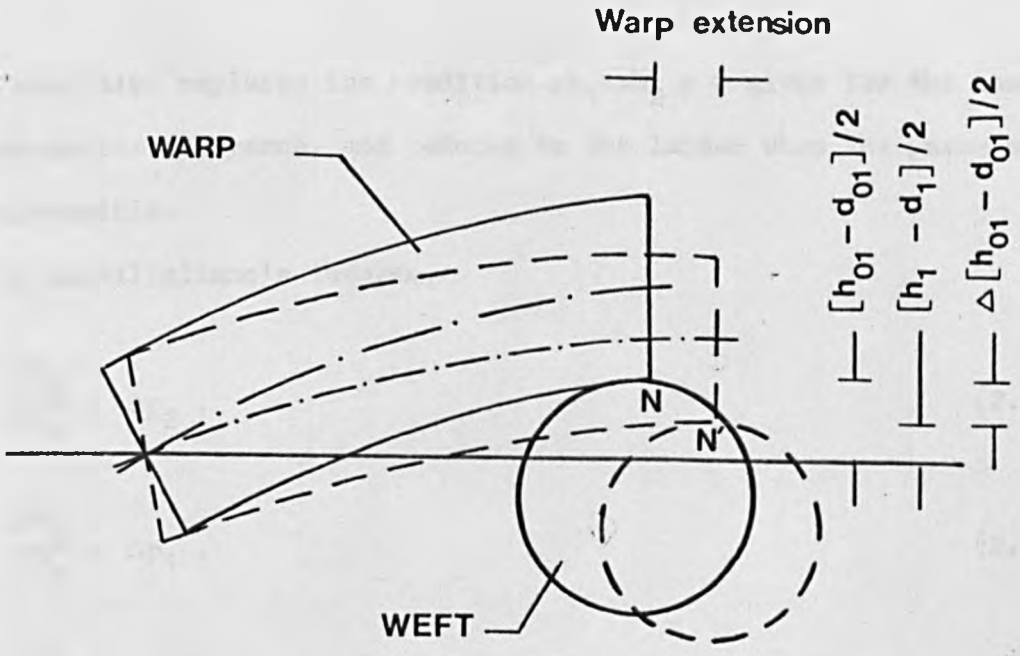

(a)

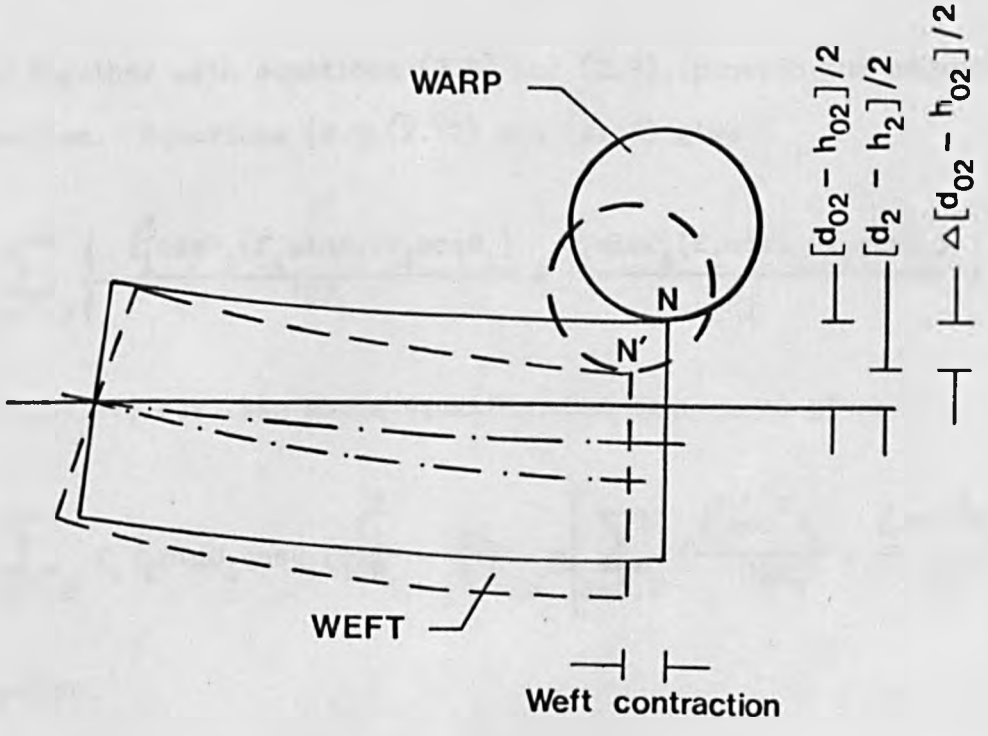

(b)

Fig. 18 shows the change in height of the point of contact, N, regarded in (a) as point on the warp and in (b) as point on the weft.

This condition replaces the condition $\Delta h_1+\Delta h_2 = 0$ given for the case of incompressible yarns, and reduces to the latter when the yarns are incompressible.

Now by Castiligliano's theorem,

$$\frac{\partial U_T}{\partial f_1} = \Delta p_2 \ , \tag{2.10}$$

$$\frac{\partial U_T}{\partial f_2} = \Delta p_1 \ , \tag{2.11}$$

$$\frac{\partial U_T}{\partial (2v_1)} = \Delta(h_1-d_1)/2 \ , \tag{2.12}$$

and

$$\frac{\partial U_T}{\partial (2v_2)} = \Delta(h_2-d_2)/2 \ . \tag{2.13}$$

These, together with equations (2.8) and (2.9), provide the solution to the problem. Equations (2.9), (2.12) and (2.13) give

$$\sum_{i=1,2}\left\{-\frac{\ell_i^3\cos\theta_i(f_i\sin\theta_i-v_i\cos\theta_i)}{12B_i}+\frac{\ell_i\sin\theta_i(f_i\cos\theta_i+v_i\sin\theta_i)}{\lambda_i}+\frac{4v_id_i}{\mu_i}\right\}=0 \ .$$

Since $v_1=v_2=v$, say, the above equation when rearranged gives

$$\sum_{i=1,2} f_i\ell_i\sin\theta_i\cos\theta_i\left(\frac{\ell_i^2}{12B_i}-\frac{1}{\lambda_i}\right) = v\left[\sum_{i=1,2}\left(\frac{\ell_i^3\cos^2\theta_i}{12B_i}+\frac{\ell_i\sin^2\theta_i}{\lambda_i}+\frac{4d_i}{\mu_i}\right)\right],$$

from which

$$v = \frac{\displaystyle\sum_{i=1,2} f_i\ell_i\sin\theta_i\cos\theta_i\left(\frac{\ell_i^2}{12B_i}-\frac{1}{\lambda_i}\right)}{\displaystyle\sum_{i=1,2}\left\{\frac{\ell_i^3\cos^2\theta_i}{12B_i}+\frac{\ell_i\sin^2\theta_i}{\lambda_i}+\frac{4d_i}{\mu_i}\right\}} . \tag{2.14}$$

Next, the extension in the warp direction Δp_2 can be obtained from equation (2.8) and (2.10) as

$$\Delta p_2 = \frac{\ell_1^3 \sin\theta_1 (f_1 \sin\theta_1 - v\cos\theta_1)}{12B_1} + \frac{\ell_1 \cos\theta_1 (f_1 \cos\theta_1 + v \sin\theta_1)}{\lambda_1}$$

$$= f_1\left[\left(\frac{\ell_1^3 \sin^2\theta_1}{12B_1}\right) + \frac{\ell_1 \cos^2\theta_1}{\lambda_1}\right] - v\left[\sin\theta_1\cos\theta_1\left(\frac{\ell_1^3}{12B_1} - \frac{\ell_1}{\lambda_1}\right)\right]. \quad (2.15)$$

Substituting the value of v from equation (2.14) gives

$$\Delta p_2 = f_1\left(\frac{\ell_1^3 \sin^2\theta_1}{12B_1} + \frac{\ell_1 \cos^2\theta_1}{\lambda_1}\right)$$

$$-\sin\theta_1\cos\theta_1\left(\frac{\ell_1^3}{12B_1} - \frac{\ell_1}{\lambda_1}\right) \frac{\sum_{i=1,2} f_i \ell_i \sin\theta_i \cos\theta_i \left(\frac{\ell_1^2}{12B_i} - \frac{1}{\lambda_i}\right)}{\sum_{i=1,2} \left(\frac{\ell_i^3 \cos^2\theta_i}{12B_i} + \frac{\ell_i \sin^2\theta_i}{\lambda_i} + \frac{4d_i}{\mu_i}\right)} . \quad (2.16)$$

Using the relations $\Delta p_2 = \mathcal{E}_1 p_2$, $f_1 = F_1 p_1$ and $f_2 = F_2 p_2$, the above equation gives

$$\mathcal{E}_1 = \frac{F_1 p_1}{p_2} \frac{M}{N} , \quad (2.17)$$

where

$$M = \left[\left\{\frac{\ell_1^3 \ell_2^3 \sin^2\theta_1 \cos^2\theta_2}{144 B_1 B_2} + \frac{\ell_1^4}{12 B_1 \lambda_1} + \frac{\ell_1 \ell_2}{12}\left(\frac{\ell_1^2 \sin^2\theta_1 \sin^2\theta_2}{B_1 \lambda_2} + \frac{\ell_2^2 \cos^2\theta_1 \cos^2\theta_2}{B_2 \lambda_1}\right)\right.\right.$$

$$\left. + \frac{\ell_1 \ell_2 \cos^2\theta_1 \sin^2\theta_2}{\lambda_1 \lambda_2} + 4\ell_1\left(\frac{\ell_1^2 \sin^2\theta_1}{12B_1} + \frac{\cos^2\theta_1}{\lambda_1}\right)\left(\frac{d_1}{\mu_1} + \frac{d_2}{\mu_2}\right)\right\}$$

$$\left. -(F_2 p_2 / F_1 p_1) \ell_1 \ell_2 \sin\theta_1 \cos\theta_1 \sin\theta_2 \cos\theta_2 \left(\frac{\ell_1^2}{12B_1} - \frac{1}{\lambda_1}\right)\left(\frac{\ell_2^2}{12B_2} - \frac{1}{\lambda_2}\right)\right] ,$$

and

$$N = \sum_{i=1,2} \left(\frac{\ell_i^3 \cos^2\theta_i}{12B_i} + \frac{\ell_i \sin^2\theta_i}{\lambda_i} + \frac{4d_i}{\mu_i}\right) \quad .$$

A similar expression for the weft-way fabric extension, $\mathcal{E}_2$, under biaxial loading could be derived from equations (2.8) and (2.11), or by the interchange of suffices in equation (2.17).

2.2.3 Special cases

The following special cases can be derived from the general expression.

1. Fabric extension of compressible and extensible yarns under uniaxial loading

In this case $F_2=0$ and the term including F_2 in equation (2.15) is eliminated. The fabric tensile modulus in this case is

$$E_1 = \frac{F_1}{\mathcal{E}_1} = \frac{p_2}{p_1}\,\frac{N}{M'} \quad , \qquad (2.18)$$

where

$$M' = \left\{\frac{\ell_1^3\ell_2^3 \sin^2\theta_1\cos^2\theta_1}{144B_1B_2} + \frac{\ell_1^4}{12B_1\lambda_1} + \frac{\ell_1\ell_2}{12}\left(\frac{\ell_1^2 \sin^2\theta_1\cos^2\theta_1}{B_1\lambda_2} + \frac{\ell_2^2\cos^2\theta_1\cos^2\theta_2}{B_2\lambda_1}\right)\right.$$

$$\left. + \frac{\ell_1\ell_2\cos^2\theta_1\sin^2\theta_1}{\lambda_1\lambda_2} + 4\ell_1\left(\frac{\ell_1^2\sin^2\theta_1}{12B_1} + \frac{\cos^2\theta_1}{\lambda_1}\right)\left(\frac{d_1}{\mu_1} + \frac{d_2}{\mu_2}\right)\right\}.$$

2. Fabric extension of inextensible and compressible yarns under biaxial loading

If the yarns are assumed inextensible, the λ's tend to infinity in equation (2.17) and the warp-wise extension is given by

$$\mathcal{E}_1 = \frac{F_1 p_1}{p_2} \frac{X}{Y} \quad , \tag{2.19}$$

where

$$X = \frac{\ell_1^3}{12} \left\{ \ell_2^3 \sin^2\theta_1 \cos^2\theta_2 + 48 B_2 \sin^2\theta_1 \left(\frac{d_1}{\mu_1} + \frac{d_2}{\mu_2}\right) \right.$$

$$\left. -(F_2 p_2 / F_1 p_1) \ell_2^3 \sin\theta_1 \cos\theta_1 \sin\theta_2 \cos\theta_2 \right\} ,$$

and

$$Y = B_2 \ell_1^3 \cos^2\theta_1 + B_1 \ell_2^3 \cos^2\theta_2 + 48 B_1 B_2 \left(\frac{d_1}{\mu_1} + \frac{d_2}{\mu_2}\right) .$$

3. Fabric extension of inextensible and compressible yarns under uniaxial loading

In this case $F_2=0$ and X is reduced to X', given by

$$X' = \frac{\ell_1^3 \sin^2\theta_1}{12} \left\{ \ell_2^3 \cos^2\theta_2 + 48 B_2 \left(\frac{d_1}{\mu_1} + \frac{d_2}{\mu_2}\right) \right\} .$$

The initial fabric modulus for this mode of deformation is then given by

$$E_1 = \frac{p_2}{p_1} \frac{Y}{X'}$$

$$= \frac{12 B_1 p_2}{p_1 \ell_1^3 \sin^2\theta_1} \left[1 + \frac{B_2 \ell_1^3 \cos^2\theta_1}{B_1 \ell_2^3 \cos^2\theta_2 + 48 B_1 B_2 (d_1/\mu_1 + d_2/\mu_2)} \right] . \tag{2.20}$$

4. The simple case

The simple case of inextensible and incompressible yarns, which was derived earlier, is a special case of the general solution (equation 2.17) when the λ's and μ's tend to infinity.

2.2.4 Fabric initial Poisson's ratio

Fabric Poisson's ratio is defined as the ratio of contraction to extension, expressed as fractions, and can be investigated by the present analysis.

Under biaxial loading, the warp-way change in fabric dimensions, Δp_2, is given by equation (2.15). By change of indices we get a similar expression for Δp_1 as follows:

$$\Delta p_1 = \left[f_2 \left(\frac{\ell_2^3 \sin^2\theta_2}{12B_2} + \frac{\ell_2 \cos^2\theta_2}{\lambda_2} \right) - \frac{1}{N} \sin\theta_2 \cos\theta_2 \left(\frac{\ell_2^3}{12B_2} - \frac{\ell_2}{\lambda_2} \right) \sum_{i=1,2} f_i \sin\theta_i \cos\theta_i \left(\frac{\ell_i^3}{12B_i} - \frac{\ell_i}{\lambda_i} \right) \right],$$

where

$$N = \sum_{i=1,2} \left(\frac{\ell_i^3 \cos^2\theta_i}{12B_i} + \frac{\ell_i \sin^2\theta_i}{\lambda_i} + \frac{4d_i}{\mu_i} \right). \qquad (2.21)$$

These expressions for Δp_2 and Δp_1 are reduced under uniaxial loading conditions, $f_2=0$, to the following

$$\Delta p_2 = \frac{f_1}{N} \left[N \left(\frac{\ell_1^3 \sin^2\theta_1}{12B_1} + \frac{\ell_1 \cos^2\theta_1}{\lambda_1} \right) - \sin^2\theta_1 \cos^2\theta_1 \left(\frac{\ell_1^3}{12B_1} - \frac{\ell_1}{\lambda_1} \right)^2 \right],$$

and

$$\Delta p_1 = - \frac{f_1}{N} \left[\sin\theta_1 \cos\theta_1 \sin\theta_2 \cos\theta_2 \left(\frac{\ell_1^3}{12B_1} - \frac{\ell_1}{\lambda_1} \right) \left(\frac{\ell_2^3}{12B_2} - \frac{\ell_2}{\lambda_2} \right) \right] .$$

A general expression for Poisson's ratio in the warp direction is then

$$\sigma_1 = -\frac{p_2}{p_1}\frac{\Delta p_1}{\Delta p_2}$$

$$= \frac{p_2 \sin\theta_1\cos\theta_1\sin\theta_2\cos\theta_2\left(\frac{\ell_1^3}{12B_1} - \frac{\ell_1}{\lambda_1}\right)\left(\frac{\ell_2^3}{12B_2} - \frac{\ell_2}{\lambda_2}\right)}{p_1\left[N\left(\frac{\ell_1^3\sin^2\theta_1}{12B_1} + \frac{\ell_1\cos^2\theta_1}{\lambda_1}\right) - \sin^2\theta_1\cos^2\theta_1\left(\frac{\ell_1^3}{12B_1} - \frac{\ell_1}{\lambda_1}\right)^2\right]}. \qquad (2.22)$$

The special cases can be obtained from the above expression by applying the following rules:

(a) If the yarns are assumed inextensible, λ_1 and λ_2 tend to infinity.

(b) If the yarns are assumed incompressible, μ_1 and μ_2 tend to infinity.

The following cases are of interest,

1. Fabric initial Poisson's ratio for inextensible and compressible yarns

In this case equation (2.22) is reduced to

$$\sigma_1 = \frac{p_2}{p_1}\frac{\sin\theta_1\cos\theta_1\sin\theta_2\cos\theta_2\left(\frac{\ell_1^3\ell_2^3}{144B_1B_2}\right)}{\left[Z\left(\frac{\ell_1^3\sin^2\theta_1}{12B_1}\right) - \sin^2\theta_1\cos^2\theta_1\left(\frac{\ell_1^3}{12B_1}\right)^2\right]},$$

where

$$Z = \sum_{i=1,2}\left(\frac{\ell_i^3\cos^2\theta_i}{12B_i} + \frac{4d_i}{\mu_i}\right),$$

or

$$\sigma_1 = \frac{p_2}{p_1}\frac{\ell_2^3\cos\theta_1\sin\theta_2\cos\theta_2}{\sin\theta_1\left[\ell_2^3\cos^2\theta_2 + 48B_2\left(\frac{d_1}{\mu_1} + \frac{d_2}{\mu_2}\right)\right]}. \qquad (2.23)$$

2. Fabric initial Poisson's ratio for inextensible and incompressible yarns

The above expression is further reduced to

$$\sigma_1 = \frac{p_2}{p_1} \frac{\tan\theta_2}{\tan\theta_1}. \qquad (2.24)$$

2.3 Solution for the Initial Bending Properties of Plain Fabrics

For this analysis, it is proposed to find a closed form solution for the relation between the fabric initial bending modulus and fabric and yarn parameters, under conditions when only small fabric bending deformations are assumed to take place in one of the major directions. The yarn's initial configuration in the fabric and its mechanical properties are assumed to be identical with those used in the previous analysis. In particular, it is important to remember that the yarns at the intersections are assumed rigidly jointed, i.e. the angle subtended between CA and AH (figure 19b) remains unchanged during deformation.

Figure 19a shows a three dimensional representation of the plain weave using the 'Saw tooth' model. When the fabric is bent, say in the warp direction, the weave unit will appear as shown in figure 20a and because of the assumption that angles like $\hat{CAH}$ remain constant, the arm AH may be treated as a cantilever fixed at A.

Figure 20b shows the elevation view of two successive bent warps according to this mechanism of fabric bending. It is apparent that the thread spacings, in the bending plane, on the outside of the bend will increase, while those on the inside of the bend will decrease. This suggests that there is a 'neutral plane' in the fabric, whose length does not change after the bending deformation. Due to the fact that the fabric is not homogeneous in structure and fabric bending involves a relative freedom for yarn deformations, including a change in their height amplitude, the 'neutral plane' will not necessarily coincide with the plane of the fabric before bending (i.e. the plane through the mid-point O of AH in figure 19b). This neutral plane is shown in figure 20b and intersects AH' at D. If the

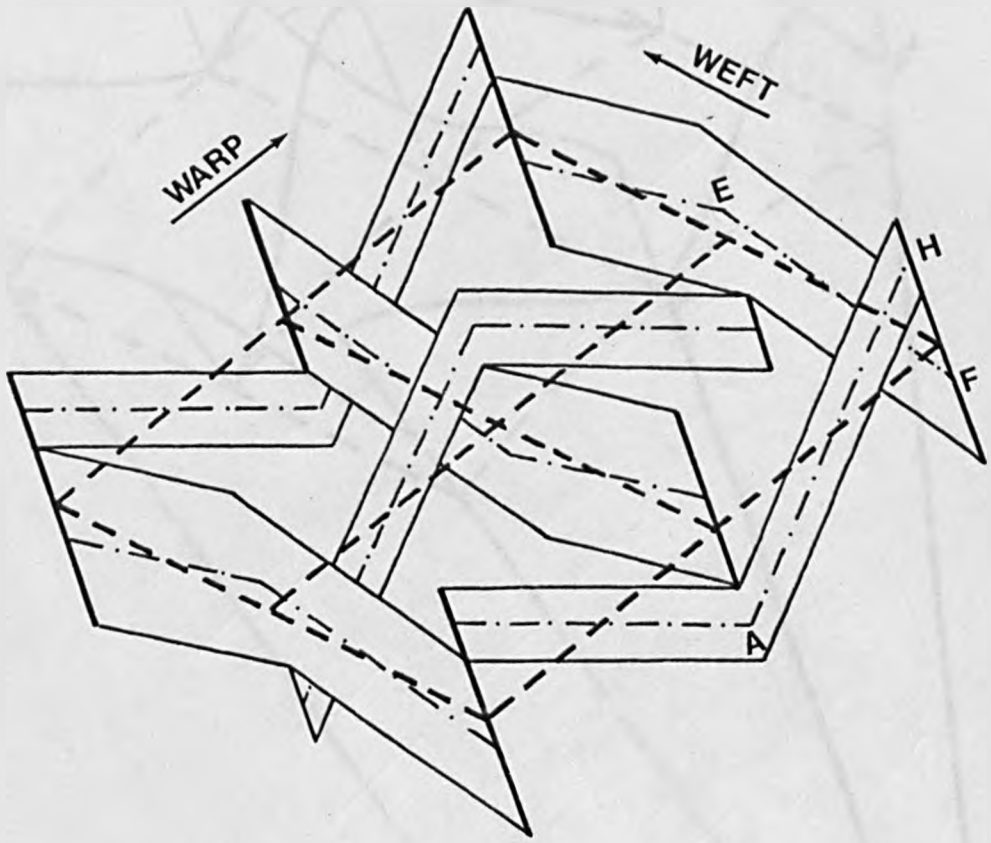

Fig. 19a

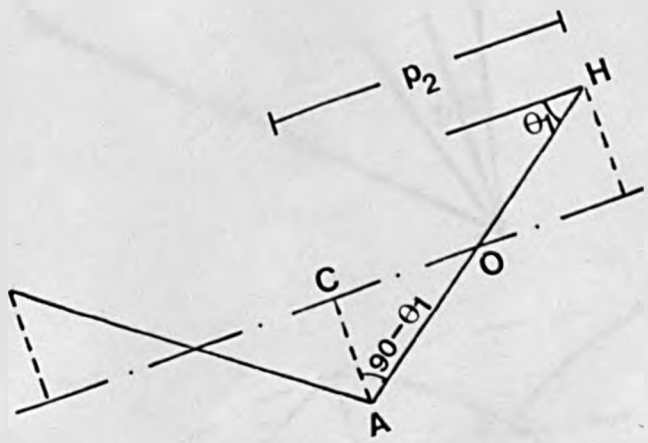

Fig. 19b

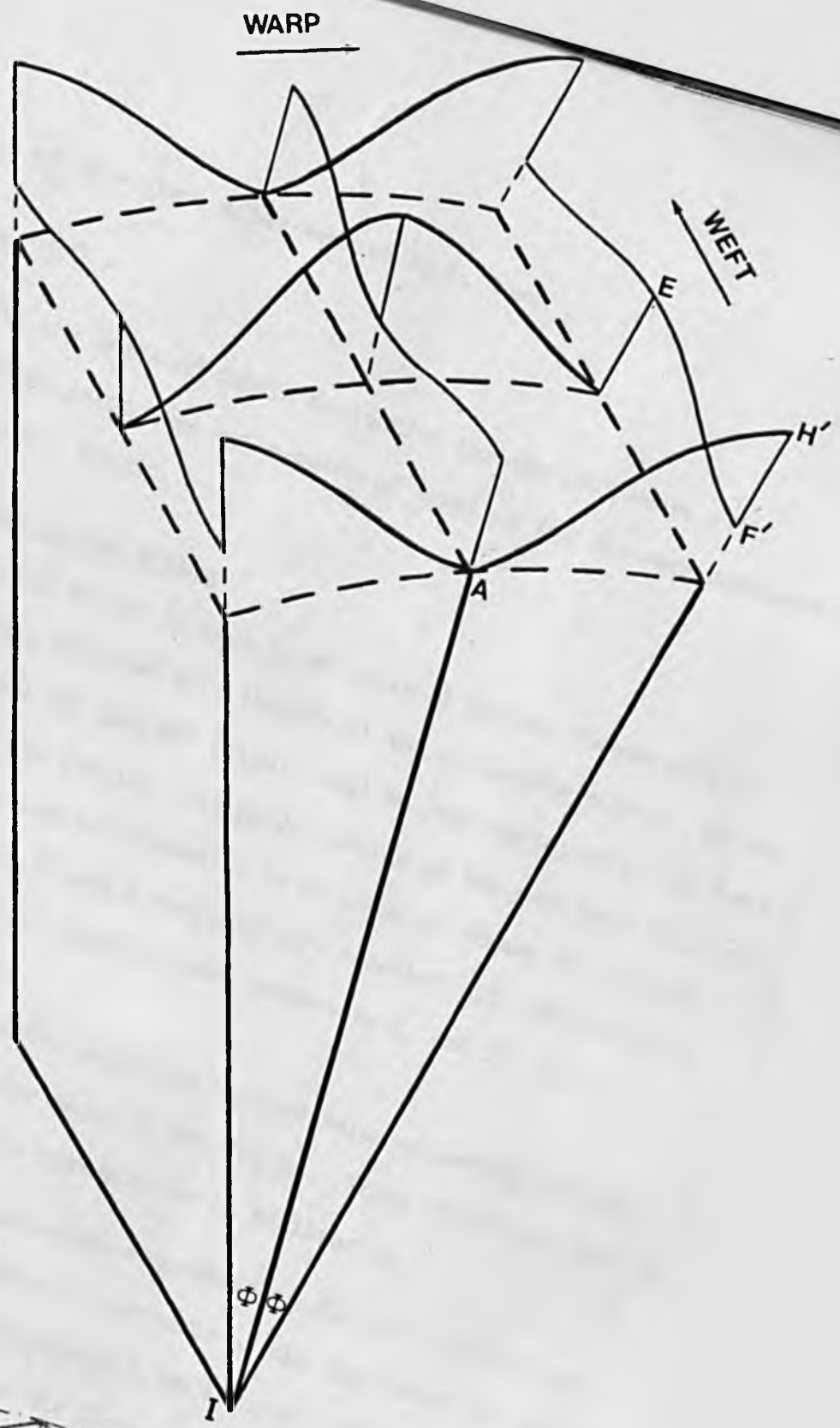

Fig. 20a

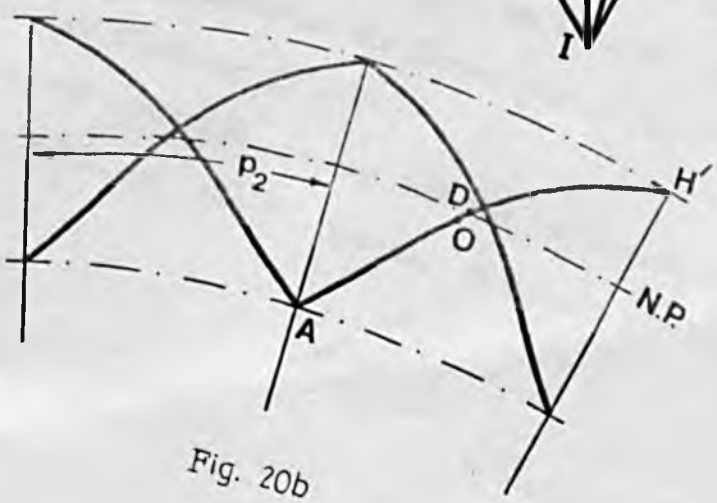

Fig. 20b

radius of this plane after bending is ρ, then

$$p_2 = \rho\Phi \ ,$$

where Φ is the angle of fabric deflection for the unit weave cell. Note that the point O is not a point of symmetry for the warp configuration in the deformed fabric.

Force analysis in the system

When the fabric is bent by an external couple, forces will be generated between warp and weft threads at the cross-over points. We may take the unit cell AH' and EF' (figure 20a) as representative of the bent configuration of the fabric. The forces acting on the warp unit AH', in the bending plane, can be assumed to be as shown in figure 21a, namely couples m_1 and m_1' at H' and A respectively, together with the forces v_1 and v_1' in the vertical direction and components f_1 and f_1' in the horizontal direction.

These forces and couples are assumed balanced, having deformed the unit warp to the shape shown in the figure. Three conditions must be satisfied in order for the system to be in equilibrium.

1. The resultant of the horizontal components of all the forces is zero.
2. The resultant of the vertical components of all the forces is zero.
3. The forces imposed by the cross yarn at A, in the radial direction AI, is of the same magnitude as the forces imposed by the cross yarn at H', in the radial direction IH'.

The last condition insures that the successive cross-yarns will be crimped by equal and opposite forces. The first two conditions give

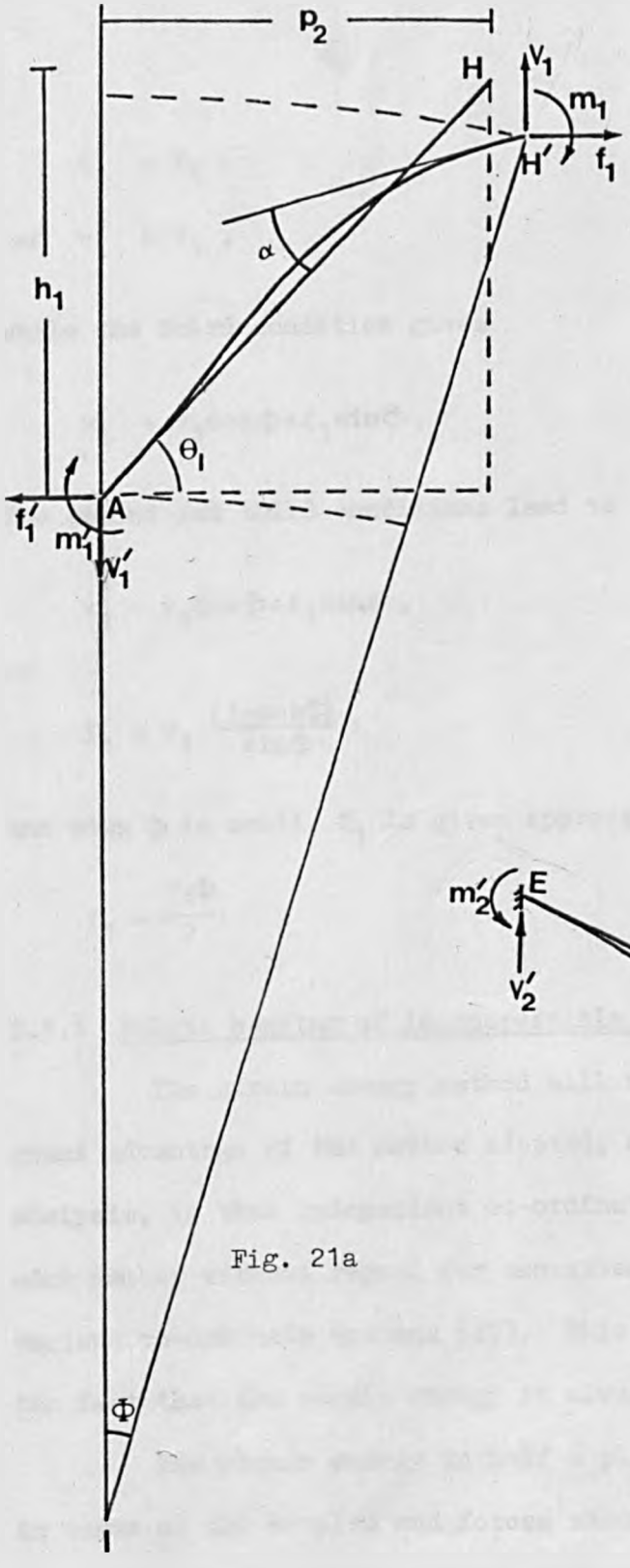

Fig. 21a

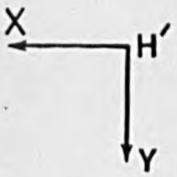

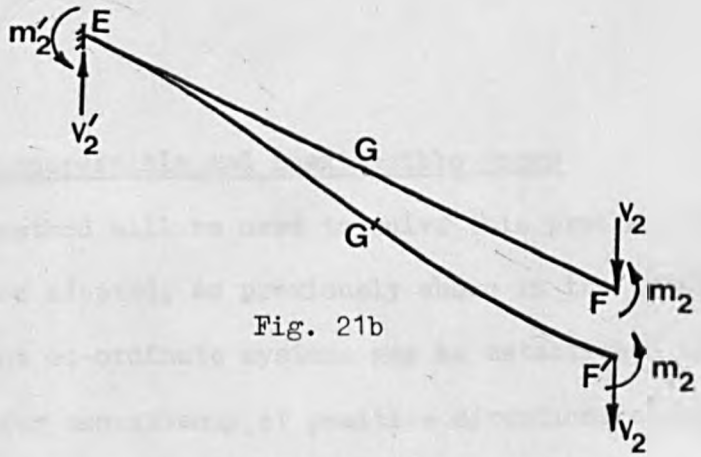

Fig. 21b

$$f_1' = f_1 ,$$

and $$v_1' = v_1 ,$$

while the third condition gives

$$v_1' = v_1\cos\Phi + f_1\sin\Phi .$$

The second and third conditions lead to

$$v_1 = v_1\cos\Phi + f_1\sin\Phi ,$$

or

$$f_1 = v_1 \frac{(1-\cos\Phi)}{\sin\Phi} ,$$

and when Φ is small, f_1 is given approximately by

$$f_1 = \frac{v_1\Phi}{2} .$$

2.3.1 Fabric bending of incompressible and inextensible yarns

The strain energy method will be used to solve this problem. A great advantage of the method adopted, as previously shown in the tensile analysis, is that independent co-ordinate systems may be established for each member without regard for consistency of positive directions of the various co-ordinate systems (47). This advantage is essentially due to the fact that the strain energy is always a positive scalar quantity.

The strain energy in half a plain weave repeat may now be calculated in terms of the couples and forces shown. When assuming inextensible and incompressible yarns, this energy will be the sum of the following terms:

(a) Bending strain energy in the warp unit AH′ (figure 21a), due to the couple m_1 and forces v_1 and f_1;

(b) Bending strain energy in the weft unit EF' (figure 21b), due to the change in its height amplitude caused by forces like v_2.

Considering the warp, referred to axes $H'X_1Y_1$ (figure 21a), the bending moment at any point $P(x_1,y_1)$ on the warp thread, a distance s_1 from H' is

$$M_1 = m_1+f_1 \cdot y_1-v_1x_1 \ .$$

Since the deformations are assumed small, the undeformed configuration may be used as a basis for the calculations instead of the unknown deformed shape.

Initially we have

$$x_1 = s_1\cos\theta_1 \qquad \text{and} \qquad y_1 = s_1\sin\theta_1.$$

Hence

$$M_1 = m_1+s_1(f_1\sin\theta_1-v_1\cos\theta_1) \ ,$$

and the strain energy, U_1, in AH' is

$$U_1 = \frac{1}{2B_1}\int_0^{\ell_1} M_1^2 ds_1$$

$$= \frac{1}{2B_1}\int_0^{\ell_1} \left[m_1+s_1(f_1\sin\theta_1-v_1\cos\theta_1)\right]^2 ds_1 \ ,$$

or

$$U_1 = \frac{1}{2B_1}\left\{\frac{\left[m_1+\ell_1(f_1\sin\theta_1-v_1\cos\theta_1)\right]^3-m_1^3}{3(f_1\sin\theta_1-v_1\cos\theta_1)}\right\}. \qquad (2.25)$$

In the weft direction, the forces acting on the unit weft yarn EF′, of length ℓ_2, are shown in figure 21b. These are the vertical forces v_2 and v_2', at E and F′ respectively, together with the couples m_2 and m_2' which balance the moment produced by v_2 and v_2' and prevent yarn rotation. Taking axes X_2Y_2 in the plane of the weft at F′, the bending moment at any point (x_2,y_2) a distance s_2 from F′ is

$$M_2 = m_2 - v_2 x_2 ,$$

and, since $x_2 \simeq s_2\cos\theta_2$ for small deformations, the bending moment is given by

$$M_2 = m_2 - v_2 s_2 \cos\theta_2 .$$

Here, the possible rotation of the plane containing the weft thread is in a direction perpendicular to the forces and couples acting on the weft, therefore this rotation will entail no change in the total elastic strain energy. Hence the strain energy in the unit weft, resulting from the change in curvature due to change in its height amplitude, is given by

$$U_2 = \frac{1}{2B_2}\int_0^{\ell_2} (v_2 s_2\cos\theta_2 - m_2)^2 ds_2$$

$$= \frac{1}{2B_2}\left[\frac{\left\{v_2\ell_2\cos\theta_2 - m_2\right\}^3 + m_2^3}{3v_2\cos\theta_2}\right]. \qquad (2.26)$$

The total bending strain energy, U, in one complete cell weave is therefore

$$U = U_1 + U_2 \ ,$$

or

$$U = \frac{1}{6B_1}\left[3m_1^2\ell_1 + 3m_1\ell_1^2(f_1\sin\theta_1 - v_1\cos\theta_1) + \ell_1^3(f_1\sin\theta_1 - v_1\cos\theta_1)^2\right]$$

$$+ \frac{1}{6B_2}\left[v_2^2\ell_2^3\cos^2\theta_2 - 3m_2v_2\ell_1^2\cos^2\theta_2 + 3m_2^2\ell_2\right] . \qquad (2.27)$$

The deformations in the system

The above expression for the strain energy was used together with Castigliano's theorem to calculate the various displacements in the system at points at which the forces are applied. The sign convention with this theorem is that the partial derivative of the energy, with respect to particular force, yields the displacement in the force direction. Accordingly, a negative value for this derivative means a displacement against the assumed force direction.

By Castigliano's theorem

$$\Delta p_2 = \frac{\partial U}{\partial f_1} \ , \quad \Delta h_1 = \frac{\partial U}{\partial v_1} \quad \text{and} \quad \alpha = \frac{\partial U}{\partial m_1} \ , \qquad (2.28)$$

also,

$$\Delta h_2 = \frac{\partial U}{\partial v_2} \quad \text{and} \quad \gamma = \frac{\partial U}{\partial m_2} \ . \qquad (2.29)$$

where Δp_2 is the change in warp spacing (as considered at the outside of the bend);

Δh_1 is the change in warp amplitude;

α is the relative angular rotation of the elastic line at H′ with respect to A (figure 21a);

Δh_2 is the change in weft amplitude;

and γ is the relative angular rotation of F′ with respect to E(figure 21b).

In the weft direction, the balance between the forces and couples acting on the unit weft cell gives $v_2=v_2'$ and $m_2=m_2'$. This means that the weft will deform symmetrically,with respect to its mid point G,as shown in figure 21b; hence the bending moment, M_2, is equal to zero at G.

The relation between m_2 and v_2 can be obtained from the above result

$$(M_2)_G = m_2-\tfrac{1}{2}v_2\ell_2\cos\theta_2 = 0 \ ,$$

or

$$m_2 = \tfrac{1}{2}v_2\ell_2\cos\theta_2 \ .$$

The relative angular rotation between F′ and E is obtained from equations (2.27)and (2.29) by

$$\Upsilon = \frac{\partial U}{\partial m_2} = \left[\frac{-\left\{v_2\ell_2\cos\theta_2-m_2\right\}^2+m_2^2}{2B_2v_2\cos\theta_2}\right] ,$$

which leads to $\Upsilon=0$ when substituting by the above value of m_2 in terms of v_2.

This, physically,means that the reaction from the warp on weft, when bending the fabric in the warp direction, may only entail changes in the weft height amplitude without any relative rotation between the ends of the weft unit cell.

We shall proceed to find the relation between m_1 and v_1 using the compatability condition of the point of contact between warp and weft.

The second condition in equation (2.28) together with equation (2.27) gives

$$\Delta h_1 = \frac{\partial U}{\partial v_1} = \frac{-3m_1\ell_1^2\cos\theta_1 - 2\ell_1^3\cos\theta_1(f_1\sin\theta_1 - v_1\cos\theta_1)}{6B_1}$$

$$= \frac{-\ell_1^2\cos\theta_1}{6B_1}\left[3m_1 + 2\ell_1(f_1\sin\theta_1 - v_1\cos\theta_1)\right].$$

The negative sign in the above equation means that the displacement of point H′(figure 21a) is against the assumed direction of the vertical reaction v_1, i.e. the system of forces and couples will produce decrimping of the warp yarn.

Similarly, the first condition in equation (2.29) together with equation (2.27) gives

$$\Delta h_2 = \frac{\partial U}{\partial v_2} = \frac{1}{6B_2}\left[2v_2\ell_2^3\cos^2\theta_2 - 3m_2\ell_2^3\cos^2\theta_2\right],$$

and since $m_2 = \frac{1}{2}v_2\ell_2\cos\theta_2$, we find

$$\Delta h_2 = \frac{v_2\ell_2^3\cos^2\theta_2}{12B_2}.$$

Note that Δh_1 is strictly the change in h_1 in a vertical direction, since v_1 is vertical. However, since Φ is small and 'ρ' large, the change of amplitude in the radial direction will, to the level of approximation being used, be equal to Δh_1. The change Δh_2 is in a radial direction, since v_2 acts radially. Thus, if the yarns are incompressible, the relation 'h_1+h_2 = constant' gives $\Delta h_1+\Delta h_2=0$; also we may put $v_2=v_1=v$ (say) and we get

$$\frac{\ell_1^2\cos\theta_1}{6B_1}\left[3m_1+2\ell_1(f_1\sin\theta_1-v\cos\theta_1)\right] = \frac{v\ell_2^3\cos^2\theta_2}{12B_2} ,$$

or

$$m_1 = \frac{vB_1\ell_2^3\cos^2\theta_2-4B_2\ell_1^3\cos\theta_1(f_1\sin\theta_1-v\cos\theta_1)}{6B_2\ell_1^2\cos\theta_1} .$$

Substituting the approximate value $f_1 = v\Phi/2$ in the equation we find

$$m_1 = v\left[\frac{B_1\ell_2^3\cos^2\theta_2-2B_2\ell_1^3\cos\theta_1(\Phi\sin\theta_1-2\cos\theta_1)}{6B_2\ell_1^2\cos\theta_1}\right]. \qquad (2.30)$$

The relative angular rotation of the elastic line at point H′ with respect to A,α, is given from equations (2.27) and (2.28) by the following expression

$$\alpha = \frac{\partial U}{\partial m_1} = \frac{6m_1\ell_1+3\ell_1^2(f_1\sin\theta_1-v_1\cos\theta_1)}{6B_1} .$$

Due to the assumption of the rigid intersections, it is apparent from figure 21a that $\alpha=\Phi$, where Φ by definition is the angular deflection of the unit fabric plane. Also since $f_1=v\Phi/2$, the above equation gives

$$\Phi = \frac{4m_1\ell_1+v\ell_1^2(\Phi\sin\theta_1-2\cos\theta_1)}{4B_1} , \qquad (2.31)$$

or

$$4B_1\Phi = 4m_1\ell_1+v\ell_1^2(\Phi\sin\theta_1-2\cos\theta_1).$$

Equations (2.30) and (2.31) can be solved for v and m_1 in terms of Φ. Thus

$$v = \frac{12\Phi B_1 B_2 \ell_1 \cos\theta_1}{2B_1\ell_2^3\cos^2\theta_2 - B_2\ell_1^3\cos\theta_1(\Phi\sin\theta_1 - 2\cos\theta_1)} ,$$

which may be approximated in the following way.

We have

$$v = \frac{6\Phi B_1 B_2 \ell_1 \cos\theta_1}{(B_2\ell_1^3\cos^2\theta_1 + B_1\ell_2^3\cos^2\theta_2)} \left[1 - \frac{\Phi B_2\ell_1^3\sin\theta_1\cos\theta_1}{2(B_2\ell_1^3\cos^2\theta_1 + B_1\ell_2^3\cos^2\theta_2)} \right]^{-1} .$$

Since Φ is assumed small, we retain only terms of order Φ and the above expression is reduced to

$$v = \frac{6\Phi B_1 B_2 \ell_1 \cos\theta_1}{(B_2\ell_1^3\cos^2\theta_1 + B_1\ell_2^3\cos^2\theta_2)} . \qquad (2.32)$$

From equations (2.30) and (2.32), m_1 in terms of Φ can be obtained:

$$m_1 = \frac{6\Phi B_1 B_2 \ell_1 \cos\theta_1}{(B_2\ell_1^3\cos^2\theta_1 + B_1\ell_2^3\cos^2\theta_2)} \left[\frac{B_1\ell_2^3\cos^2\theta_2 - 2B_2\ell_1^3\cos\theta_1(\Phi\sin\theta_1 - 2\cos\theta_1)}{6B_2\ell_1^2\cos\theta_1} \right],$$

or

$$m_1 = \frac{\Phi B_1}{\ell_1}\left[\frac{4B_2\ell_1^3\cos^2\theta_1 + B_1\ell_2^3\cos^2\theta_2}{B_2\ell_1^3\cos^2\theta_1 + B_1\ell_2^3\cos^2\theta_2} \right].$$

The strain energy in the system can now be calculated in terms of Φ. First the expression for the energy, using the relations $f_1 = v\phi/2$, $v_1 = v_2 = v$ and $m_2 = \frac{1}{2}v\ell_2\cos\theta_2$, is converted to

$$U = \frac{1}{24B_1}\left[12m_1^2\ell_1+6m_1v\ell_1^2(\Phi\sin\theta_1-2\cos\theta_1)+v^2\ell_1^3(\Phi\sin\theta_1-2\cos\theta_1)^2\right]$$

$$+\frac{v^2\ell_2^3\cos^2\theta_2}{24B_2},$$

which, upon substituting the values of v and m_1 in terms of Φ, gives

$$U = \frac{\Phi^2B_1}{2\ell_1}\left[\frac{4B_2^2\ell_1^6\cos^4\theta_1+5B_1B_2\ell_1^3\ell_2^3\cos^2\theta_1\cos^2\theta_2+B_1^2\ell_2^6\cos^4\theta_2}{(B_2\ell_1^3\cos^2\theta_1+B_1\ell_2^3\cos^2\theta_2)^2}\right]$$

$$=\frac{\Phi^2B_1}{2\ell_1}\left[1+\frac{3B_2\ell_1^3\cos^2\theta_1}{B_2\ell_1^3\cos^2\theta_1+B_1\ell_2^3\cos^2\theta_2}\right].$$

We have defined the radius of curvature of the fabric neutral plane ρ, where $\rho = p_2\Phi^{-1}$. If the external applied couple is C, then the work done to bend the single unit cell, shown in figure 21, of the fabric is

$$W.D = \tfrac{1}{2}C\Phi.$$

Also, the bending rigidity of unit width of the fabric is the sum of the interlaced yarn rigidities in this width. Therefore, the fabric warp-wise rigidity, B_W is

$$B_W = C\rho\left(\frac{1}{p_1}\right) = \frac{Cp_2}{\Phi}\left(\frac{1}{p_1}\right),$$

or

$$C = \frac{\Phi B_W}{p_2}\,p_1.$$

Therefore,

$$W.D = \frac{\Phi^2B_W}{2p_2}\,p_1.$$

Assuming the system to behave as frictionless mechanism, the external work done will be equal to the strain energy in the system. Thus

$$\frac{\Phi^2 B_w}{2p_2}\ p_1 = \frac{\Phi^2 B_1}{2\ell_1}\left[1 + \frac{3B_2\ell_1^3\cos^2\theta_1}{B_2\ell_1^3\cos^2\theta_1+B_1\ell_2^3\cos^2\theta_2}\right],$$

which gives

$$B_w = \frac{B_1 p_2}{\ell_1}\left[1 + \frac{3B_2\ell_1^3\cos^2\theta_1}{B_2\ell_1^3\cos^2\theta_1+B_1\ell_2^3\cos^2\theta_2}\right]\left(\frac{1}{p_1}\right). \qquad (2.33)$$

It is worth pointing to the result which can be obtained if the system is considered to be composed of only crimped yarns in one direction, say in the warp direction, i.e. $B_2=0$ in the above relation. This leads to

$$B_w = \frac{p_2 B_1}{\ell_1}\ \frac{1}{p_1} = \frac{B_1}{(1+c_1)}\ \frac{1}{p_1}\ ,$$

which is the same result obtained by others (41,45).

2.3.2 Inclusion of the yarn compressibility

Inclusion of the yarn compression can be achieved in the present analysis in a similar way to that used in the tensile analysis. When the fabric is bent, considering a complete repeat of the plain weave, the forces $2v_1$ and $2v_2$ are the reactions from the weft on warp and visa versa. These forces will reduce the yarn diameter and hence another term due to yarn compression is added to the energy changes inside the fabric.

The strain energy in the units AH' and EF' is then made up of:

1. The bending strain energy for warp and weft, U_B, given by

$$U_B = \frac{1}{6B_1}\left[3m_1^2\ell_1+3m_1\ell_1^2(f_1\sin\theta_1-v_1\cos\theta_1)+\ell_1^3(f_1\sin\theta_1-v_1\cos\theta_1)^2\right] + \frac{v_2^2\ell_2^2\cos^2\theta_2}{24B_2}.$$

2. The compression strain energy, U_C, given by

$$U_C = \tfrac{1}{2}\left[\frac{(2v_1)^2d_1}{\mu_1} + \frac{(2v_2)^2d_2}{\mu_2}\right]$$

$$= \frac{2v_1^2d_1}{\mu_1} + \frac{2v_2^2d_2}{\mu_2}.$$

The total strain energy, U_T, is then obtained from

$$U_T = U_B + U_C. \qquad (2.34)$$

By Castigliano's theorem

$$\frac{\partial U_T}{\partial v_1} = \Delta(h_1-d_1) \qquad \text{and} \qquad \frac{\partial U_T}{\partial v_2} = \Delta(h_2-d_2),$$

which on using equation (2.34), give

$$\Delta(h_1-d_1) = -\frac{1}{6B_1}\left[3m_1\ell_1^2\cos\theta_1+2\ell_1^3\cos\theta_1(f_1\sin\theta_1-v_1\cos\theta_1)\right] + \frac{4v_1d_1}{\mu_1},$$

and

$$\Delta(h_2-d_2) = \frac{v_2\ell_2^3\cos^2\theta_2}{12B_2} + \frac{4v_2d_2}{\mu_2}.$$

The condition which must be satisfied for the fabric deformation, assuming compressible yarns, is

$$\Delta(h_1-d_1) + \Delta(h_2-d_2) = 0.$$

Applying this condition we get

$$-\frac{1}{6B_1}\left[3m_1\ell_1^2\cos\theta_1+2\ell_1^3\cos\theta_1(f_1\sin\theta_1-v_1\cos\theta_1)\right] + \frac{4v_1d_1}{\mu_1} + \frac{v_2\ell_2^3\cos^2\theta_2}{12B_2} + \frac{4v_2d_2}{\mu_2} = 0.$$

Substituting $f_1 = \frac{v_1\Phi}{2}$ and $v_1=v_2=v$, the above relation leads to

$$m_1 = v\left[\frac{2B_2\ell_1^3\cos\theta_1(2\cos\theta_1-\Phi\sin\theta_1)+B_1\ell_2^3\cos^2\theta_2+48B_1B_2(d_1/\mu_1+d_2/\mu_2)}{6B_2\ell_1^2\cos\theta_1}\right]. \quad (2.35)$$

The angular deformation of the fabric plane, Φ, is given as before by

$$\Phi = \frac{\partial U_T}{\partial C_1} = \frac{4m_1\ell_1+v\ell_1^2(\Phi\sin\theta_1-2\cos\theta_1)}{4B_1}.$$

Hence

$$4B_1\Phi = 4m_1\ell_1+v\ell_1^2(\Phi\sin\theta_1-2\cos\theta_1). \quad (2.36)$$

Equations (2.35) and (2.36) give

$$v = \frac{\Phi(12\ B_1B_2\ell_1\cos\theta_1)}{2B_1\ell_2^3\cos^2\theta_2-B_2\ell_1^3\cos\theta_1(\Phi\sin\theta_1-2\cos\theta_1)+96B_1B_2(d_1/\mu_1+d_2/\mu_2)},$$

which can be reduced to

$$v = \frac{\Phi(6\ B_1B_2\ell_1\cos\theta_1)}{B_2\ell_1^3\cos^2\theta_1+B_1\ell_2^3\cos^2\theta_2+48B_1B_2(d_1/\mu_2+d_2/\mu_1)},$$

on neglecting Φ^2 and terms of higher order.

Substituting v in equation (2.35) and retaining only terms of order Φ gives

$$m_1 = \frac{\Phi B_1}{\ell_1}\left[\frac{4B_2\ell_1^3\cos^2\theta_1+B_1\ell_2^3\cos^2\theta_2+48B_1B_2(d_1/\mu_1+d_2/\mu_2)}{B_2\ell_1^3\cos^2\theta_1+B_1\ell_2^3\cos^2\theta_2+48B_1B_2(d_1/\mu_1+d_2/\mu_2)}\right].$$

Furthermore, following the same argument as before, the energy changes inside the fabric is equated to the work done to bend the fabric. This leads to the following expression

$$B_W = \frac{B_1\ p_2}{\ell_1}\left[1+\frac{3B_2\ell_1^3\cos^2\theta_1}{B_2\ell_1^3\cos^2\theta_1+B_1\ell_2^3\cos^2\theta_2+48(d_1/\mu_1+d_2/\mu_2)}\right]X\frac{1}{p_1}. \quad (2.37)$$

It is apparent that this expression gives lower values for the fabric rigidity, in comparison with equation (2.27) and shows the effect of yarn compression on fabric bending.

CHAPTER 3: EXPERIMENTAL WORK

CHAPTER 3

EXPERIMENTAL WORK

3.1 Planning for Experimental Work

To check the validity of the theory in Chapter 2, it was necessary to test the behaviour of a series of plain fabrics, woven and set according to predetermined specifications, under tensile and bending deformations. These experimental results were then compared with the theoretical calculations. Also, since the latter, according to the equations presented earlier, depend on the fabric construction and the constituent yarn properties it was necessary to get an accurate estimate of these parameters by a series of tests carried out on both fabrics and yarns.

The experimental part of this work can be summarized by the following sequence:

1. Weave a series of plain fabrics with different constructions.
2. 'Set' the relaxed fabric constructions.
3. Test the fabric dimensional properties.
4. Test the yarn mechanical properties.
5. Test the fabric mechanical properties.

The mechanical and dimensional properties of textiles depend on the temperature and the relative humidity under which the tests are made, and hence it was important to carry out the tests under standardized atmospheric conditions, defined (48) as $20\pm2^{\circ}C$ temperature and $65\pm2\%$ relative humidity. Samples of all materials tests were left in this atmosphere for at least 48 hours before carrying out the tests, in order

that equilibrium could be reached between temperature and humidity of the fibres inside the fabric, and the surrounding atmosphere.

3.2 Weaving the Fabrics

Planning for the experimental work included the choice of a range of different plain weave constructions. With the available range of yarn count, twist and material six fabric groups (X,Y and Z) and (A,B and C) were woven. The warp (R60/2 Tex Vincel) was common to all groups but the weft was varied according to the scheme shown in Table 3.1.

Table 3.1

Details of weft yarns used

	Weft specifications			
Fabric group	Nominal linear density (tex)	Material	Spinning method	Twist (turns/cm)
X	R60/2	Cotton	Ring	6.0
Y	R74/2	Cotton	Ring	5.2
Z	R98/2	Cotton	Open-end	4.4
A	R60/2	Vincel	Not known	4.0
B	R60/2	Cotton-vincel	Not known	4.2
C	R46/2	Cotton-vincel	Not known	7.1

Within each group, the number of ends per inch, on the loom, was kept the same while three fabrics with different numbers of picks per inch were woven. Weaving was carried out on a loom with the following specifications:

The loom is a (4x1) Multi-shuttle, automatic, Saurer Loom (Model 100W), with maximum reed space of 58 inches.

Shedding mechanism: is the Saurer positive dobby, lever type, operated by punched cards.

Let-off mechanism: is semi-positive, manually operated for tension equalization. The short term tension variation is controlled by an oscillating back rail.

Take-up mechanism: is continuous positive, and the nominal picks per inch on the loom is adjusted by a Vernier type pick scale regulator.

The reed plane was adjusted for groups X, Y and Z to give a nominal 48 ends per inch and for groups A, B and C to give 36 ends per inch. Further details about the loom timing and weave constructions are given in an appendix.

3.3 Setting the Fabrics

'Setting' is concerned with the equilibrium form which a textile material assumes. In practice this term is used to describe the stabilization of a structure in a particular form (49). The effectiveness of a fabric 'setting' treatment may be assessed by the extent to which the curvature of the yarns inside the fabric is retained when the yarn is removed from the fabric.

In the present work, because of the assumptions made in the theoretical analysis, it was necessary to obtain fabrics which were as close to 100% 'set' as possible. The finishing treatments of commercial fabrics probably satisfies this requirement, so the actual treatment used in this research was carried out as follows:

(i) Scouring at 95°C for one hour in a winch machine containing 'DTL' standard detergent and sodium carbonate (2 parts/litre each).

(ii) Two hot rinses (at 80°C), followed by one cold rinsing.

(iii) Water extraction by centrifugal hydroextractor.

(iv) Stentering, without further distortion of the fabric dimensions after hydroextraction, using a drying temperature of 110°C for one minute.

This treatment, as will be shown later, effectively 'set' the fabrics.

3.4 Testing the Fabric Dimensional Properties

3.4.1 Thread spacings

Thread spacing is one of the fabric parameters which can be relatively easily measured in several ways (50). The basic principle of most of these methods is either by counting the number of threads over a known distance normal to the thread direction or, more accurately, by precisely measuring the distance occupied by a certain number of threads. If the distance is 's' mm and the number of threads is 'n', the thread spacing, p, is given by

$$p = \frac{s}{n} \text{ mm.}$$

The method used in the present work was to count the number of threads in 5 cm wide samples, originally prepared for the fabric tensile tests, using a standard counting lens, and the average of 10 readings in each fabric direction was taken. However this method is not recommended for open fabric constructions (51) (less than 10 threads per cm). Therefore a check on the previous results was also made using a projection microscope with a magnifying power of 128.5.

For this test four samples (5x2.5 cm) of the fabric in each direction were cellotaped onto microscope slides. After adjusting the focus of the microscope and starting with a zero reading on the Vernier scale, which controls the stage movement, the sample fixed on the stage was moved normal to the threads being counted, and the number of threads was

visually observed on the screen. The distance occupied by 50 threads could then be obtained directly from the Vernier scale reading. This method gives up to 0.002 mm accuracy in measuring the thread spacings. A comparison between the results obtained by the two methods (Table A.1 in Appendix 1) gave a maximum difference of 0.015 mm (3%) in the extreme cases which suggested that most of the results obtained by the first method could be accepted with reasonable confidence.

3.4.2 Yarn modular length, crimp and degree of 'set'

The crimp, as usually defined (20), is given by the fraction $(\frac{\ell-p}{p})$. More generally, the crimp is defined as the fractional excess in length produced when straightening a crimped thread. If the crimped thread occupies a distance, S_0, inside the fabric and yields a length, S, when straightened outside the fabric, then

$$c = \frac{S-S_0}{S_0}.$$

Measuring the straightened length, S, involves applying a standard load, calculated on the basis of the yarn count (52). However the problem encountered in this measurement is that such a load is usually not enough to remove all the yarn crimp, while if a higher load is used the yarn may be stretched and still not totally eliminate the crimp. A common technique used by many researchers (16,32,42) is to obtain S by extrapolating back the load vs elongation curves of the crimped yarns from the linear stretching region of the straightened yarn, as shown by the curves in figure 22a. Such a technique relies on the following assumptions:

1. At relatively high loads, the crimp of the yarn is virtually completely eliminated and the yarn load-extension behaviour is the same as that

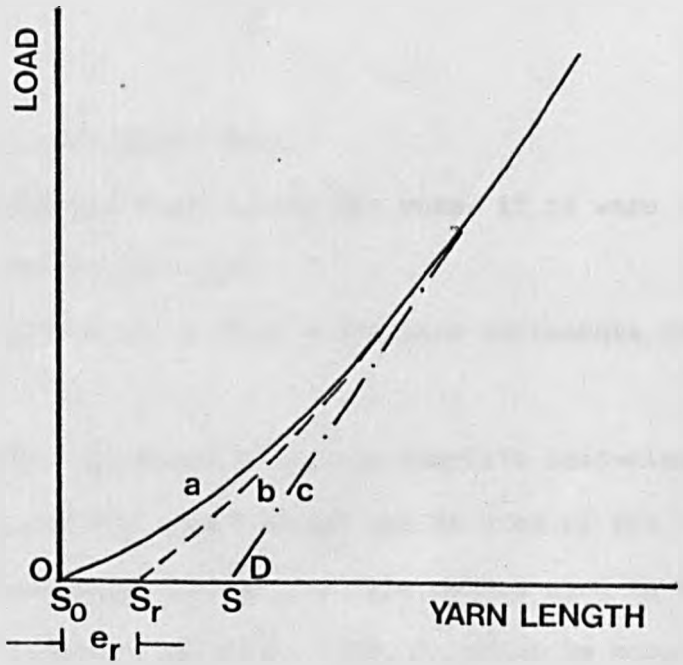

Fig. 22a shows the yarn tensile behaviour of

(a) 100% set crimped yarn
(b) partially set crimped yarn
(c) initially straight yarn of length S

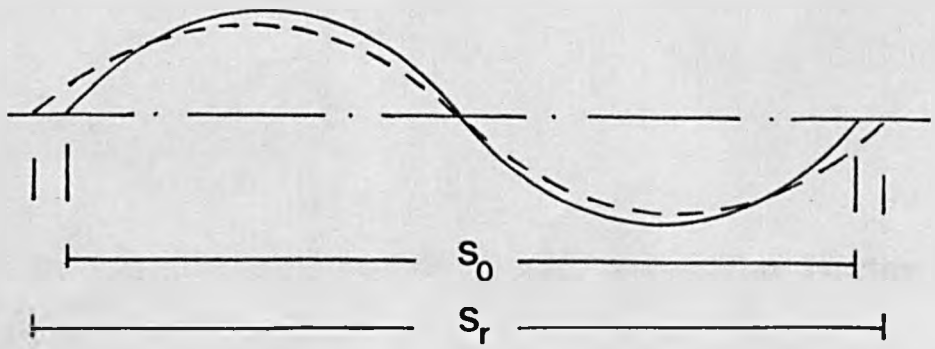

——— Crimped yarn inside the fabric

— — — Crimped yarn outside the fabric

Fig. 22b

of an initially straight yarn.

2. At these relatively high loads, the yarn, if it were initially straight, will still obey Hooke's law.

The distance OD in figure 22a then represents the excess in length $(S-S_0)$.

Actually, for simplicity, the complete load-elongation curve need not be obtained and the same concept can be used if the values at two points only of the curve are known. The method used in this work was that recommended by Grosberg and Kedia (31), in which by knowing the two straight lengths S_{30} and S_{60} corresponding to 30 and 60 g applied tension, we may write

$$\frac{S_{30}-S}{S_{60}-S} = \frac{30/\lambda}{60/\lambda} \quad ,$$

where λ is the tensile modulus of the yarn.

This gives

$$S = 2S_{30}-S_{60}.$$

Hence

$$c = \frac{(2S_{30}-S_{60}) - S_0}{S_0}.$$

Knowing the thread spacings and the crimps, the modular lengths l_1 and l_2 are given by

$$l_1 = p_2(1+c_1), \qquad \text{and} \qquad l_2 = p_1(1+c_2).$$

The apparatus used for the tests was the Shirley crimp tester, which comprises a ruler marked with a mm scale and two spring loaded clamps, one of which is mounted on a pivoted lever thus enabling the

required tension to be applied. The other clamp is mounted on a wooden block that can slide along the ruler. The test is carried out by adjusting the required tension through a sliding weight on the pivoted lever; the yarn is then mounted and the sliding clamp is moved along the ruler untilthe zero, indicated by a pointer fixed on the pivoted lever, is reached. The straight length is read directly on the ruler scale.

To take samples, the fabric was laid flat, free from tension and creases and accurately measured (25x2.5 cm) flaps along the direction of the yarns to be tested were prepared. The yarns of 25 cm crimped length were then frayed out of the fabric by means of a dissecting needle, starting from the middle. Each yarn when taken out was held firmly to prevent loss in twist, and both ends placed in the clamps of the crimp tester. The average of 30 readings taken in groups from different places in the fabric represents the final crimp value.

As the previous theoretical analysis applies mainly to completely 'set' fabrics,it was necessary to assess this parameter experimentally. This was achieved by defining the crimp values of the yarn both in the fabric, c, and in the released state, c_r, and the degree of set is then obtained by applying the relation

$$\text{'set'} = (c_r/c)^{\frac{1}{2}} .$$

The actual load-extension curve differs in the case of sompletely 'set' crimped yarn from that of a partially 'set' crimped yarn,as shown in figure 22a, and in the latter case an increase in length, e_r, is expected when the yarn is removed from the fabric. This is due to the yarn decrimping in the released state.

If the crimped length of the yarn in the released state is S_r, see figure 22b, then

$$c_r = \frac{S-S_r}{S_r} \qquad \text{where} \qquad S_r = S_0+e_r \ ,$$

and

$$\text{'set'} = \left[\left(\frac{S-S_r}{S_r}\right)/\left(\frac{S-S_0}{S_0}\right)\right]^{\frac{1}{2}} \ .$$

In order to determine 'set', 10 yarn samples were frayed out of specimens (30x2.5 cm) prepared as mentioned above. Before the yarns were removed, ink marks were made to indicate a 25 cm length of the yarns along the fabric. The yarns were then removed to the Instron tensile tester, previously set to a 25 cm gauge length. In removing the yarns and in subsequent handling great care was taken not to disturb the crimp and for this purpose it was necessary to cut the fringes protruding from the specimen after every one or two yarns had been removed. The Instron crosshead was then driven at a rate of 8% extension per minute and the load-elongation curves were obtained up to a maximum load of 200 g. The final calculated results showed that most of the fabrics were over 90% set.

Using this method, it was also possible to estimate the values of c, adopting the same principle of extrapolation previously described. A comparative study (Table A2 in Appendix 1) of the values of c obtained using the Shirley tester and the Instron showed that the first method yields lower values in most cases, which may perhaps be attributable to the higher rate of increasing the tension on the yarns that was applied with the Shirley tester method.

3.4.3 Yarn cross-section, estimated thickness and contact length

Inclusion of the yarn compressional effects in the theoretical analysis necessitates an estimation of the yarn cross-sectional shape, thickness and contact length inside the fabric to be made. In fact, the estimation of these quantities needs a variety of data and assumptions about the following:

1. The type of loads applied to the yarns and their distribution during fabric formation; also the forces produced by the possible swelling of the yarns when they are treated for relaxation.
2. The yarn behaviour under compressive forces and its behaviour when recovering from stresses.

In addition, the use of plied yarns in the present research imposes an additional difficulty about the estimation of an equivalent diameter.

In this work, the following assumptions were made.

1. An "equivalent singles" to the plied yarn is defined such that its volume is equal to that of the combined singles. Then, if 'd_s' is the diameter of the singles yarns and 'd' the diameter of the "equivalent singles", as shown in figure 23a, we have

$$\frac{\pi d^2}{4} = 2\left(\frac{\pi d_s^2}{4}\right) ,$$

if it is assumed that the yarn length is unchanged.

i.e. $d = 2^{\frac{1}{2}} d_s$.

The factor $2^{\frac{1}{2}}$ can be regarded as corresponding to the empirical factors given by Wira (53) for woollen and worsted yarns (1.6 for worsteds).

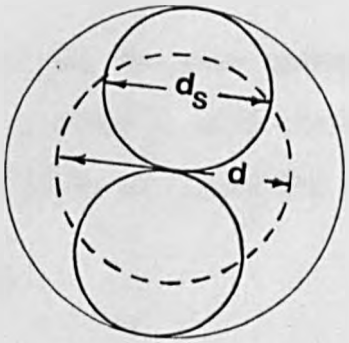

Fig. 23a

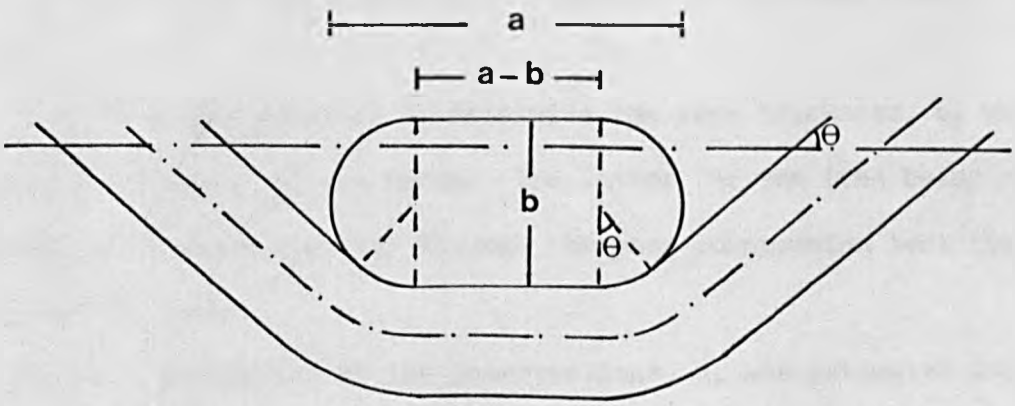

Fig. 23b

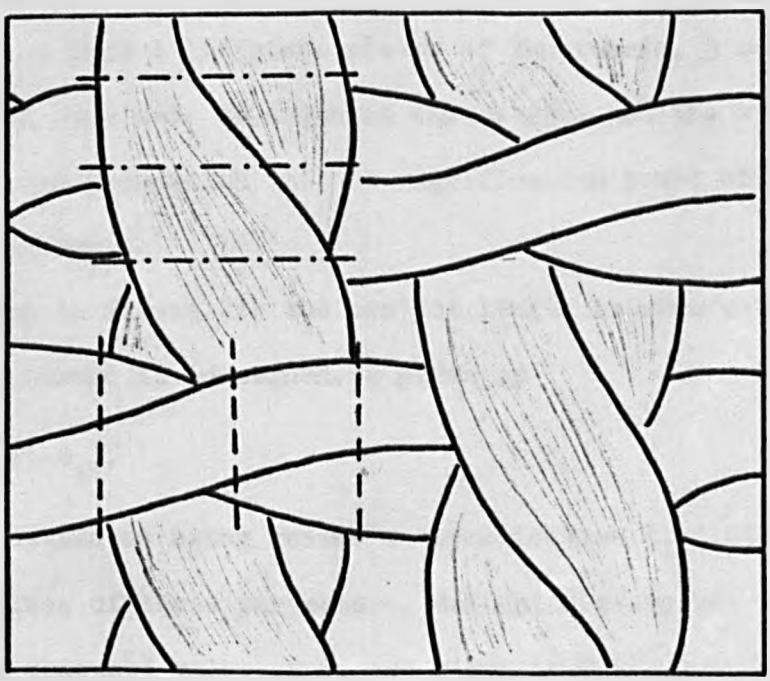

Fig. 23c

2. Due to the successive processes the yarn undergoes, its equivalent singles cross-section of diameter d, will distort at constant volume to the 'Race-track' shape shown in figure 23b. This leads to

$$b(a-b) + (\pi b^2/4) = \pi d^2/4 \ ,$$

or

$$b = 2.33\left\{a-(a^2-1.3484d_s^2)^{\frac{1}{2}}\right\} \ , \qquad (3.1)$$

where a and b are the major and minor diameters of the yarn cross-section.

It is thus now possible to determine the yarn thickness, b, when the quantities 'a' and 'd_s' are known. The latter for the time being can be considered as a known quantity through the yarn compression test that will be explained later.

The yarn projection at the intersections, a, was estimated using a projection microscope and the test was carried out for each fabric in both warp and weft directions. The unevenness of the yarns and their hairiness necessitates a large number of readings to be made. At 100 intersections taken from 4 different places of the fabric, 3 readings at every intersection were made as shown in figure 23c, and the average of these represents the projection 'a'. A magnification power of 128.5 was used on the microscope.

According to figure 23b the contact length between warp and weft, so far as a warp thread is concerned, is given by

$$\ell_{c1} = a_2-b_2(1-\theta_1), \qquad (3.2)$$

where θ_1 may be estimated using Peirce's approximation $\theta_1=1.85\sqrt{c_1}$. The numerical values of these parameters, estimated using the above equations, and a measured value of d, are given in Table 3.2.

Table 3.2

Yarn projection, estimated thickness and contact length

Fabric group	Fabric No.	Warp				Weft			
		d_1(mm)	a_1(mm)	b_1(mm)	ℓ_{c1}(mm)	d_2(mm)	a_2(mm)	b_2(mm)	ℓ_{c2}(mm)
X	1	0.321	0.439	0.204	0.518	0.398	0.564	0.242	0.327
	2	0.321	0.446	0.200	0.502	0.398	0.539	0.256	0.333
	3	0.321	0.430	0.209	0.493	0.398	0.552	0.249	0.304
Y	1	0.321	0.443	0.202	0.531	0.431	0.591	0.275	0.323
	2	0.321	0.462	0.191	0.519	0.431	0.580	0.281	0.348
	3	0.321	0.439	0.204	0.498	0.431	0.574	0.285	0.307
Z	1	0.321	0.450	0.198	0.566	0.479	0.613	0.332	0.314
	2	0.321	0.473	0.186	0.533	0.479	0.582	0.356	0.343
	3	0.321	0.452	0.197	0.586	0.479	0.625	0.324	0.326
A	1	0.321	0.460	0.193	0.376	0.321	0.416	0.219	0.354
	2	0.321	0.445	0.201	0.329	0.321	0.417	0.219	0.326
	3	0.321	0.452	0.198	0.380	0.321	0.443	0.203	0.382
B	1	0.321	0.439	0.205	0.406	0.387	0.518	0.254	0.365
	2	0.321	0.450	0.199	0.450	0.387	0.530	0.247	0.336
	3	0.321	0.445	0.201	0.441	0.387	0.540	0.241	0.328
C	1	0.321	0.437	0.206	0.311	0.299	0.396	0.199	0.347
	2	0.321	0.440	0.204	0.367	0.299	0.435	0.177	0.360
	3	0.321	0.431	0.210	0.295	0.299	0.380	0.210	0.320

$$d_1 = \frac{\text{plied yarn thickness}}{\sqrt{2}} = \sqrt{2}\, d_{s1}$$

3.5 Testing the Yarn Mechanical Properties

3.5.1 Yarn bending properties

The flexural rigidity of yarn has often been estimated by quasi-static beam (54) or loop measurements (36). However such methods do not provide sufficient information about the yarn bending characteristics. A more efficient technique (55) using samples of parallel yarns, which provides a complete bending hysteresis curve, was therefore used in this work. The apparatus used was the Shirley cyclic bending tester, originally designed for fabric tests, which is based on a principle suggested by Livesey and Owen (41).

The main idea described by the above authors is to apply an almost uniformly distributed couple along a small fabric specimen (2.5x0.5 cm) which is then taken through a pure bending cycle. Their apparatus is shown diagrammatically in figure 24a where the uniformity of couple through the specimen, AB, is achieved by using an extremely light aluminium tubing for the pointer BP and placing the weight 'p' at the end of this pointer so as to give a centre of gravity as far as possible from the sample. Under these conditions, the bending moment through out the sample is sufficiently constant for most practical purposes and its average value is taken as the moment at the sample centre point.

Both D and E in figure 24a represent circular scales calibrated in degrees. If at any position the rotatable clamp at A and the pointer make angles α and β with the vertical datum as shown in the figure, both the curvature, K, and couple per cm width, M, can be found from the relations

$$K = \frac{1}{\rho} = \frac{\alpha-\beta}{5} \qquad mm^{-1} \ ,$$

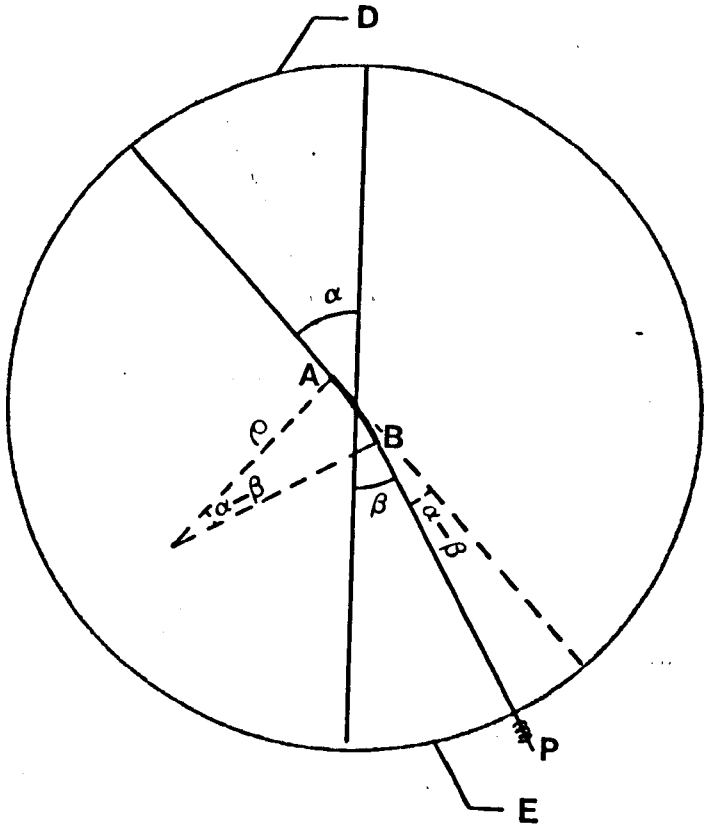

Fig. 24a

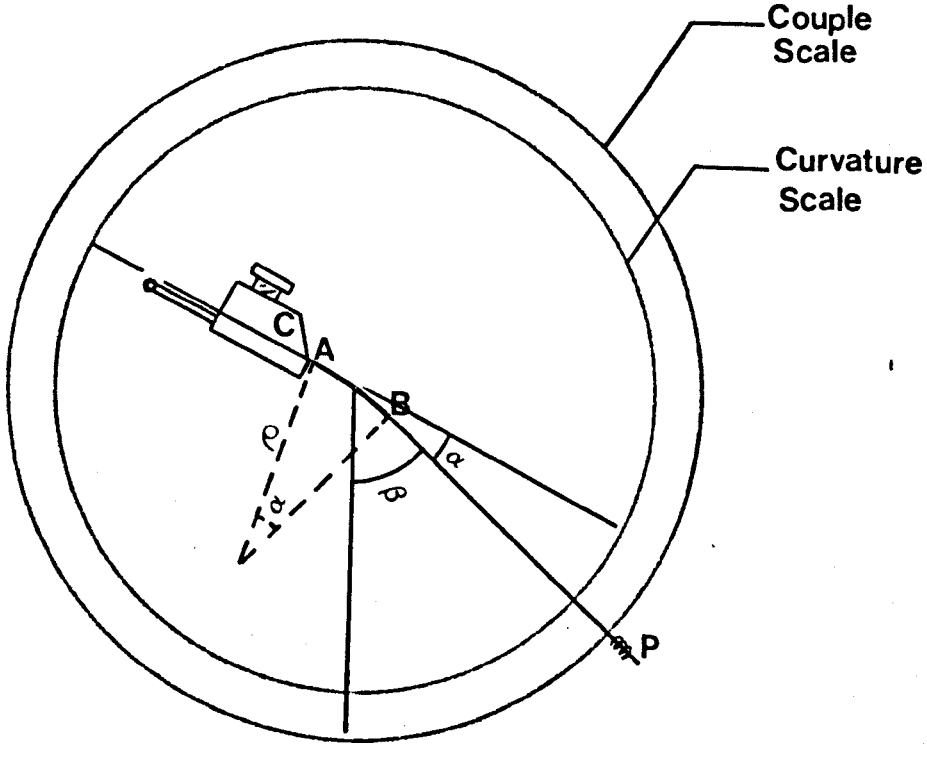

Fig. 24b

and

$$M = \frac{Wx9.81}{2.5} (L + 2.5) \sin\beta \quad (mN.mm/cm), \qquad (3.3)$$

where

ρ = the sample radius of curvature (mm),

W = the pointer weight (g),

and

L = the distance between the pointer centre of gravity to the edge of the sample (mm).

Due to the fact that at higher values of $(\alpha-\beta)$ the sample does not pass through the centre of rotation, the best estimate of the bending moment in the curvature range (± 0.3 mm^{-1}) is in fact given by

$$M = \frac{Wx9.81}{2.5} (L + 3.5) \sin\beta .$$

The Shirley tester, shown in figure 24b, differs slightly from the above arrangement in order to simplify taking readings for both the couple and curvature. AB represents the fabric specimen held at one end in a rotatable clamp C and the weighted pendulum BP is attached at the other end. The instrument has two scales, an inner one for curvature and an outer one for couple, with a mirror zone between them which enables parallax errors to be eliminated. The readings are then taken from the pendulum to each of the two scales.

The inner curvature scale rotates with the clamp, making the pendulum deflection proportional to the specimen curvature. The outer couple scale indicates the sine of the angle of the pendulum deflection, β, from the vertical position to which the couple is proportional. While the curvature is read directly, the corresponding couple per unit specimen

width is calculated from the expression

$$M = \text{calibration factor} \times \sin\beta ,$$

where

$$\text{Calibration factor} = \frac{Wx9.81}{2.5}(L + 3.5) \quad \text{mN.mm/cm} ,$$

and is given with the specific pendulum in use.

Sample preparation

To ensure that the tested yarns were fairly representative of those in the fabric, the following procedure was used. On the loom, after weaving each fabric group, several reed dents were emptied of warp threads so that straight weft threads were inserted in these sections during the ordinary weaving process. In the succeeding processes of finishing, these yarns received the same treatment as the fabric. This procedure also ensured that an equal average tension is imposed on the parallel yarns, the value of which is the same as the weaving tension. Control of the number of threads per cm was achieved by altering the rate of take-up on the loom.

These sections of parallel yarns, shown in figure 25a, were cut into specimens of the standard width (2.5 cm) to be tested on the bending apparatus. Cutting the specimens to a specified standard length was immaterial since a simple mounting jig, shown in figure 25c, was used later to adjust the specimen in its precise location on the apparatus, and to set its free length between the pointer grip and the edge of the rotatable clamp to 0.5 cm.

The specimen is shown in figure 25b where a narrow band of cellotape is shown covering the yarns on both sides at one end in order to ease their entry in the pendulum grip.

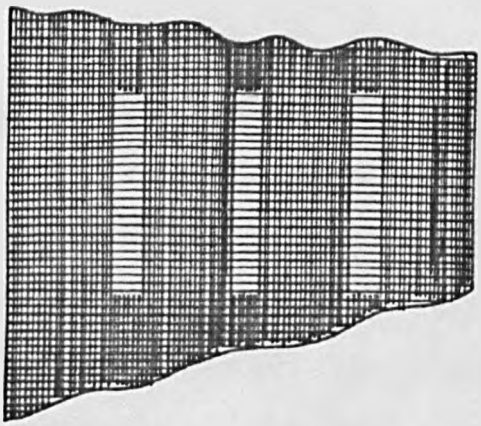

Fig. 25a

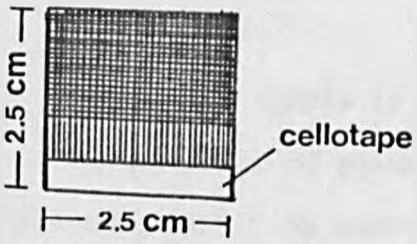

Fig. 25b

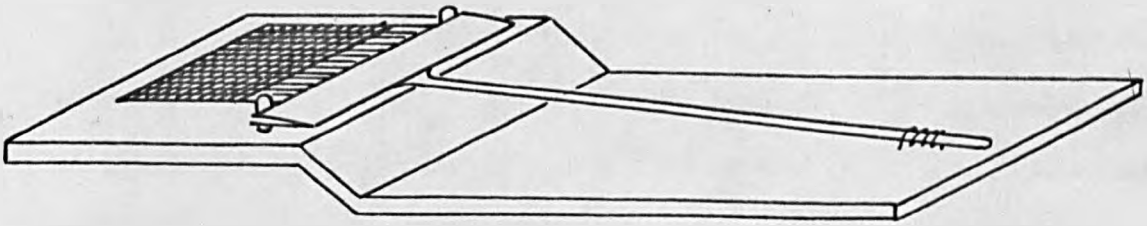

Fig. 25c

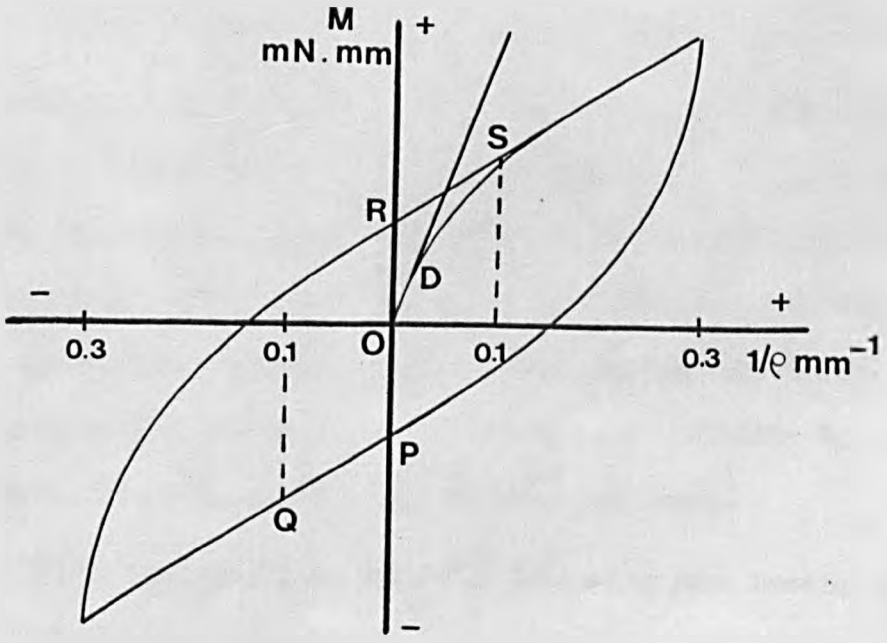

Fig. 25d

Testing procedure

For each type of yarn 8 specimens were tested. The sample is attached first to a pointer, chosen (see later) from the range of pointers provided, then mounted in the rotatable clamp with the aid of the mounting jig. The clamp with the jig plate carrying the specimen and pointer was rotated from the mounting position to the zero position, which is reached when the pointer is hanging vertically, pointing to zero on both the curvature and the couple scales. The jig is then removed and the test started.

The clamp is rotated automatically in an anti-clockwise direction so as to exert a positive couple on the specimen. The apparatus is stopped at intervals and the readings are recorded according to the procedure suggested by Livesey and Owen (39). This procedure is repeated to produce cyclic testing ($0 \rightarrow 0.3\ mm^{-1} \rightarrow -0.3\ mm^{-1} \rightarrow 0.3\ mm^{-1}$) and usually a relatively large number of readings is taken in the initial region (0 to $0.1\ mm^{-1}$) to precisely determine the initial bending behaviour.

Throughout the tests, the following precautions are essential:

1. At maximum curvatures ($\pm 0.3\ mm^{-1}$), the readings on the couple scale should be in the range of $0.4 < |\sin\theta| < 1.0$ (56). This is achieved by selecting the proper pointer with respect to the yarn stiffness.
2. The bending behaviour may differ according to the specimen mounting, face up or down, therefore half of the samples were tested starting with the face up and the rest with the face down. Finally for each tested specimen, the couple-curvature diagram was drawn.

Referring to figure 25d, the following yarn bending properties were calculated:

1. The initial flexural rigidity, B*, which is the slope of the initial part, OB, of the hysteresis loop (up to 0.02 mm^{-1}).
2. The low-curvature elastic flexural rigidity (57), B, which is the mean slope of the loop between curvatures 0 and 0.1 mm^{-1} (i.e., the mean value of the slopes PQ and RS in figure 25d).
3. The coercive couple, M_0, which is the frictional component of the initial bending resistance and is half the width of the hysteresis loop at zero curvature (i.e. the mean of PO and RO in figure 25d).

The average values of B*, B and M_0 are given in Table 3.3, while figures 26 and 27 show the curves obtained for the yarns used.

Rate of yarn bending

In spite of the fact that the test readings were taken intermittently, the total time of the test can give a reasonable estimate of the rate of yarn bending in (mm^{-1}/min). Because the deformations in textile materials are time dependent, the ideal would be to test the yarns in bending under the same rate that is expected to take place in fabric deformations.

In the fabric initial bending analysis it has been shown that the angle of deflection of the yarns can be considered as the same as that of the fabric. To estimate, roughly, the rate of yarn bending in a fabric tensile test we may follow the geometry assumed by Wilson (28) of a twin arc thread model and use his assumption that the yarn shape after deformation will still retain a twin arc shape.

Such configurations, as shown in figure 28, give the following relations:

$$p = 2\sin\theta/K \quad \text{and} \quad \theta = \ell K/2 ,$$

where $K = 1/\rho$ is the yarn curvature.

Table 3.3

Bending properties of the yarns used

No.	Yarn 'Tex' and material	B* ($mN.mm^2$)	B ($mN.mm^2$)	M_0 (mN.mm)
1	R 60/2 cotton	11.72	6.06	0.50
2	R 74/2 cotton	14.11	7.05	0.61
3	R 98/2 cotton	18.91	8.16	0.79
4	R 60/2 vincel	10.2	5.62	0.28
5	R 60/2 vincel	8.67	4.44	0.26
6	R 60/2 cotton-vincel	8.74	4.25	0.33
7	R 46/2 cotton-vincel	5.33	2.96	0.19

Note: Yarn 4 is used as warp for fabric groups X,Y and Z. Yarn 5 is used as warp for groups A,B and C and as weft for group A.

B* denotes the initial flexural rigidity at the first part of the hysteresis curve.

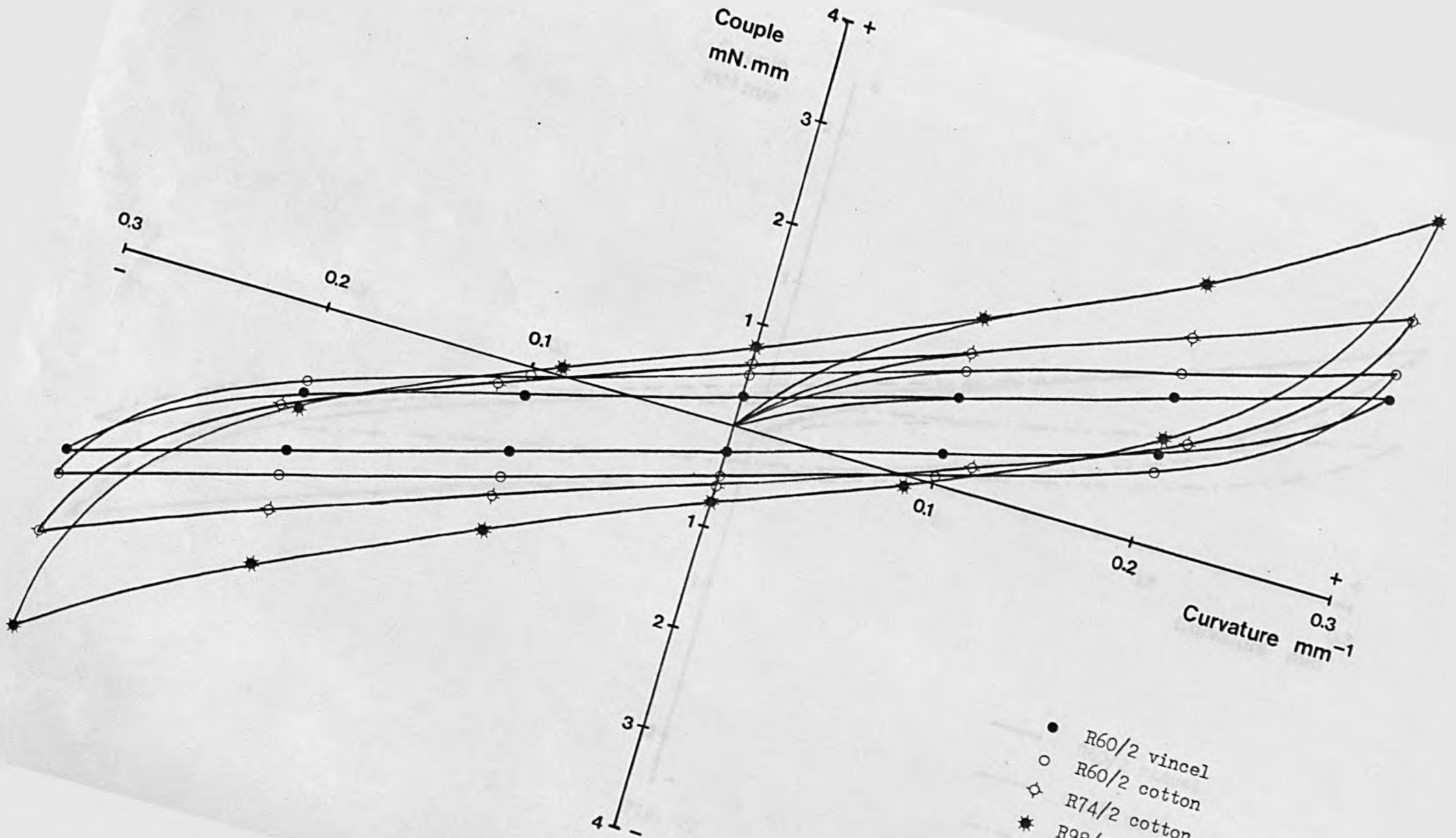
Couple
mN.mm
4
+
3
2
1
0.3
0.2
0.1
0.1
0.2
0.3
+
Curvature mm⁻¹
1
2
3
4
R60/2 vincel
R60/2 cotton
R74/2 cotton
R98/2 cotton

Fig. 26

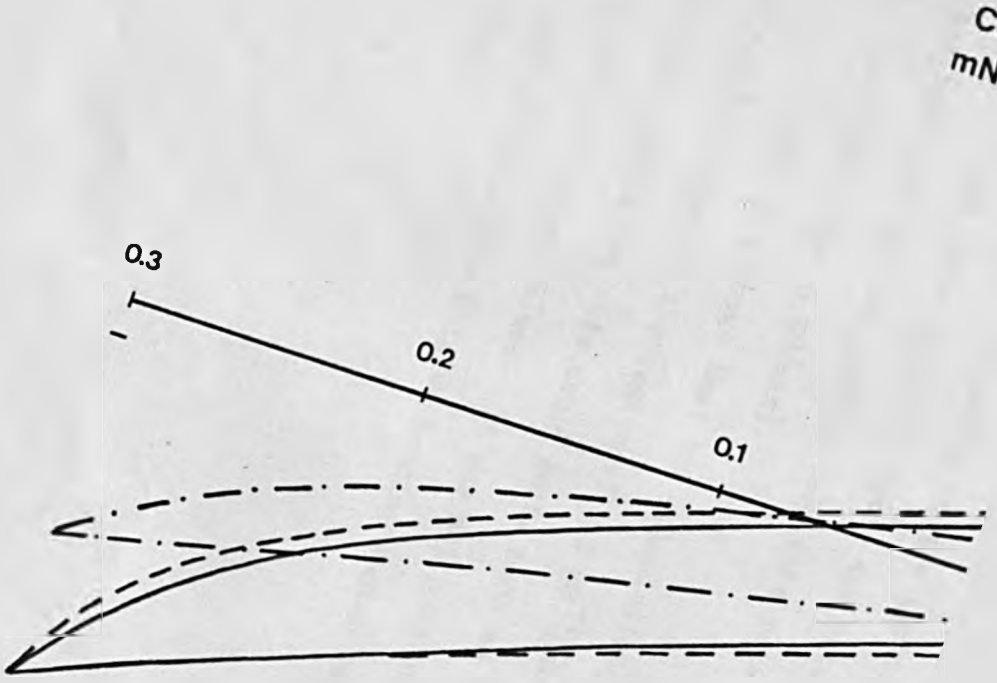
Couple
mN mm
0.3
0.2
0.1

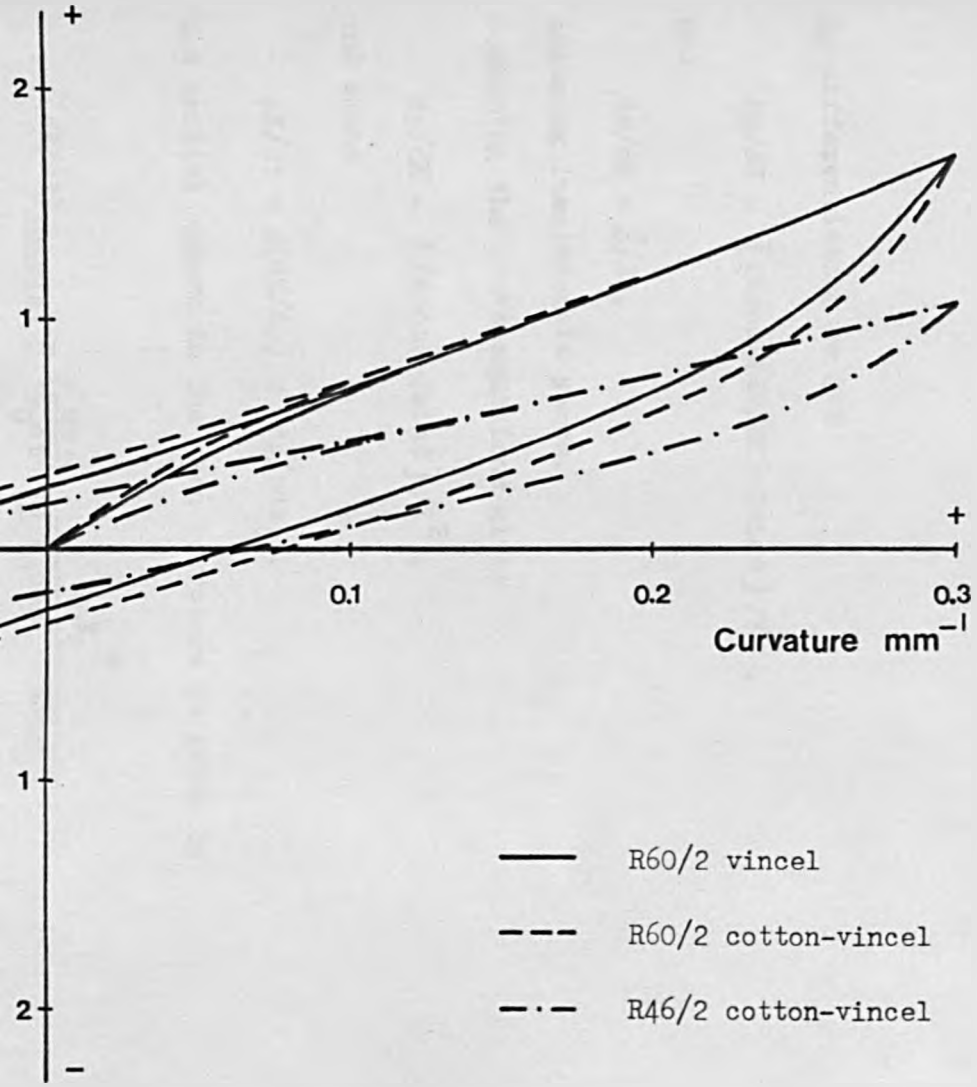
+
2
1
+
0.1
0.2
0.3
Curvature mm^{-1}
1
2
−
R60/2 vincel
R60/2 cotton-vincel
R46/2 cotton-vincel

Fig. 27

By differentiating we get

$$dp/dK = [2K\cos\theta(d\theta/dK)-2\sin\theta]/K^2 ,$$

and

$$d\theta/dK = \ell/2 ,$$

assuming inextensible yarns.

Combining the above equations gives

$$dp/dK = [\ell K\cos\theta-2\sin\theta]/K^2 ,$$

and since

$$dK/dt = p(dK/dp) \times (dp/pdt) ,$$

the initial change in the yarn curvature is given by

$$(dK/dt)_{initial} = \left(\frac{dp}{p_0 dt}\right) \frac{p_0 K_0^2}{\ell_0 K_0 \cos\theta_0 - 2\sin\theta_0} ,$$

where the suffix '0' refers to the initial parameters of the yarn shape.

The term $(dp/p_0 dt)$ gives the rate of extension per unit time which has been used in the tensile test (the rate used in our experiments, as will be seen later, was 0.08/min).

Table 3.4 shows that the calculations of the rate of yarn bending (mm^{-1}/min) is then in the region of 0.5 mm^{-1}/min. for fabrics with higher crimp values while the rate could be as much as 3 times this for the fabrics with low crimp values. It was not possible to measure the yarn bending properties on the Shirley bending tester with rates higher than 0.5 mm^{-1}/min.

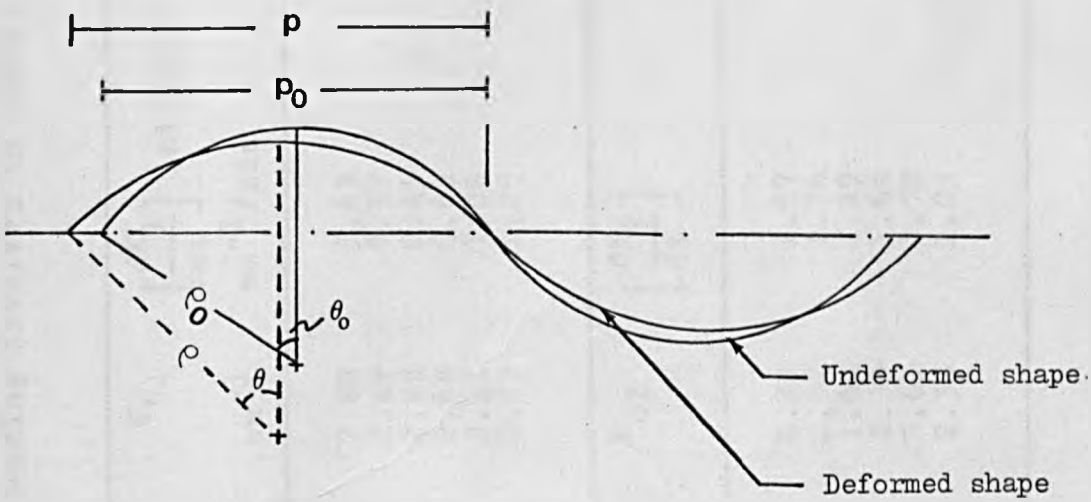

Fig. 28

Table 3.4

Theoretical rate of yarn bending involved in fabric extension

Fabric	p_{02} mm	l_{01} mm	c_1	θ_{01} radians	K_{01} mm^{-1}	$\left[\frac{dK_1}{dt}\right]$ initial mm^{-1}/min	$\left[p_{02}\frac{dK_1}{dp_2}\right]$ initial mm^{-1} per unit extension
X-1 warp	0.588	0.700	0.1916	1.01	2.89	0.63	7.88
Y-1 warp	0.677	0.798	0.1787	0.99	2.49	0.57	7.06
Z-1 warp	0.779	0.939	0.2065	1.06	2.25	0.45	5.62
A-1 warp	0.589	0.704	0.1951	1.01	2.88	0.62	7.81
B-1 warp	0.548	0.598	0.0920	0.72	2.41	1.08	13.45
C-1 warp	0.465	0.509	0.0951	0.73	2.87	1.25	15.62
	p_{01}	l_{02}	c_2	θ_{02}	K_{02}	$\left[\frac{dK_2}{dt}\right]$	$\left[p_{01}\frac{dK_2}{dp_1}\right]$ initial
X-1 weft	0.485	0.514	0.0594	0.59	2.28	1.57	19.57
Y-1 weft	0.490	0.514	0.0480	0.52	2.04	1.76	22.05
Z-1 weft	0.494	0.508	0.0285	0.41	1.62	2.29	28.57
A-1 weft	0.494	0.504	0.0587	0.58	2.31	1.66	20.75
B-1 weft	0.476	0.623	0.1189	0.81	2.61	0.78	9.10
C-1 weft	0.568	0.621	0.0934	0.72	2.33	1.03	12.89

3.5.2 Yarn tensile properties

The yarn tensile behaviour was obtained using the Instron tensile tester. The yarn was initially treated in a way which was similar to that applied to the fabrics. For this purpose continuous lengths of the yarn were prepared in the form of hanks, then soaked for one hour in a hot water bath (95°C) which contained the same chemicals that were used in the process of fabric finishing. The hanks were then left to dry in the conditioned atmosphere. For each type of yarn, 10 samples of 25 cm length were tested on the Instron using a rate of 0.08 extension/min. The behaviour of all the yarns used is shown in figures 29 and 30 where the slope of the tangent at the initial part of the tensile curve was taken to represent the initial yarn tensile modulus.

It may be worth noting that the vincel and the cotton-vincel yarns gave comparatively high load-extension behaviour, which may be expected since vincel is, in fact, a high tenacity regenerated cellulose fibre.

3.5.3 Yarn compressional properties

The apparatus used to measure the yarn compressional properties was designed by Oxtoby (58) and is based on an optical principle originally employed by Anderson and Settle (59).

General description of Oxtoby's apparatus

A general view of the apparatus is shown in figure 31a. The idea, shown in figure 31b, was to apply a compressive load on the yarn through a load lever (A), the yarn being situated between two parallel plates, the upper being fixed to the load lever and the lower to the solid base of the apparatus. By means of an optical arrangement (B,C and D), the vertical distortion of the yarn is shown, magnified, on a screen (E) where the

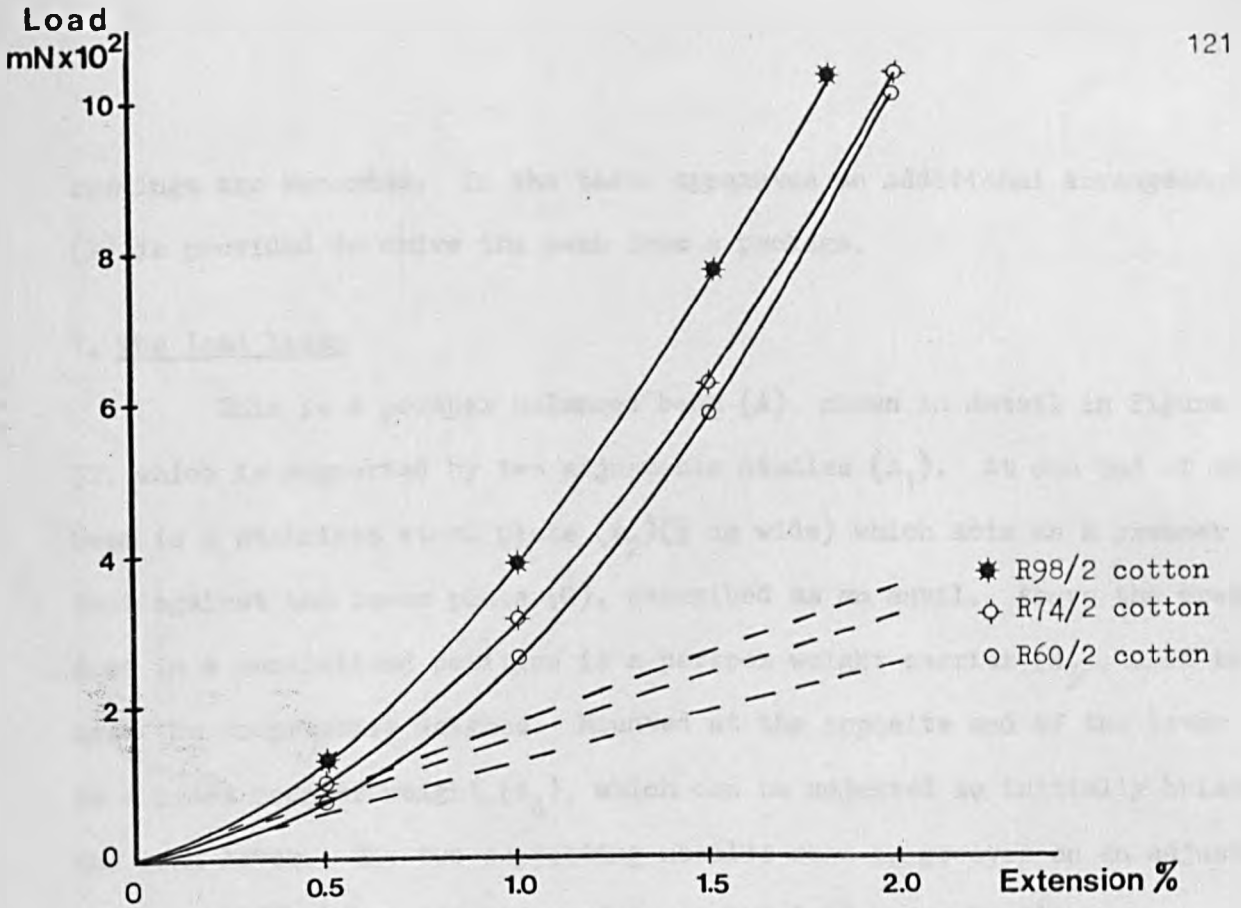
Load
mNx10²
10
8
6
4
2
0
0
0.5
1.0
1.5
2.0
Extension %
R98/2 cotton
R74/2 cotton
R60/2 cotton

Fig. 29

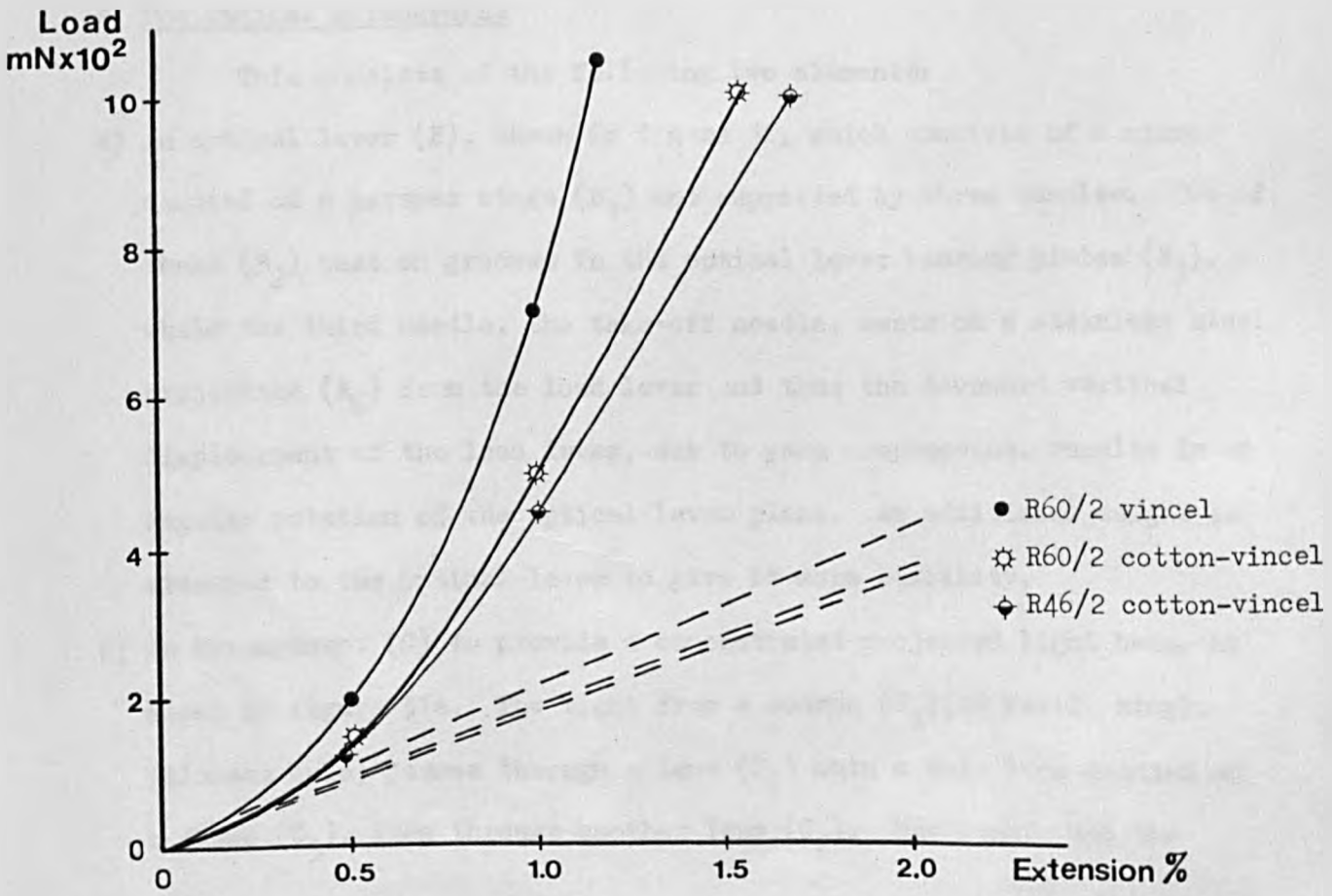
Load
mNx10²
10
8
6
4
2
0
0
0.5
1.0
1.5
2.0
Extension %
R60/2 vincel
R60/2 cotton-vincel
R46/2 cotton-vincel

Fig. 30

readings are recorded. In the basic apparatus an additional arrangement (F) is provided to drive the yarn from a package.

1. The load lever

This is a perspex balanced beam (A), shown in detail in figure 32, which is supported by two adjustable needles (A_1). At one end of the beam is a stainless steel plate (A_2)($\frac{1}{2}$ cm wide) which acts as a presser foot against the lower plate (G), described as an anvil. Above the presser foot in a centralized position is a perspex weight carrier (A_3), used to hold the compressive weights. Mounted at the opposite end of the lever is a brass counter weight (A_4), which can be adjusted to initially balance the load lever. The two supporting needles rest in grooves on an adjustable brass plate (A_5) and are referred to as the load lever bearings.

2. The optical arrangement

This consists of the following two elements:

a) An optical lever (B), shown in figure 31, which consists of a mirror mounted on a perspex stage (B_1) and supported by three needles. Two of these (B_2) rest on grooves in the optical lever bearing plates (B_3), while the third needle, the take-off needle, rests on a stainless steel projection (A_6) from the load lever and thus the downward vertical displacement of the load lever, due to yarn compression, results in an angular rotation of the optical lever plane. An additional weight is attached to the optical lever to give it more stability.

b) An arrangement (C) to provide a concentrated projected light beam, as shown in figure 31a. The light from a source (C_1)(48 Watts, single filament bulb) passes through a lens (C_2) onto a hair line mounted on a frame (C_3), then through another lens (C_4). The lenses and the

Fig. 31 a

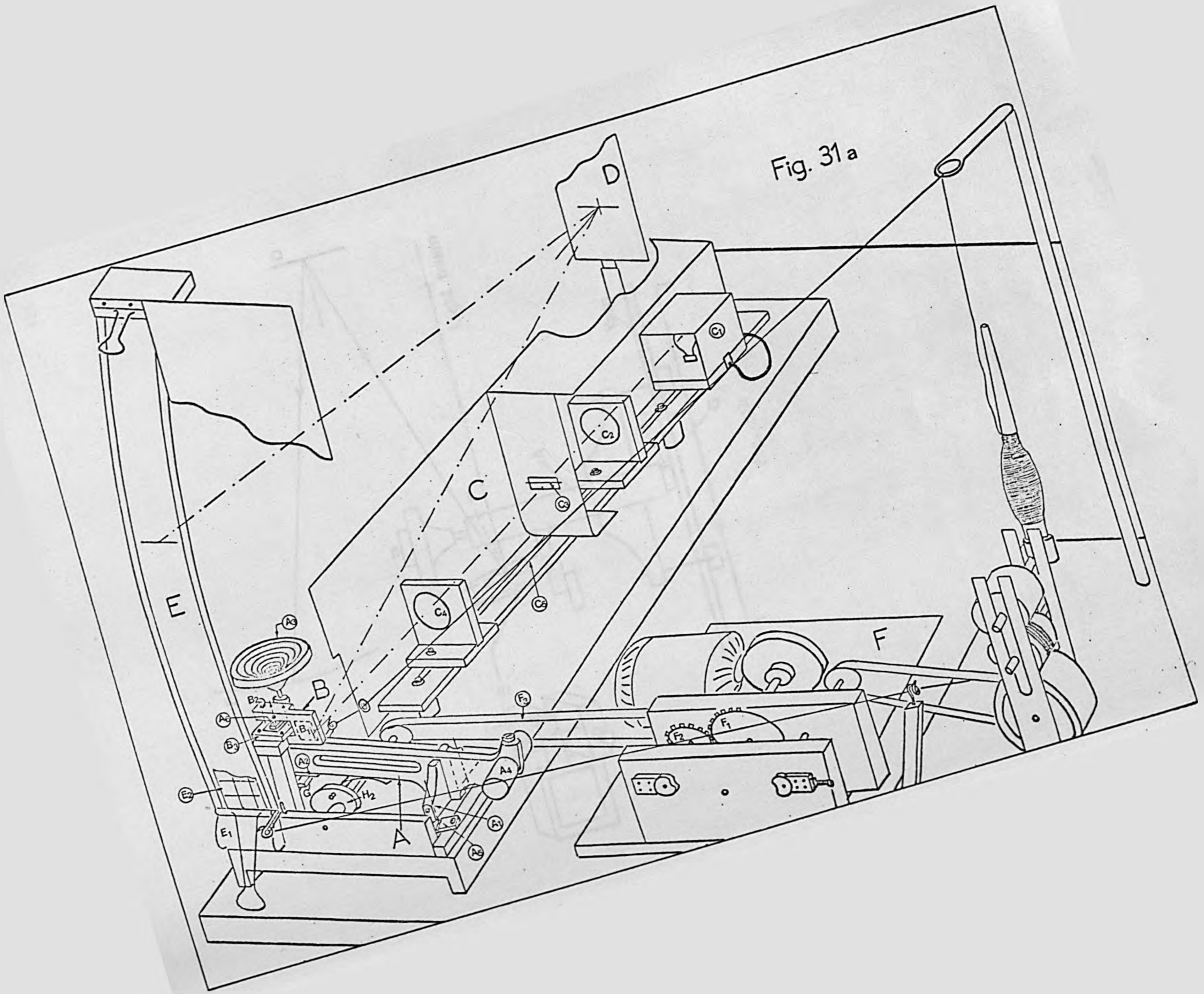

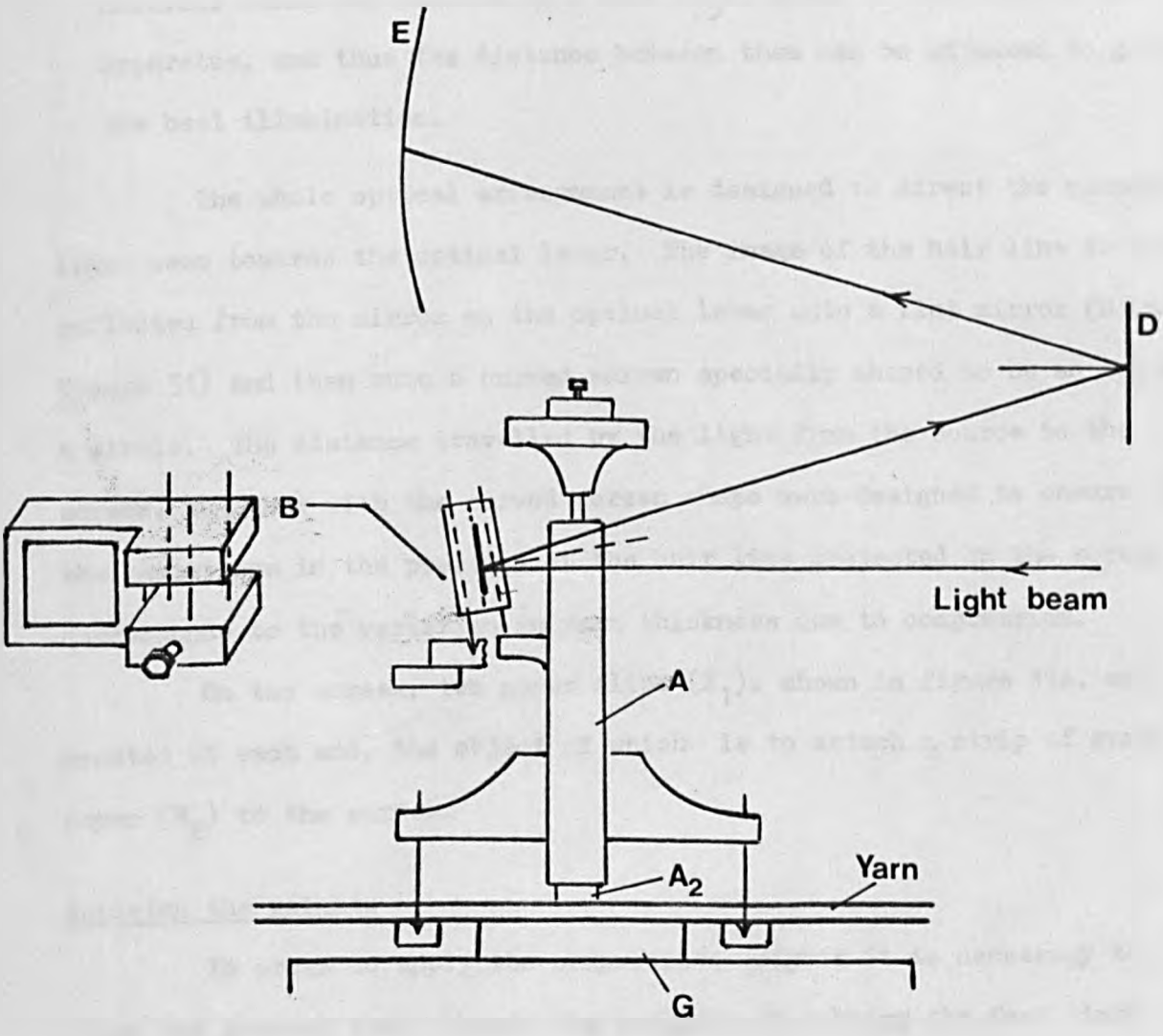

Fig. 31b

hairline frame are mounted on a rail (C_5), fixed to the base of the apparatus, and thus the distance between them can be adjusted to give the best illumination.

The whole optical arrangement is designed to direct the concentrated light beam towards the optical lever. The image of the hair line is then reflected from the mirror on the optical lever onto a flat mirror (D in figure 31) and then onto a curved screen specially shaped to be an arc of a circle. The distance travelled by the light from the source to the screen, together with the curved screen shape were designed to ensure that the variations in the position of the hair line projected on the screen corresponds to the variation in yarn thickness due to compression.

On the screen, two paper clips (E_1), shown in figure 31a, are mounted at each end, the object of which is to attach a strip of graph paper (E_2) to the screen.

Applying the weights

In order to apply the compressive weights it is necessary to raise the presser foot, change the weights, then bring the foot into contact with the yarn. The arrangement which achieves this procedure is better shown in figure 32a. This consists of an adjustable rod (H_1), mounted eccentrically on a wheel (H_2); a curved copper strip (H_3) is soldered to this rod. When the wheel is rotated, the copper strip contacts a stainless steel strip (A_7), fastened to the underside of the load lever and slowly raises the presser foot. Proceeding, the cyclic rotation of the wheel brings the presser foot back into contact with the yarn. If the compression test is to be carried out on a continuous length of the yarn, several readings for the yarn thickness, under the same load, are

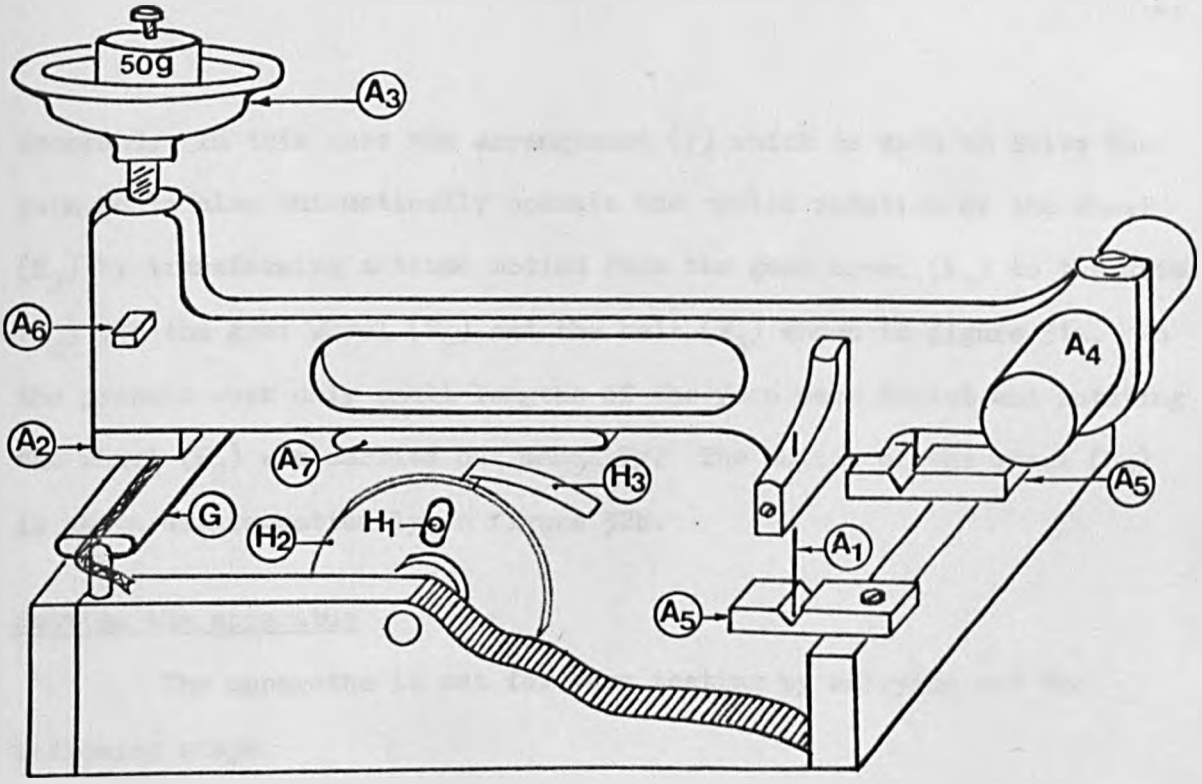

Fig. 32a

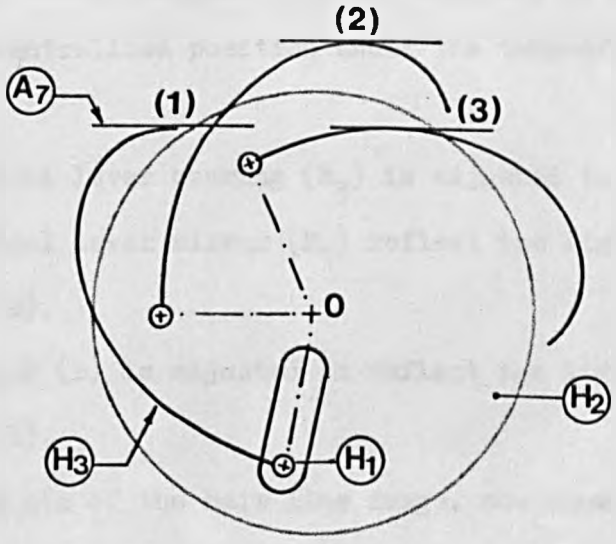

Fig. 32b

Position 1: Start of raising the load lever

Position 2: Maximum lift for the load lever

Position 3: The load lever back in contact with the yarn

recorded. In this case the arrangement (F) which is used to drive the yarn would also automatically operate the cyclic rotation of the wheel (H_2) by transforming a timed motion from the gear wheel (F_1) to the wheel (H_2) via the gear wheel (F_2) and the belt (F_3) shown in figure 31a. In the present work only small lengths of the yarn were tested and rotating the wheel (H_2) was carried out manually. The action of the wheel (H_2) is shown diagrammatically in figure 32b.

Setting the apparatus

The apparatus is set for yarn testing by carrying out the following steps.

(a) The distances between lenses, bulb and hair line are adjusted to give the best illumination (58).

(b) The load lever bearings (A_5) are adjusted to bring the projection (A_6) into a centralized position under the take-off needle of the optical lever.

(c) The optical lever bearing (B_3) is adjusted to the position which makes the optical lever mirror (B_1) reflect the light beam towards the flat mirror (D).

(d) The mirror (D) is adjusted to reflect the light beam towards the screen (E).

(e) With the aid of the hair line image, now shown on the screen, the lengths of the two load lever fulcrum needles are adjusted to achieve complete parallelization of the presser foot and the anvil. This is carried out by inserting a fine shank of a drill at different positions between the two plates, under 50 g load. The lengths of the two needles are then adjusted until a fixed reading is obtained on the screen irrespective of the position of the drill shank.

(f) The length of the optical lever take-off needle is adjusted to give zero scale reading at the lower part of the screen when the presser foot touches the anvil.

(g) The lengths of the fulcrum needles of the optical lever (B_2) are adjusted to slightly tilt the optical lever to its front under its own weight.

(h) Finally, the weight (AH) is adjusted to bring the load lever to a balanced position, nearly horizontal, when there is no load in the weight carrier (A_3).

Calibration

The method used to calibrate the instrument was to interpose engineering feeler gauges between the anvil and the presser foot, under a weight of 100 g/cm, and to record the corresponding thickness readings on the chart. The feeler gauges were initially measured accurately using the projection microscope. The calibration readings are given in the following table and in figure 33. The best fitting line for these points gave a magnification factor of 782 for the apparatus.

Table 3.5

Nominal thickness(mm)	0.05	0.1	0.15	0.2	0.3
Thickness under microscope(mm)	0.051	0.992	0.149	0.201	0.296
Chart reading (mm)	40.0	77.5	117.0	156.0	233.0

Sample preparation and test procedure

The straight parallel yarns, the same as those used in the yarn bending tests (section 3.4.1), were used to prepare the compression test samples. These yarns were frayed out of the fabric and each separated yarn was cellotaped onto a paper fibre frame, which is usually used for fibre

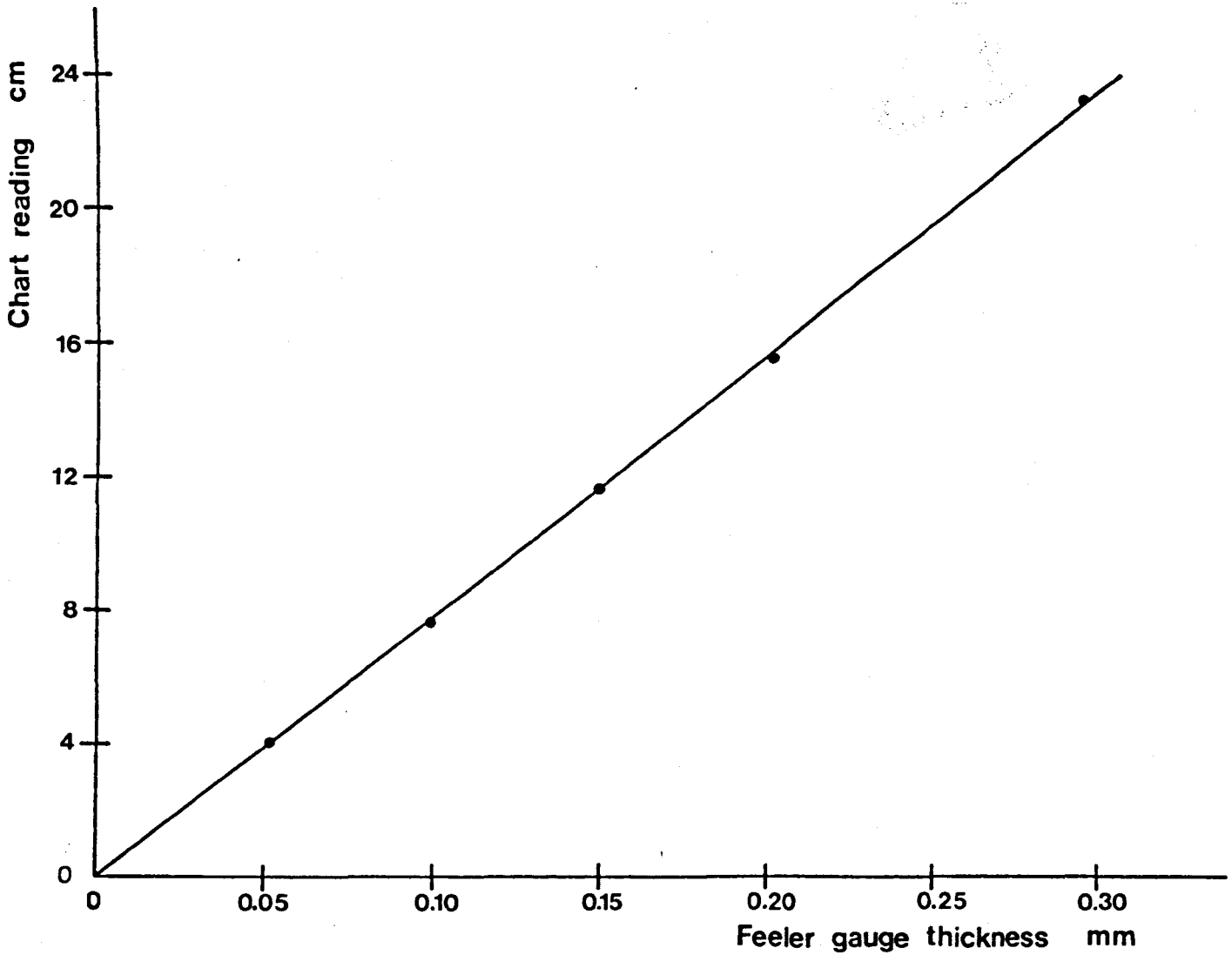
Chart reading cm
24
20
16
12
8
4
0
0
0.05
0.10
0.15
0.20
0.25
0.30
Feeler gauge thickness mm

Fig. 33

tensile tests. This process was done with great care so as not to disturb the yarn twist or impose tension on the yarn. The yarn was then situated under the raised presser foot and metal grips were used to hold the fibre frame. Raising and lowering the presser foot and changing the loads was carried out according to the procedure described above.

From the survey made (58,60) it was found that 20 variable loads, starting at 1.0 g/cm and increasing to 400 g/cm are enough to define the load-thickness relation for the yarns. For each yarn specimen, these 20 loads were applied and the corresponding thicknesses were recorded on the chart. For each type of yarn 20 specimens were tested and the average thickness for all the samples at each load was calculated.

Fitting the experimental results

An empirical formula due to Oxenham (60) was chosen to fit the experimental data. This formula is of the form

$$T = A_0 + A_1 e^{-B_1 x} + A_2 e^{-B_2 x} + A_3 e^{-B_3 x} , \qquad (3.4)$$

where

T = the yarn thickness,

x = the compressive load/unit length,

and $A_0, A_1, A_2, A_3, B_1, B_2$ and B_3 are constants.

The initial yarn thickness is obtained when the applied compressive load, x, is zero and therefore would be given by

$$(T)_{initial} = \sum_{\gamma=0}^{\gamma=3} A_\gamma \cdot \qquad (3.5)$$

Also by differentiating the formula (3.4), the rate of thickness change with load, at a load $x=x_0$, is given by

$$\left(\frac{dT}{dx}\right)_{x=x_0} = \sum_{j=1}^{j=3} A_j B_j e^{-B_j x_0} \quad . \tag{3.6}$$

The values of the constants in equation (3.4) were found by the method of least squares. Let the available data be pairs of observations (x_i, T_i), $i=1,2,3\ldots,M$. Then a residual may be defined as

$$R_i(A_\gamma, B_j) = (A_0 + A_1 e^{-B_1 x_i} + A_2 e^{-B_2 x_i} + A_3 e^{-B_3 x_i}) - T_i \, .$$

The method of least squares calculates the A's and B's so that

$$F(A_0, A_1, A_2, \ldots, B_1, B_2, \ldots) = \sum_{i=1}^{M} \left\{ R_i(A_\gamma, B_j) \right\}^2 \quad ,$$

is a minimum.

A gradient method, due to Marquardt (61), was used for minimization; and the computation, using a standard subroutine (62), was carried out on the 1906A ICL computer in Leeds University.

In the computer program it was necessary to make an initial estimate of the values of the constants. These initial values were found not to be critical and could be estimated as follows:

1. From equation (3.5) assuming, roughly, that A_0, A_1, A_2 and A_3 are equal then

   $$A_0 = A_1 = \ldots = T_{(initial)}/4 \quad ,$$

   and T(initial) is taken 30 microns above T_1 at $x_1 = 1.0$ g/cm.

2. From the knowledge that the thickness is the sum of a constant and three exponential functions, which are expected to have descending values of B, the estimates of B_1,B_2 and B_3 were taken as 0.5, 0.05 and 0.005 respectively.

The program then iteratively modifies these initial estimated values until the least squares solution is reached. In order to see how well the estimated regression curve fits the experimental values, the coefficient of determination 'C.D' was calculated, where

$$C.D. = \sum_{i=1}^{M}(Z_i-\bar{T})^2 / \left\{\sum_{i=1}^{M}(Z_i-T_i)^2 + \sum_{i=1}^{M}(Z_i-\bar{T})^2\right\},$$

and

T_i = the experimental value of the yarn thickness at a load x_i;

Z_i = predicted value of the yarn thickness (according to empirical formula) at a load x_i;

$\bar{T}$ = the mean value of the yarn thickness = $\sum_{i=1}^{M}\{T_i/M\}$.

The computer program, lay out of data, and the results are given in the appendix. The fitted empirical formulae and calculated values for the initial thickness and the equivalent yarn diameters, see section 3.4.3, are given in Table 3.6 while figures 34 to 38 show the experimental curves obtained for some of the yarns used.

Table 3.6

Experimental results for yarn thickness

Yarn 'Tex' and material	Empirical formula for thickness T in mm and 'X' in mN/mm	Initial thickness (mm)	Equivalent yarn diameter (mm)
R60/2 cotton	$T = 0.1726+0.1236e^{-0.7028X}+0.1379e^{-0.0894X}+0.1281e^{-0.0060X}$	0.562	0.398
R74/2 cotton	$T = 0.2133+0.2133e^{-0.8610X}+0.1591e^{-0.0778X}+0.1185e^{-0.0059X}$	0.601	0.431
R98/2 cotton	$T = 0.2393+0.1496e^{-0.4645X}+0.1542e^{-0.0369X}+0.1339e^{-0.0046X}$	0.677	0.479
R60/2 vincel	$T = 0.1447+0.0553e^{-0.3743X}+0.1379e^{-0.0671X}+0.1155e^{-0.0066X}$	0.453	0.321
R60/2 cotton-vincel	$T = 0.1539+0.1594e^{-0.1557X}+0.1242e^{-0.0264X}+0.1109e^{-0.0030X}$	0.548	0.387
R46/2 cotton-vincel	$T = 0.1410+0.0904e^{-0.6537X}+0.1082e^{-0.0789X}+0.0835e^{-0.0061X}$	0.423	0.299

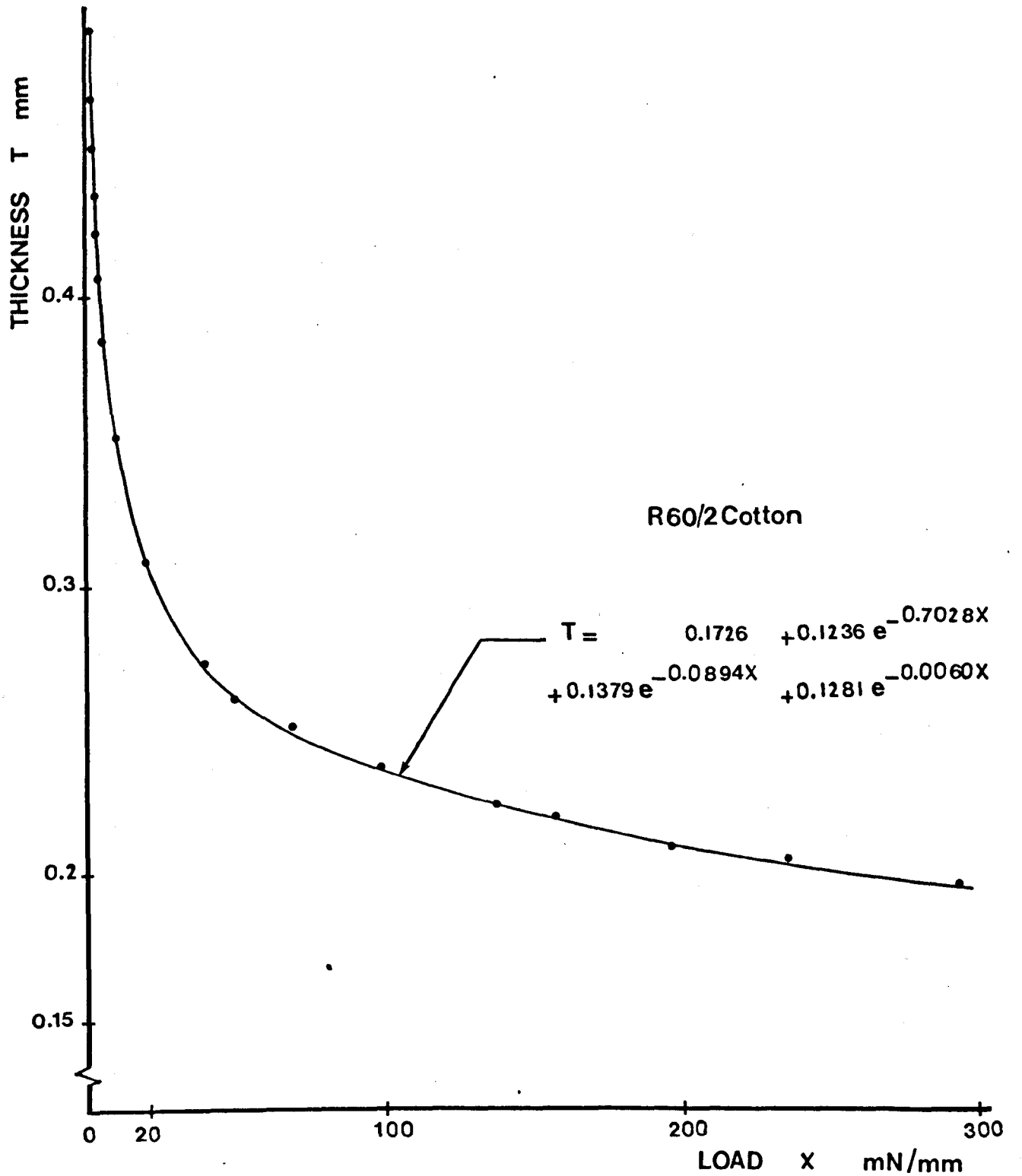
THICKNESS T mm
0.4
0.3
0.2
0.15
R60/2 Cotton
T = 0.1726 +0.1236 e^-0.7028X
+0.1379 e^-0.0894X +0.1281 e^-0.0060X
0
20
100
200
300
LOAD X mN/mm

Fig. 34

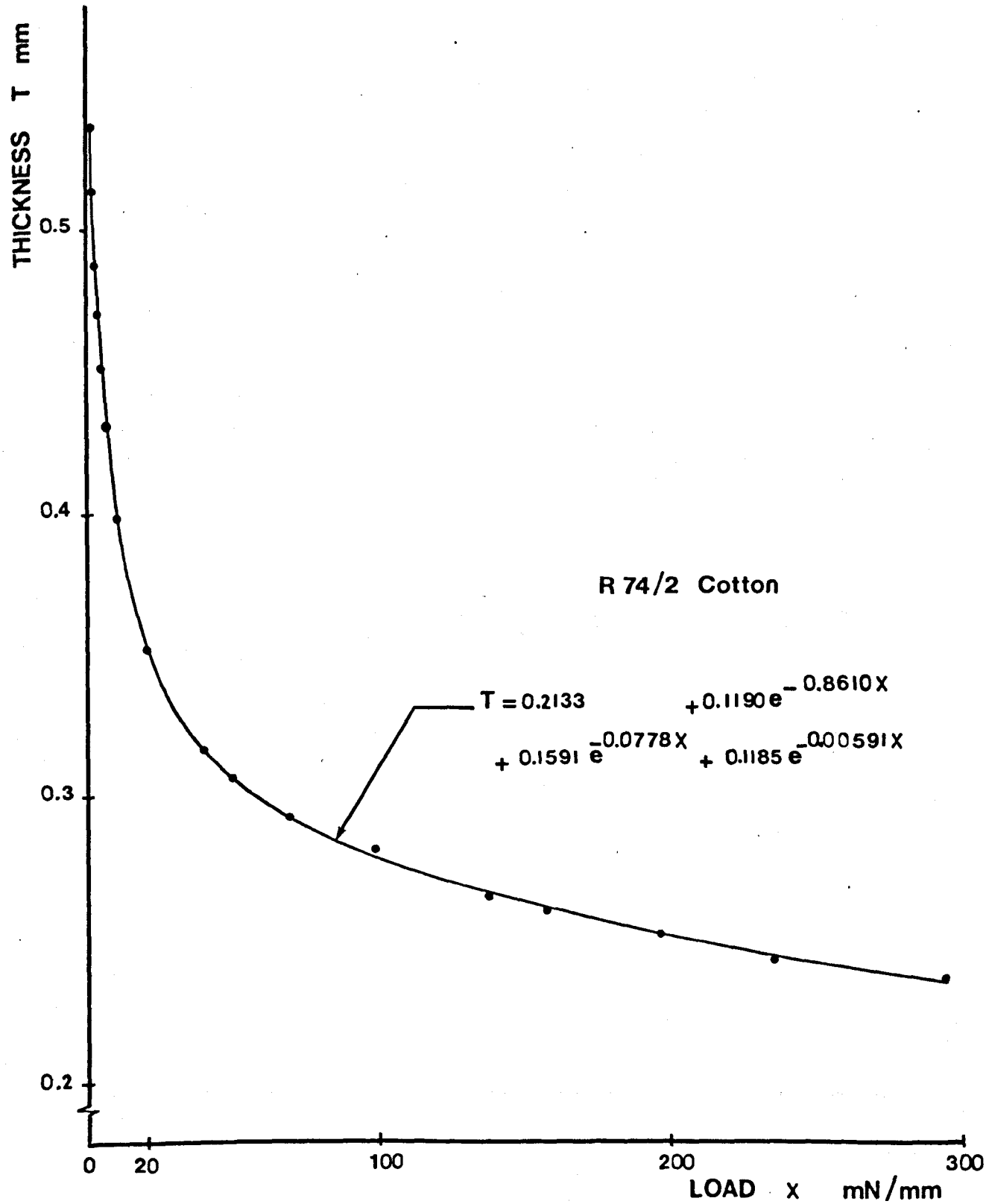
THICKNESS T mm
0.5
0.4
0.3
0.2
R 74/2 Cotton
T = 0.2133 + 0.1190 e^-0.8610X + 0.1591 e^-0.0778X + 0.1185 e^-0.00591X
0
20
100
200
300
LOAD X mN/mm

Fig. 35

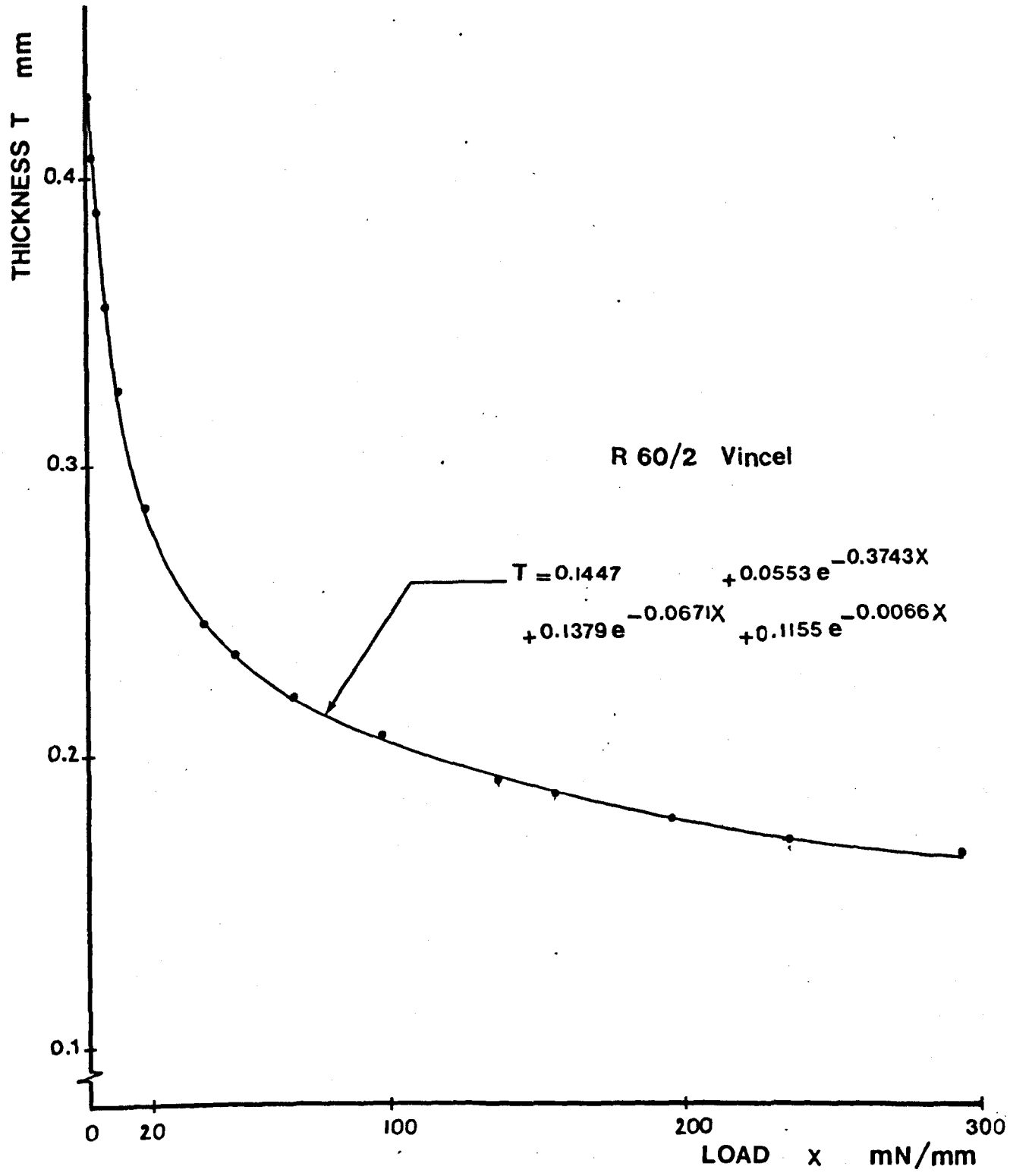
THICKNESS T mm
0.4
0.3
0.2
0.1
R 60/2 Vincel
T = 0.1447 + 0.0553 e^-0.3743X + 0.1379 e^-0.0671X + 0.1155 e^-0.0066X
0
20
100
200
300
LOAD X mN/mm

Fig. 36

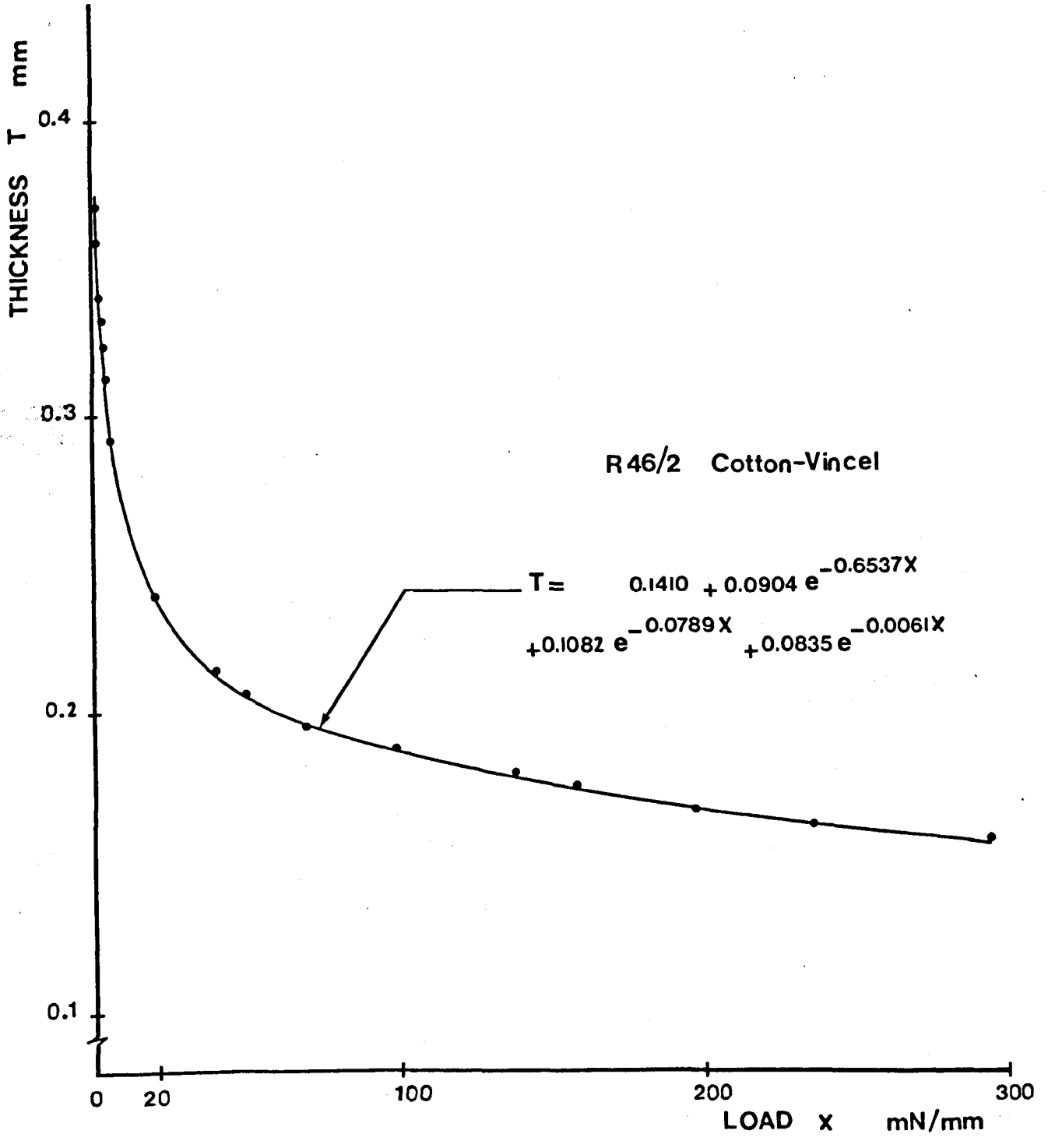
THICKNESS T mm
0.4
0.3
0.2
0.1
R 46/2 Cotton-Vincel
T= 0.1410 + 0.0904 e^-0.6537X
+0.1082 e^-0.0789X + 0.0835 e^-0.0061X
0
20
100
200
300
LOAD X mN/mm

Fig. 37

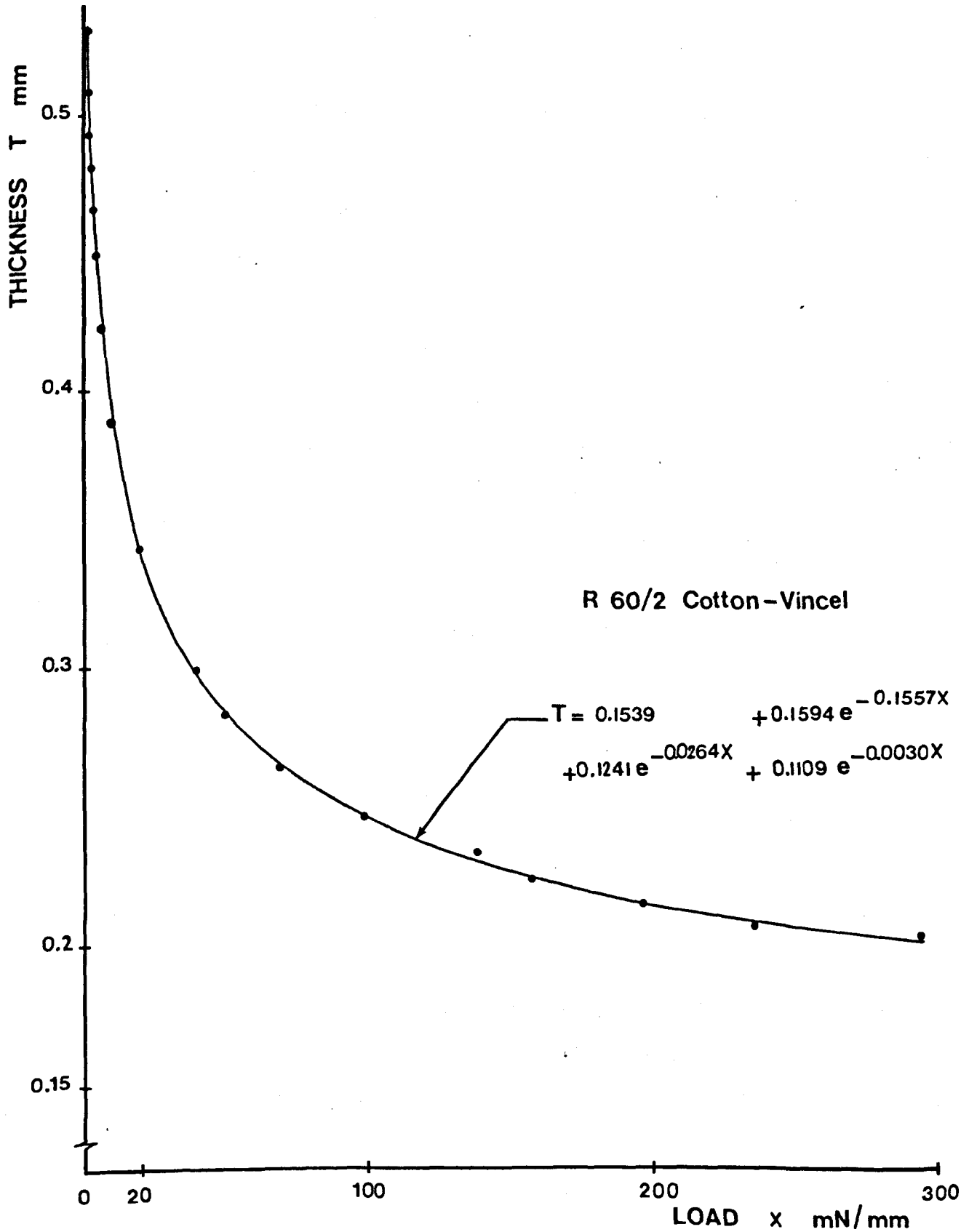
THICKNESS T mm
0.5
0.4
0.3
0.2
0.15
R 60/2 Cotton-Vincel
T = 0.1539 +0.1594 e^-0.1557X
+0.1241 e^-0.0264X + 0.1109 e^-0.0030X
0
20
100
200
300
LOAD x mN/mm

Fig. 38

3.6 Testing the Fabric Mechanical Properties

3.6.1 The fabric initial load-extension behaviour

The initial tensile behaviour of fabrics was readily found by using the Instron tensile tester. For each fabric 10 samples in each direction were tested. Each sample was rectangular, and was 30 cm long x 5 cm wide. They were initially cut to approximately 30x6 cm, and the yarns were then frayed out along the longer side until the sample width was 5 cm. The gauge length on the Instron was adjusted to give 25 cm between the jaws and a sample mounted, taking care that it was neither slack nor pretensioned. The lower jaw was then driven downwards with a speed of 2 cm per minute to give a rate of extension of 8% per minute. The Instron chart speed was adjusted to suit the fabric extensibility and the predetermined maximum extension. The ratio of the chart speed to the cross-head speed determines the 'extension scale factor' with which the extensions are represented on the charts. On the other hand the 'load scale factor' with which the loads are represented on the charts is determined by the full scale load 'F.S.L.' knob (63) on the Instron. The different positions of this knob provide different ranges of loads, with the appropriate Instron cell in use, corresponding to the chart full scale in the load direction. Since the main concern in these tests was to investigate the initial behaviour of fabrics, which usually involves relatively low loads, it was important to use the highest 'load scal factor' possible, and to achieve this the Instron 'B' cell, usually used for yarn testing, was employed. With such an arrangement specially prepared jaws were also used to fit to the 'B' cell attachment.

It is possible that the previous life history of fabrics may affect the tensile behaviour, and therefore several extension-load cycles up to

5% extension were carried out; in the event the difference between the first cycle and other cycles was regarded as insignificant. The tangent to the first cycle of the load-extension curve was then taken as the initial tensile modulus.

From the relation,

$$F = E\,\varepsilon ,$$

the fabric tensile modulus may be defined in either of the two following ways:

1. E is the force, on unit fabric width, needed to produce a 100% extension; $\varepsilon = 1$, and the units of E are therefore in 'Newtons/cm'.
2. E is the force, on unit fabric width, needed to produce 1% extension and the units are 'Newtons/cm for 0.01 extension'.

The first definition was used to express the experimental results in Table 3.7.

3.6.2 The fabric initial Poisson's ratio

Relatively few methods have been suggested for measuring the fabric Poisson's ratio, in a tensile test, under dynamic conditions (2,64,65). Amongst these a photographic method has many advantages and was used in this work. In this technique the fabrics were stretched on the Instron tensile tester. Each fabric sample was initially marked, along the line of symmetry in the direction to be extended, by 3 fine stitches; the second stitch mark was at the fabric centre while the distance between the first and third marks was approximately the same as the fabric width. An ordinary 35 mm 'S.R.L.' camera fitted with telescopic tubes was then used to take successive exposures during the fabric extension. The camera was mounted on a stand with a movable base which could be adjusted to bring the plane

containing the camera lens parallel to the fabric specimen plane when mounted on the Instron. In order to carry out the test, the Instron cross-head was driven at a speed of 2 cm per minute and the successive exposures were taken nearly at previously chosen values (0.0,0.01,0.02,0.04,0.06,0.08, 0.10 and 0.12) of the fabric extension.

To measure the specimen dimensions, when extended, the available methods were:

1. Using a mark dense-meter.
2. Projecting the negative on to a screen.
3. Printing the successive exposures and measuring the distances involved under a travelling microscope.

The first method was potentially the most accurate but was rejected as it was very laborious. On measuring the specimen dimensions, it was not necessary to know the actual magnification involved in photographing and printing, and the changes in a specimen dimensions were referred to the initial dimensions of the first photograph (at zero extension); thus the fractional extensions and the corresponding width-wise contractions could be calculated. The graphs given in figures 39-56 show the experimental results. The initial slope of these curves was taken as the initial Poisson's ratio.

Table 3.7

Experimental results of the tensile tests

Fabric group	Fabric No.	p_1 mm	p_2 mm	c_1	c_2	B_1 mN.mm^2	B_2 mN.mm^2	E_1 N/cm	E_2 N/cm	σ_1	σ_2
X	1	0.485	0.588	0.192	0.060	5.62	6.06	14.3	36.6	0.10	0.38
	2	0.488	0.624	0.214	0.056	5.62	6.06	9.4	29.8	0.11	0.42
	3	0.485	0.713	0.171	0.047	5.62	6.06	14.2	34.1	0.08	0.40
Y	1	0.490	0.677	0.179	0.048	5.62	7.05	15.9	42.9	0.08	0.40
	2	0.492	0.739	0.179	0.047	5.62	7.05	15.5	33.8	0.12	0.51
	3	0.495	0.849	0.158	0.036	5.62	7.05	14.6	28.6	0.13	0.57
Z	1	0.494	0.779	0.207	0.029	5.62	8.16	13.7	53.6	0.02	0.24
	2	0.494	0.839	0.218	0.027	5.62	8.16	10.6	45.5	0.06	0.35
	3	0.491	0.691	0.226	0.037	5.62	8.16	14.9	42.4	0.07	0.52
A	1	0.476	0.589	0.195	0.059	4.44	4.44	9.2	25.5	0.08	0.12
	2	0.587	0.749	0.104	0.049	4.44	4.44	9.1	14.8	-	0.40
	3	0.549	0.532	0.139	0.121	4.44	4.44	12.7	13.4	0.17	0.25
B	1	0.556	0.548	0.092	0.119	4.44	4.25	24.0	13.8	0.28	0.16
	2	0.591	0.637	0.134	0.053	4.44	4.25	13.3	19.7	0.32	0.52
	3	0.594	0.756	0.101	0.051	4.44	4.25	11.7	14.5	0.31	0.47
C	1	0.568	0.465	0.095	0.093	4.44	2.96	23.2	22.0	0.20	0.13
	2	0.577	0.538	0.110	0.107	4.44	2.96	18.0	12.8	0.37	0.25
	3	0.571	0.662	0.103	0.065	4.44	2.96	12.0	13.0	0.20	0.26

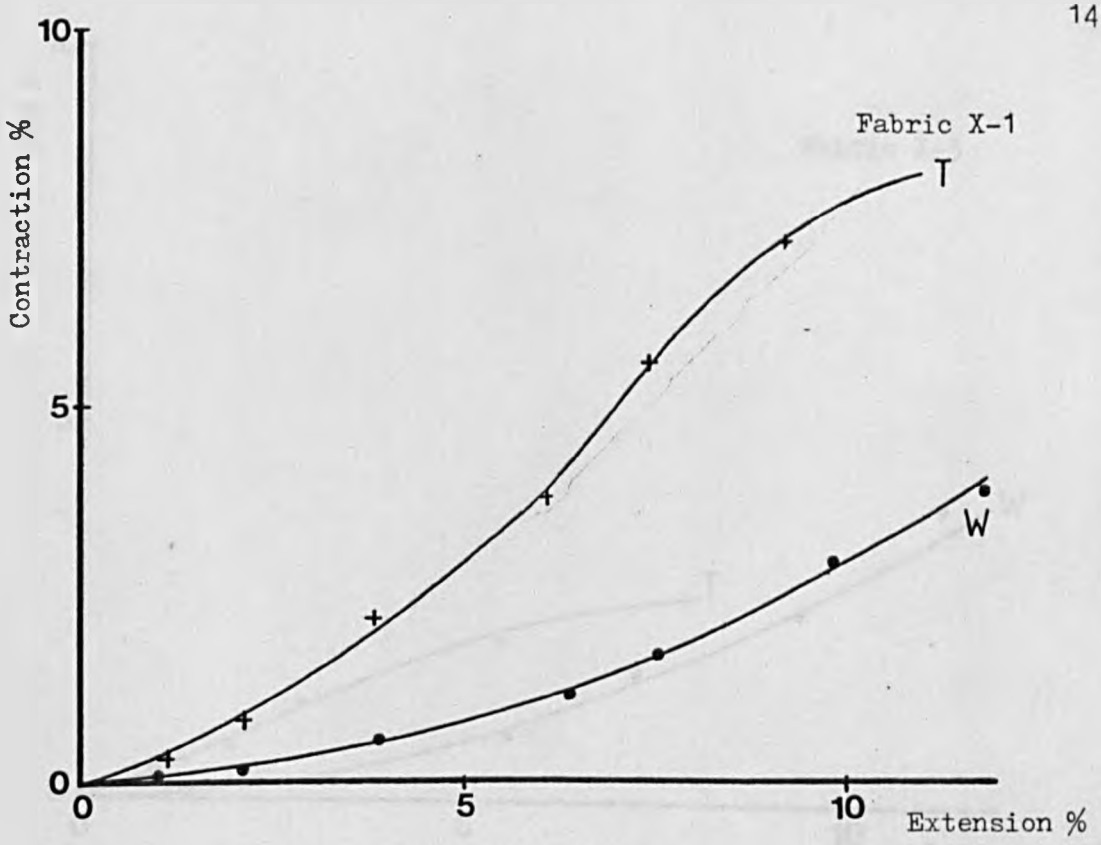

Fig. 39

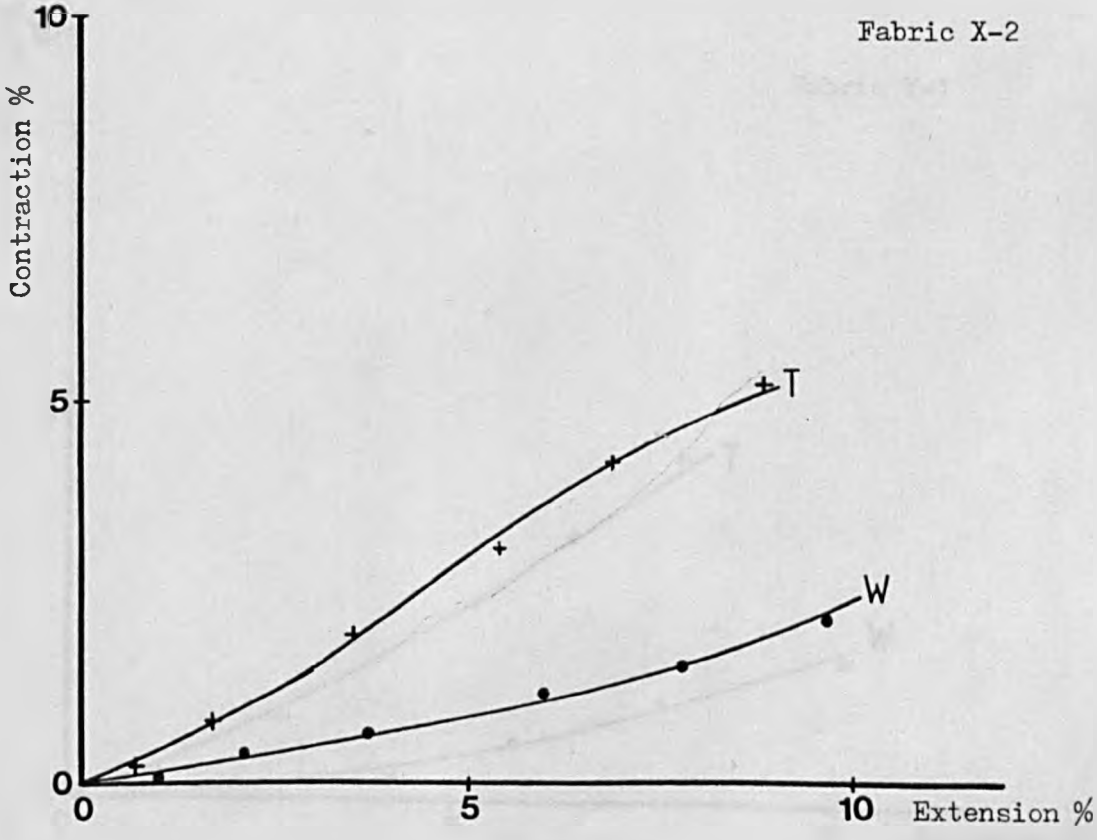

Fig. 40

W (warp) and T (weft) refer to fabric direction which was extended in the test

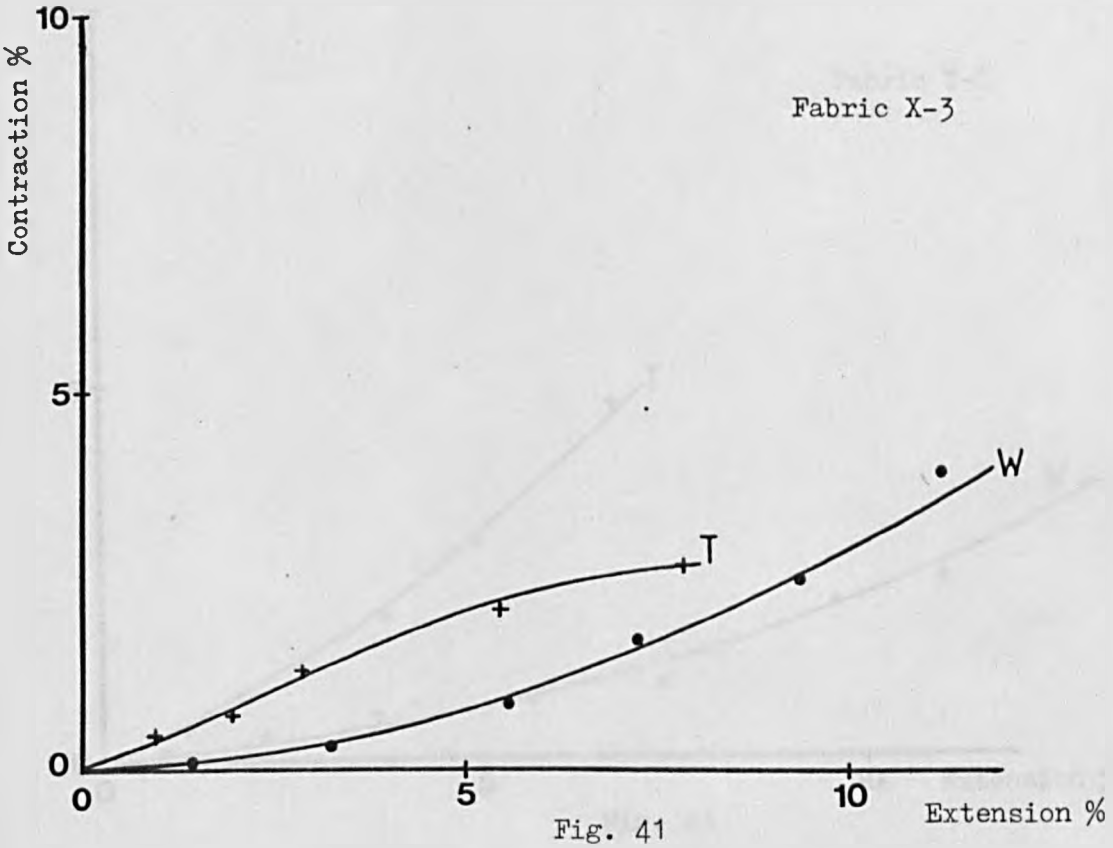
Fabric X-3
Contraction %
10
5
0
0
5
10
Extension %
T
W

Fig. 41

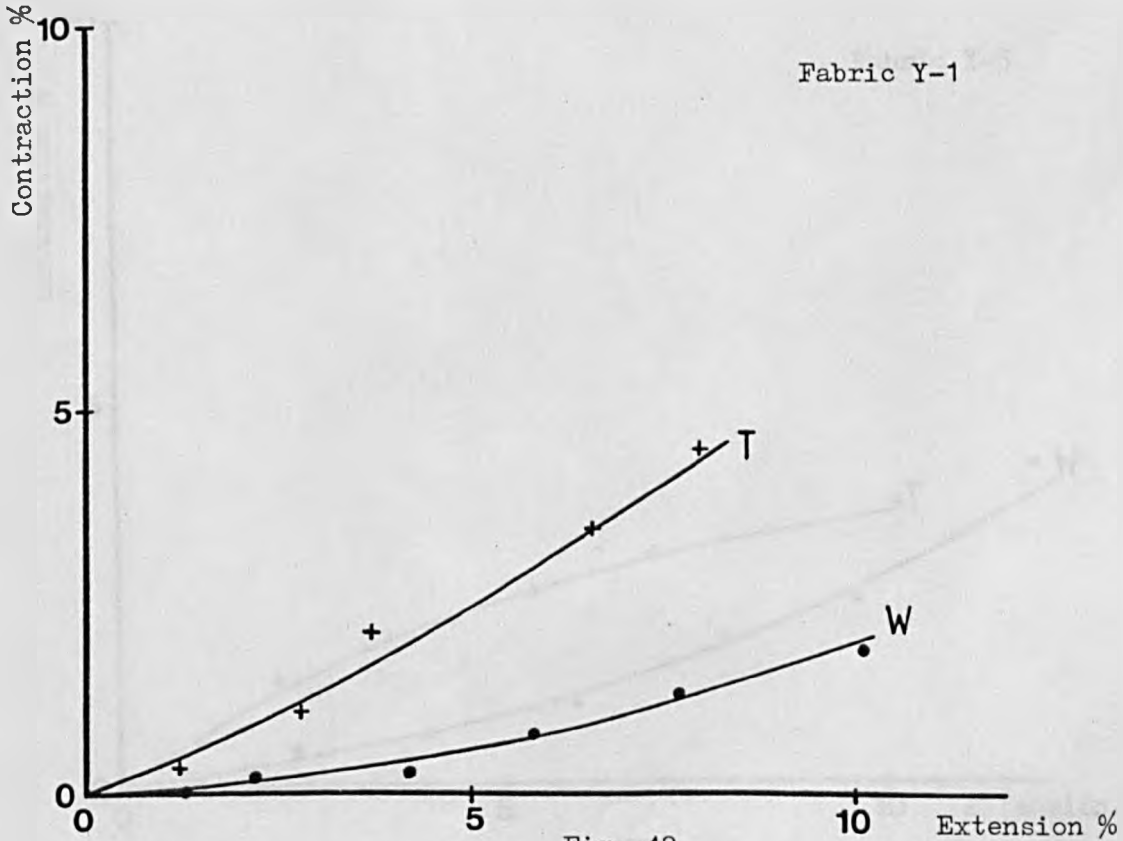
Fabric Y-1
Contraction %
10
5
0
0
5
10
Extension %
T
W

Fig. 42

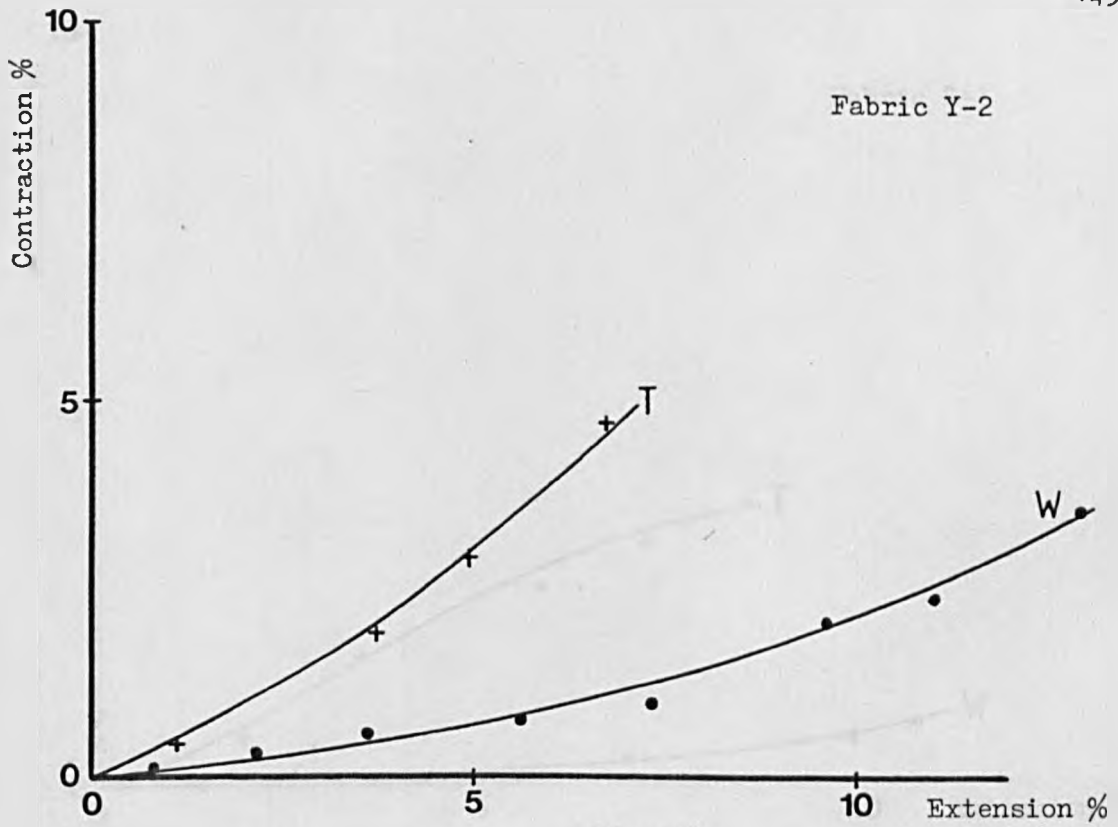
Fabric Y-2
Contraction %
10
5
0
0
5
10
Extension %
T
W

Fig. 43

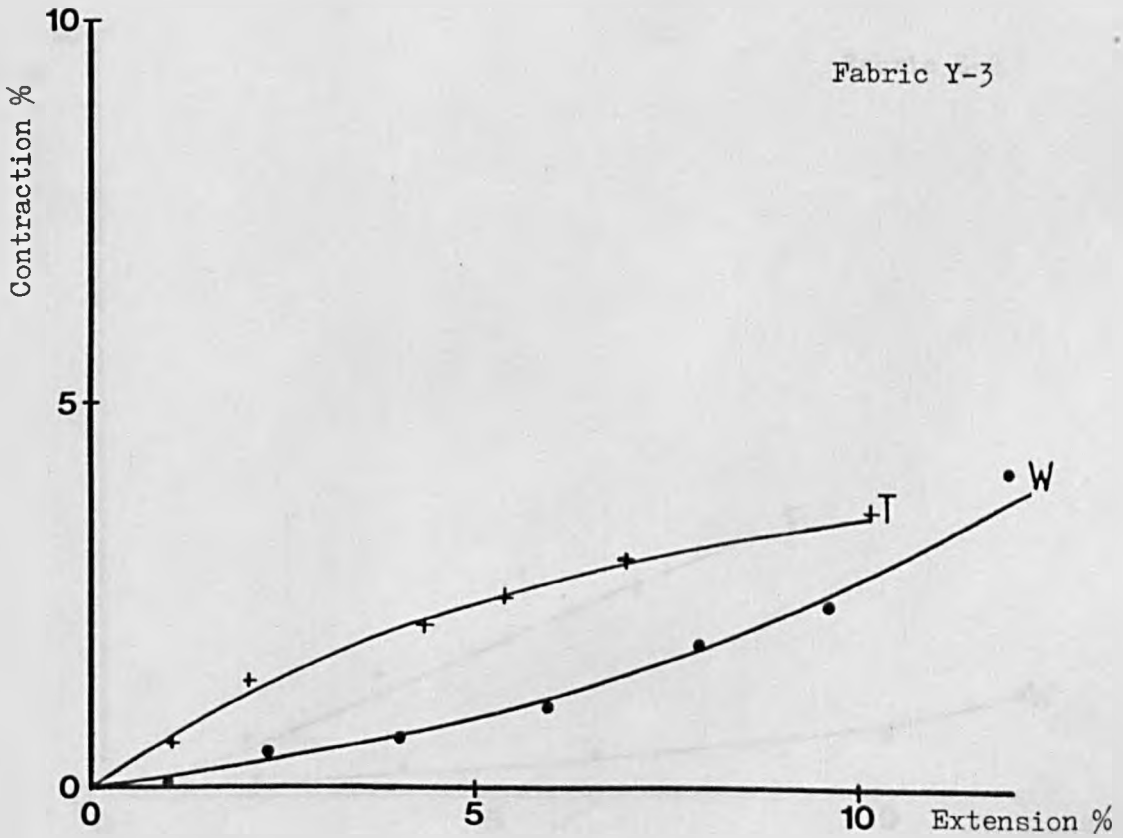
Fabric Y-3
Contraction %
10
5
0
0
5
10
Extension %
T
W

Fig. 44

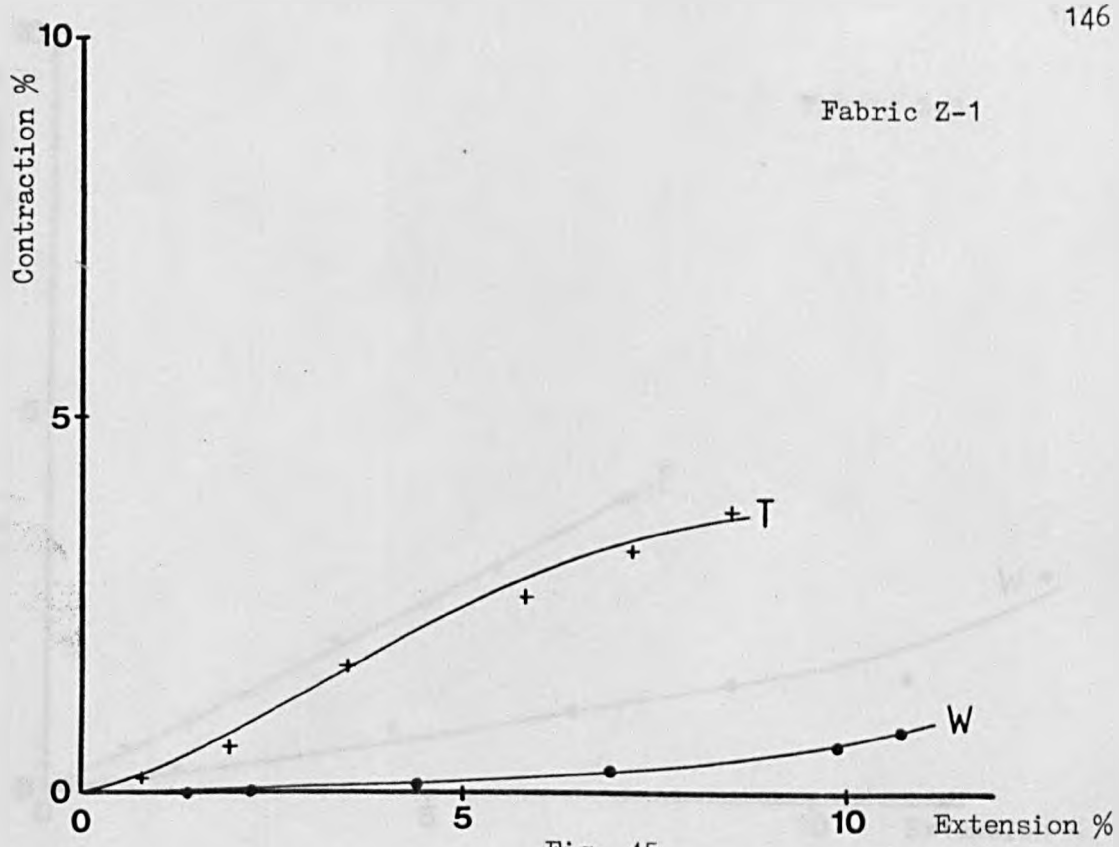
Fabric Z-1
Contraction %
10
5
0
0
5
10
Extension %
T
W

Fig. 45

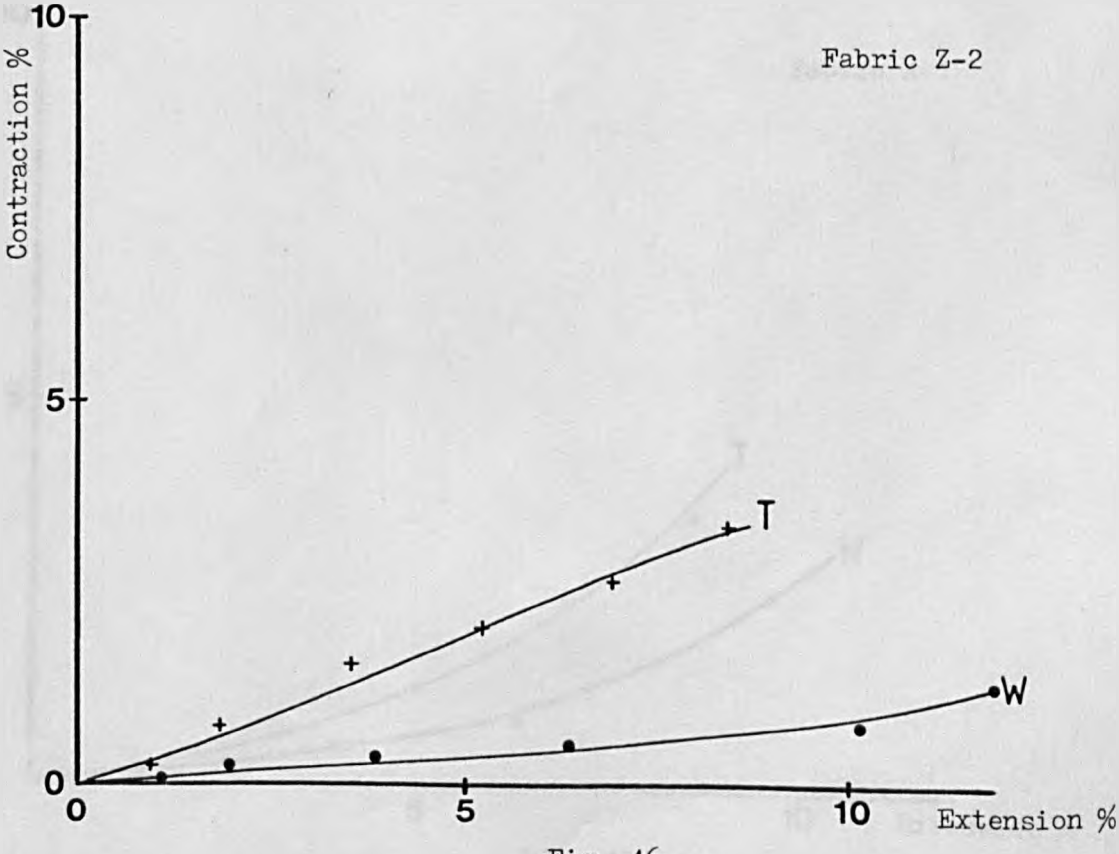
Fabric Z-2
Contraction %
10
5
0
0
5
10
Extension %
T
W

Fig. 46

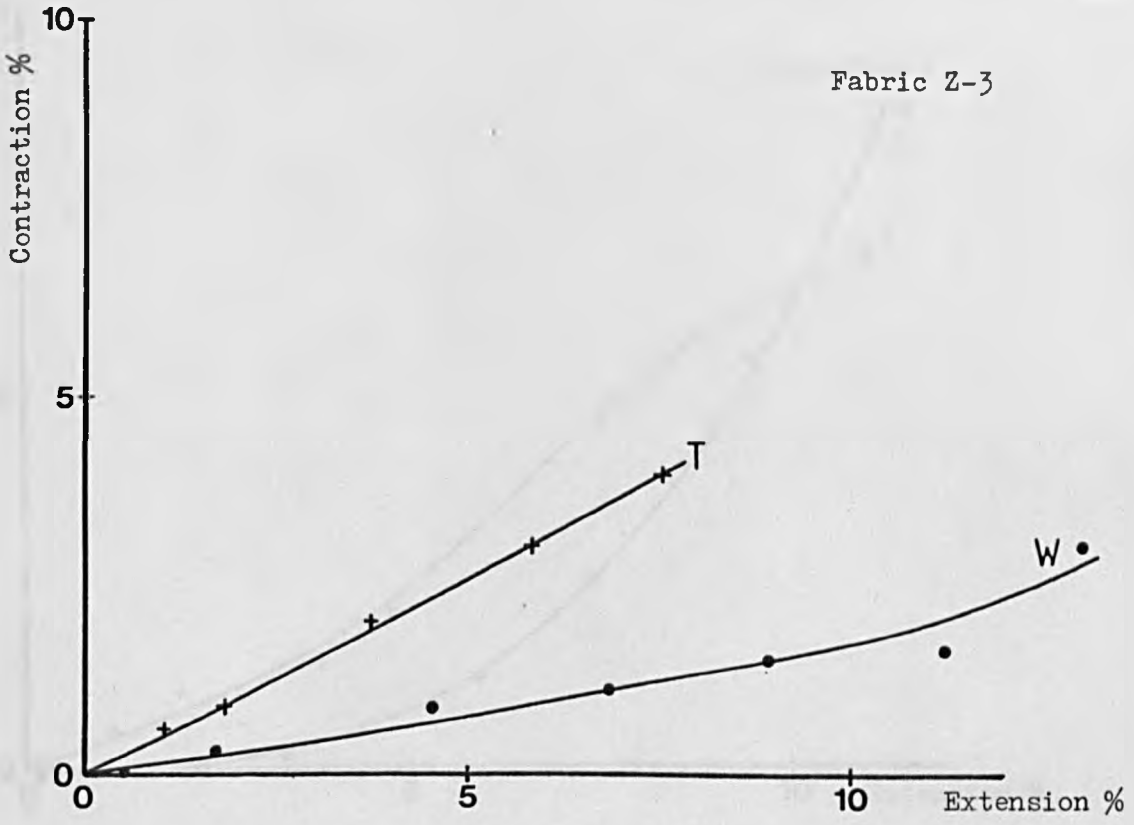
Fabric Z-3
Contraction %
10
5
0
0
5
10
Extension %
T
W

Fig. 47

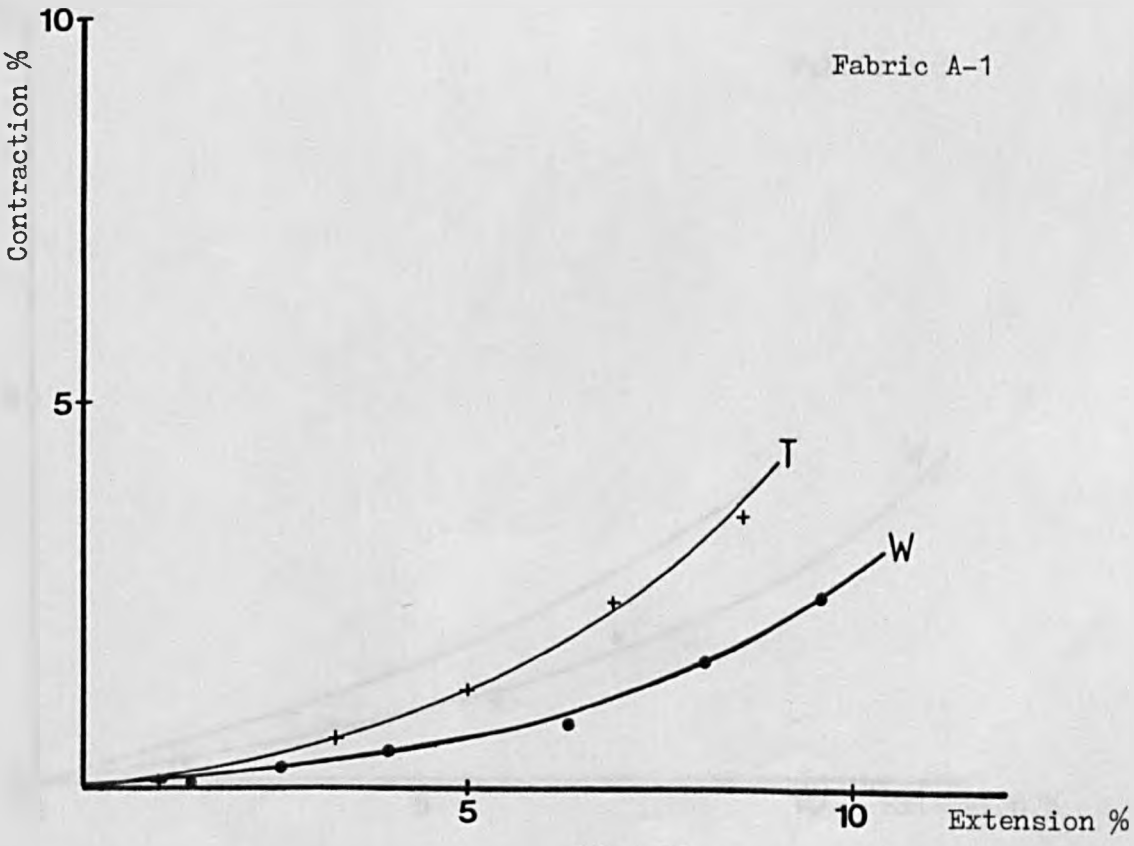
Fabric A-1
Contraction %
10
5
5
10
Extension %
T
W

Fig. 48

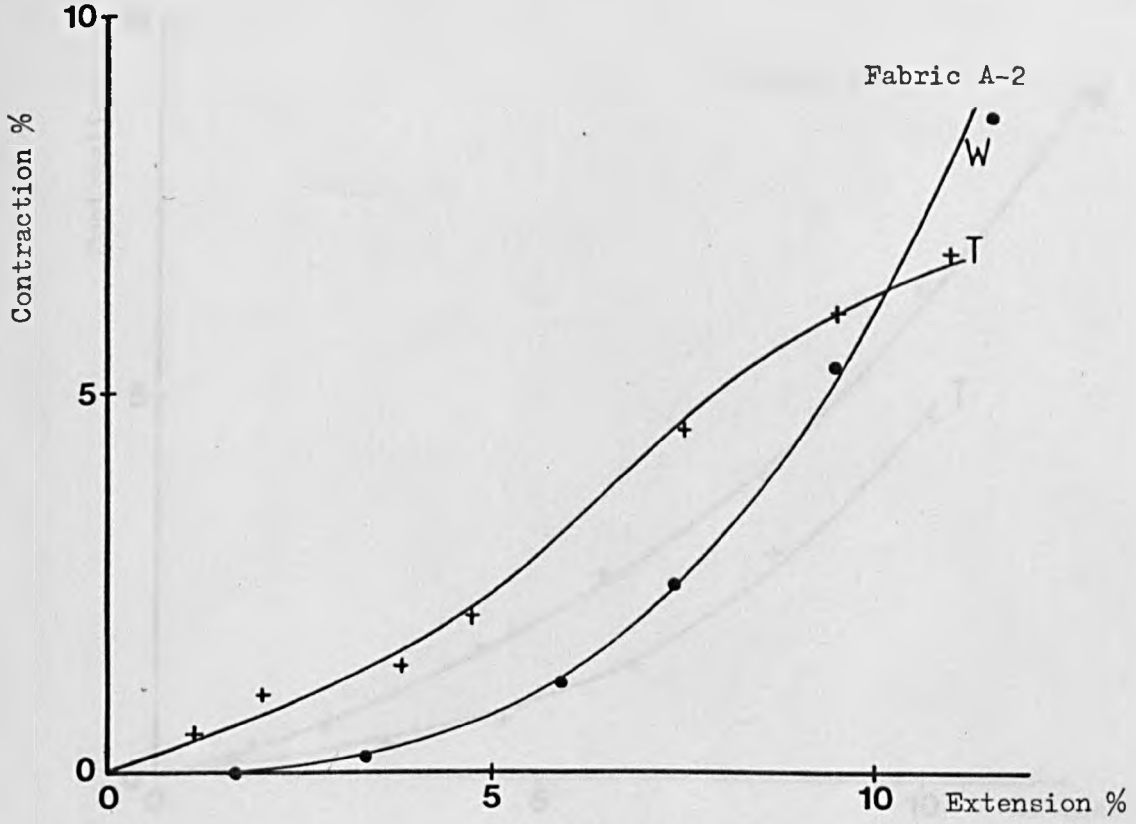
Fabric A-2
Contraction %
Extension %
W
T
10
5
0
0
5
10

Fig. 49

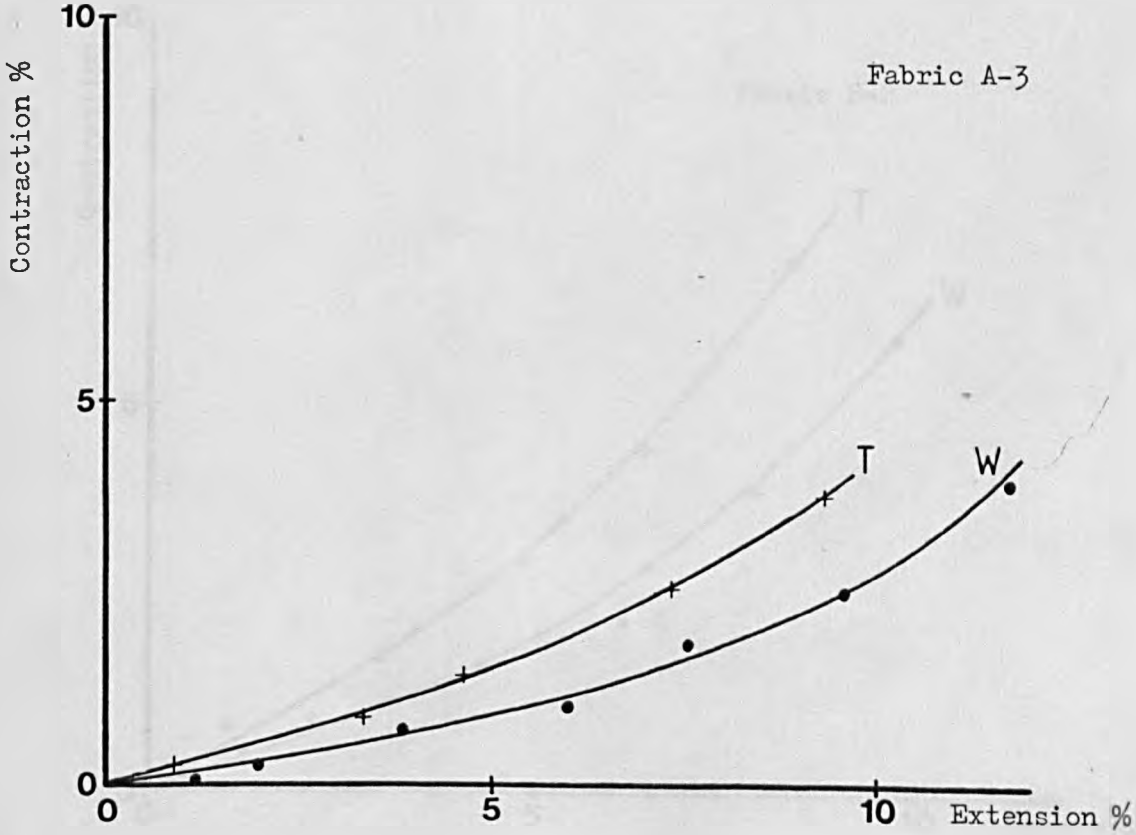
Fabric A-3
Contraction %
Extension %
T
W
10
5
0
0
5
10

Fig. 50

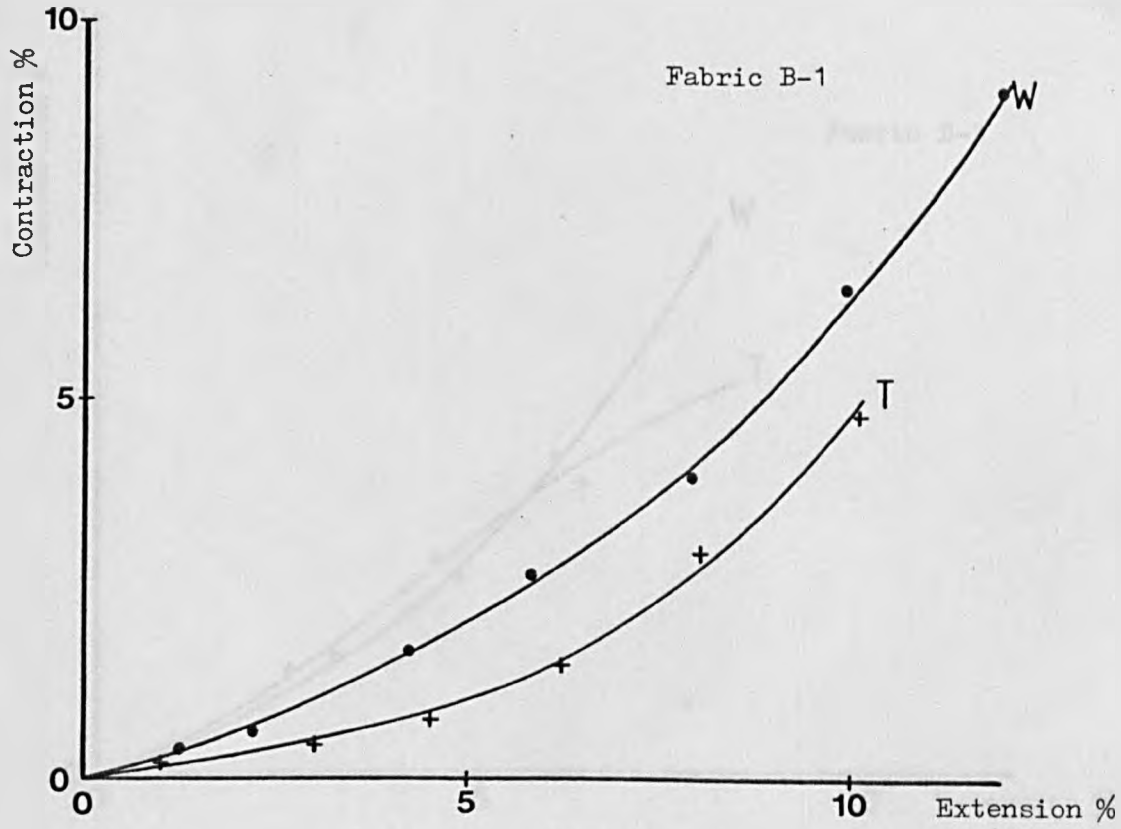
Fabric B-1
Contraction %
Extension %
10
5
0
0
5
10
W
T

Fig. 51

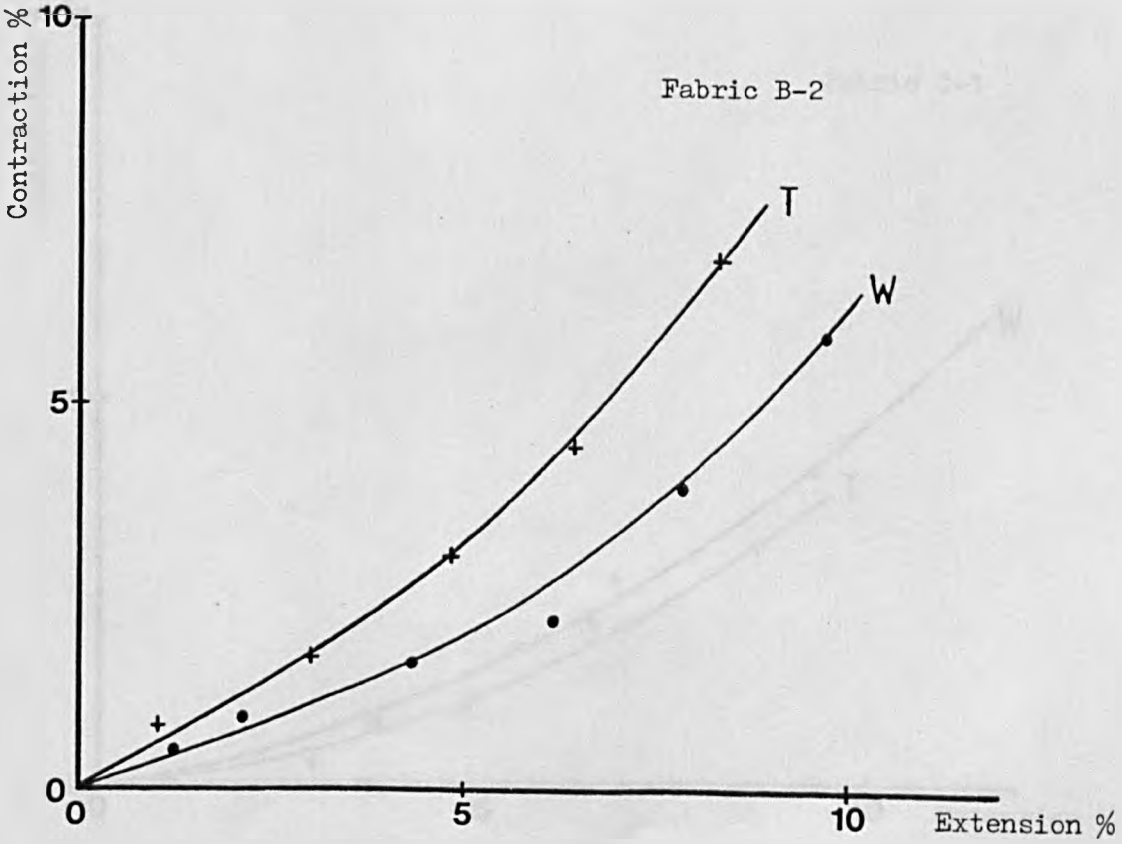
Fabric B-2
Contraction %
Extension %
10
5
0
0
5
10
T
W

Fig. 52

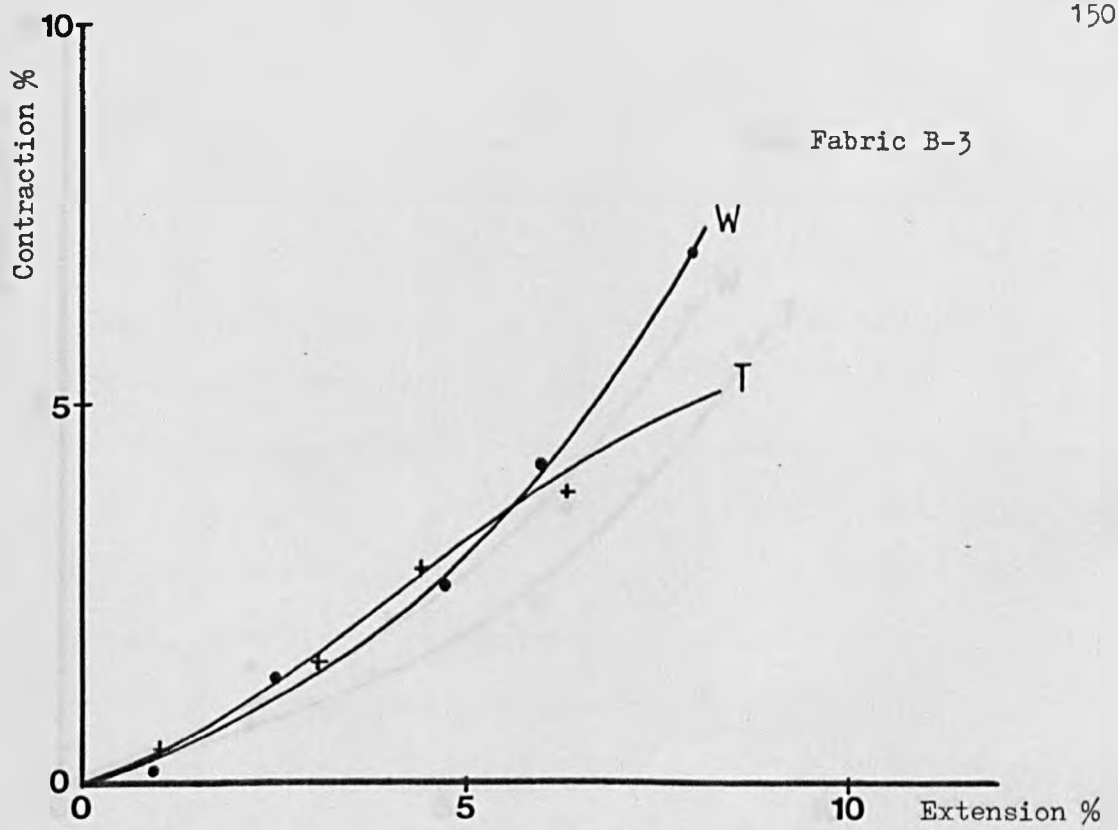
Contraction %
10
5
0
0
5
10
Extension %
Fabric B-3
W
T

Fig. 53

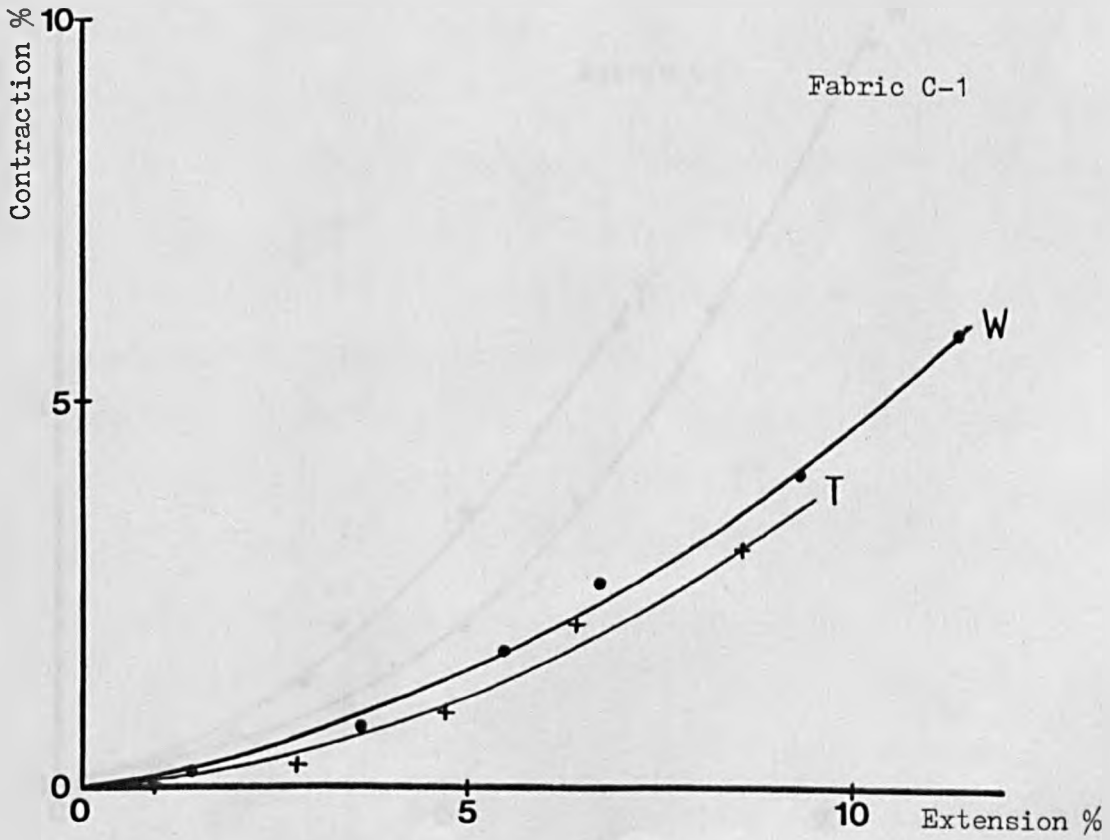
Contraction %
10
5
0
0
5
10
Extension %
Fabric C-1
W
T

Fig. 54

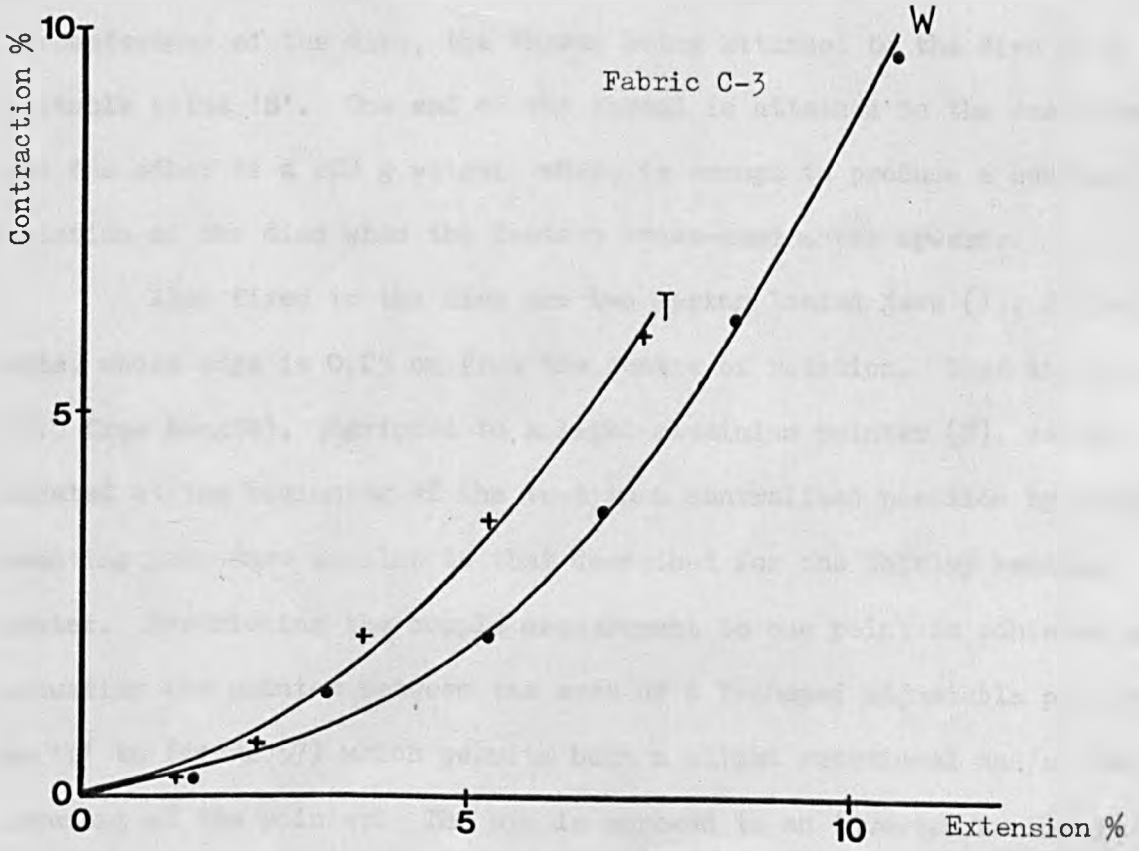

Fig. 56

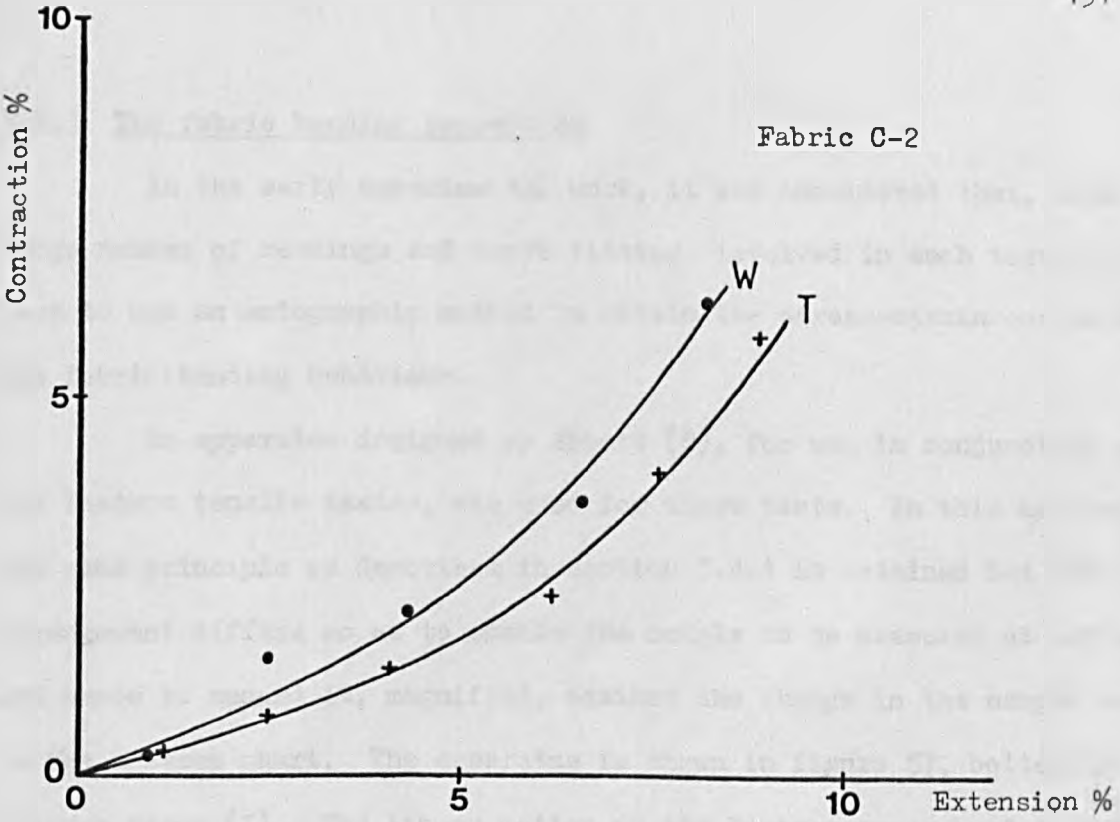

Fig. 55

3.6.3 The fabric bending properties

In the early experimental work, it was considered that, with the large number of readings and curve fitting involved in such tests, it was best to use an autographic method to obtain the stress-strain curves for the fabric bending behaviour.

An apparatus designed by Abbott (8), for use in conjunction with the Instron tensile tester, was used for these tests. In this apparatus, the same principle as described in section 3.4.1 is retained but the arrangement differs so as to enable the couple to be measured at one point and hence to record it, magnified, against the change in the sample curvature on the Instron chart. The apparatus is shown in figure 57, bolted to the Instron frame (I). The linear motion of the Instron cross-head is used to produce an angular rotation of the graduated disc (D). This is achieved by passing a folded nylon thread (T) round a grooved track in the circumference of the disc, the thread being attached to the disc at a suitable point 'S'. One end of the thread is attached to the cross-head and the other to a 200 g weight, which is enough to produce a counter rotation of the disc when the Instron cross-head moves upwards.

Also fixed to the disc are two spring loaded jaws (J), 2.5 cm wide, whose edge is 0.25 cm from the centre of rotation. Thus the sample (0.5 free length), gripped to a light aluminium pointer (P), can be located at the beginning of the test in a centralized position by using a mounting procedure similar to that described for the Shirley bending tester. Restricting the couple measurement to one point is achieved by situating the pointer between the arms of a Y-shaped adjustable pin (denoted as 'Y' in figure 57) which permits both a slight rotational and/or downward movement of the pointer. The pin is screwed to an inverted L-shaped

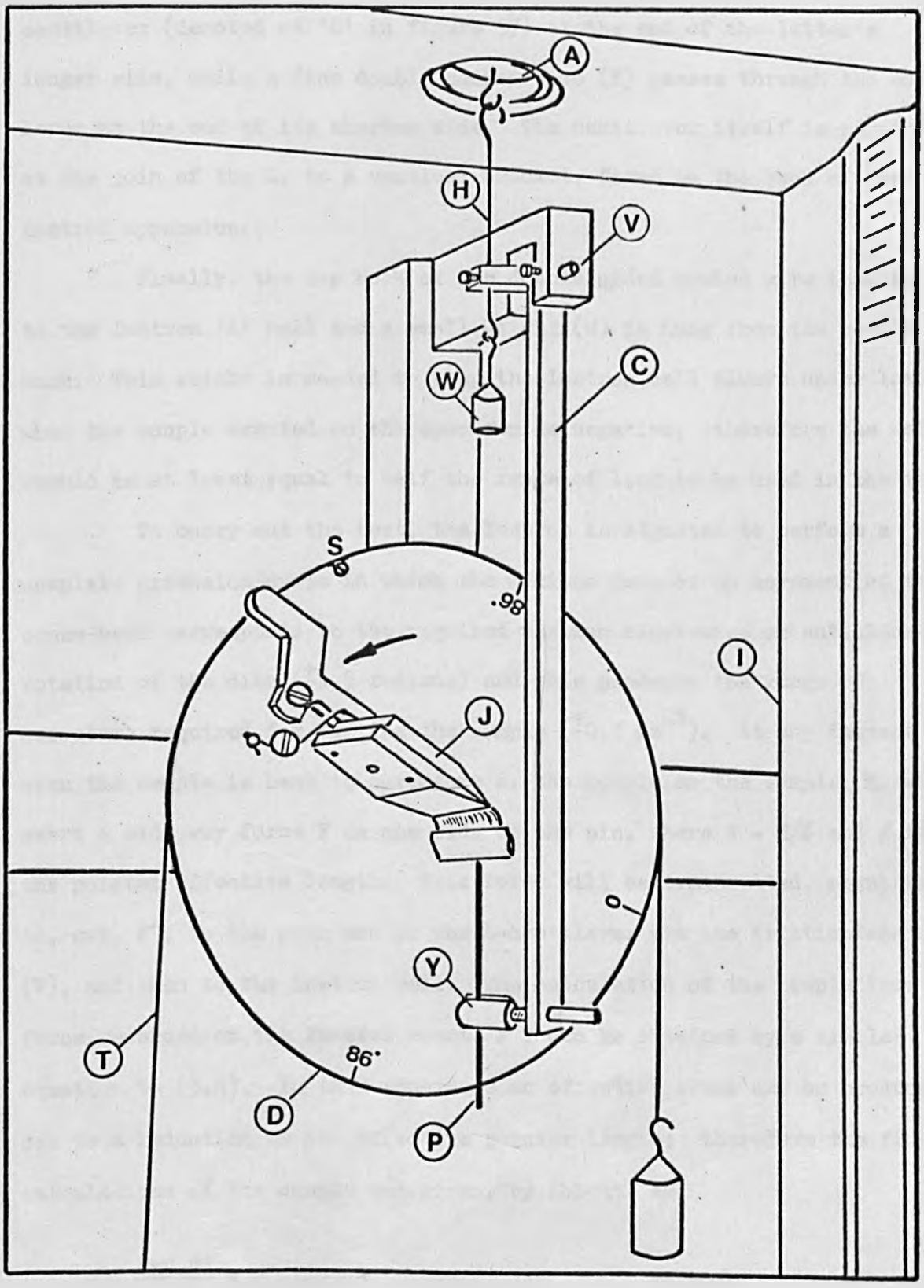

Fig. 57

cantilever (denoted as 'C' in figure 57) at the end of the latter's longer side, while a fine double hooked wire (H) passes through the cantilever at the end of its shorter side. The cantilever itself is pivoted, at the join of the L, to a vertical bracket, fixed to the back of the Instron apparatus.

Finally, the top hook of the double sided hooked wire is attached to the Instron 'A' cell and a small weight (W) is hung from the bottom hook. This weight is needed to keep the Instron cell always under load when the couple exerted on the specimen is negative; therefore the weight should be at least equal to half the range of load to be used in the test.

To carry out the test, the Instron is adjusted to perform a complete extension cycle in which the maximum down or up movement of the cross-head corresponds to the required maximum clock-wise or anticlock-wise rotation of the disc ($\pm$1.5 radians) and this produces the range of curvature required for testing the sample ($\pm$0.3 mm^{-1}). At any instant when the sample is bent to curvature K, the couple on the sample, M, will exert a side way force F on one side of the pin, where $F = M/\ell$ and ℓ is the pointer effective length. This force will be transmitted, magnified to, say, F', to the rear end of the L-cantilever via the frictionless pivot (V), and then to the Instron cell. The calculation of the couple from the force recorded on the Instron chart, F , can be obtained by a similar equation to (3.3). In this apparatus an effective error may be produced due to a reduction in the effective pointer length; therefore the final calculations of the couple was given, by Abbott, as

$$M = \frac{Rx9.81}{2.5} \times F'(L+2.0) \ , \qquad \text{mN.mm/cm}$$

where R is the length ratio of the short side to the long side of the L-cantilever (0.1 in this arrangement),

L is the effective length (mm) of the pointer at zero sample curvature,

and F' is the force recorded on the Instron chart in g.

The results of the fabric bending (per yarn), using the above method at 0.68 mm^{-1}/min bending rate, are given in Table 3.8. Each value is the average of 4 tested samples. In this table (3.8), the corresponding values, using the Shirley tester, are also included and it is evident that the two methods may lead to different results. The main reason is, probably, due to the different conditions under which the samples are tested. In Abbott's apparatus, the samples are tested under dynamic conditions while in the Shirley method the testing procedure may allow some stress relaxation. In addition, the following are some sources of error associated with Abbott's method.

1. Abbott's apparatus is mounted on the Instron, and it was found that mechanical vibrations through the frame of the instrument severely affected the traces obtained for fabrics of low bending rigidities (e.g. fabrics in groups A,B and C).
2. The Instron is actually operated, in cases of fabrics of low rigidities, under its minimum rated capacity of 1 g.

The Shirley cyclic bending tester was finally used to test the fabric bending behaviour and for this purpose 4 face and 4 back samples were examined following the same testing procedure as that described for the yarn bending tests. The results obtained using the Shirley tester (Table 3.9) were considered more reliable and will be used for comparison with the theoretical

calculations of the fabric bending. The fabric behaviour, under bending, was sometimes very close to the bending behaviour of the component yarns, in the load direction, as can be seen in figure 58. Another case is shown in figure 59, in which the fabric bending behaviour is considerably different than that of the yarns.

Table 3.8

Fabric	Bending Direction	Abbott's apparatus			Shirley Tester		
		B* $mN.mm^2/yarn$	B $mN.mm^2/yarn$	M_0 mN.mm /yarn	B* $mN.mm^2/yarn$	B $mN.mm^2/yarn$	M_0 mN.mm /yarn
X-1	warp	9.61	5.61	0.23	9.46	4.80	0.27
X-1	weft	12.64	6.59	0.41	12.93	5.56	0.48
X-2	warp	8.68	5.01	0.18	9.02	5.00	0.31
X-2	weft	13.13	7.10	0.55	12.79	6.24	0.68
X-3	weft	13.39	6.70	0.46	16.04	6.77	0.53
Y-2	warp	8.44	5.53	0.25	10.59	5.45	0.30
Y-2	weft	-	10.48	0.50	20.42	6.27	0.55
Z-2	warp	9.28	4.66	0.20	9.63	3.88	0.27
Z-2	weft	30.73	12.38	1.20	57.03	10.69	1.34
Z-3	warp	10.80	7.35	0.34	16.45	7.09	0.41
Z-3	weft	36.47	18.31	1.40	55.96	15.02	1.45

Table 3.9

Experimental results of the fabric bending characteristics

Fabric group	Fabric No.	Warp			Weft		
		B_W^* mN.mm^2/cm	B_W mN.mm^2/cm	M_{OW} mN.mm/cm	B_T^* mN.mm^2/cm	B_T mN.mm^2/cm	M_{OT} mN.mm/cm
X	1	195.88	98.90	5.50	220.88	94.61	8.11
	2	184.82	102.50	6.38	205.50	99.98	10.89
	3	204.00	76.82	6.00	225.00	95.00	7.49
Y	1	205.48	113.71	5.99	330.00	151.22	12.99
	2	215.16	110.97	6.12	414.98	127.93	11.09
	3						
Z	1	194.78	81.21	5.24	789.28	174.85	17.98
	2	194.98	78.63	5.49	679.86	127.46	15.99
	3	335.05	144.49	8.24	806.79	217.35	20.98
A	1	172.50	96.84	5.35	202.50	104.65	5.36
	2	143.54	71.47	3.60	116.83	51.15	2.51
	3	182.50	130.54	6.28	196.19	105.80	5.06
B	1	285.00	143.78	8.49	160.00	79.04	4.75
	2	140.94	73.17	4.14	130.59	60.99	4.03
	3	165.23	83.74	3.83	136.80	52.57	4.73
C	1	205.04	120.46	7.19	120.03	68.77	4.15
	2	152.00	80.22	5.00	100.00	46.49	2.59
	3	116.00	68.72	3.14	73.64	41.98	2.33

B_W^*, B_T^* are the initial flexural rigidities of the fabric (per cm width)

B_W, B_T are the elastic flexural rigidities of the fabric (per cm width)

M_{OW}, M_{OT} are the frictional couples of the fabric (per cm width)

Couple mN.mm
2
1
0.3
0.2
0.1
1
2

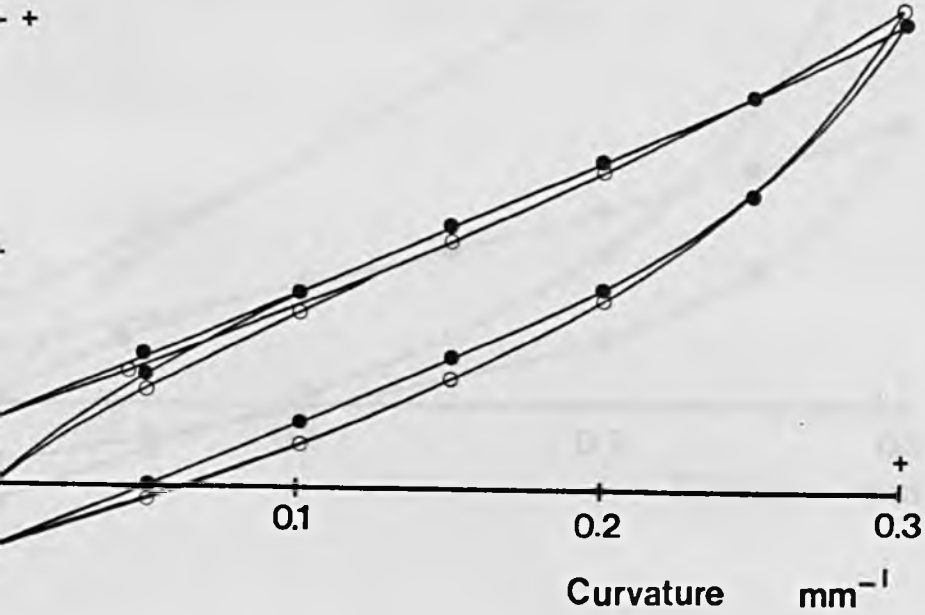

● R60/2 cotton/vincel
○ Warp-wise bending
of fabric X-2

Fig. 58

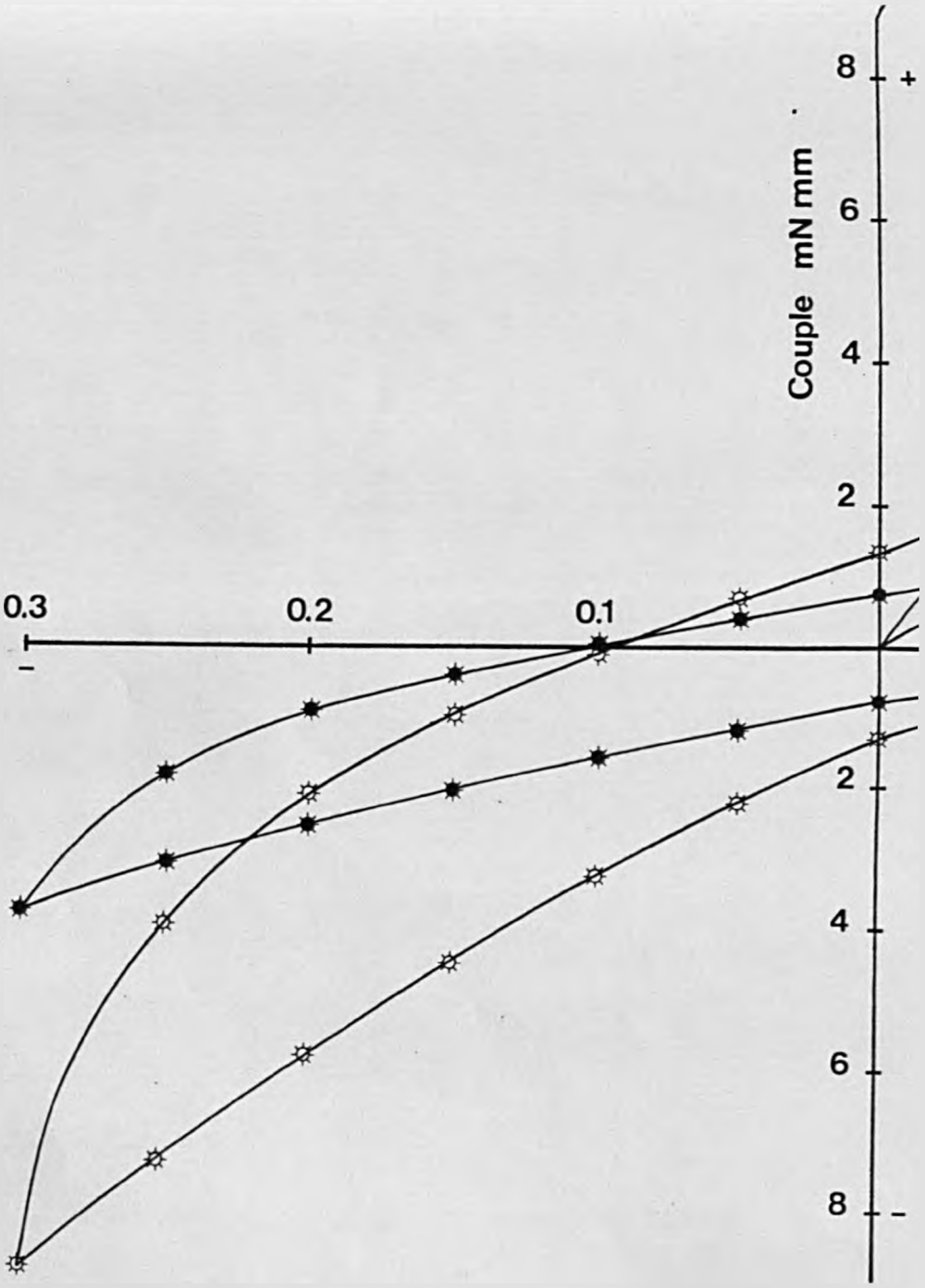
Couple mN mm
8
+
6
4
2
0.3
0.2
0.1
–
2
4
6
8
–

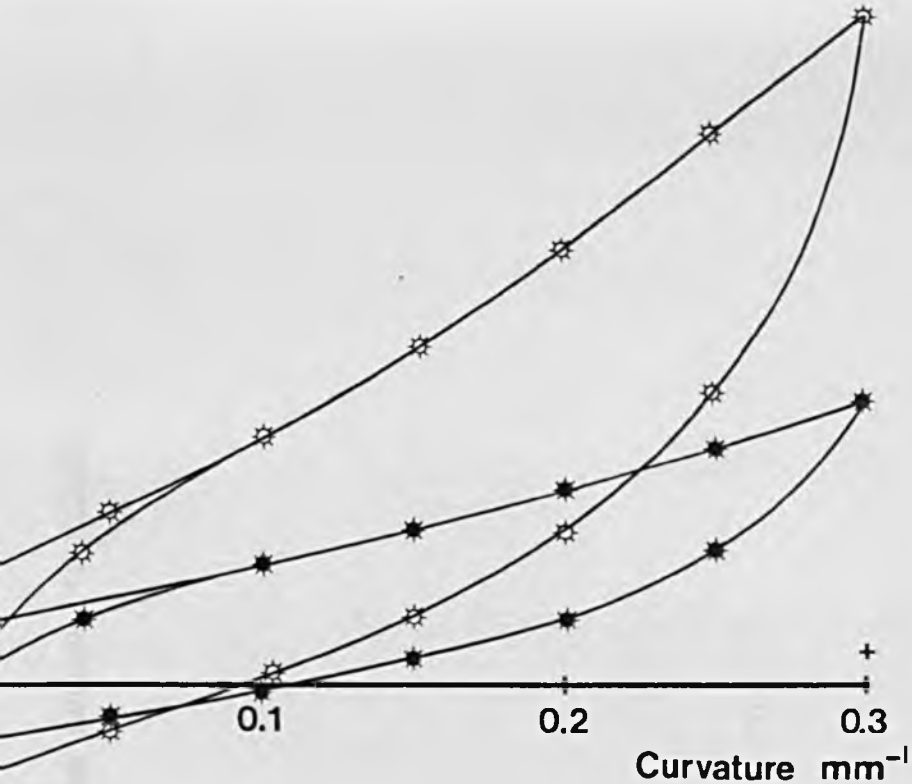

✸ R98/2 cotton
✡ Weft-wise bending of fabric Z-3

Fig. 59

CHAPTER 4: RESULTS AND DISCUSSION

CHAPTER 4

RESULTS AND DISCUSSION

4.1 Introduction

In this chapter the experimental data obtained for both the fabric dimensional properties and for the yarn mechanical properties, previously presented, are used in conjunction with the theoretical relations, derived earlier, to calculate the initial fabric behaviour under tensile and bending deformations. The discrepancies and agreements of these calculations with the actual fabric behaviour, as obtained experimentally, will then be discussed, especially with regard to the theoretical assumptions and difficulties encountered in some experimental measurements.

4.2 A Discussion of the Initial Tensile Properties of Plain Fabrics

In the theoretical analysis of the fabric initial tensile properties, the behaviour under both uniaxial and biaxial tensions was described. However, due to the absence of an apparatus which tests the fabric under biaxial loading, most of the experimental work was directed to checking the validity of the theory under uniaxial loading conditions. The theoretical equations related to biaxial loading will only be briefly discussed later in this chapter.

It may be useful at this stage to reconsider the general aspects of the mechanism of fabric tensile behaviour, that may be observed from the experimental curves of the fabrics used.

4.2.1 The experimental curves of the fabric load-extension

Figures 60-65 show the behaviour, under tensile test, of all the fabrics used in the experiments; the fabrics were extended up to 10-12% in the warp direction and 6-8% in the weft direction. The general features of these curves can be summarized as follows:

1. Unlike what is theoretically expected, the majority of these finished fabrics do not exhibit the relatively high initial moduli of a typical fabric, as shown in figure 1, and which is attributed to friction effects. On the contrary, most of the fabrics showed a relatively easy initial extension, linearly increasing with the load, up to a value of extension in the range 1.5% to 4%. This initial neo-Hooke behaviour (referred to as OE in the figures), with the fabrics used, holds valid up to the relatively high region of 3-4% fabric extension in cases where the yarns in the load direction have a considerable amount of crimp. Such conditions are usually associated with a relatively low fabric modulus and this can be seen with all fabrics in groups X,Y and Z when extended in the warp direction. On the other hand, the straight line relation represents the initial tensile behaviour only up to a value of fabric extension in the range 1.5% to 2%, if the yarns in the load direction have a low crimp value, and the resultant initial fabric modulus in such cases is relatively high. This latter behaviour is noticeable with all the fabrics in groups X,Y and Z, when extended in the weft direction. The rate of initial extension therefore undoubtedly depends on the crimp.

   It is of interest to note that De Jong and Postle (66) defined the initial tensile deformation by the extension which corresponds to a load/yarn in the range $0 \leqslant f \leqslant 2B/\ell^2$. In the above discussion of the

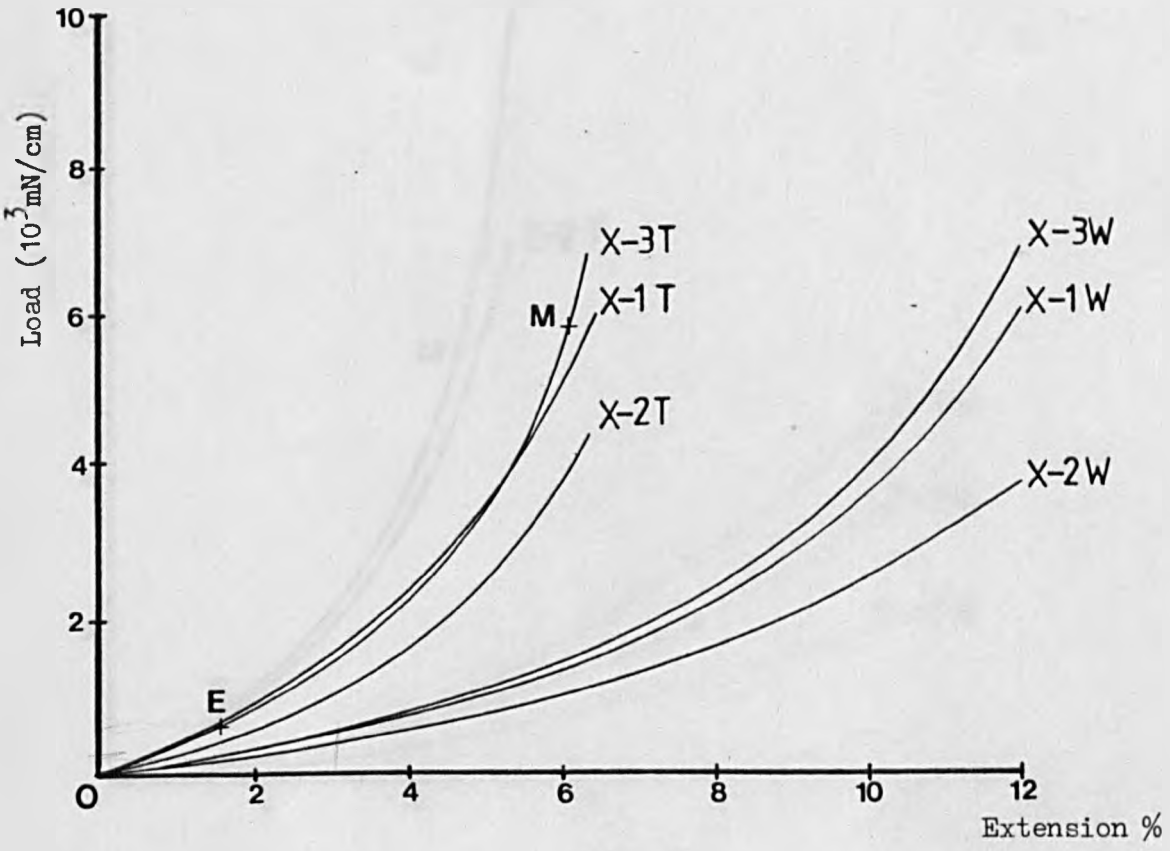

Fig. 60

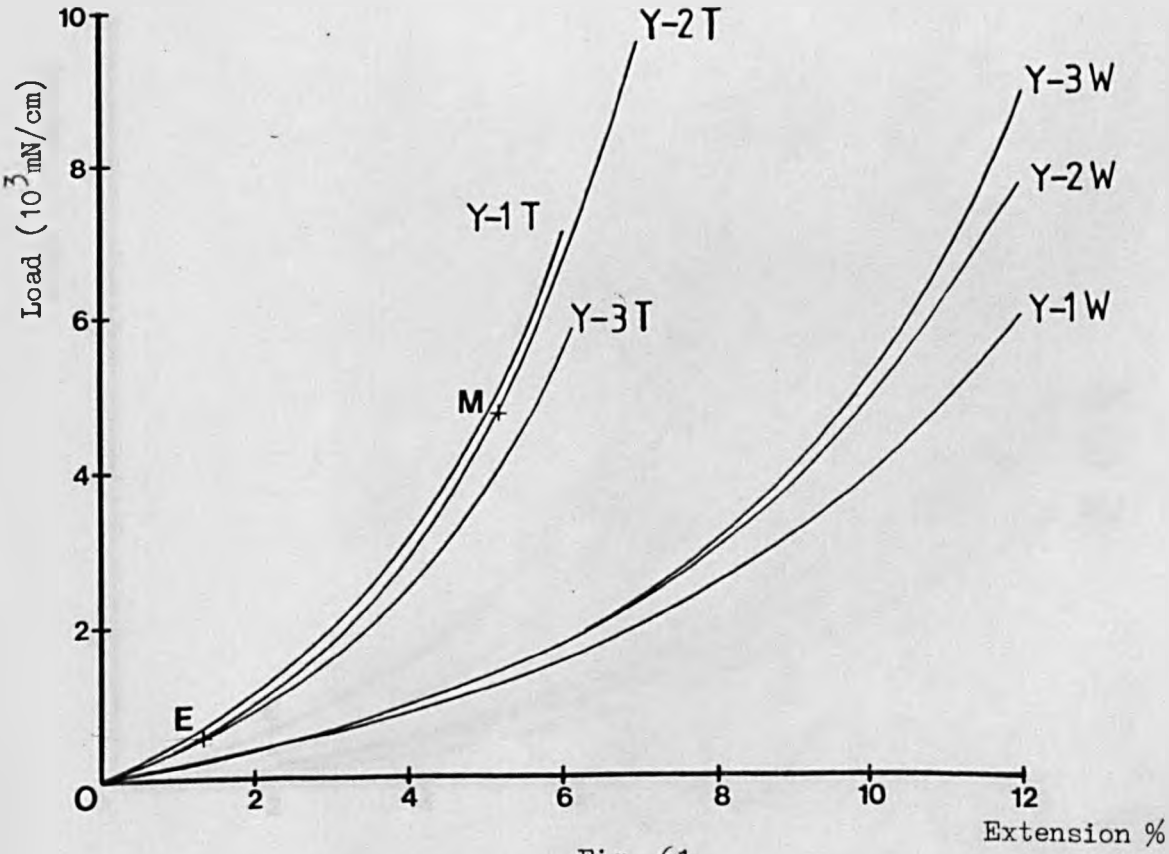

Fig. 61

W (warp) and T (weft) indicate the direction of fabric extension

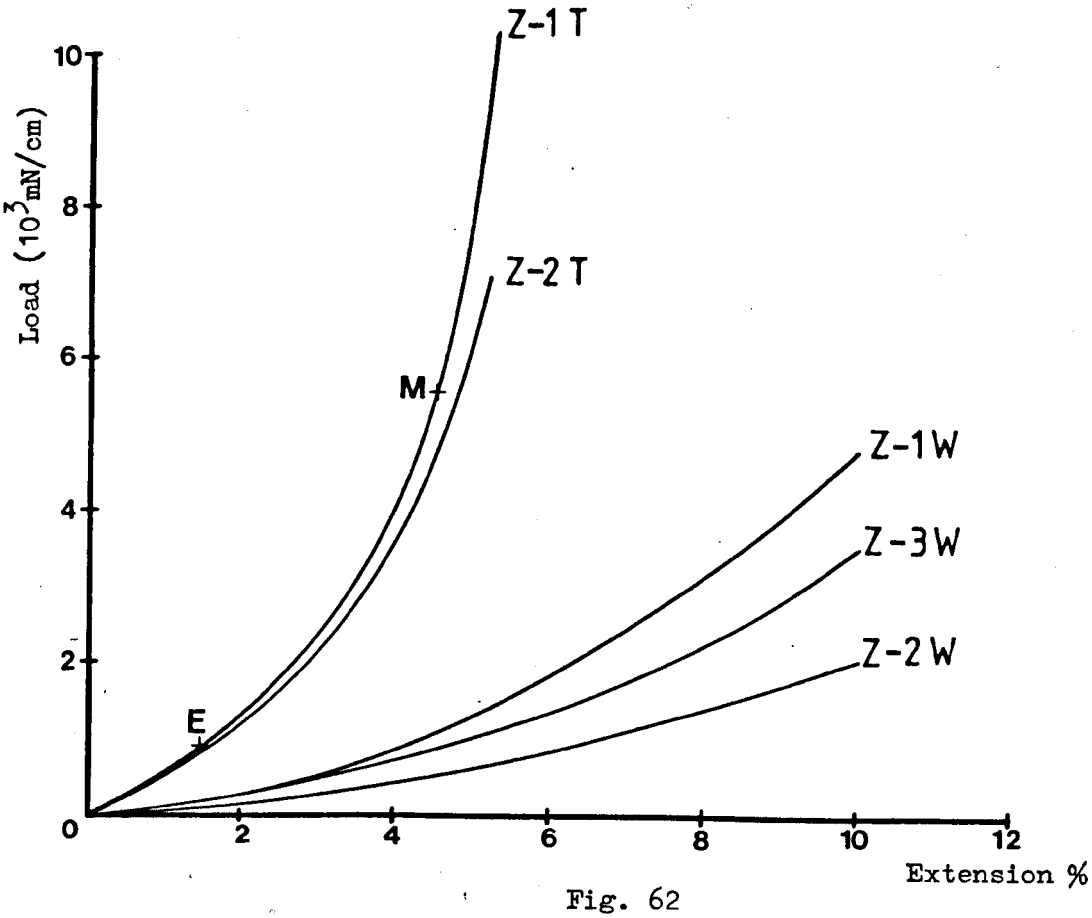
Z-1 T
Z-2 T
Z-1W
Z-3W
Z-2W
M
E
Load (10^3mN/cm)
Extension %
0
2
4
6
8
10
12

Fig. 62

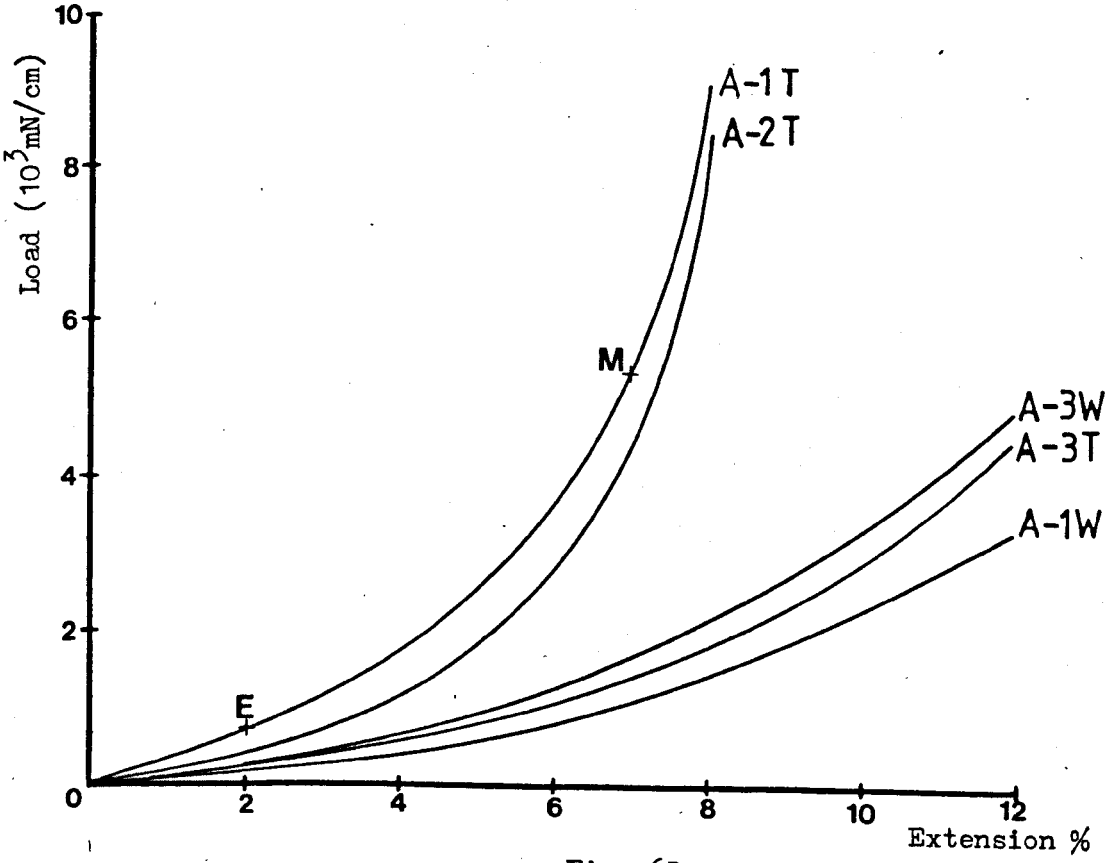
A-1 T
A-2T
A-3W
A-3T
A-1W
M
E
Load (10^3mN/cm)
Extension %
0
2
4
6
8
10
12

Fig. 63

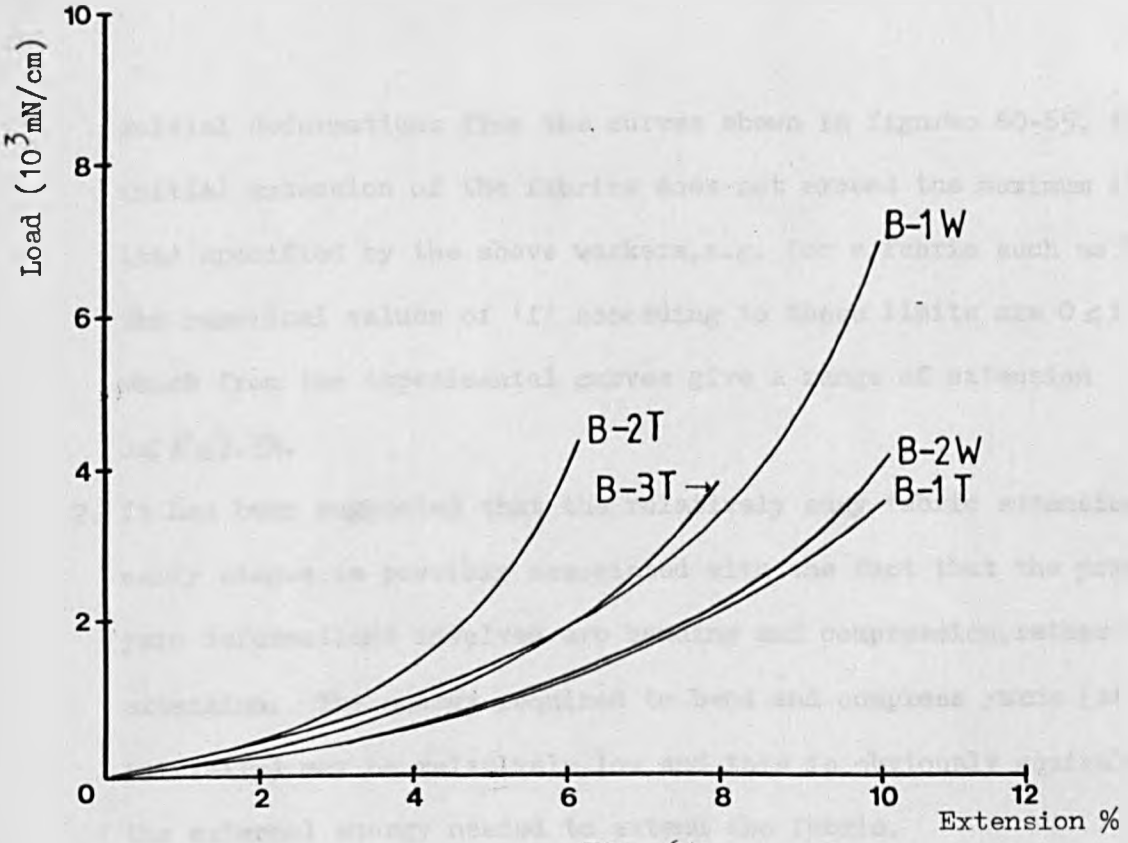
Load (10^3mN/cm)
10
8
6
4
2
0
2
4
6
8
10
12
Extension %
B-1W
B-2T
B-3T
B-2W
B-1T

Fig. 64

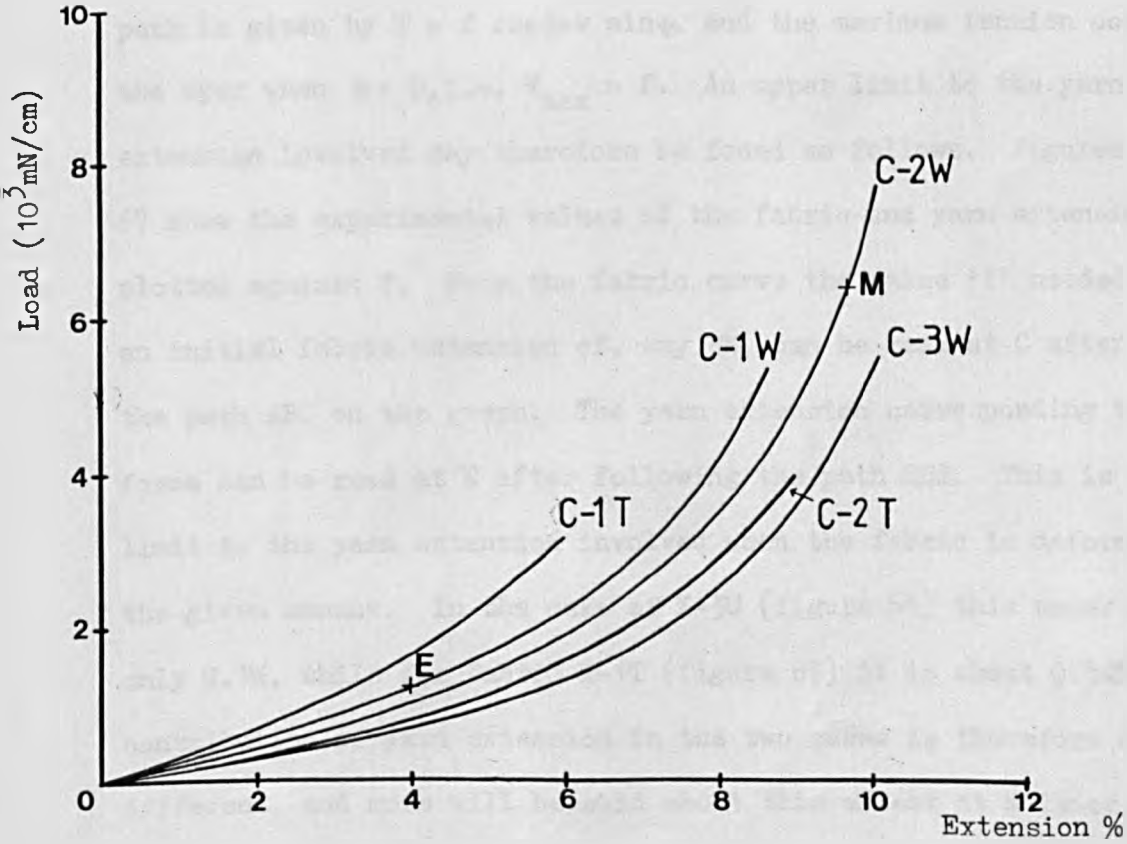
Load (10^3mN/cm)
10
8
6
4
2
0
2
4
6
8
10
12
Extension %
C-2W
M
C-1W
C-3W
C-1T
C-2T
E

Fig. 65

initial deformations from the curves shown in figures 60-65, the initial extension of the fabrics does not exceed the maximum limit of load specified by the above workers, e.g. for a fabric such as X-1W, the numerical values of 'f' according to these limits are $0 \leqslant f \leqslant 23$mN, which from the experimental curves give a range of extension $0 \leqslant \varepsilon \leqslant 3.3\%$.

2. It has been suggested that the relatively easy fabric extension in the early stages is possibly associated with the fact that the primary yarn deformations involved are bending and compression, rather than extension. The energy required to bend and compress yarns (at least initially) may be relatively low and this is obviously equivalent to the external energy needed to extend the fabric.

   It is possible to examine the magnitude of the role played by yarn extension in the following way. The yarn tension at any point on its path is given by $T = f \cos\Psi + v \sin\Psi$, and the maximum tension occurs at the apex when $\Psi = 0$, i.e. $T_{max} = f$. An upper limit to the yarn extension involved may therefore be found as follows. Figures 66 and 67 show the experimental values of the fabric and yarn extensions plotted against f. From the fabric curve the value 'f' needed to produce an initial fabric extension of, say 3%, can be read at C after following the path ABC on the graph. The yarn extension corresponding to this force can be read at E after following the path CDE. This is an upper limit to the yarn extension involved when the fabric is deformed by the given amount. In the case of X-3W (figure 66) this upper limit is only 0.1%, while for fabric X-1T (figure 67) it is about 0.54%. The contribution of yarn extension in the two cases is therefore quite different, and more will be said about this effect at a later stage.

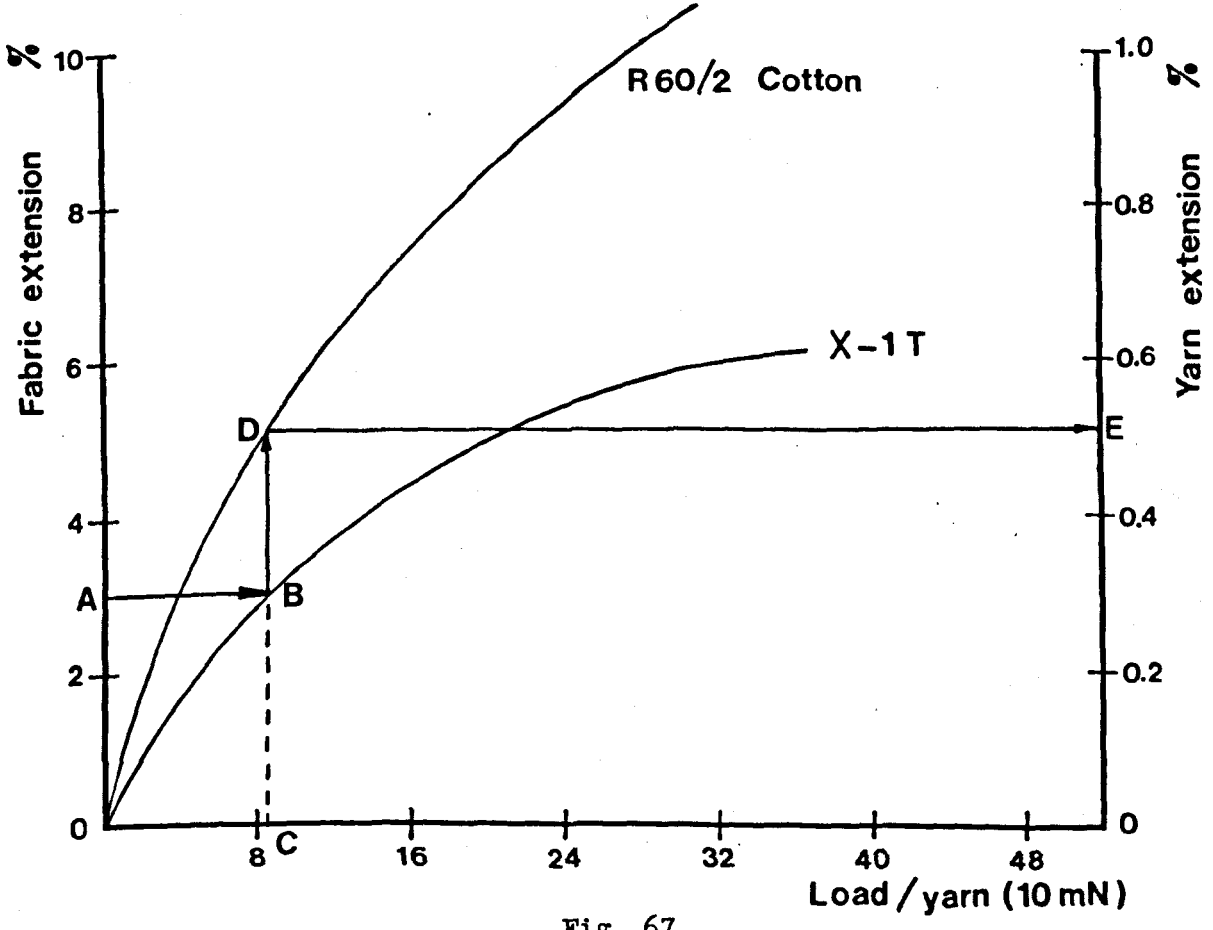
%
10
8
6
4
2
0
Fabric extension
R60/2 Cotton
X-1T
D
E
A
B
C
1.0
0.8
0.6
0.4
0.2
0
%
Yarn extension
8
16
24
32
40
48
Load / yarn (10 mN)

Fig. 67

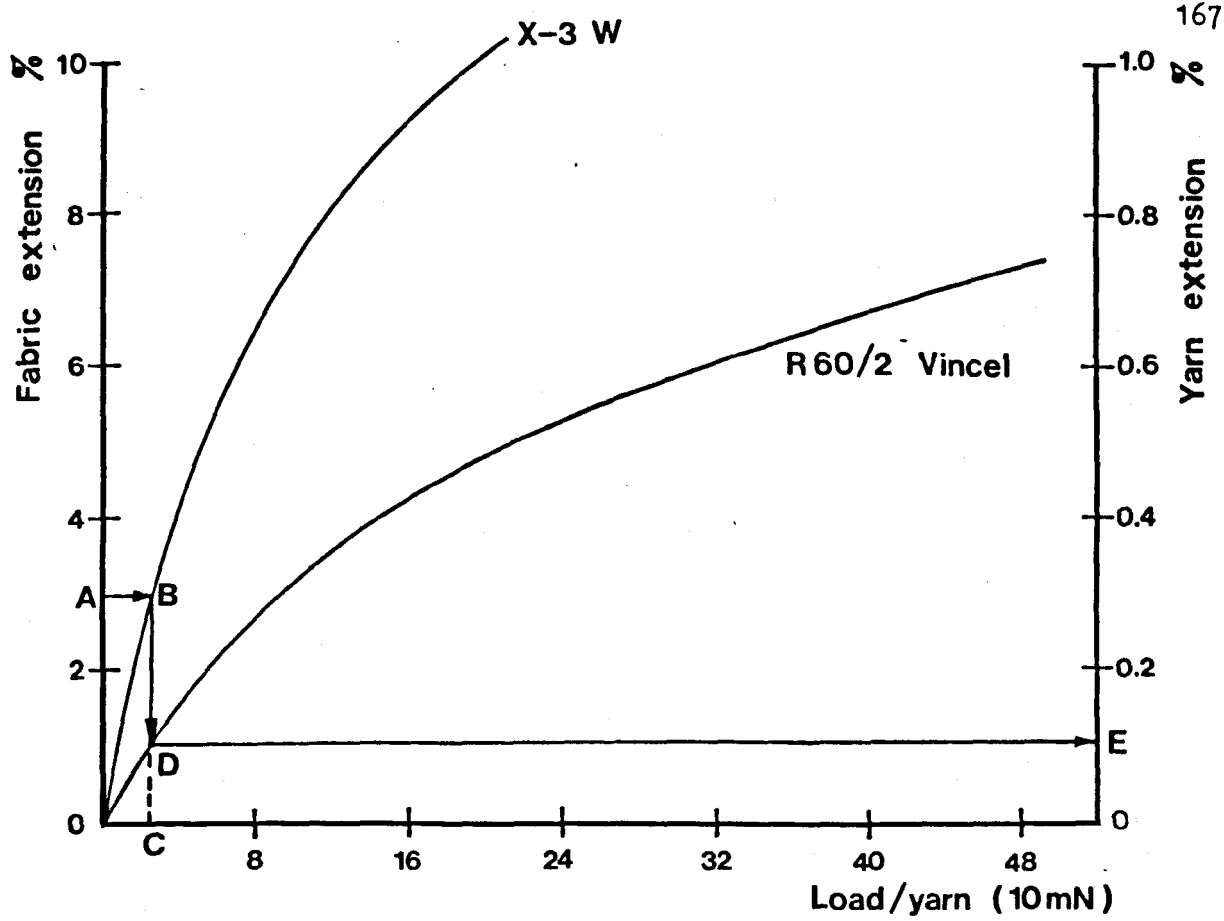
X-3 W
R60/2 Vincel
Fabric extension %
Yarn extension %
10
8
6
4
2
0
1.0
0.8
0.6
0.4
0.2
0
A
B
C
D
E
8
16
24
32
40
48
Load/yarn (10mN)

Fig. 66

3. The next phase, after the initial (indicated by EM in figures 60-65), shows non-linear increasing values of load as the fabric extension develops, yielding higher values for the fabric modulus. This suggests that the fabric deformation has 'taken up the slack' and that the tensile behaviour is progressively becoming more dependent on those yarn properties which require greater energy changes to deform them. Also, the contribution of the crossing threads to the fabric resistance to extension is probably increasing. Unless jamming occurs, this crimp redistribution is expected to continue.
4. The fabric behaviour eventually reaches a phase of very rapid increase in modulus. This seems to occur at, or a little beyond, the point when the fabric extension is equal to the yarn crimp value, e.g. for fabric X-3T (c_2 = 0.046) this point is indicated by M in figure 60 where it can be seen that the corresponding fabric extension is nearly 6%. The above mentioned phase probably starts when the yarn crimp is totally eliminated or when jamming occurs; consequently, no further crimp interchange or yarn flattening would take place and the fabric extension would be mainly dependent on the yarn tensile properties.

4.2.2 The experimental curves of the fabric length extension-width contraction

The behaviour of the fabrics under this test is shown in figures 39-56. An important feature of these curves is the fact that they lead to low values of the initial Poisson's ratio. In some cases there is a delayed contraction (sometimes it does not take place until there is as much as 2-3% fabric length extension e.g. Z-1W and A-2W in figures 45 and 49). This suggests that a mechanism of fabric extension with yarn compression as an important factor is taking place, which reduces the value of the width

contraction. Obviously this effect depends on how easily compressed are both of the two systems of yarns, and on other factors which determine the magnitude of the interyarn forces at the intersections.

When the test was carried out on fabrics having high crimp values in the load direction, such as the fabrics in groups X,Y and Z when extended in the warp direction (c_1 = 17-22%), the trend of the Poisson's ratio,up to the maximum extension employed on the tests (12%),can be described to be of ever increasing values. However, this was not the case for the fabrics which have low crimp values in the load direction, such as fabrics in groups X,Y and Z when extended in the weft direction e.g. X-3T and Z-2T in figures 41 and 46. A point which is worth noting is that the width contraction vs. length extension produces curves that sometimes show an inflection point. Such behaviour may be associated with the crimp interchange mechanism in the following way. Since the latter takes place until the yarns in the load direction are almost straight (assuming no jamming occurs), the fabric length extension beyond this limit becomes almost independent of the crossing yarn resistance and little or no further changes in the interyarn forces may occur; consequently one should expect correspondingly little or no further width contraction. The fabric Poisson's behaviour could, then, be expected to be in the form shown in figure 68a,which shows the experimental data for fabrics in group X, extended in the weft direction (note that the weft crimp values of these fabrics are less than the maximum extension employed in the tests).

Based on the analysis described earlier in section 1.3.3, Huang (4) gave theoretical curves for the relation between the fabrics' load-length extension and load-width contraction. From these curves it is

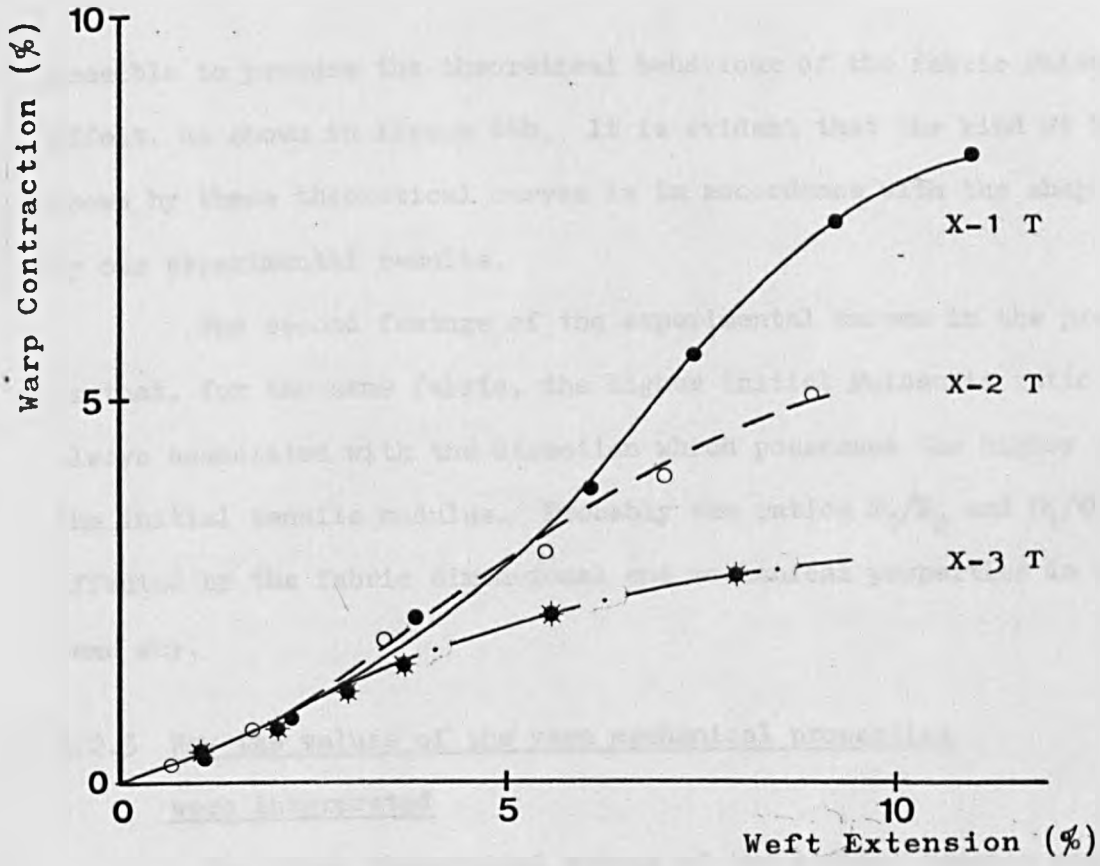

Fig. 68a

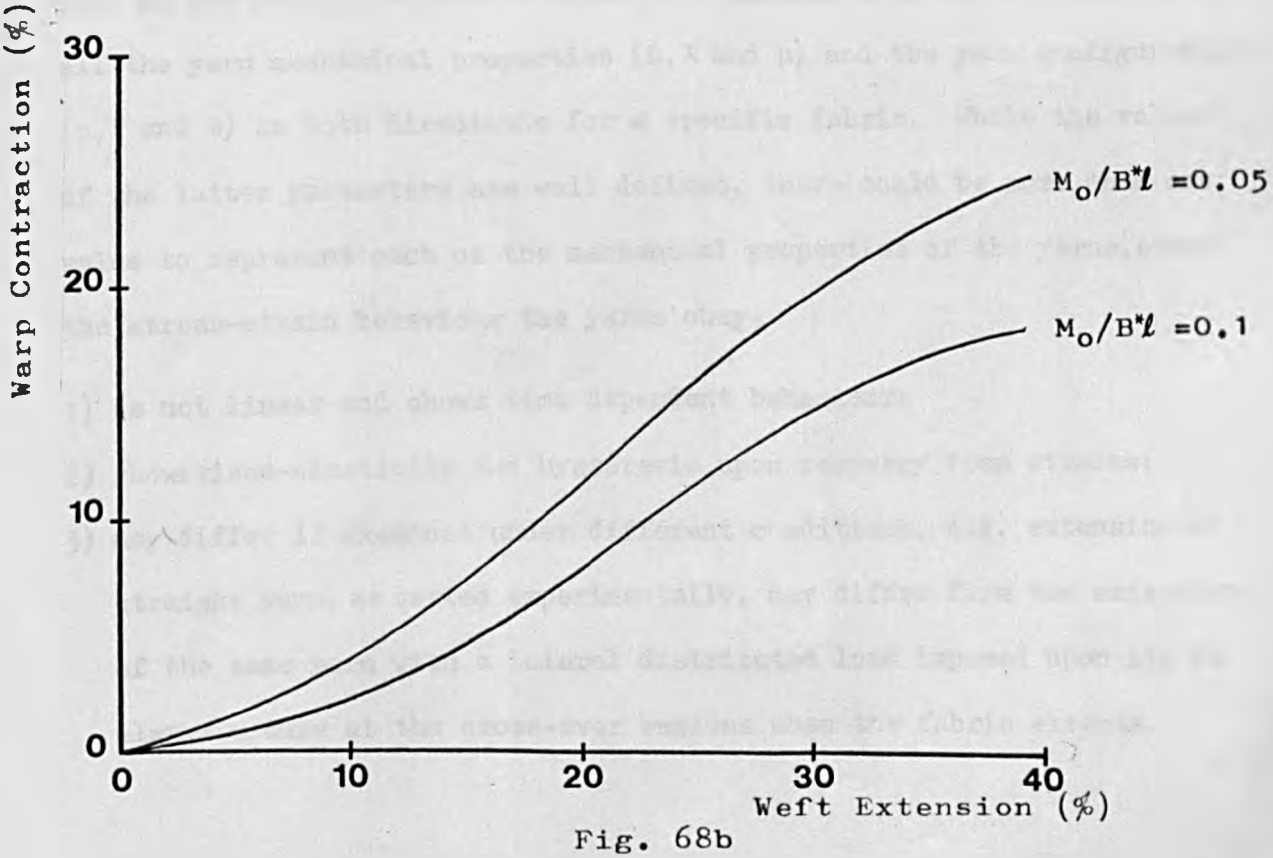

Fig. 68b

$c_2 \simeq 0.19$, $c_1 \simeq 0.14$, $B^*/B=10$, $\lambda/\mu=0.3$, fabric warp and weft yarns are of the same mechanical properties

possible to produce the theoretical behaviour of the fabric Poisson's effect, as shown in figure 68b. It is evident that the kind of behaviour shown by these theoretical curves is in accordance with the shape obtained by our experimental results.

The second feature of the experimental curves in the present work is that, for the same fabric, the higher initial Poisson's ratio is always associated with the direction which possesses the higher value of the initial tensile modulus. Probably the ratios E_1/E_2 and σ_1/σ_2 are affected by the fabric dimensional and mechanical properties in much the same way.

4.2.3 How the values of the yarn mechanical properties were interpreted

The final theoretical values of the initial tensile modulus, as well as the initial Poisson's ratio, are dependent on the interaction of all the yarn mechanical properties (B, λ and μ) and the yarn configurations (p, ℓ and θ) in both directions for a specific fabric. While the values of the latter parameters are well defined, there could be more than one value to represent each of the mechanical properties of the yarns, since the stress-strain behaviour the yarns obey:

1) is not linear and shows time dependent behaviour;
2) shows visco-elasticity and hysteresis upon recovery from strains;
3) may differ if examined under different conditions, e.g. extension of straight yarn, as tested experimentally, may differ from the extension of the same yarn with a lateral distributed load imposed upon it, as always occurs at the cross-over regions when the fabric extends.

These are obviously complicating factors, which will be discussed for each yarn property individually.

The yarn bending property involved in the initial fabric extension

A major factor affecting the initial fabric extension behaviour is the mode of bending of the component yarns. In the analysis, this bending behaviour is assumed to be linear and represented by a flexural rigidity B. However, a number of workers (41,45) have shown that, in fact, the bending behaviour of a yarn is non-linear and is more nearly represented by a curve of the type (2) in figure 69. The stress-strain relation tends to be linear beyond a certain value M_0 of the bending couple, and approximations to this behaviour are represented by curves (1) and (3). In these approximations the bending law is:

(1) $M \leqslant M_0$: $1/\rho = 0$

$M > M_0$: $M-M_0 = B/\rho$

(3) $M \leqslant M_0$: $M = B^*/\rho$

$M > M_0$: $M-M_0 = B/\rho$

In the above relations, B is the slope of the linear part of curve (2), and it was decided to use this value in the following work for the following reasons:

(a) Based on the rough analysis in section 3.4.1, it can be shown that a mean value of the initial change in the yarn curvature involved in 1% fabric extension is of the order of 0.08 mm^{-1}, when the yarns in the load direction are of high crimp, and of the order of 0.2 mm^{-1} for the lower crimped yarns (see the values of $p_{02}dK_1/100dp_2$ in Table3.4). Hence, the initial yarn bending modulus (as commonly defined by the slope of the couple-curvature behaviour up to 0.02 mm^{-1}) will not in

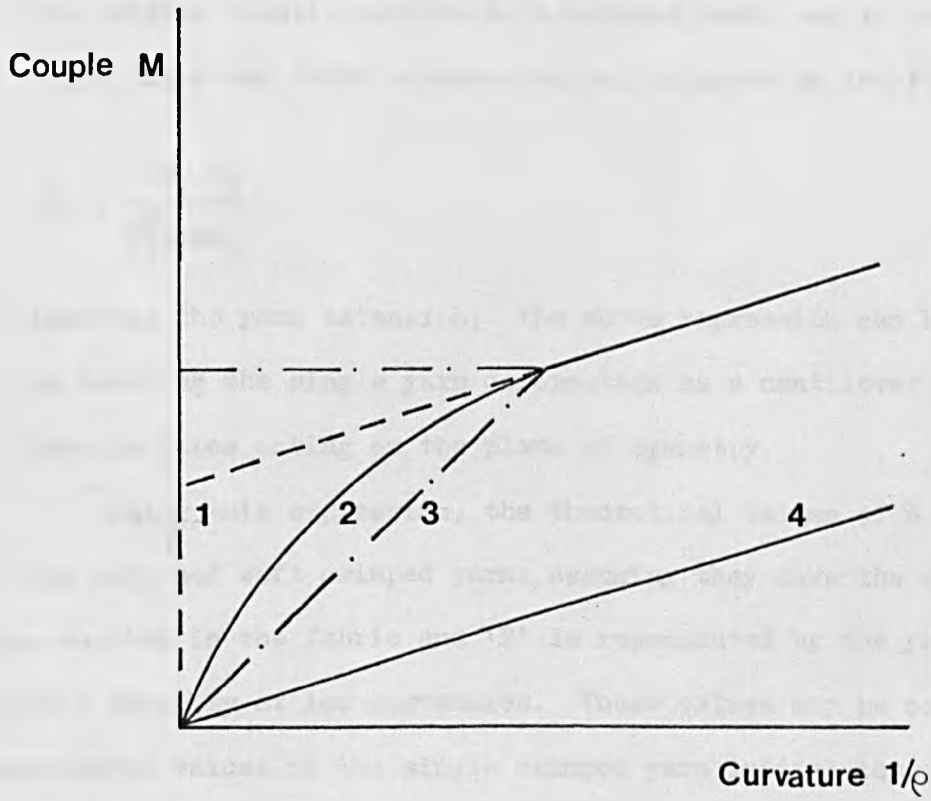

Fig. 69 shows the bending behaviour of yarns

1. Grosberg
2. Experimental
3. Huang
4. Present analysis

general, reasonably represent the yarn behaviour likely to be met in the experiments.

(b) The initial tensile modulus of a crimped yarn, say in the warp direction, which has a saw tooth representation, is given by the following

$$E_1 = \frac{12B_1 p_2}{\ell_1^3 \sin\theta_1} , \qquad (4.1)$$

ignoring the yarn extension; the above expression can be obtained by treating the single yarn deformation as a cantilever deformed by a tensile force acting on the plane of symmetry.

Using this expression, the theoretical values of E were calculated for the warp and weft crimped yarns, assuming they have the same dimensional shape as that in the fabric and 'B' is represented by the yarn elastic flexural rigidity at low curvatures. These values may be compared with the experimental values of the single crimped yarn initial tensile modulus, calculated from the curves described in section 3.4.2. The comparison, given in Table 4.1, suggests that the values of B chosen will, in general, give a fair representation of the yarn bending property involved in the initial fabric extension.

The yarn compressional property involved in the initial fabric extension

The initial compression behaviour of previously undistorted yarn obviously differs from the initial behaviour of the same yarn inside the fabric, since the latter can be regarded as already having undergone cyclic compression strains during the fabric formation. A partial recovery from these strains has then taken place during the succeeding finishing process. After relaxation, the fabric is finally set into shape when dried, with a

Table 4.1

Theoretical and experimental values for the crimped yarn initial tensile modulus ($\lambda = \infty$)

Fabric group	Fabric No.	E_1(mN)		E_2(mN)	
		Theoretical	Experimental	Theoretical	Experimental
X	1	392	372	2384	1780
	2	299	285	2537	1651
	3	305	321	3050	2726
Y	1	319	349	3324	2724
	2	270	252	3455	2868
Z	2	162	183	7264	4359
	3	229	238	5308	4967
A	1	300	323	1826	1425
	2	394	405	1457	1214
	3	555	580	620	671
B	1	849	854	576	568
	2	406	490	1286	1187
	3	402	516	1331	1343

smaller yarn thickness than the initial value. When the fabric deforms in extension or in bending, the interyarn forces, thus developed, will cause the yarn cross-section to start another cycle. The best estimate of the yarn initial compression modulus in the fabric can therefore be obtained experimentally by an apparatus that can provide such cyclic compression strains in which the second cycle should start at the same thickness as that of the yarn inside the fabric. The apparatus actually used, however, does not provide this facility, and a procedure therefore had to be developed that would provide an estimate of the necessary information.

The compression modulus, μ, is defined by the following relation

$$V = \mu \varepsilon_d,$$

where V is the compressive force (considered as a point load) and ε_d is the fractional change in yarn thickness $(\frac{T-T_0}{T_0})$.
Differentiating the above expression we get

$$dV = \mu d\varepsilon_d .$$

In practice a point load does not exist and therefore V may be defined in terms of the intensity of load x(mN/mm), assumed uniformly distributed over the contact length, ℓ_c, between warp and weft i.e. $V = \ell_c\, x$ and $dV = \ell_c dx$. Substituting in the above expression we get

$$\ell_c . dx = \mu d\varepsilon_d$$

$$= \mu \frac{dT}{T_0} ,$$

or

$$\mu = (\ell_c . T_0)/(\frac{dT}{dx}) .$$

In the above expression 'T_0' corresponds to the initial yarn thickness inside the fabric, denoted previously by b, which was defined by the experimental procedure in section 3.3.3; this procedure also enables ℓ_c to be estimated. From the experimental curve or the fitted empirical formula of the yarn compressional behaviour, the equivalent load, say x_0, to the thickness b can be found either by a graphical or by an interpolation method. Assuming that the change in yarn thickness under cyclic loading will have the behaviour shown in figure 70, we may regard the slopes of the tangents to the curve at the points 'e' and 'g'as nearly equal. Thus the rate of change of the yarn thickness inside the fabric is given by $(\frac{dT}{dx})_{x=x_0}$. This is obtained from the empirical formula (3.6) by

$$(\frac{dT}{dx})_{x=x_0} = \sum_{j=1}^{j=3} A_j B_j e^{-B_j x_0} .$$

The compression modulus is thus finally given by the expression

$$\mu = \ell_c . b / \sum_{j=1}^{j=3} A_j B_j e^{-B_j x_0} .$$

The yarn tensile property involved in the initial fabric extension

The tensile behaviour of yarns of normal twist such as those used in this work show a low initial modulus, rapidly increasing with the further extension. This behaviour may be fitted to a relation, as suggested by Nordby (2), of the form

$$\varepsilon_y = kT^n , \qquad 0<n<1$$

where ε_y is the yarn extension, T is the tensile load, and k and n are constants.

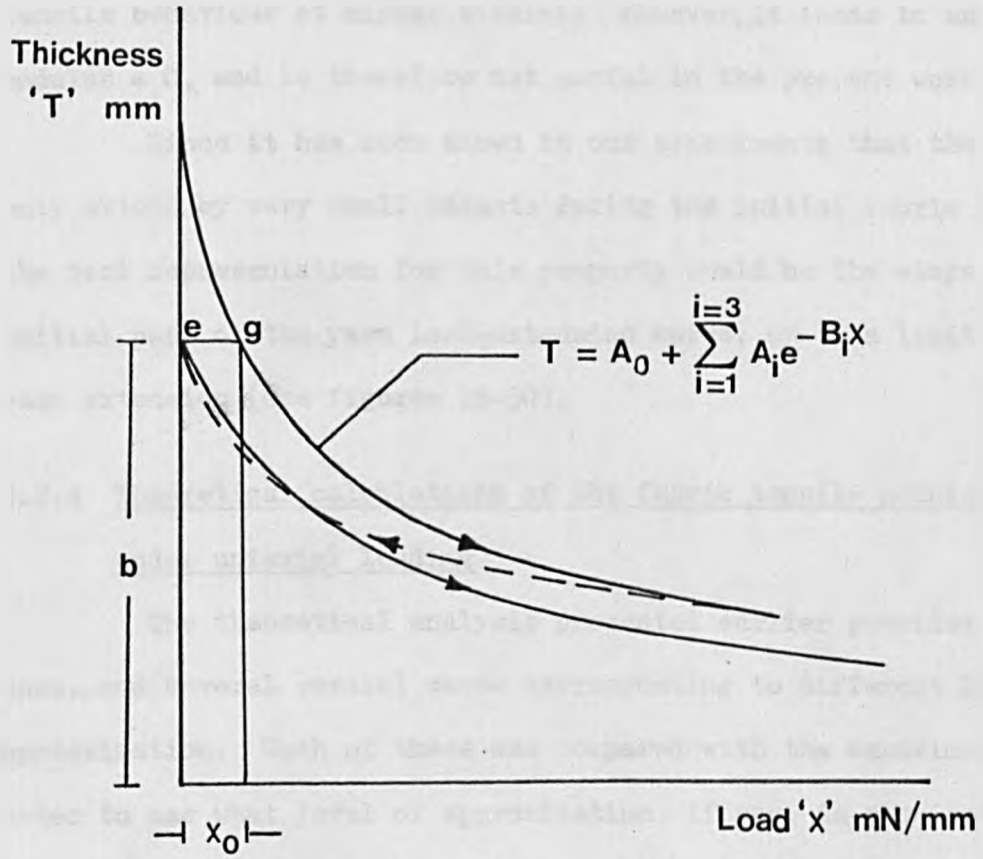

Fig. 70

Such a relation may be useful when investigating the fabric tensile behaviour at higher strains; however, it leads to an initial modulus = 0, and is therefore not useful in the present work.

Since it has been shown in our experiments that the yarns would only extend by very small amounts during the initial fabric extension, the best representation for this property would be the slope of the very initial part of the yarn load-extension curve, up to a limit of 0.1%-0.2% yarn extension (see figures 29-30).

4.2.4 Theoretical calculations of the fabric tensile modulus under uniaxial loading

The theoretical analysis presented earlier provides a general case, and several special cases corresponding to different levels of approximation. Each of these was compared with the experimental data in order to see what level of approximation, if any, is required to give reasonable agreement between theory and experiments.

Case 1: Calculations assuming inextensible and incompressible yarns

The simplest theoretical expression for the fabric initial tensile modulus is provided by this case and is given by equation (2.7), namely

$$E_1 = \frac{12B_1p_2}{p_1\ell_1^3\sin^2\theta_1}\left[1+\frac{B_2\ell_1^3\cos^2\theta_1}{B_1\ell_2^3\cos^2\theta_2}\right]. \qquad (2.7)$$

In order to calculate E_1 from this equation it was necessary to evaluate the weave angles θ_1 and θ_2. According to the fabric model, we have

$$\theta_1 = \cos^{-1}(p_2/\ell_1) \qquad \text{and} \qquad \theta_2 = \cos^{-1}(p_1/\ell_2).$$

The theoretical calculations for E_1 and E_2 plotted against the experimental values are shown as circles in figure 71, and these deviate considerably from the straight line drawn on the graph which indicates perfect agreement between theory and experiment. In fact, the mean value of $\frac{E(\text{experimental})}{E(\text{theoretical})}$ is 0.49 which means that the theoretical values are, on average, nearly twice the experimental values. The reason for this can be explained if we consider the force needed to extend the fabric to a unit extension (100%). This force can be divided into a force F_1', which is the contribution of the warp threads to the fabric resistance to extension, and a force F_1'' which is the cross yarn's contribution. Equation (4.1) shows that

$$F_1' = \frac{12B_1 \cdot p_2}{p_1 \ell_1^3 \sin^2\theta_1} \quad , \tag{4.2}$$

and from equation (2.7) F_1'' is then given by

$$F_1'' = \frac{12B_1 p_2}{p_1 \ell_1^3 \sin^2\theta_1} \; \frac{B_2 \ell_1^3 \cos^2\theta_1}{B_1 \ell_2^3 \cos^2\theta_2} \quad , \tag{4.3}$$

for incompressible and inextensible yarns.

In fact, if the yarns are compressible, the contribution F_1'' would be far less, as will be seen later by considering a similar expression of F_1'' in Case 2. In addition, depending on the value of θ_1, both warp and weft contributions to the fabric resistance to extension are further reduced if the yarn extensibility is also included, as will be shown by examining the general case.

In the hope that for practical purposes we can avoid the necessity to define the tensile and compressional properties of the yarn, another

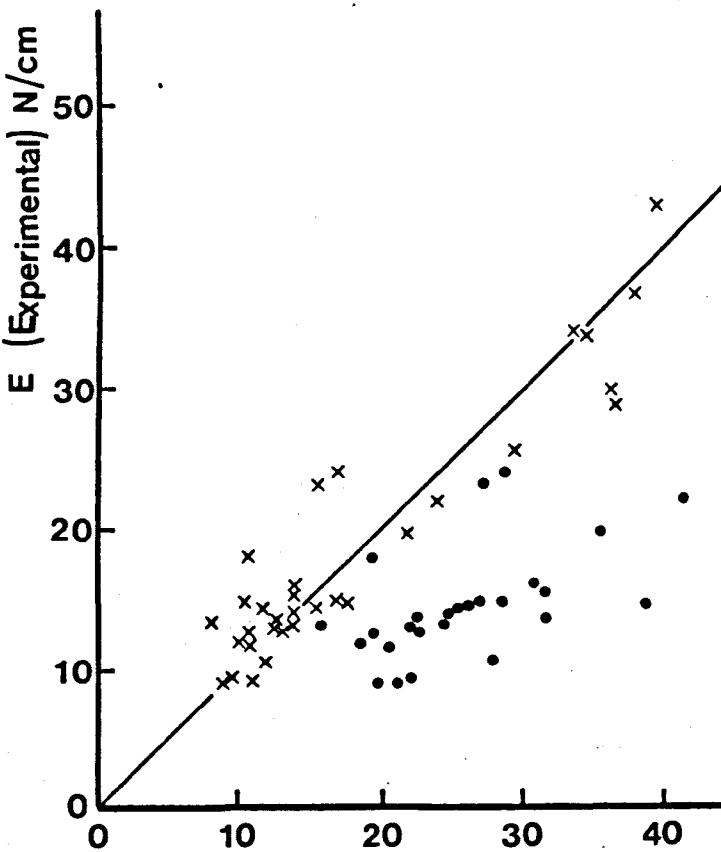
E (Experimental) N/cm
50
40
30
20
10
0
0
10
20
30
40

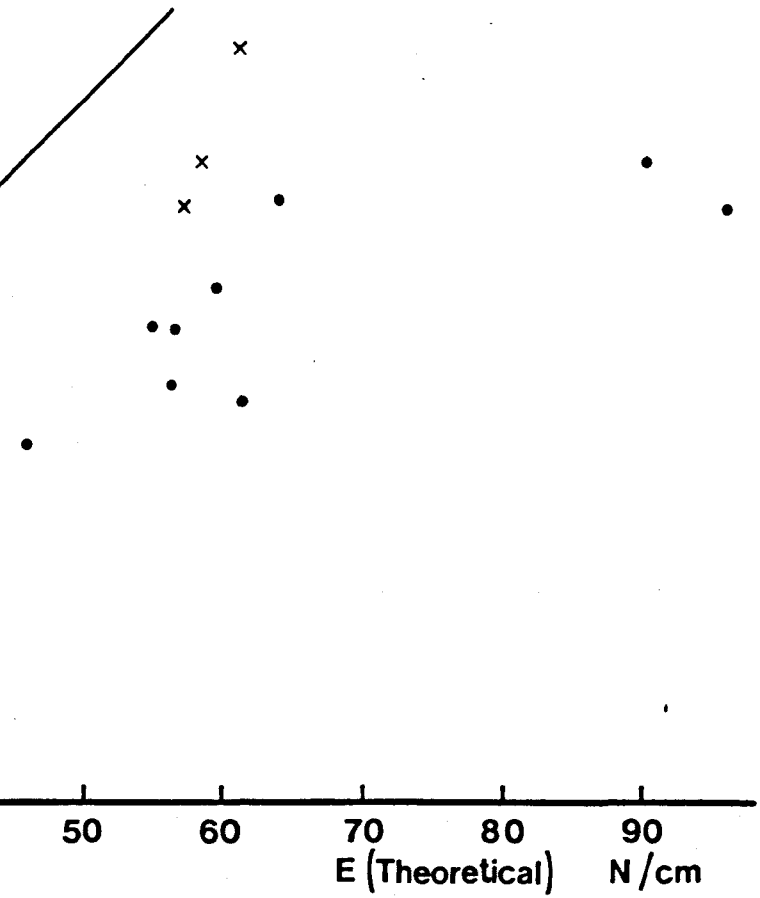

Fig. 71

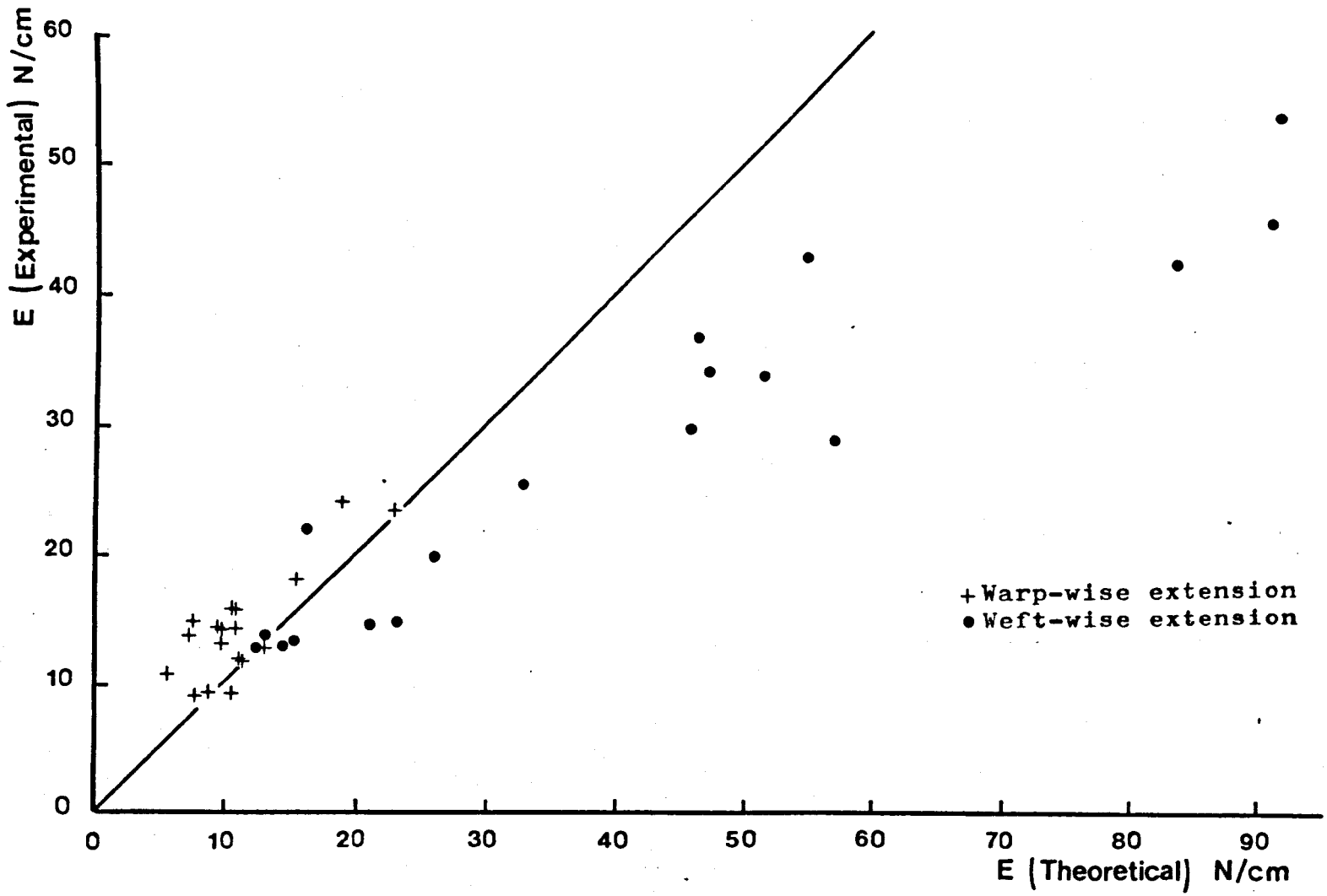

Fig. 72

Theoretical and experimental values of the fabric initial tensile modules (yarns are assumed inextensible)

approach was followed. When presenting his rigid-thread model, Peirce showed that

$$\theta_1 = 106(\ell_1/p_2-1)^{\frac{1}{2}} \qquad \text{and} \qquad \theta_2 = 106(\ell_2/p_1-1)^{\frac{1}{2}} ,$$

where the angles are measured in degrees. When the values calculated from these relations were used in equation (2.7), quite good agreement between the theory and the experimental results were obtained, as can be seen from the points plotted as crosses in figure 71. It is obvious that in employing this procedure there is an element of inconsistency in that two fabric models have been used, one to derive the expression for the initial modulus and another to estimate the weave angles, but the resulting agreement seems to justify it. However, while this procedure has resulted in reasonable agreement between theory and experiment, so far as initial fabric moduli are concerned, it will be shown later that it does not produce satisfactory estimates of the initial Poisson's ratios. Consequently, we proceed to investigate the effect of the yarn compression on the initial modulus.

Case 2: Calculations assuming compressible but inextensible yarns

The expression for the tensile modulus in this case is given by equation (2.20), i.e.

$$E_1 = \frac{12B_1 \cdot p_2}{p_1 \ell_1^3 \sin^2\theta_1} \left[1 + \frac{B_2 \ell_1^3 \cos^2\theta_1}{B_1 \ell_2^3 \cos^2\theta_2 + 48 B_1 B_2 (d_1/\mu_1 + d_2/\mu_2)} \right]. \qquad (2.20)$$

In this case, the warp contribution to the force needed to produce unit extension has not changed and is still given by equation (4.2); however, the weft contribution is changed to

$$F_1'' = \frac{12B_1 \cdot p_2}{p_1 \ell_1^3 \sin^2\theta_1} \quad \frac{B_2 \ell_1^3 \cos^2\theta_1}{B_1 \ell_2^3 \cos^2\theta_2 + 48 B_1 B_2 (d_1/\mu_1 + d_2/\mu_2)} \cdot \qquad (4.4)$$

When the theoretical calculations were carried out including the effect of yarn compression, a generally better agreement between the theory and experimental was obtained. However, this procedure gives a reasonably close agreement for some fabrics but not for all, as can be seen from figure 72. The best agreement with experimental results is observed with fabrics having high to medium crimp values in the load direction. On the other hand, fabrics in groups X,Y and Z gave high theoretical weft-wise fabric initial moduli, and these represent poor agreement with the experimental data when the yarns in the load direction possess low crimp values. The reason for this is associated with the neglect of the yarn extensibility, as will be discussed in the next case.

General case: Calculation assuming compressible and extensible yarns

Some plain fabrics are made, purposely, with nearly straight yarns in one direction in order to achieve, for example, a rib effect or to obtain certain properties such as better drapability in the cross-wise direction. Such constructions are shown in figure 73. From our point of view, when these fabrics are extended in the direction of the straight yarns, i.e. the weft direction shown in figure 73a, the initial tensile behaviour can not be explained on the basis of crimp redistribution only. Most probably such a mechanism almost vanishes, and the fabric is virtually extended by extending the yarns themselves; thus a comparatively high tensile modulus for the fabric is expected.

Calculations for the general case including the yarn extensibility, as well as its compressibility, were carried out using equation (2.18),

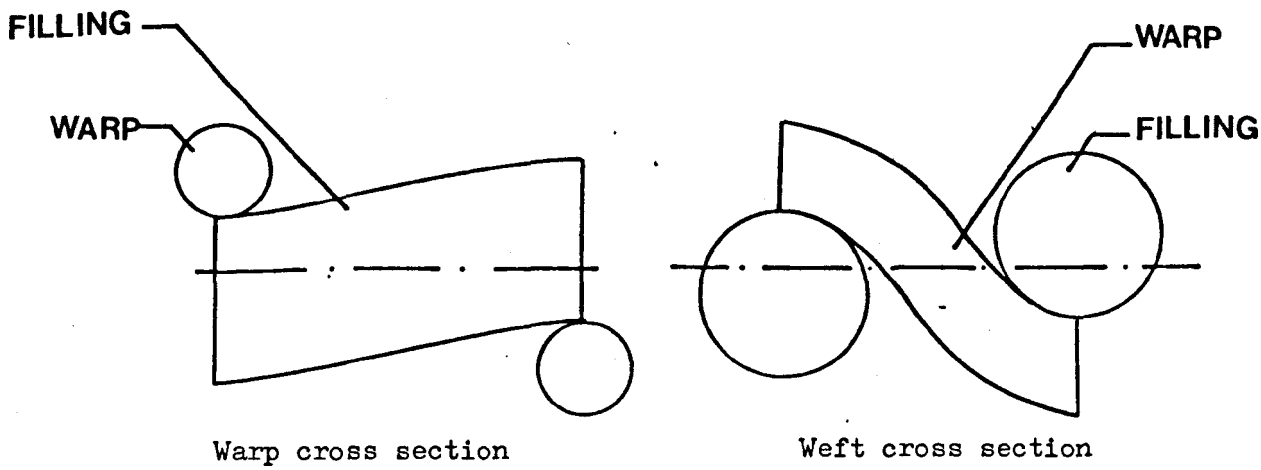

(a) Rib effect produced by using coarse filling and open structure fine slack warp

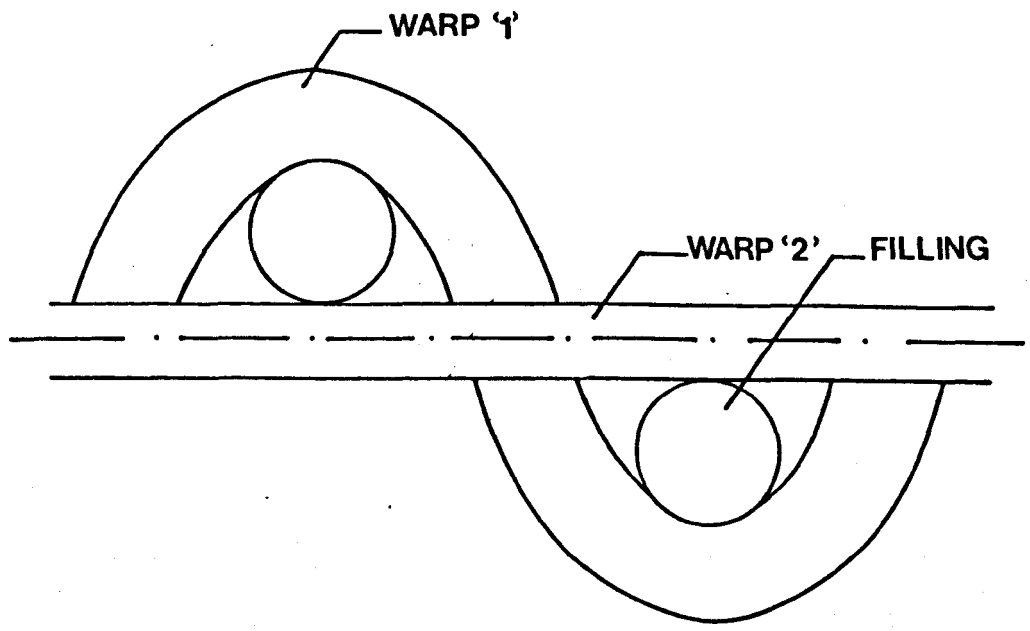

(b) Rib effect produced by using coarse filling and fine highly tensioned warps alternated with coarse slack ones

Fig. 73

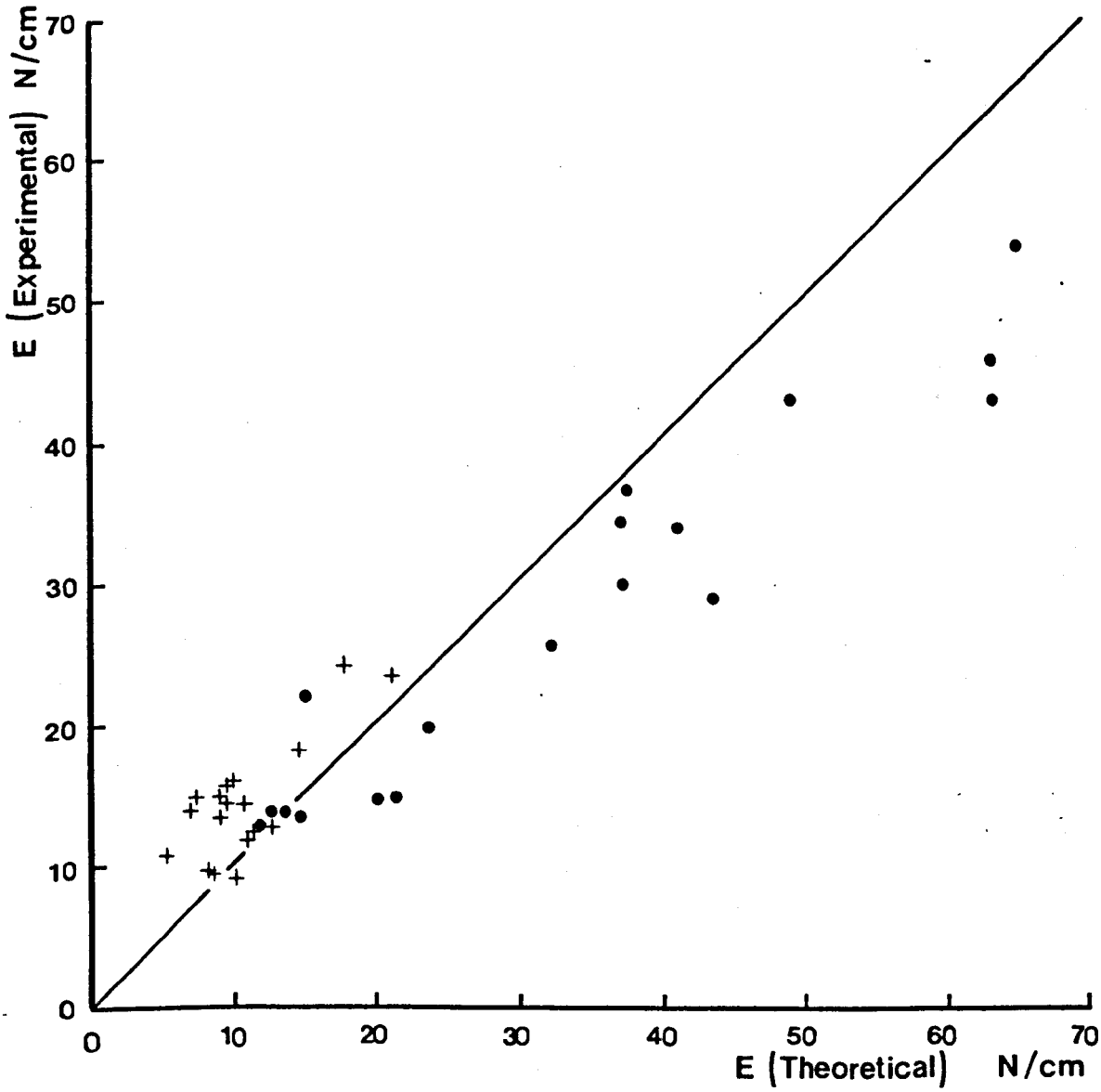

Fig. 74

Theoretical and Experimental values of fabric initial tensile modulus (general case).

+ Fabric extended in warp direction
• Fabric extended in weft direction

Table 4.2

Theoretical and experimental calculations of the initial tensile modulus

Fabric group	Fabric No.	E_1(N/cm) $\lambda's=\infty$ $B_2=0$	$\lambda's=\infty$ $\mu's=\infty$	$\lambda's=\infty$	General case	Experimental values	E_2(N/cm) $\lambda's=\infty$ $B_1=0$	$\lambda's=\infty$ $\mu's=\infty$	$\lambda's=\infty$	General case	Experimental values
X	1	8.09	25.52	11.02	10.72	14.3	40.55	59.36	46.27	38.28	36.6
	2	6.14	22.07	8.62	8.43	9.4	40.67	56.33	45.75	37.55	29.8
	3	6.30	30.41	9.81	9.56	14.2	42.78	53.95	47.19	37.52	34.1
Y	1	6.53	30.79	10.55	10.23	15.9	49.10	62.31	54.69	44.25	42.9
	2	5.50	31.87	10.08	9.79	15.5	46.75	56.50	51.64	41.54	33.8
	3	4.79	38.71	9.64	9.38	14.6	53.25	60.77	57.06	43.72	28.6
Z	1	4.13	31.71	7.20	7.05	13.7	85.81	98.65	91.67	65.38	53.6
	2	3.29	31.10	5.56	5.48	10.6	86.59	96.84	90.99	63.61	45.5
	3	4.68	27.04	7.59	7.43	14.9	76.82	92.88	83.52	63.05	42.4
A	1	6.32	19.85	8.76	8.57	9.2	31.07	45.57	35.72	32.42	25.5
	2	6.72	21.40	10.52	10.19	9.1	19.46	28.39	23.32	21.48	14.8
	3	10.11	19.46	12.99	12.55	12.7	11.67	24.29	15.35	14.75	13.4
B	1	15.27	28.87	18.80	17.88	24.0	10.52	22.33	13.33	12.80	13.8
	2	6.88	15.76	9.63	9.36	13.3	20.20	35.85	25.95	23.74	19.7
	3	6.77	20.78	11.45	11.05	11.7	17.61	26.13	21.95	20.09	14.5
C	1	20.07	27.42	22.71	21.39	23.2	11.11	41.41	16.26	15.58	22.0
	2	12.40	19.11	15.53	14.87	18.0	7.90	22.49	12.58	12.10	12.8
	3	8.96	18.60	11.38	11.17	12.0	11.52	22.22	14.54	13.80	13.0

and are shown plotted against the experimental values in figure 74. It can be seen that most of the discrepancies noted in figure 72 for the weft-wise direction in fabric groups X,Y and Z, were improved.

The experimental and theoretical values, according to all the cases examined, are given in the general table 4.2.

4.2.5 Theoretical calculations of the fabric initial Poisson's ratio

Case 1: Calculations assuming incompressible and inextensible yarns

The simplest expression for the fabric Poisson's ratio, met with in literature, is due to Grosberg, which was derived by differentiating the relations

$$\ell = p(1+c) \qquad \text{and} \qquad h = \frac{4}{3} p\sqrt{c} \ ,$$

for both warp and weft, assuming that the yarns are incompressible and inextensible.

Thus

$$d\ell_1 = d\ell_2 = 0 \qquad \text{and} \qquad dh_1+dh_2 = 0 .$$

The final expression for the Poisson's ratio is then obtained as

$$\sigma_1 = -\frac{p_2}{p_1}\frac{dp_1}{dp_2} = \frac{p_2}{p_1}\frac{(1-c_1)}{(1-c_2)}\frac{\sqrt{c_2}}{\sqrt{c_1}} \simeq \frac{p_2}{p_1}\frac{\tan\theta_2}{\tan\theta_1} .$$

The same result was derived by Hearle and Shanahan (22) using Peirce's flexible-thread model. In the present analysis,the simplest expression was derived with the same assumptions of yarn inextensibility and incompressibility, and was given by

$$\sigma_1 = \frac{p_2}{p_1}\frac{\tan\theta_2}{\tan\theta_1} \ ,$$

which is similar to the above result. It may be worth pointing to the fact that both expressions are independent of the yarn rigidities.

The theoretical calculations carried out using the above expression are given in Table 4.3 where it can be shown that the values obtained for this case ($\lambda=\infty$, $\mu=\infty$) are much higher than the experimental results. We therefore go on immediately to consider the case of compressible yarns.

Case 2: Calculations assuming compressible but inextensible yarns

The theoretical expression for this case is given by equation (2.23). This expression can in fact be written in the form

$$\sigma_1 = \frac{p_2}{p_1} \frac{\tan\theta_2}{\tan\theta_1} \times K_c ,$$

where

$$K_c = \frac{\ell_2^3 \cos^2\theta_2/12B_2}{(\ell_2^3\cos^2\theta_2/12B_2)+4(d_1/\mu_1+d_2/\mu_2)} , \qquad (4.5)$$

and K_c may be thought of as a correction factor for case '1' if the yarn compression is to be taken into account. It is obvious that the theoretical value of Poisson's ratio is reduced since K_c is always less than unity, and is dependent on both warp and weft compressibilities. Further, in this case it is possible to get values for σ_1 and σ_2 which are both less than unity, while in the previous case a theoretical value of σ less than unity in one direction leads to a value higher than unity in the other direction. The calculations, carried out according to this case, give much better agreement for most of the fabrics, as can be seen in Table 4.3 ($\lambda=\infty$) and in Figure 75.

Table 4.3

Theoretical and experimental calculations of the fabric initial Poisson's ratio

Fabric group	Fabric No.	σ_1				σ_2			
		$\lambda's=\infty$ $\mu's=\infty$	$\lambda's=\infty$	General case	Experimental values	$\lambda's=\infty$ $\mu's=\infty$	$\lambda's=\infty$	General case	Experimental values
X	1	0.66	0.11	0.10	0.10	1.53	0.46	0.37	0.38
	2	0.63	0.10	0.09	0.11	1.60	0.52	0.41	0.42
	3	0.75	0.11	0.10	0.08	1.33	0.53	0.41	0.40
Y	1	0.70	0.12	0.11	0.08	1.42	0.60	0.47	0.40
	2	0.75	0.13	0.12	0.12	1.33	0.67	0.52	0.51
	3	0.80	0.11	0.11	0.13	1.25	0.68	0.50	0.57
Z	1	0.57	0.06	0.06	0.02	1.76	0.80	0.56	0.24
	2	0.57	0.05	0.04	0.06	1.76	0.76	0.52	0.35
	3	0.54	0.07	0.07	0.07	1.85	0.77	0.57	0.52
A	1	0.66	0.12	0.11	0.08	1.52	0.55	0.43	0.12
	2	0.87	0.23	0.22	–	1.15	0.49	0.45	0.40
	3	0.90	0.28	0.26	0.17	1.12	0.33	0.31	0.25
B	1	1.14	0.30	0.28	0.28	0.88	0.21	0.19	0.16
	2	0.66	0.21	0.20	0.32	1.51	0.55	0.50	0.52
	3	0.89	0.30	0.28	0.31	1.12	0.57	0.52	0.47
C	1	0.81	0.29	0.27	0.20	1.23	0.21	0.20	0.13
	2	0.92	0.43	0.41	0.37	1.09	0.35	0.33	0.25
	3	0.92	0.25	0.23	0.20	1.09	0.31	0.29	0.26

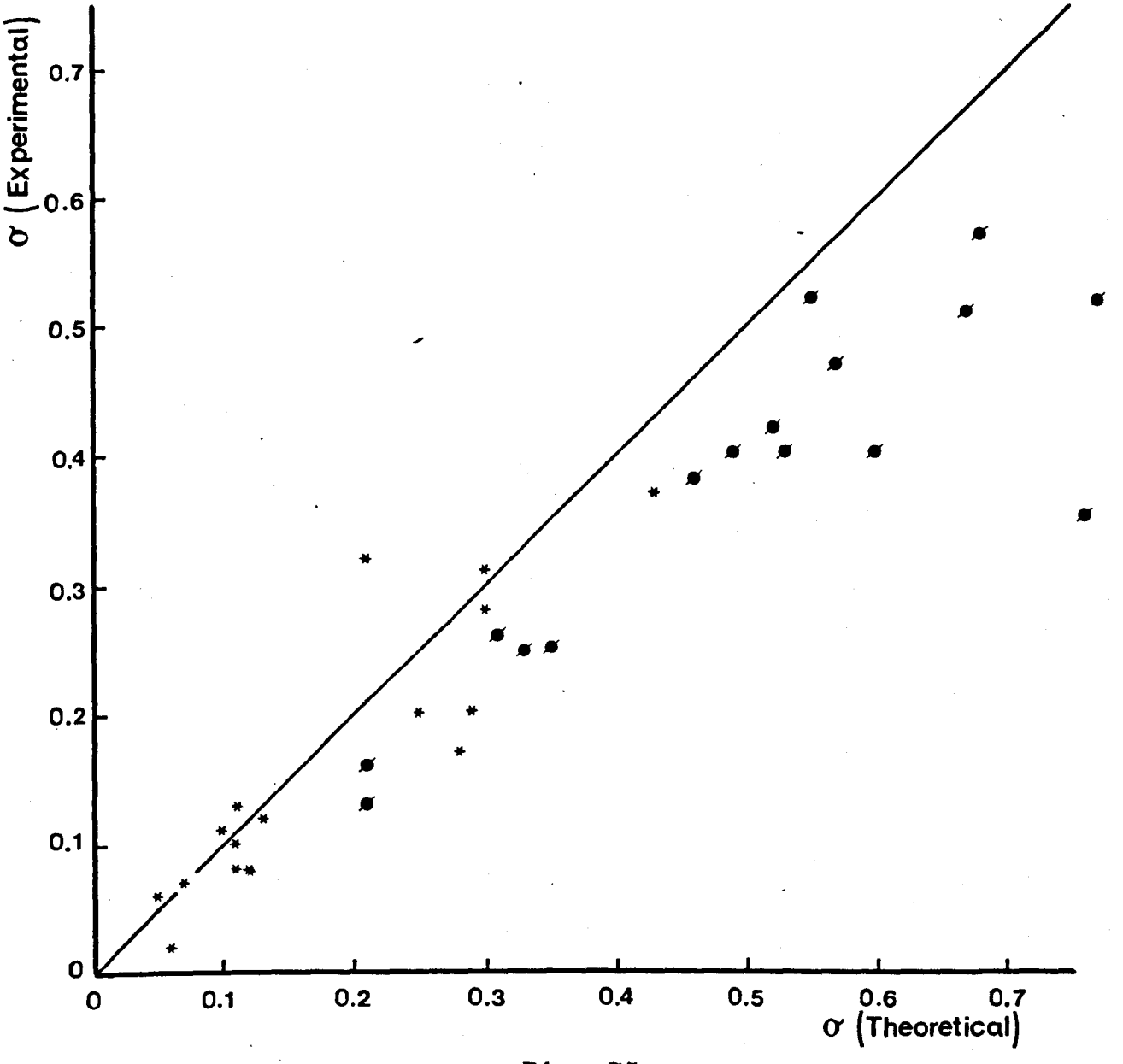

Fig. 75

Theoretical and Experimental values of fabric initial Poisson's ratio (yarns assumed inextensible)

* Fabric extended in warp direction
● Fabric extended in weft direction

General case: Calculations assuming compressible and extensible yarns

The theoretical expression of this case is given by equation (2.22) and may be put in the form

$$\sigma_1 = \frac{p_2}{p_1} \frac{\tan\theta_2}{\tan\theta_1} K_{ct} ,$$

where

$$K_{ct} = \frac{\sin^2\theta_1\cos^2\theta_2\left(\frac{\ell_1^3}{12B_1} - \frac{\ell_1}{\lambda_1}\right)\left(\frac{\ell_2^3}{12B_2} - \frac{\ell_2}{\lambda_1}\right)}{N\left(\frac{\ell_1^3\sin^2\theta_1}{12B_1} + \frac{\ell_1\cos^2\theta_1}{\lambda_1}\right) - \sin^2\theta_1\cos^2\theta_1\left(\frac{\ell_1^3}{12B_1} - \frac{\ell_1}{\lambda_1}\right)^2} , \qquad (4.6)$$

and

$$N = \sum_{i=1,2} \left(\frac{\ell_i^3\cos^2\theta_i}{12B_i} + \frac{\ell_i\sin^2\theta_i}{\lambda_i} + \frac{4d_i}{\mu_i}\right).$$

'K_{ct}' may be termed a correction factor to include both the yarn compressibility and extensibility. The calculations, carried out according to this case, are included in Table 4.3 and are illustrated in figure 76.

4.2.6 Discrepancies and agreements between the theoretical and experimental results

Generally, the theoretical calculations give a reasonable estimation for the fabric initial tensile modulus and Poisson's ratio. The case which gives the best agreement is that which includes both yarn compressibility and yarn extensibility. A complete agreement is seldom possible for the following reasons:

1. errors in the experimental measurements of the fabric initial behaviour;

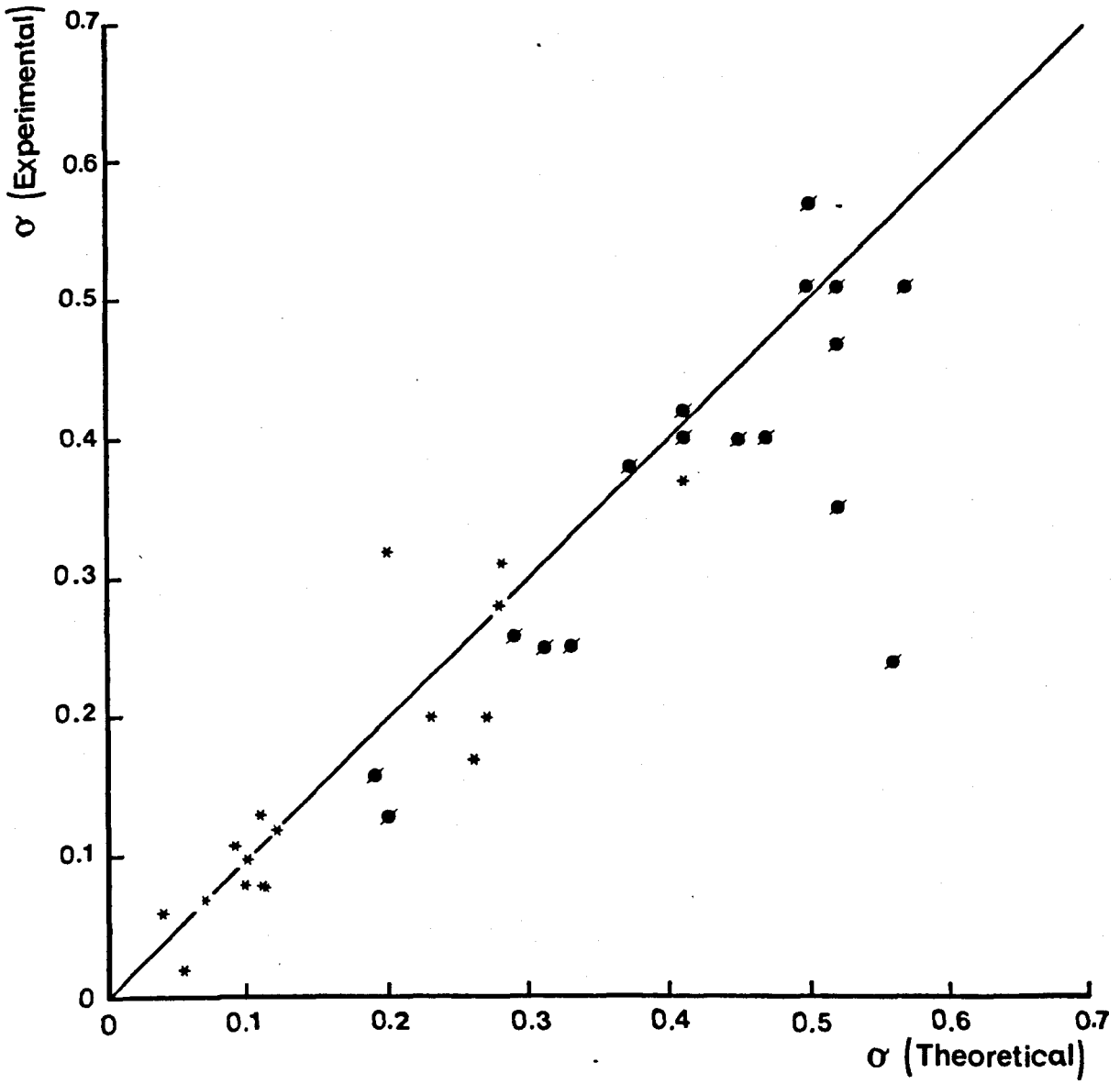

Fig. 76

Theoretical and Experimental values of fabric initial Poisson's ratio (general case).

* Fabric extended in warp direction
● Fabric extended in weft direction

2. errors due to basic assumptions;

3. errors in defining the yarn mechanical properties.

These will be discussed separately.

1. Errors in the experimental measurements of the fabric initial behaviour

The value of the fabric tensile modulus is ideally defined by the slope of the initial part of the load-extension curve, and this is sometimes not easy to determine with great accuracy. Also a slightly slack or slightly pretensioned fabric, when inserted in the jaws of the Instron, leads to an indeterminancy of the origin i.e. the point on the chart corresponding to zero load and extension. The coefficient of variation of the initial fabric tensile modulus is in the range of 4.4% to 13%. This variation may also, of course, reflect some variation in the fabric properties at different parts of the woven fabric piece.

The quoted values of the Poisson's ratio are based on testing one or two samples for each fabric direction, this small number of tests being done because of the lengthy testing procedure. From the preliminary investigation it was clear that it is necessary to extend the fabric to a sensible amount, beyond the initial, since the resultant initial changes in width are very small. Such a procedure clarifies the extension-contraction behaviour and reduces errors in interpreting the initial Poisson's ratio from the resulting curves representing the behaviour. In this test, a crucial error may result from the samples being pretensioned, since the curve will be interpreted from the experimental measurements as shown in figure 77a referred to axes $O'X'Y'$. The behaviour, in fact, should actually have been started from the point O, where axes OXY represent the correct datum for extension and contraction, and it is clear that the correct value of the

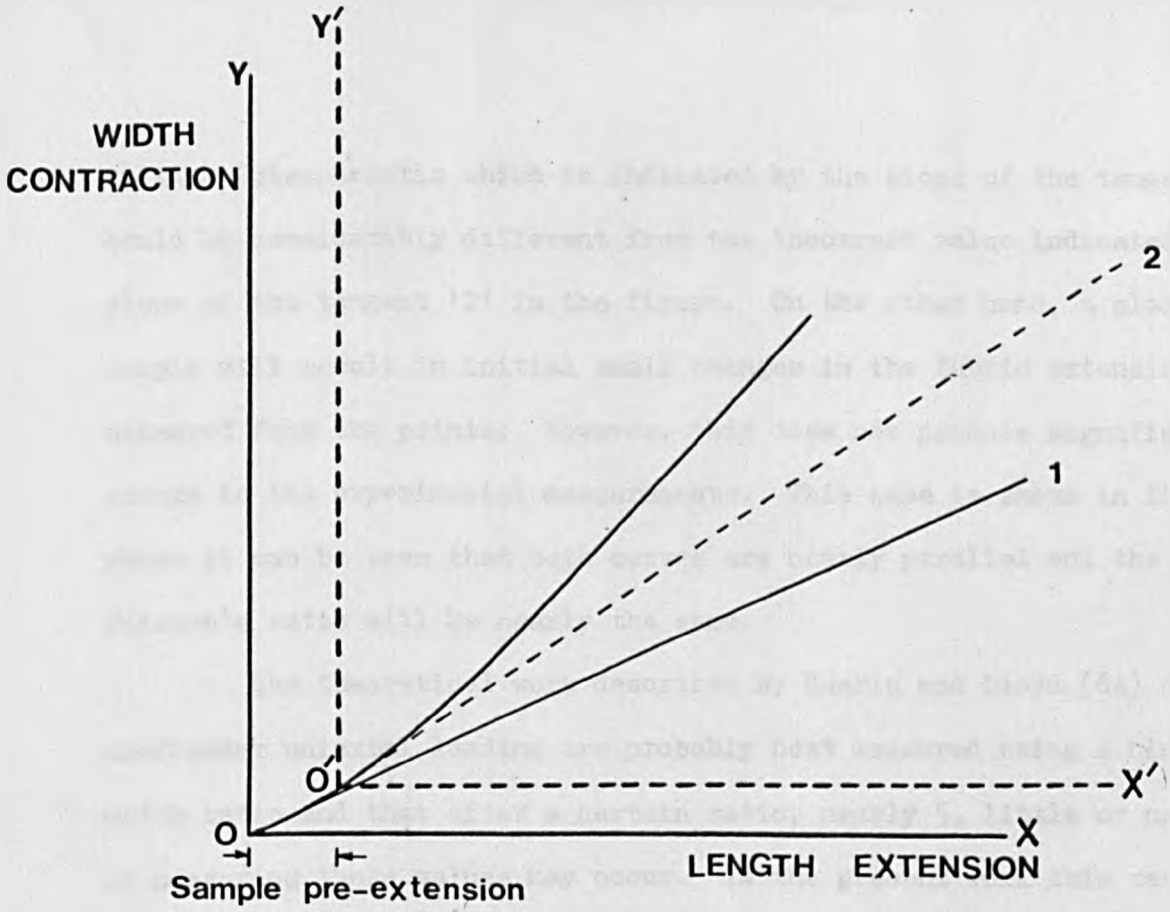

Fig. 77a

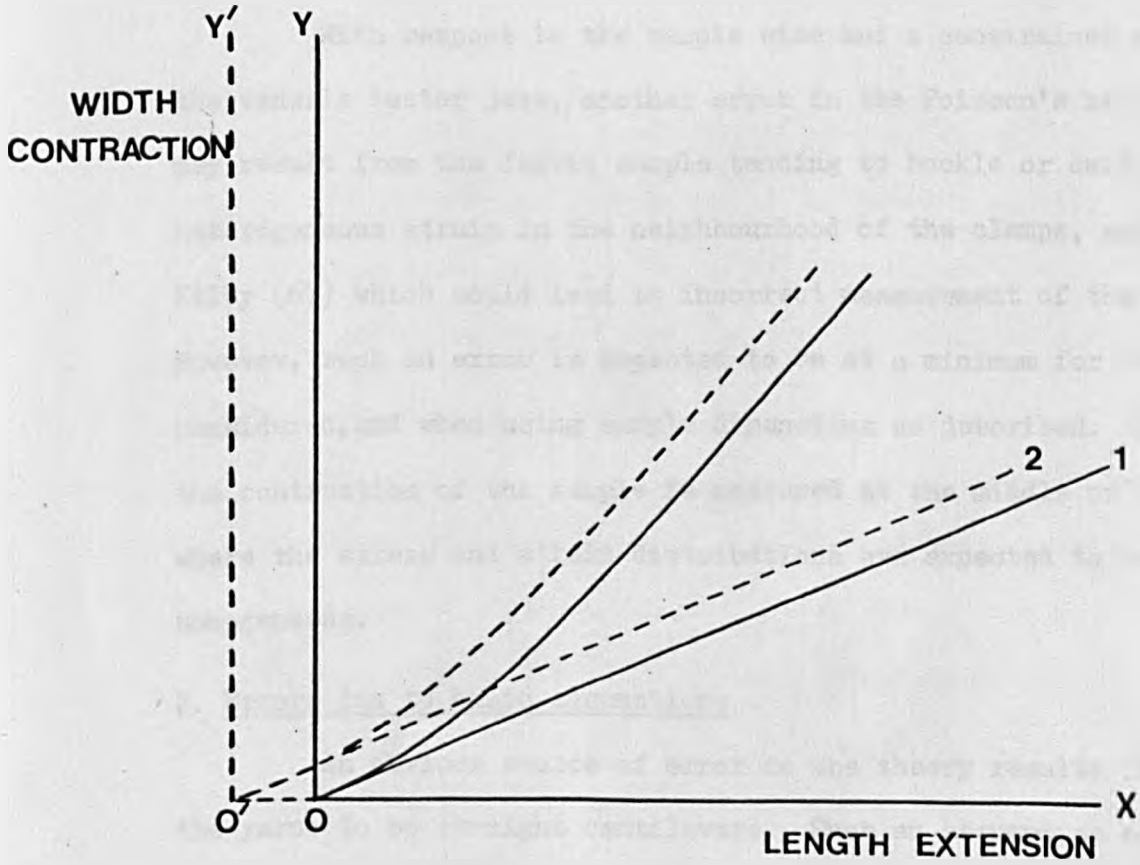

Fig. 77b

initial Poisson's ratio which is indicated by the slope of the tangent '1' could be considerably different from the incorrect value indicated by the slope of the tangent '2' in the figure. On the other hand, a slack fabric sample will result in initial small changes in the fabric extension, as measured from the prints; however, this does not produce significant errors in the experimental measurements. This case is shown in figure 77b where it can be seen that both curves are nearly parallel and the measured Poisson's ratio will be nearly the same.

The theoretical work described by Hearle and Lloyd (64) shows that E and σ under uniaxial loading are probably best measured using a high length: width ratio and that after a certain ratio, nearly 5, little or no changes in measuring these values may occur. In the present work this ratio was 5, and an additional check was made using a ratio of 10; both results were similar.

With respect to the sample size and a constrained contraction at the tensile tester jaws, another error in the Poisson's ratio measurements may result from the fabric sample tending to buckle or curl due to the heterogeneous strain in the neighbourhood of the clamps, as described by Kilby (67) which could lead to incorrect measurement of the width contraction. However, such an error is expected to be at a minimum for the small strains considered, and when using sample dimensions as described. In addition, the contraction of the sample is measured at the middle of the specimen where the stress and strain distributions are expected to be nearly homogeneous.

2. Errors due to basic assumptions

An obvious source of error in the theory results from assuming the yarns to be straight cantilevers. Such an assumption could be a

reasonable approximation for both warp and weft in conditions which lead to an open fabric construction with low to medium crimp in both directions. If the structure is highly unbalanced so that the ratio of diameters, rigidities and spacing of the yarns in one direction to the other is high (figure 73a), the straight line representation holds reasonably accurately in the direction which possesses the low crimp value, while giving less accurate estimates for the modulus in the crossing direction. This can be seen clearly in figure 78, where the mean values of $\frac{E(\text{experimental})}{E(\text{theoretical})}$ for each fabric group are plotted against the crimp value of the yarns in the load direction, the theoretical values being calculated according to the general case. The graph shows that the best agreements between theory and experimental ($\frac{E(\text{experimental})}{E(\text{theoretical})} \simeq 0.75\text{-}1.2$) are given by fabrics of low crimp to medium values in the load direction (0.03-0.12), while the maximum discrepancies are related to the warp-wise fabric extension of groups X, Y and Z, which have high crimp values in this direction.

3. Errors in defining the yarn mechanical properties

The mechanical properties of the yarns have been measured in isolation, and these could be different from those that apply when the yarn is inside the fabric. For example, the following might be cited:

(a) The yarns inside the fabric may be regarded, approximately, as consecutive arcs of different radii, as suggested by Nordby (2), and the bending properties of these might be dependent on their initial curvature.

(b) The yarn compression under zero axial tension could be different from the yarn compression produced when the yarn is also acted upon by axial loading (3), such as may occur during the fabric tensile deformation. In addition, the procedure used to define the compression modulus relies

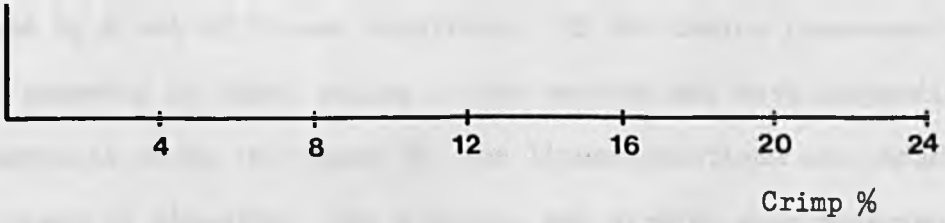

Fig. 78

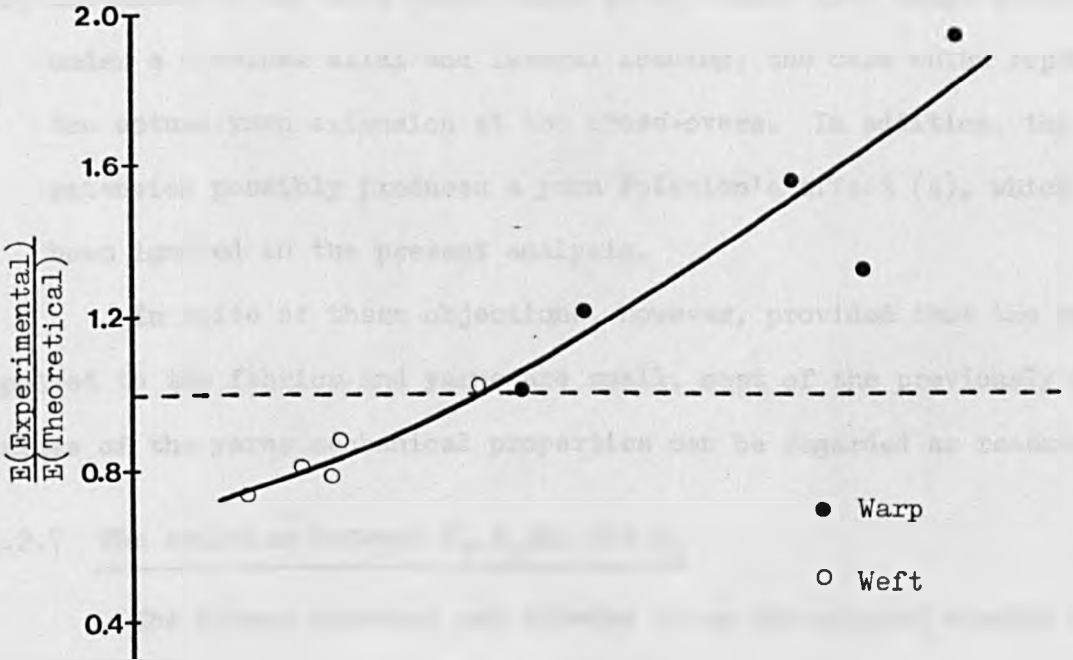
2.0
1.6
1.2
0.8
0.4
E(Experimental)
E(Theoretical)
Warp
Weft

on assumptions such as a race-track cross-sectional shape and that the yarn is compressed at constant volume, which may not, in fact, be satisfied.

(c) Extension of the free yarns could be different from their extension under a combined axial and lateral loading, the case which represents the actual yarn extension at the cross-overs. In addition, the yarn extension possibly produces a yarn Poission's effect (4), which has been ignored in the present analysis.

In spite of these objections, however, provided that the strains applied to the fabrics and yarns are small, most of the previously estimated values of the yarns mechanical properties can be regarded as reasonable.

4.2.7 The relation between E_1, E_2, σ_1 and σ_2

The planar stresses and strains of an anisotropic elastic lamina are related by a set of linear equations. If the lamina possesses two planes of symmetry at right angles to one another and both perpendicular to the lamina, as shown in figure 79, the linear equations are reduced from considerations of symmetry. The stresses and strains, when referred to the principal axes defined by the intersections of the planes of symmetry with the lamina, i.e. axes X and Y, are defined by

$$\left.\begin{aligned} e_{XX} &= A_{11}S_{XX}+A_{12}S_{YY} \ , \\ e_{YY} &= A_{21}S_{XX}+A_{22}S_{YY} \ , \\ e_{XY} &= A_{33}S_{XY} \ , \end{aligned}\right\} \quad (4.7)$$

where S_{XX} and S_{YY} are the normal tensile stresses and S_{XY} is the shear stress.

e_{XX}, e_{YY} and e_{XY} are the corresponding tensile and shear strains.

$A_{11}, A_{12}, A_{21}, A_{22}$ and A_{33} are influence coefficients.

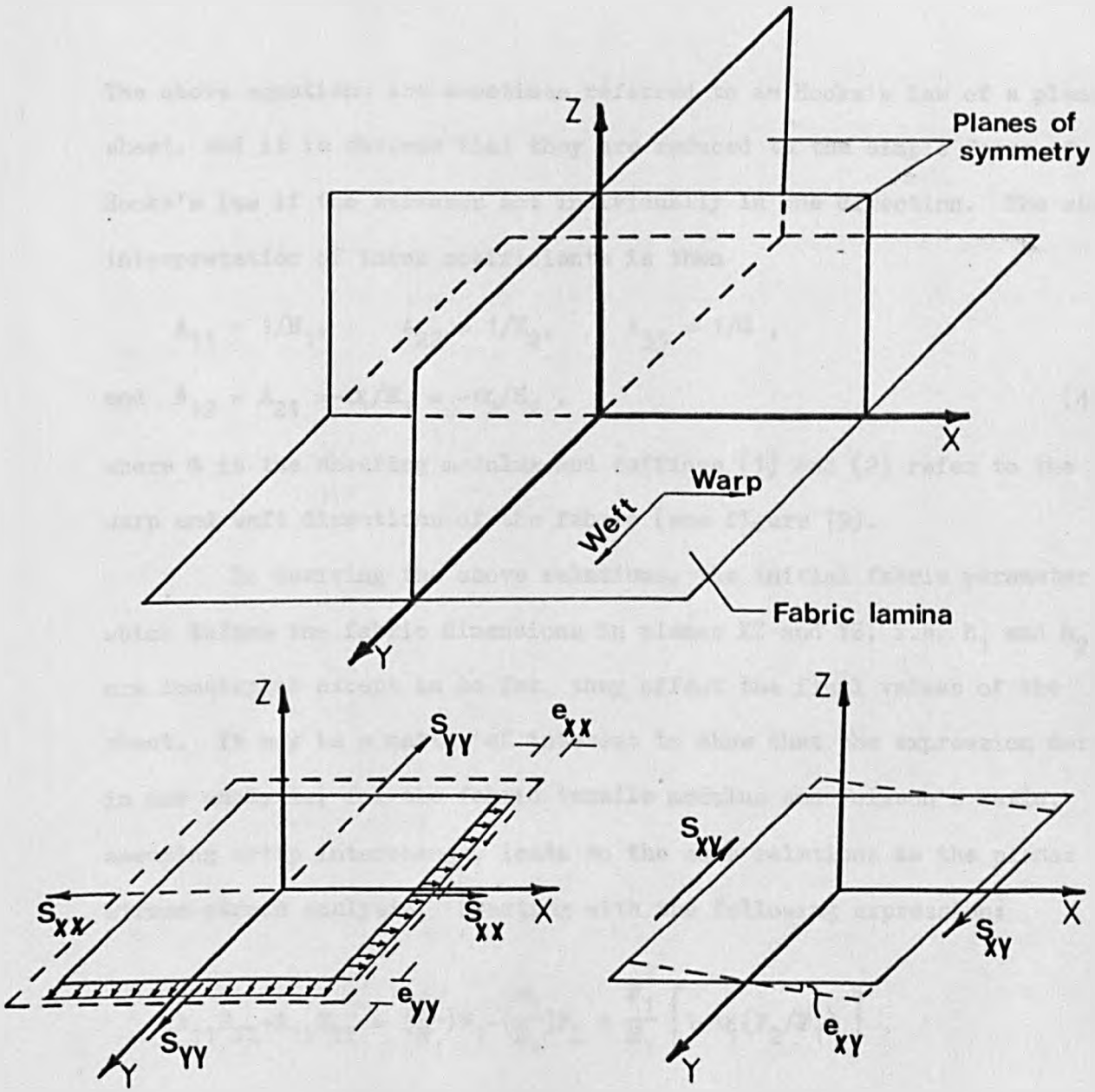
Z
Planes of symmetry
X
Warp
Weft
Fabric lamina
Y
Z
S_{YY}
e_{XX}
S_{XX}
X
S_{XX}
e_{YY}
S_{YY}
Y
Z
S_{XY}
X
S_{XY}
e_{XY}
Y

Fig. 79

The above equations are sometimes referred to as Hooke's Law of a planar sheet, and it is obvious that they are reduced to the simple forms of Hooke's law if the stresses act individually in one direction. The simple interpretation of these coefficients is then

$$A_{11} = 1/E_1, \qquad A_{22} = 1/E_2, \qquad A_{33} = 1/G ,$$

$$\text{and} \quad A_{12} = A_{21} = -\sigma_1/E_1 = -\sigma_2/E_2 , \tag{4.8}$$

where G is the shearing modulus and suffices (1) and (2) refer to the warp and weft directions of the fabric (see figure 79).

In deriving the above relations, the initial fabric parameters which define the fabric dimensions in planes XZ and YZ, i.e. h_1 and h_2, are immaterial except in so far they affect the final values of the sheet. It may be a matter of interest to show that the expression derived in our analysis, for the fabric tensile modulus and Poisson's ratio, assuming crimp interchange, leads to the same relations as the planar stress-strain analysis. Starting with the following expression:

$$A_{11}S_{XX}+A_{12}S_{YY} = (\frac{1}{E_1})F_1-(\frac{\sigma_1}{E_1})F_2 = \frac{F_1}{E_1}\left[1-\sigma_1(F_2/F_1)\right] ,$$

and substituting the equivalent values of E_1 and σ_1 from equations (2.7) and (2.24) gives

$$\frac{F_1 l_1^3 l_2^3 p_1 \sin^2\theta_1 \sin^2\theta_2}{12p_2(l_1^3 B_2\cos^2\theta_1+l_2^3 B_1\cos^2\theta_2)}\left[1-\frac{p_2\tan\theta_2}{p_1\tan\theta_1}(F_2/F_1)\right]$$

$$= \frac{F_1 l_1^3 l_2^3 p_1 \sin^2\theta_1 \sin^2\theta_2 - F_2 l_1^3 l_2^3 p_2 \sin\theta_1\cos\theta_1\sin\theta_2\cos\theta_2}{12p_2(l_1^3 B_2\cos^2\theta_1+l_2^3 B_1\cos^2\theta_2)} ,$$

which is the expression previously derived for the warp extension under biaxial loading with the assumption of inextensible and incompressible yarns.

Similarly, it can be shown that the planar stress-strain relation (4.8), arising from symmetry considerations holds valid when substituting for E and σ from our analysis i.e.

$$\sigma_1 E_2 = \left(\frac{p_2 \tan\theta_2}{p_1 \tan\theta_1}\right) \frac{12 B_2 p_1}{p_2 \ell_2^3 \sin^2\theta_2} \left[\frac{B_1 \ell_2^3 \cos^2\theta_2 + B_2 \ell_1^3 \cos^2\theta_1}{B_2 \ell_1^3 \cos^2\theta_1}\right] ,$$

and

$$\sigma_2 E_1 = \left(\frac{p_1 \tan\theta_1}{p_2 \tan\theta_2}\right) \frac{12 B_1 p_2}{p_1 \ell_1^3 \sin^2\theta_1} \left[\frac{B_1 \ell_2^3 \cos^2\theta_2 + B_2 \ell_1^3 \cos^2\theta_1}{B_1 \ell_2^3 \cos^2\theta_2}\right] ,$$

and these in fact equal.

It can also be shown that the above equivalence is consistent in any case, when using the other expressions obtained with the different assumptions for the yarn mechanical properties. The theoretical relation (4.8) confirms the experimental finding, discussed in section 4.2.2, that for the same fabric, the direction which possesses the higher value of E, also shows a higher value of σ.

4.2.8 The fabric initial behaviour under biaxial tensile deformation

In a biaxial tensile deformation two quantities are involved, namely the two tensile loads (F_1 and F_2) and the two extensions (ε_1 and ε_2). In order to carry out an experimental test, two of these quantities are regarded as specified independent variables, while the other will be dependent on them and obviously on the weave construction. The specified variables

can be varied according to several schemes (3,68, 4); for example, their ratio may be held constant. The following discussion applies to the case where F_2 and F_1 are varied so that F_2/F_1 = constant during the test.

To predict the initial biaxial tensile behaviour, it is possible to rely directly on the relations derived from the planar stress-strain analysis, since it has been shown that the expression in our work which assumes crimp interchange leads to the same conclusion. The particular value of the sheet (E_1,E_2,α_1 and α_2 under uniaxial loading) should be predicted using the case which best agrees with the experimental results, i.e. with the assumption of extensible and compressible yarns. The fabric extension, regarded as the dependent variable, under biaxial loading in a warp direction, can then be calculated from

$$\varepsilon_1 = F_1 \frac{1}{E_1}\left[1-\alpha_1(F_2/F_1)\right]$$

There will be 3 possibilities for the fabric initial tensile behaviour, namely

1. Warp-wise fabric extension if $\alpha_1(F_2/F_1) < 1$.
2. Zero warp-wise fabric extension if $\alpha_1(F_2/F_1) = 1$.
3. Warp-wise fabric contraction if $\alpha_1(F_2/F_1) > 1$.

4.2.9 Comparison with other theories

The theoretical results based on the expressions derived in our analysis were compared with some results obtained by De Jong and Postle (66,69) Their analysis uses an energy method, and should be more accurate since it relies on a more realistic shape for the yarn path. We shall use here the same dimensionless units used by the above authors. These are:

f_r: dimensionless decrimping load per yarn (fl^2/B);

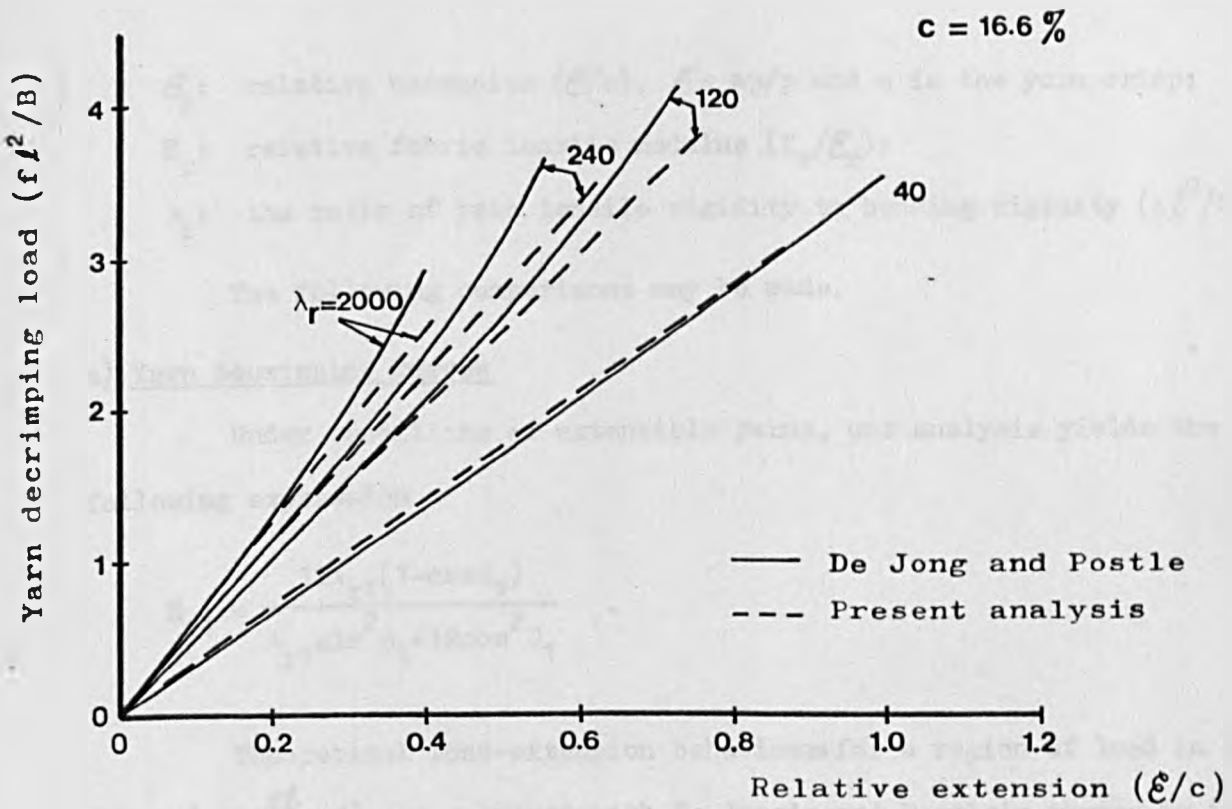
c = 16.6 %
120
240
40
λ_r=2000
De Jong and Postle
Present analysis
Yarn decrimping load ($f\ell^2$/B)
Relative extension (ε/c)
0
1
2
3
4
0.2
0.4
0.6
0.8
1.0
1.2

Fig. 80

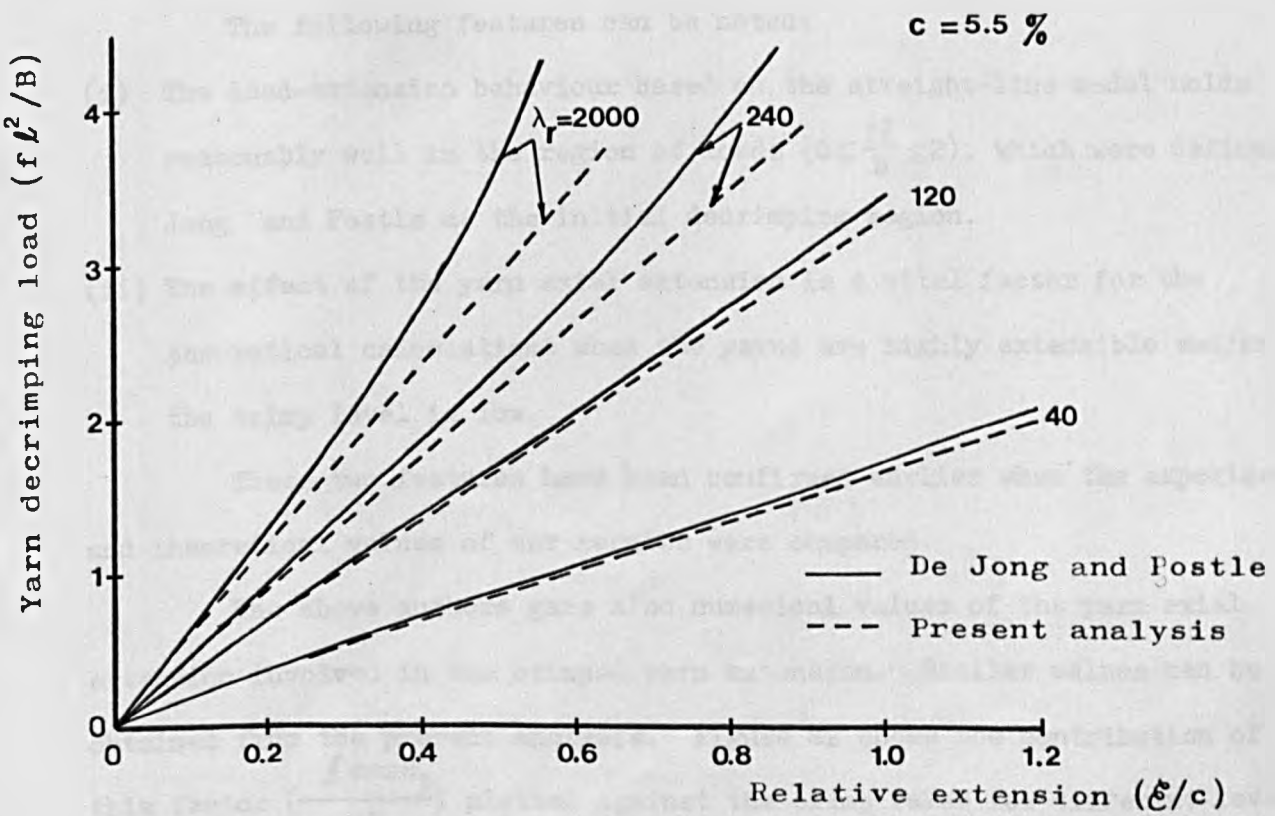
c = 5.5 %
λ_r=2000
240
120
40
De Jong and Postle
Present analysis
Yarn decrimping load ($f\ell^2$/B)
Relative extension (ε/c)
0
1
2
3
4
0.2
0.4
0.6
0.8
1.0
1.2

Fig. 81

$\mathcal{E}_r$: relative extension ($\mathcal{E}/c$), $\mathcal{E} = \Delta p/p$ and c is the yarn crimp;

E_r: relative fabric tensile modulus ($f_r/\mathcal{E}_r$);

λ_r: the ratio of yarn tensile rigidity to bending rigidity ($\lambda \ell^2/B$).

The following comparisons may be made.

a) Yarn decrimping curves

Under conditions of extensible yarns, our analysis yields the following expression

$$E_{r1} = \frac{12\lambda_{r1}(1-\cos\theta_1)}{\lambda_{r1}\sin^2\theta_1 + 12\cos^2\theta_1} \quad .$$

Theoretical load-extension behaviours for a region of load in the range ($0 \leqslant \frac{f\ell}{B} \leqslant 4$) are compared with De Jong's and Postle's curves in figures 80 and 81, these being shown at two levels of crimp values and for different values of λ_r.

The following features can be noted:

(i) The load-extension behaviour based on the straight-line model holds reasonably well in the region of loads ($0 \leqslant \frac{f\ell}{B} \leqslant 2$), which were defined by De Jong and Postle as the initial decrimping region.

(ii) The effect of the yarn axial extension is a vital factor for the theoretical calculations when the yarns are highly extensible and/or the crimp level is low.

These two features have been confirmed earlier when the experimental and theoretical values of our results were compared.

The above authors gave also numerical values of the yarn axial extension involved in the crimped yarn extension. Similar values can be obtained from the present analysis. Figure 82 shows the contribution of this factor ($\frac{\ell \cos\theta_1}{p}$) plotted against the crimp value for different levels of λ_r.

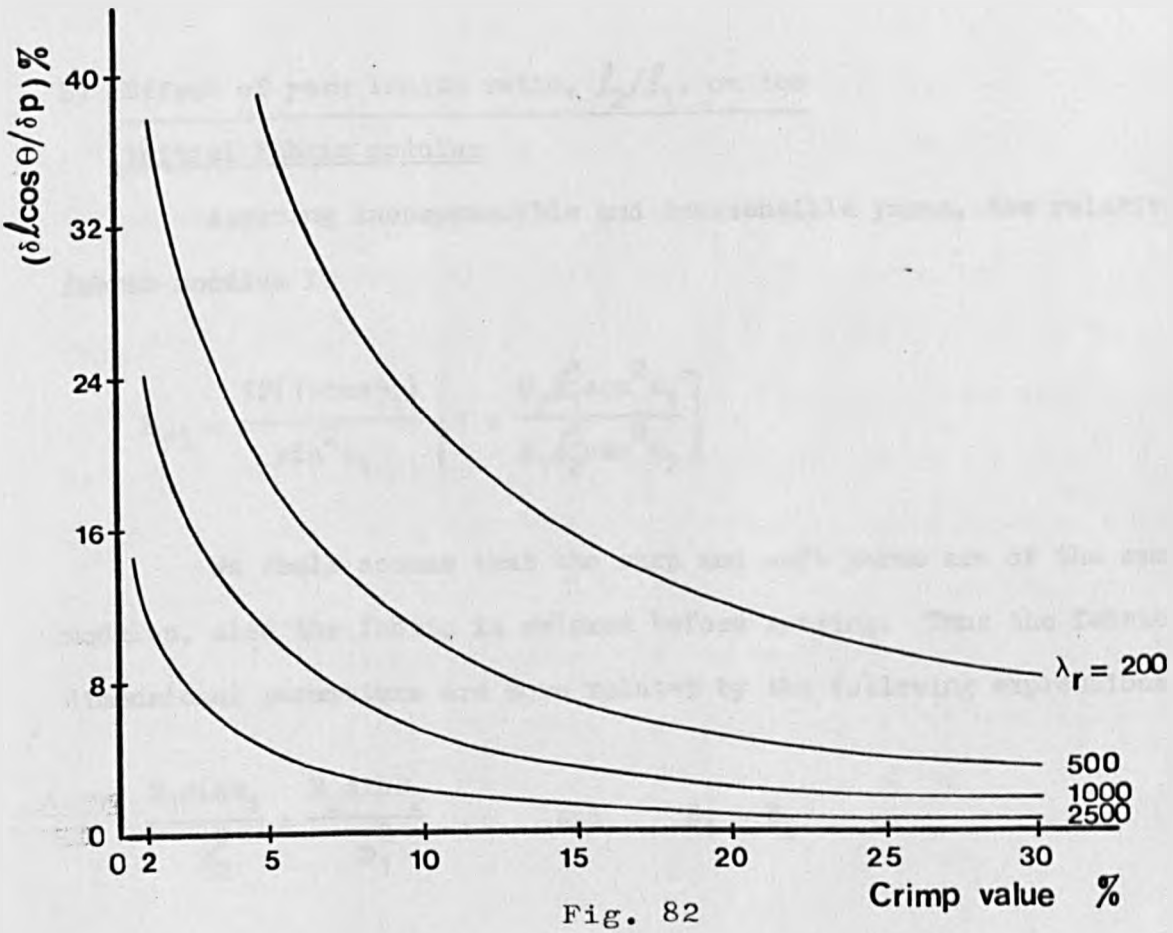
(δl cosθ/δp)%
40
32
24
16
8
0
0 2
5
10
15
20
25
30
Crimp value %
λr = 200
500
1000
2500

Fig. 82

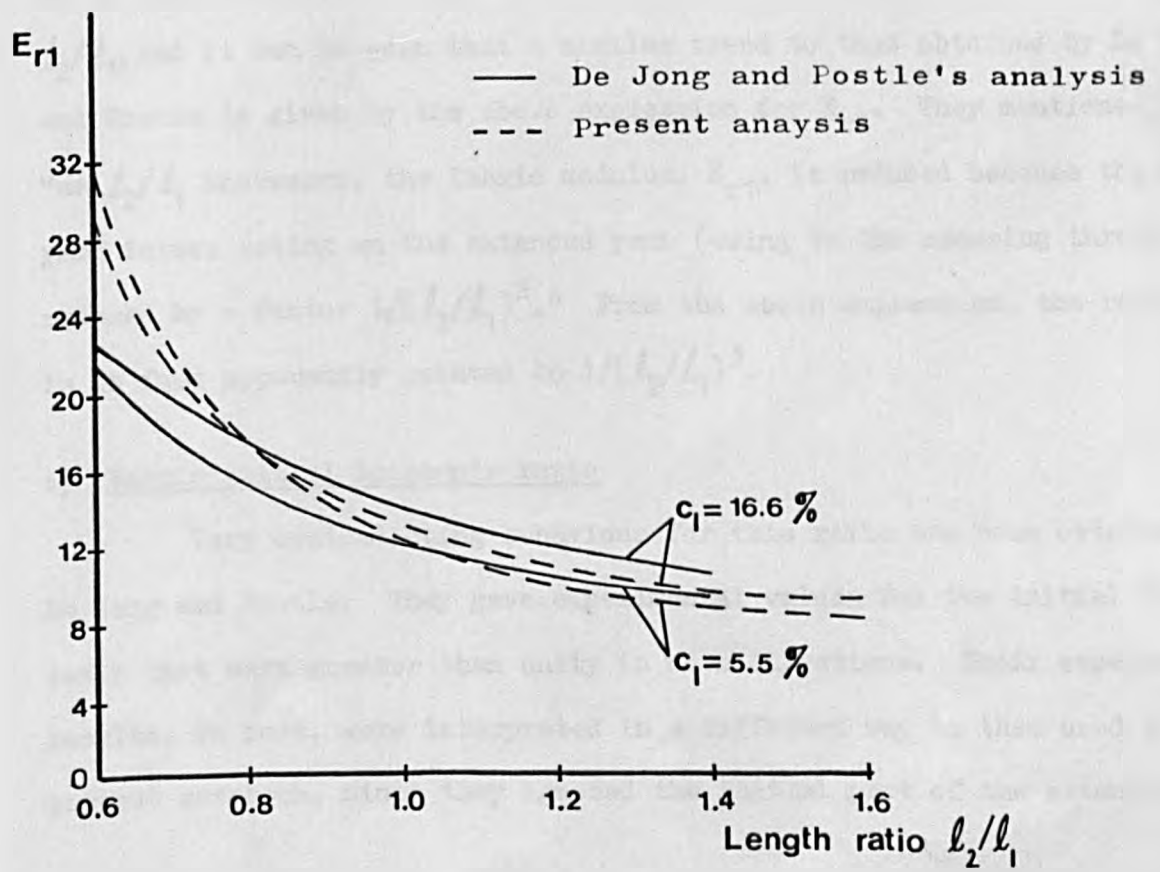
Er1
—— De Jong and Postle's analysis
- - - Present anaysis
32
28
24
20
16
12
8
4
0
0.6
0.8
1.0
1.2
1.4
1.6
Length ratio l2/l1
c1 = 16.6 %
c1 = 5.5 %

Fig. 83

b) Effect of yarn length ratio, ℓ_2/ℓ_1, on the initial fabric modulus

Assuming incompressible and inextensible yarns, the relative fabric modulus is

$$E_{r1} = \frac{12(1-\cos\theta_1)}{\sin^2\theta_1}\left[1 + \frac{B_2\ell_1^3\cos^2\theta_1}{B_1\ell_2^3\cos^2\theta_2}\right] .$$

We shall assume that the warp and weft yarns are of the same bending modulus, also the fabric is relaxed before setting. Thus the fabric dimensional parameters are more related by the following expressions

$$\frac{B_1\sin\theta_1}{p_2^2} = \frac{B_2\sin\theta_2}{p_1^2} \quad , \qquad \text{and} \qquad B_1 = B_2 .$$

It is thus possible to draw the curves shown in figure 83, relating E_{r1} and ℓ_2/ℓ_1, and it can be seen that a similar trend to that obtained by De Jong and Postle is given by the above expression for E_{r1}. They mentioned that "as ℓ_2/ℓ_1 increases, the fabric modulus, E_{r1}, is reduced because the inter-yarn forces acting on the extended yarn (owing to the crossing thread) are reduced by a factor $1/(\ell_2/\ell_1)^2$." From the above expression, the reduction is in fact apparently related to $1/(\ell_2/\ell_1)^3$.

c) Fabric initial Poisson's ratio

Very contradicting behaviour for this ratio has been obtained by De Jong and Postle. They gave experimental values for the initial Poisson's ratio that were greater than unity in both directions. Their experimental results, in fact, were interpreted in a different way to that used in the present research, since they ignored the initial part of the extension-

contraction behaviour in the cases where no contraction was observed. They attributed this delayed contraction to the possibility that the interyarn forces during the initial fabric extension are insufficient to upcrimp the crossing yarn. De Jong and Postle also attributed the values of $\sigma>1$, in both directions, to the effect of the axial tension applied to the yarns on yarn rounding (rather than flattening). They suggested that the interyarn distance is therefore predominantly controlled by the effect of tension on the yarn cross-sectional shape rather than by the interyarn forces. In the present work, the values of the initial σ were always less than unity and the theoretical justification that we have presented for this highlights the effect of yarn compression on the initial length extension-width contraction.

4.3 A Discussion of the Initial Bending Properties of Plain Fabrics

The general trends of the experimental results, referring to Table 3.9, for all the tested fabrics can be summarized in the following remarks.

1. The general shape of the bending hysteresis curve, previously described, was observed for all the fabrics. These curves for plain fabrics are expected to show symmetry about the origin, since the weave cell is symmetrical with respect to the fabric plane. However such symmetry was not always found in the experimental curves, probably due to an initial in-plane couple or to different treatment of the two faces when the fabric was dried in the stenter during the finishing process. The procedure used to interpret the results,(section 3.5.1), effectively reduced these differences, since the mean values of all the tested samples of a particular fabric finally produced a nearly symmetrical curve.

2. The trends for the fabric bending modulus are probably better discussed by examining the experimental data with respect to a simple model of fabric bending. The simplest mechanism for this behaviour assumes that the effect of the crossing yarns may be regarded as reducing the effective length of the yarns, in the bending plane, that will bend when the fabric plane is deformed (38,45). The yarns are therefore considered as alternate rigid and flexible segments. The fabric stiffness per yarn, as far as warp-wise bending is concerned, is given by

$$B_W = B_1 \frac{p_2}{\ell_{f1}} \quad ,$$

where ℓ_{f1} is the length of the flexible segment of the warp thread in the fabric unit cell.

An obvious difficulty in applying this simple model is how to define these segments, since a preknowledge about the yarn compressibility and its cross-sectional shape, before bending, is required. One possibility is shown in figure 84, which gives the warp-wise fabric rigidity (per unit width) as

$$B_W = \frac{B_1}{p_1} \frac{p_2}{\ell_1-(a_2-b_2)} \quad . \tag{4.9}$$

Using the available data referring to the yarn projections, the calculated values of the initial bending modulus, according to this model, are given in Table 4.4 and are plotted against the measured values in figure 85. It is apparent that most of the measured flexural rigidities of the finished fabrics tend to be lower than those estimated by the simple model.

If the bending behaviour of fabrics does follow a mechanism like that assumed, the discrepancies between the measured and calculated data can possibly be explained on the basis that the rigid parts of the yarn length in the unit weave cell might be smaller than those given by the fabric model. Furthermore, there could be a possible interaction due to the yarn compression, during fabric bending, which leads to lower values of the experimental fabric rigidity. On the other hand, for some fabrics, the measured initial bending moduli are higher than those calculated from equation (4.9). This can be seen in connection with the tighter fabric constructions, and suggests that increasing values of the frictional resistance to the initial fabric bending have resulted and caused the noted discrepancies in these cases. The values of the 'coercive couple/yarn' for both the initially straight yarns (M_{01} and M_{02}) and the yarns inside the

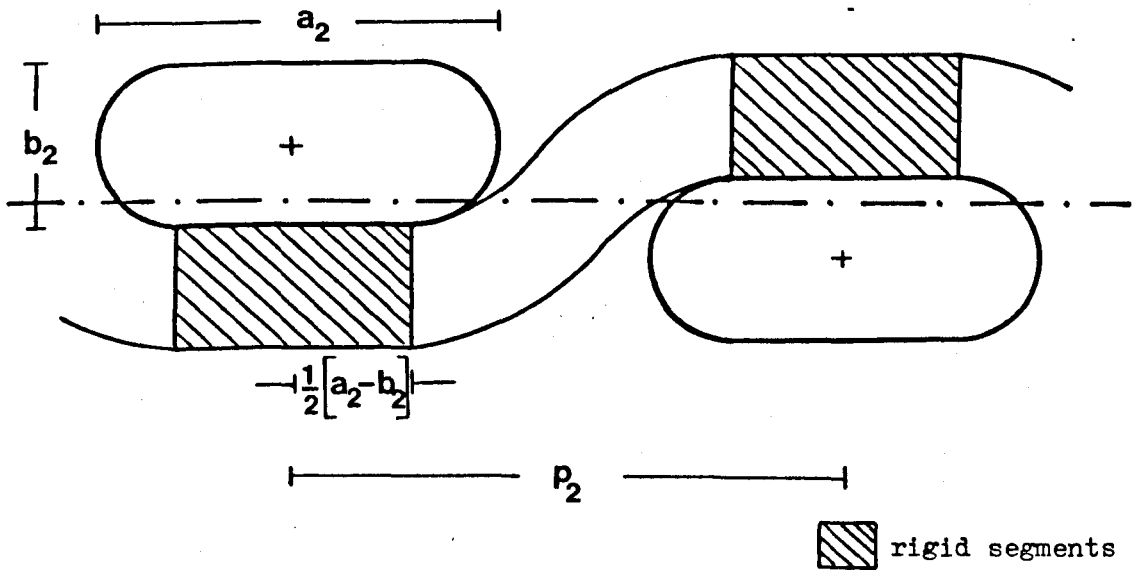

Fig. 84

Table 4.4

Fabric group	Fabric No.	Warp M_{01} mN.mm	Warp M_{0W} mN.mm	Warp B_W (equation 4.9) mN.mm^2/cm	Weft M_{02} mN.mm	Weft M_{0T} mN.mm	Weft B_T (equation 4.9) mN.mm^2/cm	No.in Fig.85
X	1	0.28	0.27	327	0.50	0.48	346	1
	2	0.28	0.31	275	0.50	0.68	341	2
	3	0.28	0.29	282	0.50	0.52	278	3
Y	1	0.28	0.29	292	0.61	0.88	374	4
	2	0.28	0.30	268	0.61	0.82	385	5
	3	0.28	-	252	0.61	-	296	6
Z	1	0.28	0.26	245	0.79	1.40	469	7
	2	0.28	0.27	218	0.79	1.34	505	8
	3	0.28	0.41	263	0.79	1.45	529	9
A	1	0.26	0.26	212	0.26	0.32	296	10
	2	0.26	0.21	176	0.26	0.19	183	11
	3	0.26	0.35	230	0.26	0.27	248	12
B	1	0.26	0.47	256	0.33	0.26	228	13
	2	0.26	0.25	213	0.33	0.26	219	14
	3	0.26	0.23	207	0.33	0.36	281	15
C	1	0.26	0.41	227	0.19	0.19	167	16
	2	0.26	0.29	239	0.19	0.14	142	17
	3	0.26	0.18	180	0.19	0.15	119	18

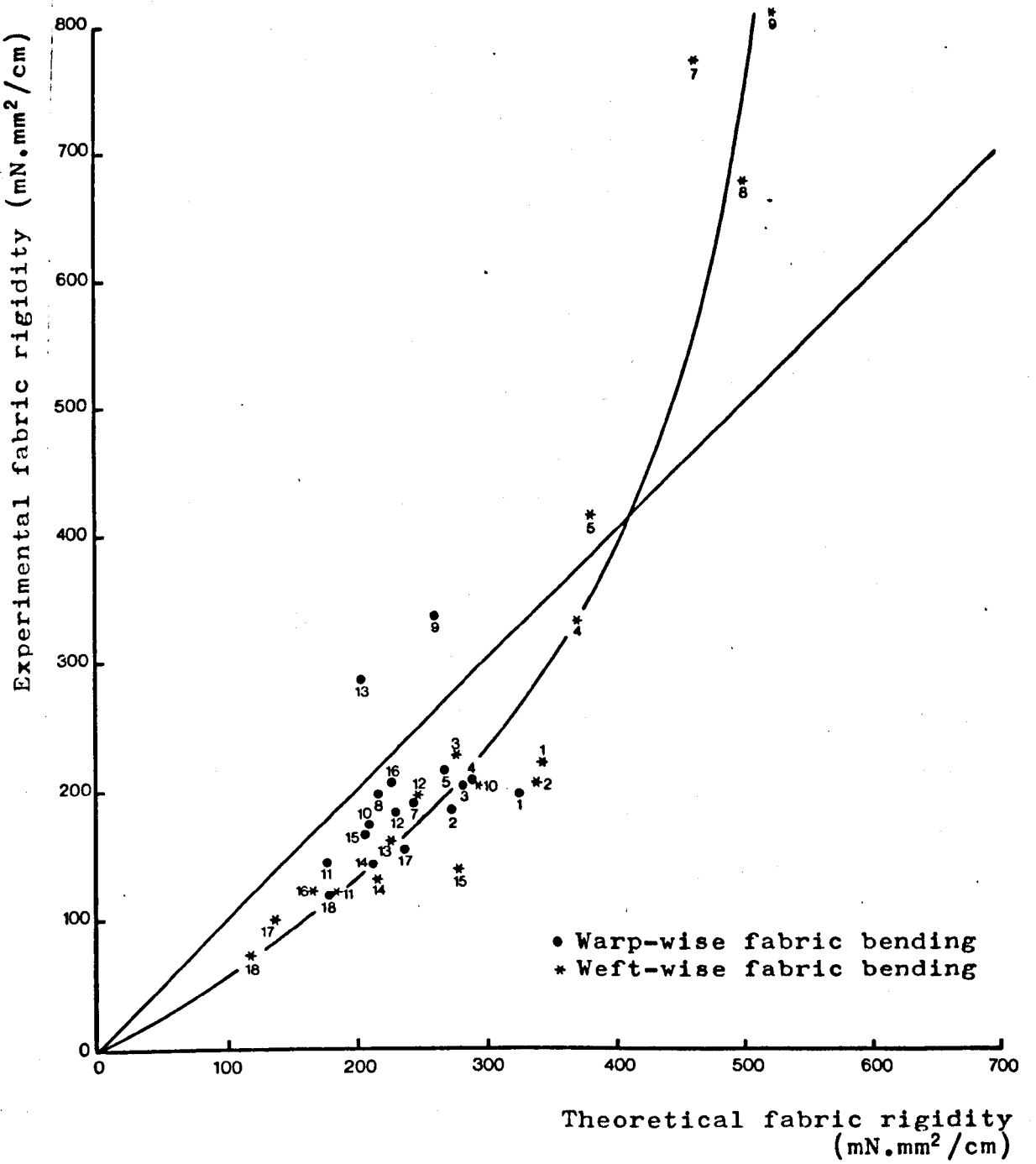
Experimental fabric rigidity (mN.mm²/cm)
800
700
600
500
400
300
200
100
0
0
100
200
300
400
500
600
700
Theoretical fabric rigidity (mN.mm²/cm)
• Warp-wise fabric bending
* Weft-wise fabric bending

Fig. 85

fabric (M_{OW} and M_{OT}) are included in Table 4.4, from which it can be seen that the high values of M_{OT} are associated with the coarser weft yarns being used in fabric groups Y and Z, and the high values of M_{OW} are associated with fabrics Z-3,A-3,B-1 and C-1, which have high cover factors. These constructions gave higher experimental values of the fabric stiffness than the theoretical ones (figure 85).

4.3.1 Theoretical calculations of the fabric initial bending modulus

The mechanical properties of the component yarns were discussed when considering the tensile behaviour of fabrics. The yarn bending property involved, was chosen based on an analysis of the possible change in yarn curvature, produced by extending the fabric by a small amount. A further comparison between the theoretical and experimental values, obtained for the initial tensile modulus of the isolated crimped yarns, confirmed that yarn bending is best represented by its elastic flexural rigidity.

In the following calculations, the yarn bending property, involved in the fabric initial bending, will be redefined taking into consideration the following aspects:

1. In the bending analysis, it has been assumed that the yarns are bent to the same angle as that of the fabric plane, i.e. the initial change in curvature of both are nearly the same.
2. The initial bending modulus of the isolated straight yarn takes into account the effect of the fibre frictional restraints. This effect is very likely to act in the same way when the yarns are bent during fabric bending, and may indeed be accentuated.

Based on the above arguments it is reasonable to represent the yarn modulus 'B' by its initial value, i.e. the slope of the initial part of the hysteresis loop (up to the range 0.02 mm^{-1}). With the other geometrical and mechanical properties involved in the calculations having the same values as before, the theoretical calculations of the fabric bending modulus can then be compared with the experimental initial bending modulus of the real fabrics.

Before discussing the theoretical calculations we must point out the following reservations:

1. The theory assumes a point contact between the crossing yarns. The yarn shape and the contact length between warp and weft are only taken into consideration in determining values for the yarn's compression moduli. The theory, therefore, ignores any interference between the yarns associated with the real contact and their possible effect on the fabric initial bending modulus.

2. The theory does not consider the interaction between the yarns in the load direction, which may lead to a rubbing action, or additional frictional restraints, between the adjacent yarns when the fabric is bent. This interaction causes both the frictional couple and the initial bending modulus to increase. This effect was discussed by Olofsson (43), Owen (6) and Cooper (70) and a common agreement between them is that such interaction is more likely to occur with the tighter fabric constructions. Because of the above two reasons, the theoretical calculations would not be expected to be comparable to the actual bending behaviour of fabrics such as Z-1 and A-3 in the warp direction and groups Y and Z in the weft direction, in which tight fabric constructions have increased the frictional restraints, leading to significantly higher values of the experimental bending modulus

than are given by the calculations.

The first set of calculations was carried out assuming the yarns to be incompressible and inextensible (μ's, λ's $=\infty$). The expression derived in the theoretical analysis for the fabric initial modulus, per unit width, is then

$$B_W = \frac{B_1}{1+c_1}\left[1+\frac{3B_2\ell_1^3\cos^2\theta_1}{B_1\ell_2^3\cos^2\theta_2+B_2\ell_1^3\cos^2\theta_1}\right]\left(\frac{1}{p_1}\right) , \qquad (2.33)$$

where B_W is the warp-wise fabric initial bending modulus.

The estimated and measured values are compared in Table 4.5, where large discrepancies can be seen with this assumption (μ's $=\infty$). In the majority of cases, the calculated values are greater than the measured ones. The reason probably is associated with the overestimation of the crossing yarn's contribution to the fabric resistance to bending, which, in terms of the couple needed to counteract the interyarn forces involved in bending the fabric to a unit curvature, is given by

$$C_1'' = \frac{B_1}{1+c_1}\,\frac{3B_2\ell_1^3\cos^2\theta_1}{B_1\ell_2^3\cos^2\theta_2+B_2\ell_1^3\cos^2\theta_1}\left(\frac{1}{p_1}\right) . \qquad (4.10)$$

Fabrics made from highly compressible yarns tend to feel softer and seem to bend more easily than those made from hard twisted yarns of high compression moduli. This suggests that yarn compression behaviour might effect the bending properties of fabrics, and the theory confirms this. The final expression for B_W, taking account of yarn compression, was

$$B_W = \frac{B_1}{1+c_1}\left[1+\frac{3B_2\ell_1^3\cos^2\theta_1}{B_1\ell_2^3\cos^2\theta_2+B_2\ell_1^3\cos^2\theta_1+48B_1B_2(d_1/\mu_1+d_2/\mu_2)}\right]\frac{1}{p_1} , \qquad (2.37)$$

from which it can be seen that the weft contribution to the fabric bending resistance is reduced.

The values calculated using the above equation are given in Table 4.5, and are plotted against the measured values in figure 86. The underlined cases in Table 4.5 are excluded from the figure since the theory does not apply to them. It is apparent that a better agreement between the theory and experiment is achieved by including the yarn compressibility, though the differences are still considerable.

The remaining discrepancies between theory and experimental may be attributed to the same general sources of errors as were mentioned in the tensile analysis. Applied to the fabric bending, these are:

1. Errors in the experimental measurements of the fabric bending behaviour. In spite of the fact that a relatively large number of samples has been tested for each fabric construction, the fact that the standard size used with the Shirley tester is so small (0.5x2.5 cm), leaves some doubt about whether the fabric is best represented by the samples.
2. Errors due to the theoretical assumptions and the level of approximations used in deriving the final expressions.

In order to follow the theoretical trends suggested by the general equation (2.37), we shall use the following relative quantities:

μ_r: the ratio of yarn compression rigidity to bending rigidity ($\mu l^2/B$),

and D_r: the ratio of interyarn spacing to yarn modular length, in the bending plane (D/l).

We shall only consider the case when the warp and weft are made of the same yarns, i.e. $B_1=B_2$ and $\mu_1=\mu_2$. Equation (2.37) is then converted to

Table 4.5

Fabric group	Fabric No.	B_W(mN.mm^2/cm) Calculated (Equation 2.33)	B_W(mN.mm^2/cm) Calculated (Equation 2.37)	B_W(mN.mm^2/cm) Measured	B_T(mN.mm^2/cm) Calculated (Equation 2.33)	B_T(mN.mm^2/cm) Calculated (Equation 2.37)	B_T(mN.mm^2/cm) Measured	No. in Fig. 86
X	1	545.42	217.17	195.88	359.29	232.07	220.88	1
	2	515.44	272.52	184.82	319.59	215.41	205.50	2
	3	612.23	313.21	204.00	249.81	185.72	225.00	3
Y	1	602.50	319.14	205.48	315.88	238.02	330.00	4
	2	619.56	352.23	215.16	269.29	216.90	414.98	5
	3	651.13	378.12	–	215.13	183.57	–	6
Z	1	630.73	327.60	194.78	310.26	261.29	789.28	7
	2	635.11	314.69	194.98	275.34	236.91	679.86	8
	3	606.06	306.98	335.05	375.24	298.98	809.79	9
A	1	464.15	234.03	172.50	271.76	173.79	202.50	10
	2	409.17	233.74	143.54	214.22	148.04	116.83	11
	3	338.38	199.50	182.50	371.96	214.45	196.19	12
B	1	350.16	194.22	285.00	363.19	197.26	160.00	13
	2	353.08	205.59	140.94	295.95	186.70	130.59	14
	3	405.13	251.66	165.23	213.90	155.42	136.80	15
C	1	244.97	170.41	205.04	339.91	173.92	120.03	16
	2	270.65	192.38	152.00	268.49	164.87	100.00	17
	3	343.49	196.92	116.00	189.37	108.33	73.64	18

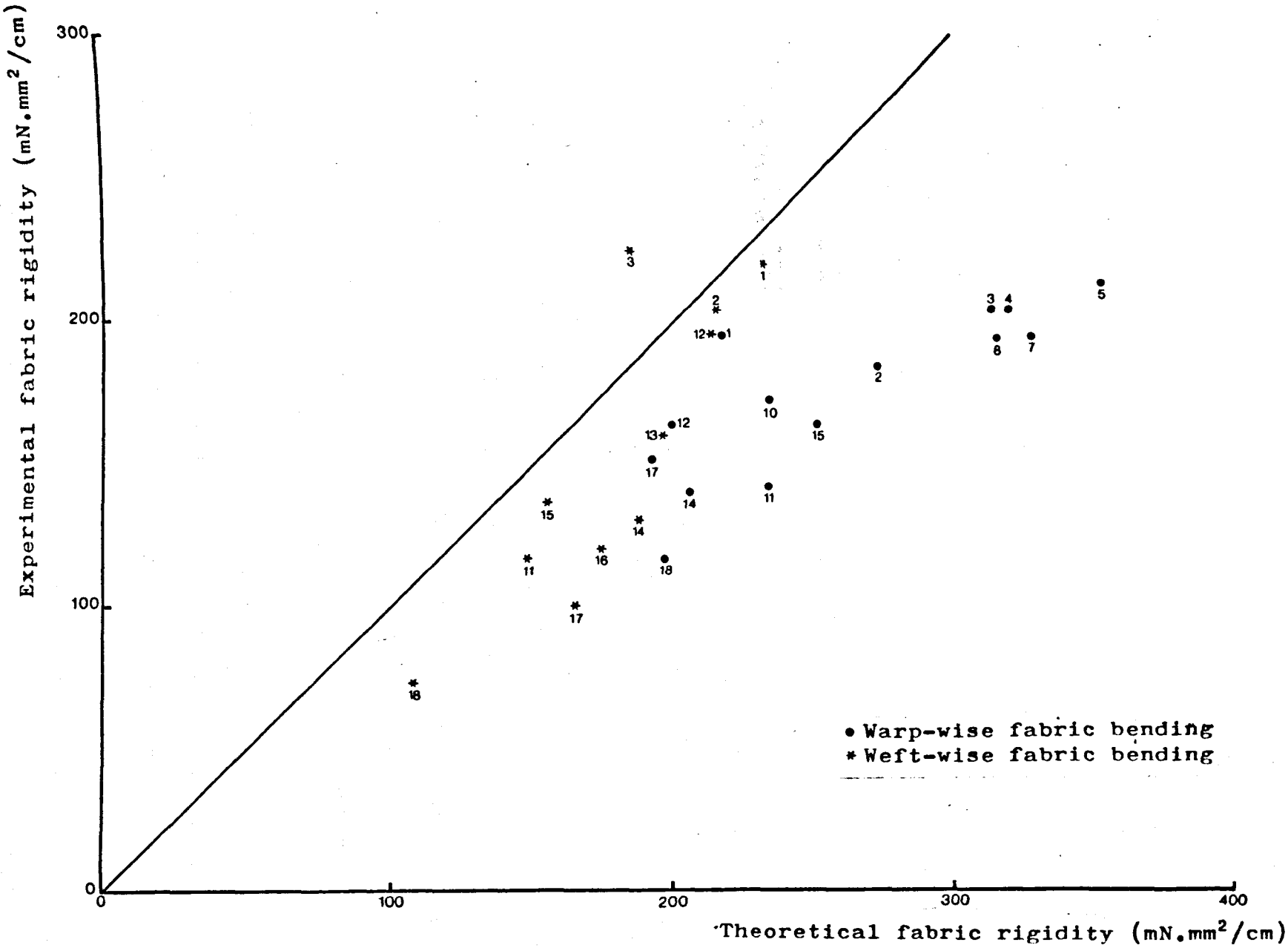
Experimental fabric rigidity (mN.mm²/cm)
300
200
100
0
0
100
200
300
400
Theoretical fabric rigidity (mN.mm²/cm)
• Warp-wise fabric bending
* Weft-wise fabric bending

Fig. 86

$$B_w/B_1 = \left[\cos\theta_1 + \frac{3\cos^3\theta_1}{(l_2/l_1)^3\cos^2\theta_1+\cos^2\theta_2+48\frac{D_r}{\mu_r}}\right],$$

where B_w is the warp-wise bending rigidity, per yarn, of the fabric.

The theoretical trends shown in figures 87-89 can be easily obtained from the above equation. The graphs show the effect of yarn length ratio (l_2/l_1) on the ratio B_w/B_1. Figures 87 and 88 show this effect at two levels of crimp (5.5% and 16.6%), and for three levels of D_r/μ_r (0,0.05 and 0.1); the latter two values of D_r/u_r represent realistic values of this ratio and are typical of some of the yarns used in the present work.

The curves in figures 87 and 88 exhibit the following features:

1. In the chosen range of fabrics where $0.6 \leqslant l_2/l_1 \leqslant 1.6$ and $0 \leqslant D_r/\mu_r \leqslant 0.1$, the fabric initial flexural rigidity is always higher than the yarn initial rigidity.
2. A reduction in the fabric modulus (B_w) is obtained by increasing the length ratio (l_2/l_1). This trend resembles the trend obtained for the initial tensile modulus. The reduction has a steeper rate in the case of the lower crimp value (5.5%).
3. For the same ratio of (l_2/l_1), increasing the warp crimp reduces the warp-wise fabric bending rigidity.
4. The effect of yarn compression, i.e. increasing the value of D_r/μ_r, is interesting. Initially, as D_r/μ_r changes from 0 to 0.05, the effect on B_w/B_1 is, in general, relatively large. However, as D_r/μ_r increases from 0.05 to 0.1, the change in B_w/B_1 is rather small.

The effect of the crossing yarn rigidity is shown in figure 89 where it can be seen that, in general, an increase in the crossing yarn

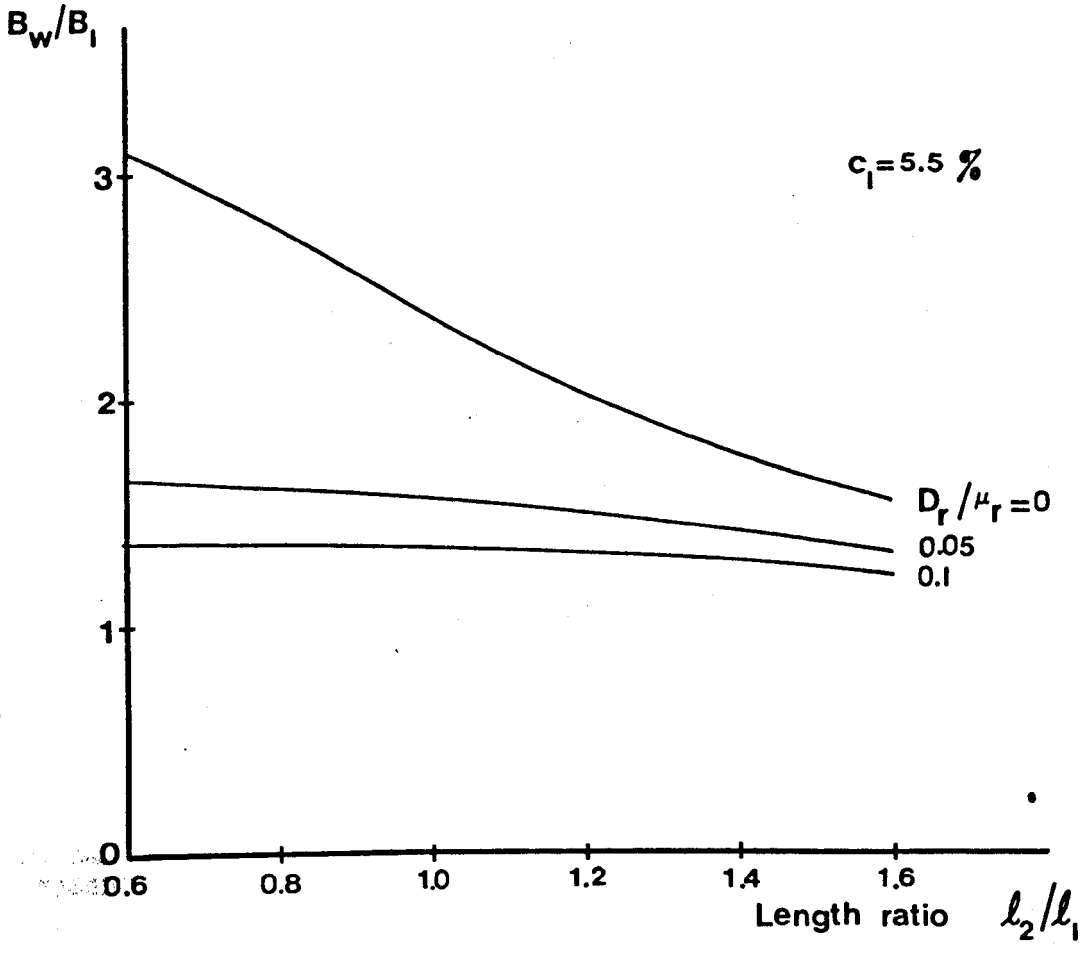
B_w/B_l
c_l=5.5 %
D_r/μ_r=0
0.05
0.1
3
2
1
0
0.6
0.8
1.0
1.2
1.4
1.6
Length ratio ℓ_2/ℓ_1

Fig. 87

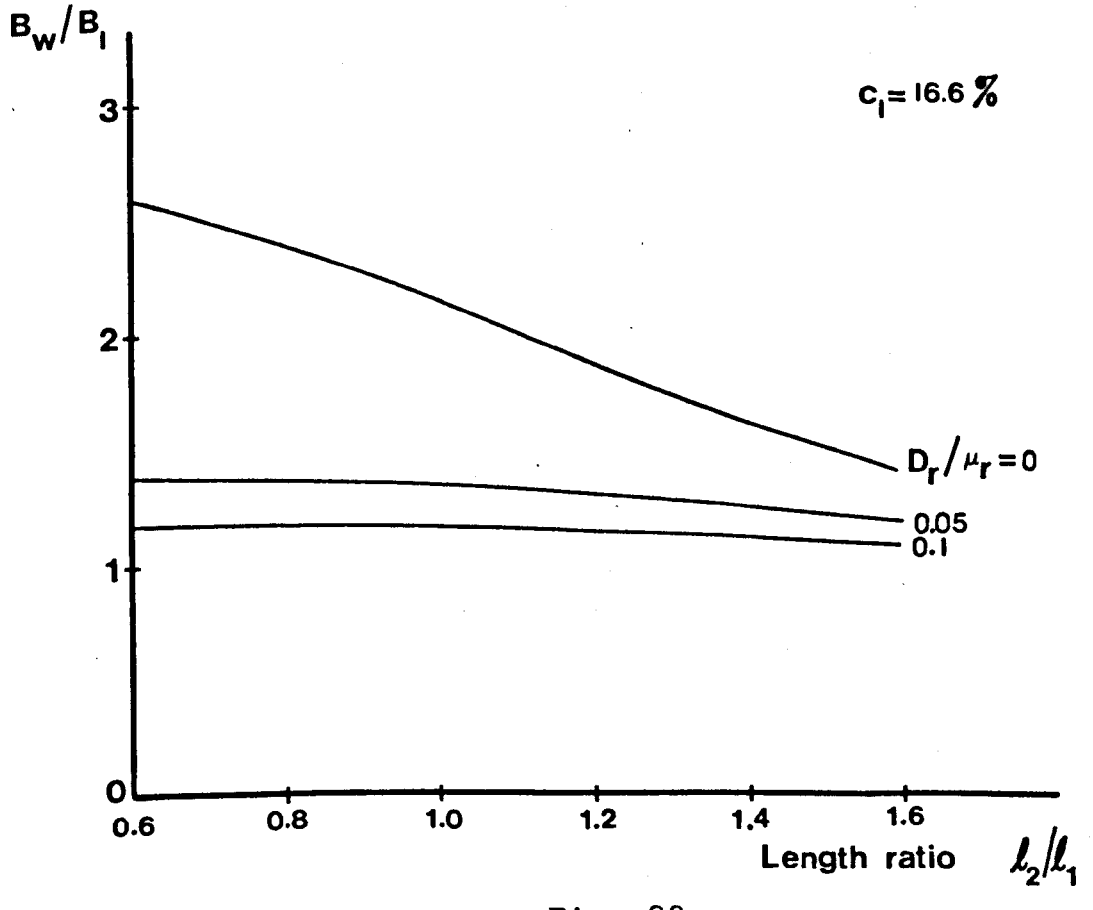
B_w/B_l
c_l= 16.6 %
D_r/μ_r=0
0.05
0.1
3
2
1
0
0.6
0.8
1.0
1.2
1.4
1.6
Length ratio ℓ_2/ℓ_1

Fig. 88

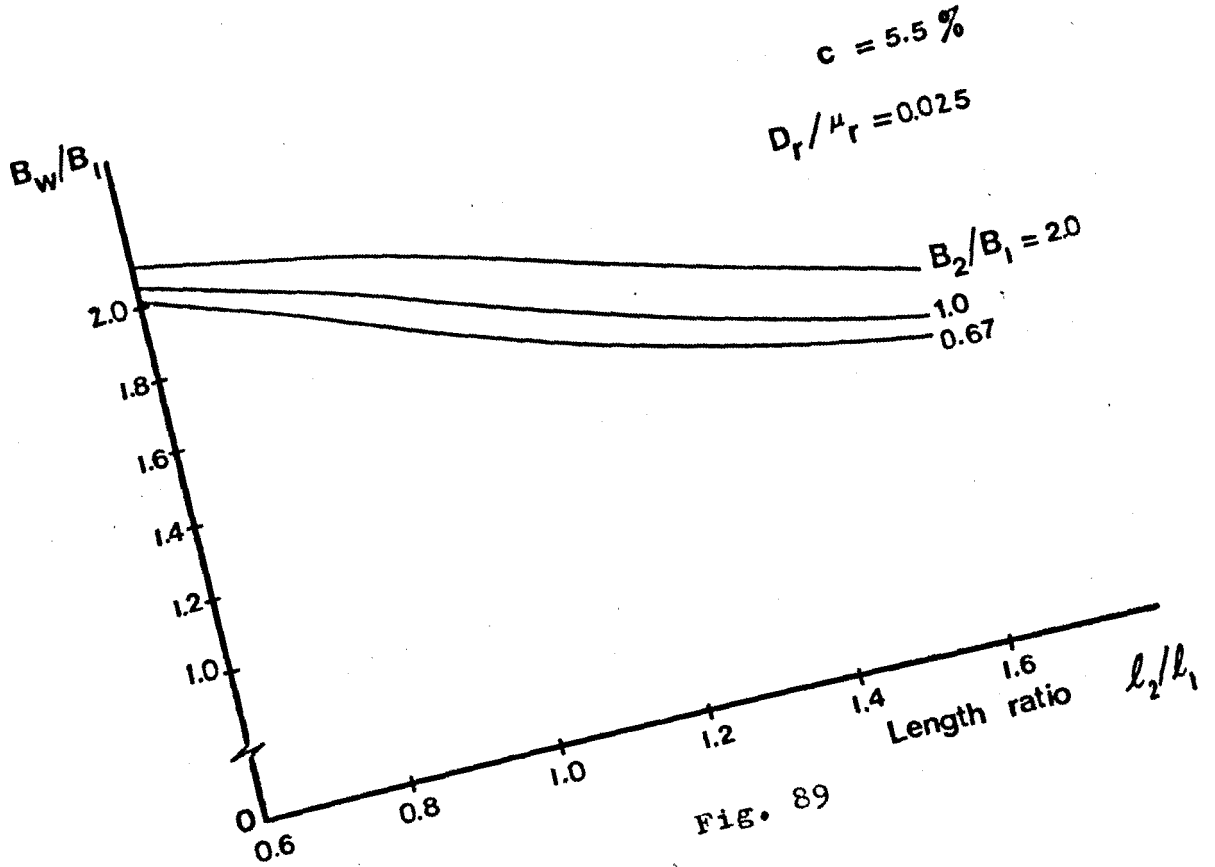
c = 5.5 %
D_r/μ_r = 0.025
B_w/B_1
B_2/B_1 = 2.0
1.0
0.67
2.0
1.8
1.6
1.4
1.2
1.0
0
0.6
0.8
1.0
1.2
1.4
1.6
Length ratio
ℓ_2/ℓ_1

Fig. 89

bending modulus stiffens the fabric. This is more prominent at the higher values of length ratio ℓ_2/ℓ_1.

From equation (3.27) and the trends shown in figures 87-89, it is possible to obtain fabrics of $B_W/B_1 < 1$ if the fabric construction is very open, i.e. ℓ_2/ℓ_1 is high enough, also when the yarns are highly compressible and/or the crossing yarns are very easy to bend. The minimum value of B_W/B_1 is $1/(1+c_1)$. Obviously the same applies to the ratio B_T/B_2 when considering the corresponding parameters involved.

4.3.2 Comparison with other theories

The only other closed form solution, met with in the literature, which provides a theoretical expression for the fabric initial bending modulus, is due to Abbott (8). The ratio B_W/B_1 of a warp yarn inside the fabric was given in his analysis by

$$B_W/B_1 = \frac{1}{1+c_1} + \frac{b_1^2}{h_1^2}\left[\tfrac{1}{2} + 2(1-L)^2\right] + \frac{9.3B_2}{4p_1^3B_1}\, b_1^2L^2p_2\,\left(\frac{\ell_1-2p_2}{h_1}\right)^2, \qquad (4.11)$$

where b_1 is the minor diameter of the yarn, in the load direction, $b_1L/2$ defines the yarn neutral axis as shown in figure 90, and L is given by

$$L = \frac{B_1/B_2}{B_1/B_2 + \left[\dfrac{1.16p_2(\ell_1-2p_2)^2}{p_1^3}\right]} \qquad (4.12)$$

It may be shown that the expression given in equation (4.11) can, in fact, be reduced to

$$B_W/B_1 = \frac{1}{1+c_1} + \frac{b_1^2}{2h_1^2}\,(5-4L)$$

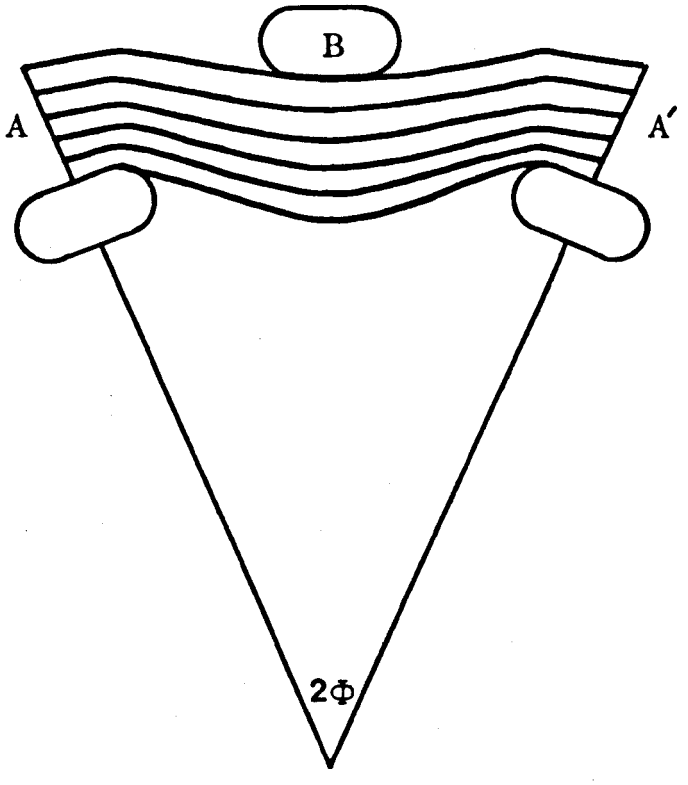

Fig. 90a

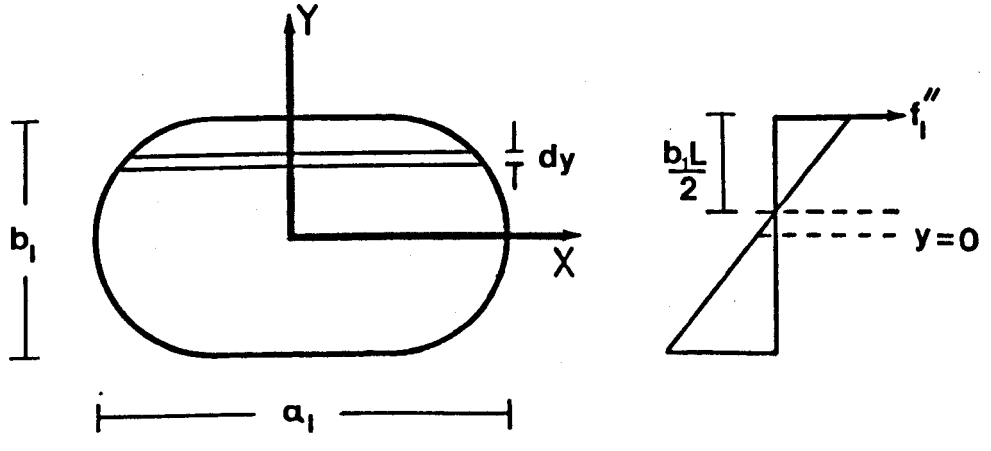

Fig. 90b

Abbott's expression for the ratio (B_w/B_1) was derived by using certain relations developed by Grosberg and Kedia (concerning the crimped shape of the yarns) and applying them to individual fibre deformations.

Using a similar method to that adopted by Abbott and using the relations obtained in our tensile analysis, which are equivalent to those derived by Grosberg and Kedia, the following expression for the fabric bending behaviour can be reached, (see Appendix 2)

$$B_w/B_1 = \frac{1}{1+c_1}\left[1 + \frac{3b_1^2}{h_1^2}(1-L)\right] , \qquad (4.13)$$

where L is defined by

$$L = \frac{B_1/B_2}{B_1/B_2+(\ell_1^3\cos^2\theta_1/\ell_2^3\cos^2\theta_2)} \qquad (4.14)$$

From equations (4.13) and (4.14), if p_2 has a fixed value, then an increase in θ_1 will reduce the fabric rigidity. This trend can be shown by putting equation (4.13) in the form

$$B_w/B_1 = \cos\theta_1 + \frac{3b_1^2}{\tan^2\theta_1}\left[\frac{B_2p_2}{B_1\ell_2^3\cos^2\theta_2+B_2p_2^3\sec\theta_1}\right] .$$

The numerical values obtained using equation (4.11) and (4.13) were examined with respect to the experimental data. Both expressions give higher calculated values than those actually measured, possibly due to ignoring the yarn compression.

In the tensile analysis, it was shown that including the yarn compression reduces the weft contribution to the fabric deformation. Doing

this for the bending analysis leads to a value of L which is now given by (see Appendix)

$$L = \frac{B_1/B_2}{B_1/B_2 + \dfrac{\ell_1^3\cos^2\theta_1}{\ell_2^3\cos^2\theta_2+48B_2(d_1/\mu_1+d_2/\mu_2)}} \quad , \qquad (4.15)$$

and this gives an increased value of L when the yarns are compressible (L=1 when μ_1 and/or μ_2 equal zero).

The final expression (4.13) is still valid but with the above value of L, and may be put in the form

$$B_W/B_1 = \frac{1}{1+c_1}\left[1+\frac{3b_1^2}{h_1^2}\left\{\frac{B_2\ell_1^3\cos^2\theta_1}{B_1\ell_2^3\cos^2\theta_2+B_2\ell_1^3\cos^2\theta_1+48B_1B_2(d_1/\mu_1+d_2/\mu_2)}\right\}\right] \quad , \qquad .....(4.16)$$

which may be regarded as a modification to the expression obtained by the earlier theory (equation 2.37), in which the weft contribution is multiplied by the factor b_1^2/h_1^2 .

Numerical values calculated using equation (4.16) are given in Table 4.6, and are plotted against the corresponding experimental results in figure 91. It can be seen that this is the best agreement between theory and experimental so far found. The fabrics which give considerably higher experimental values than the calculated results are those of tight construction discussed earlier.

Table 4.6

Fabric group	Fabric No.	Warp C_1	Warp L_1	Warp mN.mm²/cm	Weft C_2	Weft L_2	Weft mN.mm²/cm	No.in Fig. 91
X	1	0.1916	0.8210	203.79	0.0594	0.9222	277.52	1
	2	0.2143	0.8060	193.75	0.0557	0.9297	268.45	2
	3	0.1712	0.7519	210.54	0.0466	0.9392	235.09	3
Y	1	0.1787	0.7310	209.11	0.0480	0.9344	320.90	4
	2	0.1789	0.6657	206.26	0.0472	0.9368	299.00	5
	3	0.1580	0.6250	211.88	0.0359	0.9519	264.53	6
Z	1	0.2065	0.6953	193.48	0.0285	0.9643	431.53	7
	2	0.2177	0.7147	184.91	0.0269	0.9736	387.29	8
	3	0.2264	0.7292	191.67	0.0371	0.9556	470.87	9
A	1	0.1951	0.8215	172.91	0.0587	0.9167	199.65	10
	2	0.1041	0.7509	166.77	0.0490	0.8861	162.25	11
	3	0.1394	0.8535	166.94	0.1210	0.8416	182.55	12
B	1	0.0920	0.8800	180.38	0.1189	0.8720	187.27	13
	2	0.1336	0.8039	155.48	0.0532	0.8556	205.98	14
	3	0.1011	0.7005	172.53	0.0506	0.8625	182.35	15
C	1	0.0951	0.9258	170.22	0.0934	0.7803	148.30	16
	2	0.1097	0.8598	170.71	0.1074	0.7190	120.51	17
	3	0.1027	0.8567	164.29	0.0652	0.8556	105.00	18

$$B_W = \frac{B_1}{1+c_1}\left[1 + \frac{b_1^2}{h_1^2}(3.0 - 3\,L_1)\right] \cdot \frac{1}{p_1}$$

$$L_1 = \frac{B_1 \ell_2^3 \cos^2\theta_2 + 48 B_1 B_2 (d_1/\mu_1 + d_2/\mu_2)}{B_1 \ell_2^3 \cos^2\theta_2 + B_2 \ell_2^3 \cos^2\theta_1 + 48 B_1 B_2 (d_1/\mu_1 + d_2/\mu_2)}$$

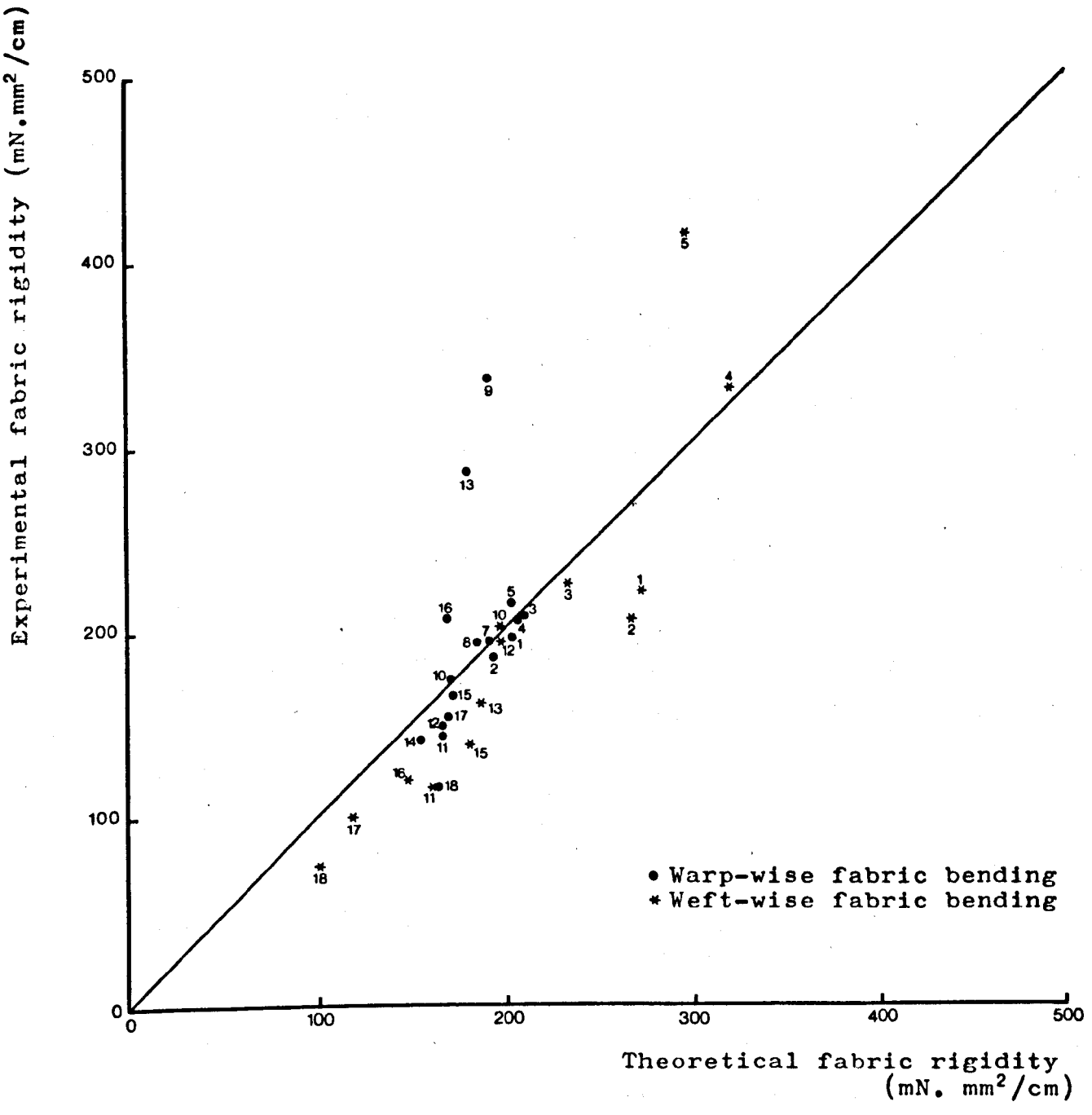
Experimental fabric rigidity (mN.mm²/cm)
500
400
300
200
100
0
0
100
200
300
400
500
Theoretical fabric rigidity
(mN. mm²/cm)
• Warp-wise fabric bending
* Weft-wise fabric bending

Fig. 91

SUMMARY AND CONCLUSION

The theoretical behaviour of the initial tensile and bending deformations of plain fabrics have been analysed. The aim was to provide a closed form solution for these deformations, Castigliano's theorem being used as the principal method of attack. The theory was then compared with experimental results.

The analysis showed that the resistance of fabrics to deformation should be regarded, in general, as two resistances contributed by both warp and weft; both are highly affected by the crimp value in the load direction.

In the tensile analysis, the yarn extensibility and compressibility in addition to its rigidity were taken into consideration; however, the first of these is only important when the yarns in the load direction are of low crimp value. If the effect of the yarn extensibility is ignored, the initial tensile modulus in a warp direction under uniaxial loading, lies between the following limits:

$$\frac{12B_1p_2}{p_1\ell_1^3\sin^2\theta_1} \leqslant E_1 \leqslant \frac{12B_1p_2}{p_1\ell_1^3\sin^2\theta_1}\left[1+\frac{B_2\ell_1^3\cos^2\theta_1}{B_1\ell_2^3\cos^2\theta_2}\right],$$

where the maximum limit corresponds to incompressible yarns and the minimum to extremely compressible yarns. The weft contribution is independent of the warp rigidity, but dependent on its own rigidity and on geometrical factors. This has resulted from the mechanism of crimp interchange that has been assumed for the initial deformation.

Practically, most of the fabric's initial tensile moduli lie between the above extremes, and for a reasonably simple estimate of E

equation (2.20) may be used, which reduces the predicted upper limit of fabric modulus by a factor in the range 1.2-4.

Using the same analysis it is possible to predict the fabric initial Poisson's ratio with considerable accuracy by equation (2.23). It has been found that the Poisson's ratio is nearly independent of the yarn rigidity in the load direction and depends on the yarn extensibility only when the fabric has a low crimp value in the load direction. For other fabrics, of medium to high crimp value, the Poisson's ratio lies between the limits $0 \leqslant \sigma_1 \leqslant \frac{p_2 \tan\theta_2}{p_1 \tan\theta_1}$, and a reasonable estimate can be obtained by multiplying the maximum limit by the factor K_c, given by equation (4.5). This factor depends on the compressibilities of the yarns used, i.e. on the ratio $\frac{48(d_1/\mu_1 + d_2/\mu_2)}{\ell_2^3 \cos^2\theta_2 / B_2}$. For the fabrics used, the estimated Poisson's ratio is reduced 2-8 times below the maximum limit mentioned above, in agreement with the experimental results.

In the bending analysis, the yarn bending rigidity and its compressibility were taken into consideration to derive the expression given by equation (2.37); however, considerable differences between experiment and theory have been found, possibly due to ignoring the real contact between warp and weft and the associated frictional restraints. A similar approach to Abbott's was later followed which gave a closer estimate of the fabric initial bending modulus.

Possibly the most important feature of the theoretical analysis is the effect of yarn compressibility on the fabric initial behaviour. It is recommended for further work in this area to develop a more accurate and simpler technique to define this property in the fabric structure.

REFERENCES

1. K.B. Iyer, K. Hepworth and D.C. Snowden. J.Text.Inst., 1964, 55, T99.

2. H.A. Nordby. Ph.D. thesis, Leeds University, 1968.

3. S. Kawabata, M. Niwa and H. Kawai. J.Text.Inst., 1973, 64, Y21.

4. N.C. Huang. Technical report SM.7801, Solid Mechanics Group, Dept. of Aerospace and Mechanical Engineering, University of Notre Dame, U.S.A., Sept. 1978.

5. G.A.V. Leaf and K.H. Kandil. J.Text.Inst., 1980, 72, T1.

6. J.D. Owen. J.Text.Inst., 1968, 59, T313.

7. E.F. Denby. J.Text.Inst., 1974, 65, T239.

8. G.M. Abbott. Ph.D. thesis, Leeds University, 1968.

9. J. Skelton and M.M. Schoppee. Text.Res.J., 1976, 46, 44.

10. J.W.S. Hearle; in "Structural Mechanics of Fibres, Yarns and Fabrics"; by J.W.S. Hearle, P. Grosberg and S. Backer, Wiley, 1969, p.372.

11. B. Behre. Text.Res.J., 1961, 31, 87.

12. G.E. Cusick. J.Text.Inst., 1961, 52, T395.

13. G.E. Cusick. Text.Res.J., 1964, 34, 1102.

14. J. Lindberg, B. Behre and B. Dahlberg. Text.Res.J., 1961, 31, 99.

15. L.R. Treloar. J.Text.Inst., 1965, 56, T533.

16. P. Grosberg and B.J. Park. Text.Res.J., 1966, 36, 420.

17. P. Grosberg, G.A.V. Leaf and B.J. Park. Text.Res.J., 1968, 38, 1085.

18. Brierley. Textile Manufacturer, 1931, 57, 3.

19. W. Watson. "Textile Design and Colour", Longmans, London, 5th edition, 1946, pp.487-496.

20. F.T. Peirce. J.Text.Inst., 1937, 28, T45.

21. P. Grosberg. Contributions of Science to the Development of the Textile Industry, Proceedings of the Joint Conference of the Institute Textile de France, The Textile Institute, Paris, 1975, p.179.

22. J.W.S. Hearle and W.J. Shanahan. J.Text.Inst., 1978,69, T81.

23. L. Love. Text.Res.J., 1954, 24, 1073.

24. P. Grosberg; in "Structural Mechanics of Fibres, Yarns and Fabrics"; by J.W.S. Hearle, P. Grosberg and S. Backer, Wiley, 1969, pp.323-342.

25. A. Kemp. J.Text.Inst., 1958, 49, T44.

26. W.J. Shanahan and J.W.S. Hearle. J.Text.Inst., 1978, 69, T92.

27. B. Olofsson. J.Text.Inst., 1964, 55, T351.

28. N. Wilson. Bulk, stretch and Texture, Papers at the 51st Annual Conference of the Textile Institute, 1966, p.217.

29. P.R. Lord and M.H. Mohamed. "Weaving, Conversion of yarn into fabric", Merrow, England, 1973, p.137.

30. B. Olofsson. J.Text.Inst., 1964, 55, T541.

31. P. Grosberg and S. Kedia. Text.Res.J., 1966, 36, 72.

32. P. Ellis. Text.Inst. and Indust., 1974, Nov., p.339.

33. R.I. Mashaly. Ph.D. thesis, Leeds University, 1979.

34. S. Kawabata, M. Niwa and H. Kawai. J.Text.Inst., 1973, 64, T62.

35. S. Kawabata and M. Niwa. J.Text.Inst., 1979, 70, T417.

36. F.T. Peirce. J.Text.Inst., 1930, 21, T377.

37. N.J. Abbott, M.J. Caplan and M.M. Platt. J.Text.Inst., 1960, 51, T1384.

38. M.M. Platt, W.G. Klein and W.J. Hamburger. Text.Res.J., 1959, 29, 611.

39. P. Grosberg. Text.Res.J., 1966, 36, 205.

40. G.M. Abbott, P. Grosberg and G.A.V. Leaf. Text.Res.J., 1971, 41, 345.

41. R.G. Livesey and J.D. Owen. Shirley Inst. Memories, 1964, 37, 35.

42. G.A.V. Leaf. J.Text.Inst., 1979, 70, T323.

43. T.Eeg-Olofsson. "A contribution to the experimental study of the bending properties of fabrics". Doctorial thesis, A. Rydberg & Co., Gothenberg, 1957.

44. T. Eeg-Olofsson. J.Text.Inst., 1959, 50, T112.

45. G.M. Abbott, P. Grosberg and G.A.V. Leaf. J.Text.Inst., 1973, 64, T346.

46. S.P. Timoshenko and D.H. Young. "Theory of Structure", McGraw-Hill, Tokyo, 1965, Chapter 5.

47. W.A. Nash. 'Strength of Materials 2/ed.', McGraw-Hill, U.S.A., 1972, Chapter 16.

48. British Standard No. 1051, B.S. Handbook No. 11: "Methods of Tests for Textiles", British Standard Institution, London, 1963, p.10.

49. J.W.S. Hearle and L.W.C. Miles. "The Setting of Fibres and Fabrics", Merrow, England, 1971, p.2.

50. British Standard No. 2862, B.S. Handbook No. 11: "Methods of Tests for Textiles", British Standard Institution, London, 1963, p.222.

51. J.E. Booth. "Principles of Textile Testing", Newness-Butterworths, London, 1968, p.265.

52. British Standard No. 2863, B.S. Handbook No. 11: "Methods of Tests for for Textiles", British Standard Institution, London, 1963, p.230.

53. "The Wira Textile Data Book", Wira, Leeds, 1973, B80.

54. P.W. Carlene. J.Text.Inst., 1947, 38, T38; 1950, 41, T159.

55. H.M. Elder and M. El-Tawashi. J.Text.Inst., 1977, 68, T.188.

56. Instruction manual of the Shirley cyclic bending tester, Shirley Development LT, Manchester.

57. V.H. Dawes and J.D. Owen. J.Text.Inst., 1971, 62, 233.

58. E. Oxtoby. M.Sc. thesis, University of Leeds, 1966.

59. S.L. Anderson and S.E. Settle. 3rd Wool Textile Research Conference, 1965, Cirtel Section 4.

60. W. Oxenham. Ph.D. thesis, University of Leeds, 1974.

61. D.W. Marquardt. J.Soc. Industrial and Applied Mathematics, 1963, 11, p.431.

62. Subroutine E04GAF (NAGFLIB; 1326/427: MK5: Dec.75). NAG Library, vol. 3.

63. The Instron Tensile Tester Manual.

64. D.W. Lloyd and J.W.S. Hearle. J.Text.Inst., 1977, 68, T399.

65. J.W.S. Hearle and V. Ozsanlav. J.Text.Inst., 1979, 70, T439.

66. S. De Jong and R. Postle. J.Text.Inst., 1977, 68, T350.

67. W.F. Kilby. J.Text.Inst., 1963, 54, T9.

68. E.E. Clulow and H.M. Taylor. J.Text.Inst., 1963, 45, T323.

69. S. De Jong and R. Postle. J.Text.Inst., 1979, 70, T359

70. D.N.E. Cooper. J.Text.Inst., 1960, 51, T317.

Some loom details

1-Let-off motion

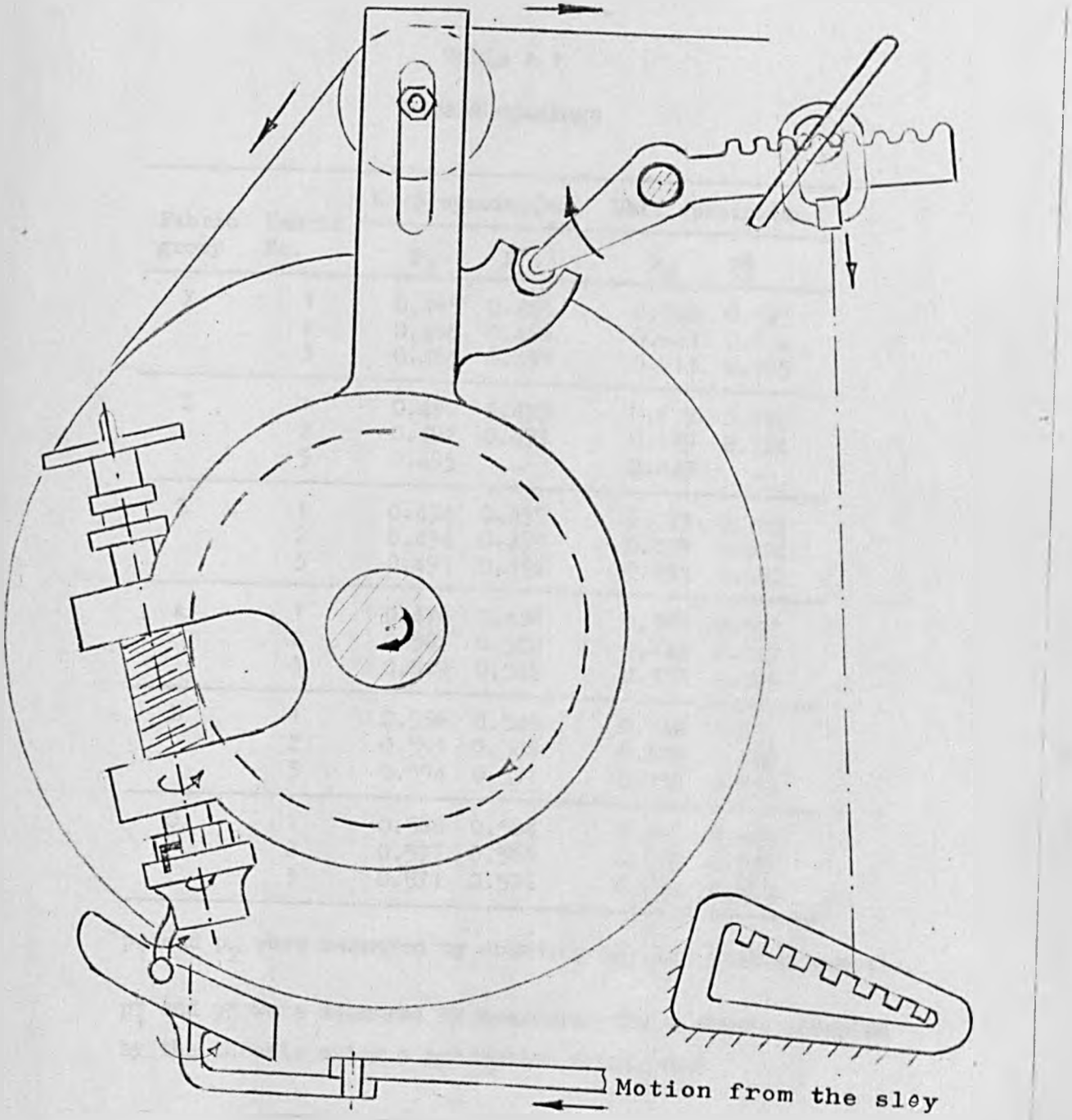

2-Loom Cycle
A-Beat up point at zero
B-Start of dwelling at 64
C-End of dwelling at 154
D-Crossing point at 290
E-Start of mechanical picking at 60
F-End of mechanical picking at 100

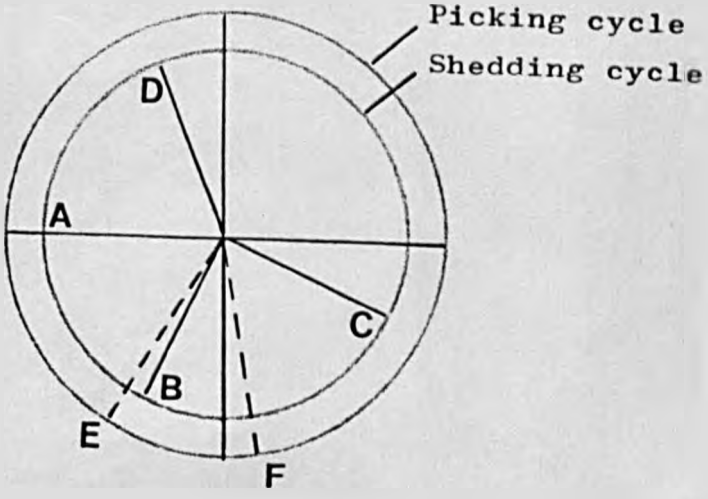

Table A.1

Thread spacings

Fabric group	Fabric No.	Warp spacing(mm)		Weft spacing(mm)	
		p_1	p_1^*	p_2	p_2^*
X	1	0.485	0.485	0.588	0.593
	2	0.488	0.486	0.624	0.618
	3	0.485	0.491	0.713	0.705
Y	1	0.490	0.495	0.677	0.696
	2	0.492	0.491	0.739	0.724
	3	0.495	-	0.849	-
Z	1	0.494	0.495	0.779	0.769
	2	0.494	0.499	0.839	0.824
	3	0.491	0.492	0.691	0.680
A	1	0.476	0.486	0.589	0.591
	2	0.587	0.592	0.749	0.727
	3	0.549	0.545	0.532	0.529
B	1	0.556	0.548	0.548	0.557
	2	0.591	0.588	0.637	0.660
	3	0.594	0.591	0.756	0.755
C	1	0.568	0.584	0.465	0.469
	2	0.577	0.566	0.538	0.536
	3	0.571	0.591	0.662	0.655

p_1 and p_2 were measured by counting threads in 5 cm samples.

p_1^* and p_2^* were measured by measuring the distance occupied by the threads using a projection microscope.

Table A.2

Yarns crimp and degree of 'set'

Fabric group	Fabric No.	Warp crimp (%) c_1	Warp crimp (%) c_1^*	Warp 'set' (%)	Weft crimp (%) c_2	Weft crimp (%) c_2^*	Weft 'set' (%)
X	1	19.16	19.20	92	5.94	6.19	91
	2	21.43	21.72	95	5.57	5.70	92
	3	17.12	18.17	91	4.66	4.21	89
Y	1	17.87	19.19	90	4.80	4.65	90
	2	17.89	18.63	91	4.72	4.15	91
	3	15.80	16.27	96	3.59	3.58	93
Z	1	20.65	23.22	93	2.85	2.82	96
	2	21.77	22.65	90	2.69	2.84	96
	3	22.64	23.83	93	3.71	2.72	97
A	1	19.51	19.48	97	5.87	6.48	97
	2	10.41	10.30	96	4.90	5.28	98
	3	13.94	13.56	96	12.10	12.43	94
B	1	9.20	9.69	94	11.89	12.07	93
	2	13.36	13.64	94	5.32	5.68	91
	3	10.11	10.89	86	5.06	5.67	88
C	1	9.51	10.22	88	9.34	9.91	85
	2	10.97	12.78	89	7.31	8.79	85
	3	10.27	10.12	89	6.52	6.88	85

c_1 and c_2 were measured using the Shirley crimp tester.

c_1^* and c_2^* were measured using the 'Instron'.

Big differences are underlined.

Table A.3

Experimental data of the cyclic bending test for various yarns

Curvature ($10^{-1}mm^{-1}$)	Couple (mN.mm per thread)						
	R60/2 vincel*	R60/2 cotton	R74/2 cotton	R98/2 cotton	R60/2 vincel**	R60/2 cotton/ vincel	R46/2 cotton/ vincel
0.0	0.0	0.0	0.0	0.0	0.0	0.0	0.0
0.2	0.22	0.36	0.38	0.50	0.18	0.32	0.11
0.4	0.38	0.55	0.65	0.80	0.31	0.45	0.22
0.6	0.56	0.80	0.88	1.14	0.44	0.51	0.28
0.8	0.69	1.00	1.08	1.33	0.56	0.62	0.36
1.0	0.84	1.12	1.30	1.56	0.68	0.75	0.46
1.5	1.14	1.40	1.67	2.08	0.95	0.97	0.60
2.0	1.42	1.67	2.01	2.59	1.21	1.22	0.76
2.5	1.73	1.92	2.40	3.15	1.46	1.47	0.91
3.0	2.03	2.26	2.79	3.75	1.72	1.75	1.07
2.5	1.27	1.17	1.49	1.76	1.04	0.95	0.67
2.0	0.87	0.73	0.87	0.98	0.70	0.61	0.44
1.5	0.57	0.41	0.46	0.46	0.42	0.33	0.29
1.0	0.30	0.11	0.12	0.03	0.17	0.11	0.12
0.5	0.04	0.18	0.22	0.34	0.09	0.11	0.04
0.0	-0.28	0.50	0.61	0.79	0.26	0.33	0.19
-0.5	-0.57	0.82	0.96	1.19	0.48	0.50	0.29
-1.0	-0.84	1.12	1.30	1.56	0.71	0.75	0.46

* Yarn used as warp with fabric groups X,Y and Z

** Yarn used as warp with fabric groups A,B and C, also for weft with fabric group A

```
C      MINIMIZATION OF FUNCTION
       DIMENSION ZL(16)
       INTEGER M,N,METHOD,IW,IPRINT,MAXCAL,IFAIL,I
       REAL X(16),Z(16),F,A(7),SCALE(7),R(16),W(100) ,XTOL(7)
       EXTERNAL RESID,LSQ,MONIT
       COMMON/AAAA/X,Z
       WRITE (2,99999)
       READ (1,10) M
    10 FORMAT (I2)
       N=7
       SUM1 =0.0
       DO 500   IK=1,M
       READ (1,200) X(IK),Z(IK)
   200 FORMAT (2F5.1)
       SUM1 =SUM1+Z(IK)
   500 CONTINUE
       ZM =SUM1/M
       READ (1,300)(A(J) ,J=1,7)
   300 FORMAT(7F10.5)
       XTOL (1) =10.E-8
       XTOL (2) =10.E-8
       XTOL (3) =10.E-8
       XTOL (4) =10.E-8
       XTOL (5) =10.E-8
       XTOL (6) =10.E-8
       XTOL (7) =10.E-8
       METHOD =2
       IW =N*(N+4)+M
       IPRINT =1
       MAXCAL =100
       IFAIL =0
       CALL E04GAF (M,N,A,R,F,XTOL,METHOD,SCALE,W,IW,RESID,LSQ  ,MONIT,
      *IPRINT,MAXCAL,IFAIL)
       WRITE (2,99998) F
       WRITE (2,99997) (A(I),I =1,N)
       WRITE (2,99996) IFAIL
       WRITE (2,99995)
99995 FORMAT (36HOLOAD       THICKNESS   L.S.THICKNESS,1X)
       SUM2 =0.0
       DO 310  LL=1,M
       ZL(LL) =R(LL) +Z(LL)
       SS =ZL(LL) -ZM
       SUM2 =SUM2+SS*SS
       WRITE(2,99994) X(LL),Z(LL),ZL(LL)
99994 FORMAT(1H ,3(2X,F6.1,5X))
   310 CONTINUE
       DC =SUM2/(SUM2+F)
       WRITE (2,99993) DC
99993 FORMAT(13HODETER.COEF,=, F5,4)
       TINT =A(1) +A(2) +A(4) +A(6)
       WRITE(2,99992) TINT
99992       FORMAT(8HOTINT, =,F6,1)
       CI =-A(2)*A(3) -A(4)*A(5) -A(6)*A(7)
       CM =1/CI
       WRITE (2,99991) CI,CM
99991 FORMAT(14HOCOMP. INDE, =,F15,5/13HOCOMP. MOD, =,F15,5)
99999 FORMAT (4(1X/),31H  COMPRESION RESULTS          ,1X)
SEPARATOR OMITTED AT ABOUT COL 55, LINE 0063, COMMA ASSUMED

99998 FORMAT (25H FINAL SUM OF SQUARES IS ,F12,4)
99997 FORMAT (15H AT THE POINT, 2F12,6/1H ,5F12,6)
99996 FORMAT (22HO THIS HAS  ERROR NUM  , I3)
       END
```

```
C      CALCULATES THE VALUES OF THE RESIDUALS RC AT AC
       LOGICAL  IFL
       INTEGER M,N ,JJ
       REAL AC,RC(16),AJC(16,7)
       DIMENSION AC(N)
       COMMON/AAAA/X(16),Z(16)
       COMMON/BBBB/AJC
       DO  700  JJ=1,M
       Y2 =AC(3)*X(JJ)
       IF (17.0-Y2)  4,4,5
    4  G2 =0.0
       GO TO 6
    5  G2 =1/EXP(Y2)
    6  TOT2 =AC(2)*G2
       G3 =-X(JJ)*TOT2
       Y4 =AC(5)*X(JJ)
       IF (17.0-Y4)  7,7,8
    7  G4 =0.0
       GO TO 9
    8  G4 =1/EXP(Y4)
    9  TOT4 =AC(4)*G4
       G5 =-X(JJ)*TOT4
       Y6 =AC(7)*X(JJ)
       IF (17.0 -Y6)  10,10,11
   10  G6 =0.0
       GO TO  12
   11  G6 =1/EXP(Y6)
   12  TOT6 =AC(6)*G6
       G7 =-X(JJ)*TOT6
       FA =(AC(1) +TOT2 +TOT4 +TOT6) -Z(JJ)
       RC(JJ)=FA
       AJC(JJ,1) =1
       AJC(JJ,2) =G2
       AJC(JJ,3) =G3
       AJC(JJ,4) =G4
       AJC(JJ,5) =G5
       AJC(JJ,6) =G6
       AJC(JJ,7) =G7
  700  CONTINUE
       RETURN
       END

       SUBROUTINE LSQ(M,N,AC,RC,AJTJC,GC)
C      CALCULATES THE JACOBIAN RC AT AC
        INTEGER M,N,I,K,II
       REAL AC,RC,AJTJC,GC,AJC,SUM
       DIMENSION AC(N),RC(M),GC(N),AJTJC(N,N),AJC(16,7)
       COMMON/BBBB/AJC
C      EVALUATE GC(I)
       DO 80  I=1,N
            SUM =0.0
            DO 20 K =1,M
                 SUM =SUM+AJC(K,I)*RC(K)
   20       CONTINUE
            GC(I) =SUM
            II=I
C      EVALUATE  AJTJC(J,I)
            DO 60 J =1,II
                 SUM =0.0
                 DO 40 K =1,M
                      SUM =SUM +AJC(K,I)*AJC(K,J)
   40            CONTINUE
                 AJTJC(J,I) =SUM
   60       CONTINUE
   80  CONTINUE
       RETURN
       END
```

```
      SUBROUTINE MONIT(M,N,AC,RC,FC,GC,NCALL)
C     PRITES THE VALUES EVERY IPRINT INTERATION
      INTEGER M,N,NCALL,I
      REAL XC,GC,RC,FC
      DIMENSION AC(N),GC(N),RC(M)
C     EVALUATION OF AJTJC(J,I)
      WRITE (2,99999) NCALL,FC
      WRITE (2,99997) (GC(I),I=1,N)
      WRITE (2,99998) (AC(I),I=1,N)
      RETURN
99999 FORMAT(6H AFTER,I4,16H   CALLS OF RESID,, 19H THE SUM OF SQUARES,
     *2HIS, F12,4)
99998 FORMAT(13H AT THE POINT, 6F12,6/5F12,6)
99997 FORMAT(13H GRADIENT IS , 5F16,4/4F16,4)
      END
```

COMPUTER RESULTS FOR YARN THICKNESS

(1) R60/2 cotton

Load (g/cm)	Load (mN/mm)	Experimental thickness(mm)	Corrected thickness(mm)
1.0	0.98	0.493	0.490
1.4	1.37	0.468	0.471
2.0	1.96	0.451	0.449
2.4	2.23	0.438	0.437
3.0	2.94	0.422	0.423
4.0	3.92	0.406	0.407
6.0	5.89	0.384	0.384
10.0	9.81	0.351	0.355
20.0	19.62	0.308	0.310
40.0	39.24	0.272	0.270
50.0	49.05	0.260	0.261
70.0	68.67	0.251	0.249
100.0	09.10	0.236	0.236
140.0	137.34	0.223	0.224
160.0	156.96	0.218	0.219
200.0	196.20	0.208	0.210
240.0	235.44	0.204	0.203
300.0	294.30	0.195	0.195
340.0	333.54	0.191	0.190
400.0	392.40	0.187	0.186

A_0 = 0.1726
A_1 = 0.1236
B_1 = 0.7028
A_2 = 0.1379
B_2 = 0.0894
A_3 = 0.1281
B_3 = 0.0060

C.D. = 0.9997

T(initial) = 0.562 mm

d(equivalent) = 0.398 mm

(2) R74/2 cotton

Load (g/cm)	Load (mN.mm)	Experimental thickness(mm)	Corrected thickness(mm)
1.0	0.98	0.535	0.530
1.4	1.37	0.513	0.510
2.0	1.96	0.488	0.490
2.4	2.35	0.479	0.478
3.0	2.94	0.470	0.466
4.0	3.92	0.451	0.450
6.0	5.89	0.430	0.429
10.0	9.81	0.399	0.399
20.0	19.62	0.351	0.353
40.0	39.24	0.316	0.315
50.0	49.05	0.306	0.306
70.0	68.67	0.292	0.293
100.0	98.10	0.281	0.280
140.0	137.34	0.264	0.266
160.0	156.96	0.259	0.260
200.0	196.20	0.251	0.251
240.0	235.44	0.242	0.243
300.0	294.30	0.235	0.234
340.0	333.54	0.230	0.230
400.0	392.40	0.224	0.225

$A_0 = 0.2133$
$A_1 = 0.1190$
$B_1 = 0.8610$
$A_2 = 0.1591$
$B_2 = 0.0778$
$A_3 = 0.1185$
$B_3 = 0.0059$

C.D. = 0.9997

T(initial) = 0.601 mm

d(equivalent) = 0.431 mm

(3) R98/2 cotton

Load (g/cm)	Load (mN.mm)	Experimental thickness(mm)	Corrected thickness(mm)
1.0	0.98	0.619	0.616
1.4	1.37	0.597	0.598
2.0	1.96	0.575	0.576
2.4	2.23	0.563	0.563
3.0	2.94	0.547	0.548
4.0	3.92	0.527	0.529
6.0	5.89	0.502	0.503
10.0	9.81	0.476	0.476
20.0	19.62	0.436	0.436
40.0	39.24	0.388	0.387
50.0	49.05	0.371	0.371
70.0	68.67	0.349	0.349
100.0	98.10	0.331	0.329
140.0	137.34	0.310	0.311
160.0	156.96	0.305	0.305
200.0	196.20	0.291	0.294
240.0	235.44	0.284	0.285
300.0	294.30	0.274	0.274
340.0	333.54	0.269	0.268
400.0	392.40	0.261	0.261

$A_0 = 0.2393$
$A_1 = 0.1496$
$B_1 = 0.4645$
$A_2 = 0.1542$
$B_2 = 0.0369$
$A_3 = 0.1339$
$B_3 = 0.0046$

C.D. = 0.999

T(initial) = 0.677 mm

d(equivalent) = 0.479 mm

(4) R60/2 vincel

Load (g/cm)	Load (mN.mm)	thickness(mm)	Corrected thickness(mm)
1.0	0.98	0.429	0.427
1.4	1.37	0.416	0.418
2.0	1.96	0.406	0.406
2.4	2.35	0.399	0.399
3.0	2.94	0.388	0.390
4.0	3.92	0.379	0.376
6.0	5.89	0.355	0.355
10.0	9.81	0.325	0.326
20.0	19.62	0.283	0.283
40.0	99.24	0.245	0.244
50.0	49.05	0.233	0.233
70.0	68.67	0.219	0.220
100.0	98.10	0.205	0.205
140.0	137.34	0.192	0.191
160.0	156.96	0.185	0.186
200.0	196.20	0.177	0.176
240.0	235.44	0.169	0.169
300.0	294.30	0.162	0.161
340.0	333.54	0.156	0.158
400.0	392.40	0.154	0.153

A_0 = 0.1447
A_1 = 0.0053
B_1 = 0.3743
A_2 = 0.1379
B_2 = 0.0671
A_3 = 0.1155
B_3 = 0.0066

C.D. = 0.998

T(initial) = 0.453 mm

d'equivalent = 0.321 mm

(5) R60/2 cotton-vincel

Load (g/cm)	Load (mN.mm)	thickness(mm)	Corrected thickness(mm)
1.0	0.98	0.532	0.522
1.4	1.37	0.509	0.513
2.0	1.96	0.493	0.499
2.4	2.35	0.481	0.491
3.0	2.94	0.466	0.480
4.0	3.92	0.449	0.462
6.0	5.89	0.422	0.433
10.0	9.81	0.388	0.392
20.0	19.62	0.342	0.340
40.0	39.24	0.298	0.297
50.0	49.05	0.282	0.284
70.0	68.67	0.263	0.264
100.0	98.10	0.246	0.245
140.0	137.34	0.233	0.230
160.0	156.96	0.223	0.225
200.0	196.20	0.214	0.216
240.0	235.44	0.207	0.208
300.0	294.30	0.202	0.199
340.0	333.54	0.193	0.194
400.0	392.40	0.187	0.187

$A_0 = 0.1539$
$A_1 = 0.1594$
$B_1 = 0.1557$
$A_2 = 0.1241$
$B_2 = 0.0264$
$A_3 = 0.1109$
$B_3 = 0.0030$

C.D. = 0.9998

T(initial) = 0.548 mm

d(equivalent) = 0.387 mm

(6) R46/2 cotton-vincel

Load (g/cm)	Load (mN.mm)	thickness(mm)	Corrected thickness(mm)
1.0	0.98	0.370	0.372
1.4	1.37	0.359	0.358
2.0	1.96	0.341	0.342
2.4	2.35	0.334	0.333
3.0	2.94	0.323	0.322
4.0	3.92	0.312	0.309
6.0	5.89	0.292	0.292
10.0	9.81	0.268	0.270
20.0	19.62	0.240	0.239
40.0	39.24	0.214	0.212
50.0	49.05	0.206	0.206
70.0	68.67	0.195	0.197
100.0	98.10	0.187	0.187
140.0	137.34	0.179	0.178
160.0	156.96	0.174	0.173
200.0	196.20	0.167	0.167
240.0	235.44	0.161	0.161
300.0	294.30	0.156	0.155
340.0	333.54	0.152	0.152
400.0	392.40	0.149	0.149

$A_0 = 0.1410$
$A_1 = 0.0904$
$B_1 = 0.6537$
$A_2 = 0.1082$
$B_2 = 0.0789$
$A_3 = 0.0835$
$B_3 = 0.0061$

C.D. = 0.9997

T(initial) = 0.423 mm

d(equivalent) = 0.299 mm

Appendix 2

Initial fabric bending: an approach similar to Abbott's

For the purpose of the following analysis, it is best to examine the behaviour of two adjacent cells of a completely set plain weave, although the bent configuration of each is similar. The yarns are assumed effectively clamped at section A and A′ (figure 90a), and the planes containing these sections are then rotated through an angle ϕ so that the angle subtended by the deformed shape of the two cells is 2ϕ. Since both unit cells are identical, the movement of fibres between the two cells is not allowed, and under such conditions it is possible to consider each unit cell in isolation when the fabric is bent. The fibres in the idealized twisted yarn geometry take helical paths with different radii from the yarn centre line; it is possible to greatly simplify the analysis by assuming that the fibres in the isolated weave cell run parallel to the yarn centre line. This assumption seems reasonable when the yarn twist is sufficiently small relative to the length of the unit weave cell, and a typical value of this twist with the fabrics used is of the order of 0.25 turns per unit cell.

When the fabric is bent, as shown in figure 90a, the outer layer of fibres in the yarn, i.e. the layers above the neutral axis (N.A.), are in a state of tension, while the layers under the N.A. are in a state of compression. Obviously there is a greater likelihood of fibre extension at large deflections, but since the following theory applies only to small fabric deformations, the fibres may only extend by very small amounts so that they can be considered as inextensible. If the fibres inside the yarn are assumed to bend independently, the fibres above the N.A. would

move upwards at the region B rather than extend in length, while the fibres below the N.A. will buckle rather than decrease in length. When there is no resistance to the upward fibre movement at B, the distribution of forces acting at A' to bend the unit weave cell will be symmetrical with respect to the neutral axis. However, due to the crossing yarn rigidity an additional force f_1'' is needed to bend the unit cell to the same angle ϕ. Since the fibres are inextensible, the outer layer of fibres which suffers the highest strains would mainly support the crossing yarn and consequently the force f_1'' acts at a distance y=b/2 (referred to figure 90). The displacement of the fibre ends and the force distribution at A', for this case, are shown in figure 90b, where the N.A. is displaced upwards due to the extra force f_1'' required to uncrimp the cross yarn.

The following assumptions will now be used to solve this problem:

1. The fibres in the yarn, of a total number n, are uniformly distributed over the cross-section. It is convenient to assume a 'race track' yarn cross-sectional shape; the method of analysis is equally applicable to other shapes.
2. The fibres are regarded as parallel elasticas which have the same initial crimped shape as that of the yarn centre line before deformation i.e. are defined by p, ℓ and θ.
3. The fibres, because they are assumed to bend independently, will have the sum of their flexural rigidities equal to that of the yarn. Therefore, the single fibre rigidity may be taken as B/n, where B is the yarn flexural rigidity and n is the total number of fibres in the yarn cross-section.
4. The energies due to fibre extension and yarn compression are ngelected in comparison with the bending energy involved.

Consider now an element of area of cross-section, da, of thickness dy, a distance y from the line of symmetry of the yarn cross-section (figure 90b). Using the first of the above assumptions, the number of fibres n(y) in this element is

$$n(y) = n\,\frac{da}{A} = \frac{n\left[(a-b)+2\left(\frac{b^2}{4} - y^2\right)^{\frac{1}{2}}\right]}{(a-b)b+\pi b^2/4}\,dy$$

$$= n.F(y)dy, \qquad (A.1)$$

where A is the total area of cross-section.

By definition we can write the following relations for a symmetrical cross-section

$$\bar{y} = \int_{-b/2}^{b/2} yF(y)dy = \int_{-A/2}^{A/2} y.\,\frac{da}{A} = 0\ , \qquad (A.2)$$

and

$$I = A\int_{-b/2}^{b/2} y^2F(y)dy = \int_{-A/2}^{A/2} y^2da\ . \qquad (A.3)$$

In the tensile analysis, it was shown that the force required to extend a warp crimped yarn inside the fabric, due only to bending energy changes, through a distance Δp_2, can be regarded as the sum of two forces, namely f_1', the warp contribution, and f_1'', the weft contribution, where

$$f_1' = \Delta p_2\,\frac{12B_1}{\ell_1^3\sin^2\theta_1}\ , \qquad (A.4)$$

and

$$f_1'' = \Delta p_2\,\frac{12B_1}{\ell_1^3\sin^2\theta_1}\,\frac{B_2\ell_1^3\cos^2\theta_1}{B_1\ell_2^3\cos^2\theta_2} \qquad (A.5)$$

For an individual fibre inside the warp yarn, if its flexural rigidity is B_1/n_1, then the force needed to displace its end by Δp_2 is, using (A.4)

$$H_1' = \Delta p_2 \frac{12B_1/n_1}{\ell_1^3 \sin^2\theta_1} = K_1 \Delta p_2 \quad \text{say} \tag{A.6}$$

According to the bending mechanism shown in figure 90, Δp_2 depends on the position of the fibre, being zero at the neutral axis. Above the N.A., $\Delta p_2 > 0$ and below it, $\Delta p_2 < 0$.

In general

$$\Delta p_2 = [y - \tfrac{b}{2}(1-L)]\phi \ ,$$

where L is a fraction $(0 \leqslant L \leqslant 1)$ that defines the position of the yarn N.A. as shown in figure 90b.

In using the tensile theory together with the above expression for Δp_2, we are in fact assuming the following:

1. The warp spacing, unchanged in the bent configuration, is defined as the horizontal distance between the two planes containing the yarn N.A. at A' and B. Obviously, this distance should be defined parallel to the bent fabric plane, but little error will be introduced by using the above definition.
2. The fibre deforms symmetrically with respect to its midpoint.
3. Only geometrical fibre extension or compression are taking place, whose moduli, K_1, are assumed to be the same for small deformations.

Now, consider the forces acting on all the fibres. Above the N.A. we have the sum of the tensile forces

$$T = f_1'' + \int_{N.A.}^{outside} K_1 \Delta p_2 \, n(y)dy$$

$$= f_1'' + \int_{b(1-L)/2}^{b/2} K_1 \left[y - \frac{b}{2}(1-L) \right] \phi \, . n_1 F(y)dy$$

$$= f_1'' + n_1 K_1 \phi \int_{b(1-L)/2}^{b/2} \left[y - \frac{b}{2}(1-L) \right] F(y)dy \, .$$

Below the N.A., the sum of the compressive forces is

$$C = - \int_{-b/2}^{b(1-L)/2} K_1 . \Delta p_2 . n(y)dy.$$

For the pure bending condition, we must have

$$(T-C) = 0 \, ,$$

i.e.

$$f_1'' + n_1 K_1 \phi \int_{b(1-L)/2}^{b/2} \left[y - \frac{b}{2}(1-L) \right] F(y)dy$$

$$+ n_1 L_1 \phi \int_{-b/2}^{b(1-L)/2} \left[y - \frac{b}{2}(1-L) \right] F(y)dy = 0$$

This gives

$$f_1'' + n_1 K_1 \phi \int_{-b/2}^{b/2} \left[y - \frac{b}{2}(1-L) \right] F(y)dy = 0 \, ,$$

which, on using the definition in (A.2), $\bar{y}=0$, leads to

$$f_1'' - n_1 K_1 \phi \int_{-b/2}^{b/2} \frac{b}{2} (1-L)F(y)dy = 0 ,$$

and since

$$\int_{-b/2}^{b/2} F(y)dy = 1, \text{ see (A.1), we get}$$

$$f_1'' = n_1 K_1 \phi . \frac{b}{2}(1-L) .$$

Substituting the value of K_1 from (A.6) we get

$$f_1'' = \phi \frac{12B_1}{\ell_1^3 \sin^2\theta_1} \frac{b}{2} (1-L) .$$

Substituting the displacement $\Delta p_2 = \phi \frac{bL}{2}$, at the outer layer, in equation (A.5), we find

$$f_1'' = \frac{12B_1}{\ell_1^3 \sin^2\theta_1} \frac{B_2 \ell_1^3 \cos^2\theta_1}{B_1 \ell_2^3 \cos^2\theta_2} \phi \frac{bL}{2} . \qquad (A.7)$$

Equating the above two expressions for f_1'' , we obtain

$$L = \frac{B_1/B_2}{B_1/B_2 + \dfrac{\ell_1^3 \cos^2\theta_1}{\ell_2^3 \cos^2\theta_2}} . \qquad (A.8)$$

The flexural rigidity of the system can now be found by summing the internal energy changes for one unit cell and equating this sum to the work done by the external moment.

The total internal energy change is the sum of the following terms:

1. The energy change, U_1, due to the geometrical extension and compression of all fibres. This is given by

$$U_1 = \tfrac{1}{2} \int_{-b/2}^{b/2} n_1 K_1 . (\Delta p_2)^2 F(y) dy$$

$$= \tfrac{1}{2} \int_{-b/2}^{b/2} K_1 . \left[y - \frac{b}{2} (1-L) \right]^2 \phi^2 . n_1 F(y) dy$$

or

$$U_1 = \tfrac{1}{2} \int_{-b/2}^{b/2} K_1 . y^2 . \phi^2 . n_1 F(y) dy + \tfrac{1}{2} \int_{-b/2}^{b/2} -K_1 b(1-L) \phi^2 . n_1 F(y) dy$$

$$+ \tfrac{1}{2} \int_{-b/2}^{b/2} K_1 . \frac{b^2}{4} (1-L)^2 . \phi^2 . n_1 F(y) dy$$

Using the relations (A.1-3), U_1 is reduced to

$$U_1 = \tfrac{1}{2} n_1 K_1 \phi^2 \frac{I}{A} + n_1 K_1 \phi^2 \left[(1-L)^2 \frac{b^2}{8} \right] \qquad (A.9)$$

The first term, U_{11} say, in the above expression will now be considered in more detail. Since K_1 represents the modulus of geometrical extension of a single crimped fibre, the tensile modulus of a yarn having 'n_1' fibres can be regarded as $n_1 K_1$, if the fibres behave independently, in 'force/elongation' units. The Young's modulus of this crimped yarn is then

$$E = \frac{n_1 K_1}{A} \quad p_2 \qquad \text{(force per unit area/unit extension)}$$

The energy term, U_{11}, is then converted to

$$U_{11} = \tfrac{1}{2}\, n_1 K_1 \phi^2 \frac{I}{A} = \frac{1}{2p_2}\ \phi^2\ (EI)_c . \qquad (A.10)$$

$(EI)_c$ is the bending modulus for the crimped yarn as it lies in the fabric since the distribution of the force $K_1\left[y - \frac{b}{2}(1-L)\right]\phi$, shown in figure 90b, displace the fibre ends parallel to the fabric plane. The relation between the bending rigidity of the crimped yarn to its rigidity as it lies straight is given by the ratio of yarn projection in the fabric plane, p, to its straight length, ℓ.

$$\text{i.e. } \frac{(EI)_{\text{crimped yarn}}}{(EI)_{\text{straight yarn}}} = \frac{(EI)_c}{B_1} = \frac{1}{1+c_1} . \qquad (A.11)$$

Substituting in (A.10) from (A.11) gives

$$U_{11} = \frac{1}{2p_2(1+c_1)}\ \phi^2\ B_1 ,$$

Hence

$$U_1 = \frac{1}{2p_2(1+c_1)}\ \phi^2 B_1 + n_1 K_1 \phi^2 \left[(1-L)^2\ \frac{b^2}{8}\right]$$

2. The second energy term, U_2, is due to the force f_1'' needed to upcrimp the crossing yarn, and is given by

$$U_2 = \tfrac{1}{2}\, f_1''\ \Delta p_2 ,$$

Since f_1'' is given by (A.7) and Δp_2 is the distance moved by f_1'' at the outside of the yarn ($= \frac{bL}{2}$), U_2 is

$$U_2 = \tfrac{1}{2}\, n_1 K_1\ \phi^2\ \frac{B_2 \ell_1^3 \cos^2\theta_1}{B_1 \ell_2^3 \cos^2\theta_2}\ \frac{b^2 L^2}{4}$$

The total internal energy change is therefore

$$U_T = U_1 + U_2$$

$$= \frac{\phi^2 B_1}{2p_2(1+c_1)} + n_1 K_1 \phi^2 \left[(1-L)^2 \frac{b^2}{8}\right] + n_1 K_1 \phi^2 \frac{B_2 \ell_1^3 \cos^2\theta_1}{B_1 \ell_2^3 \cos^2\theta_2} \frac{b^2 L^2}{8}$$

$$= \frac{\phi^2 B_1}{2p_2(1+c_1)} + n_1 K_1 \phi^2 \frac{b^2}{8} \left[(1-L^2) + \frac{B_2 \ell_1^3 \cos^2\theta_1}{B_1 \ell_2^3 \cos^2\theta_2} L^2\right] .$$

From (A.6) and (A.8), we have

$$\frac{1-L}{L} = \frac{B_2 \ell_1^3 \cos^2\theta_1}{B_1 \ell_2^3 \cos^2\theta_2} , \qquad \text{and} \qquad K_1 = \frac{12 B_1/n_1}{\ell_1^3 \sin^2\theta_1} .$$

Substituting in the above expression we get

$$U_T = \frac{\phi^2 B_1}{2p_2(1+c_1)} + \frac{3\phi^2 B_1 b^2}{2\ell_1^3 \sin^2\theta_1} \left[(1-L)^2 + L(1-L)\right] ,$$

and since $\ell_1 \sin\theta_1 = h_1$ and 'b' as considered above is the warp minor diameter, then

$$U_T = \frac{\phi^2 B_1}{2\ell_1} + \frac{3\phi^2 B_1 b_1}{2\ell_1 h_1^2} (1-L) .$$

The external work done is $\frac{\phi^2 B_W}{2p_2}$, where B_W is the warp-wise fabric rigidity per thread. Equating U_T and the external work done, we get

$$B_W = \frac{B_1 p_2}{\ell_1} + \frac{B_1 p_2}{\ell_1} \frac{3b_1^2}{h_1^2} (1-L) .$$

This may be compared with Abbott's expression by putting the above equation in the form

$$B_W/B_1 = \frac{1}{1+c_1} \left[1 + \frac{3b_1^2}{h_1^2} (1-L) \right] .$$

It can also be compared with the expression derived in the earlier analysis by substituting the value of L to get

$$B_W = \frac{B_1}{1+c_1} \left[1 + \frac{3b_1^2}{h_1^2} \left(\frac{B_2 \ell_1^3 \cos^2\theta_1}{B_1 \ell_2^3 \cos^2\theta_2 + B_2 \ell_1^3 \cos^2\theta_1} \right) \right] . \qquad (A.12)$$

Inclusion of the yarn compressibility

For this case, the force required to extend the crimped shape of the yarn was given by the tensile analysis as follows,

$$f_1 = \Delta p_2 \frac{12B_1}{\ell_1^3 \sin^2\theta_1} \left[1 + \frac{B_2 \ell_1^3 \cos^2\theta_1}{B_1 \ell_2^3 \cos^2\theta_2 + B_1 B_2 (d_1/\mu_1 + d_2/\mu_2)} \right],$$

and this was regarded as the sum of two force namely, f_1', the warp contribution and f_1'' , the weft contribution, where now

$$f_1' = \Delta p_2 \frac{12B_1}{\ell_1^3 \sin^2\theta_1} = \Delta p_2 \; n_1 K_1 \quad \text{say,}$$

and

$$f_1'' = \Delta p_2 \frac{12B_1}{\ell_1^3 \sin^2\theta_1} \frac{B_2 \ell_1^3 \cos^2\theta_1}{B_1 \ell_2^3 \cos^2\theta_1 + 48 B_1 B_2 (d_1/\mu_1 + d_2/\mu_2)} .$$

Substituting $\Delta p_2 = \phi \frac{bL}{2}$ at the outer layer of the yarn cross-section in the above equation we get

$$f_1'' = \frac{12B_1}{\ell_1^3 \sin^2\theta_1} \frac{B_2 \ell_1^3 \cos^2\theta_1}{B_1 \ell_2^3 \cos^2\theta_2 + 48 B_1 B_2 (d_1\mu_1 + d_2/\mu_2)} \phi \frac{bL}{2} \qquad (A.13)$$

Following the same argument as before, i.e. putting (T-C)=0, we get another expression for f_1'' in the form

$$f_1'' = \frac{12B_1}{\ell_1^3 \sin^2\theta_1} \phi \frac{b}{2} (1-L) . \qquad (A.14)$$

Dividing equation (A.13) by equation (A.14) we now get

$$\frac{1-L}{L} = \frac{B_2 \ell_1^3 \cos^2\theta_1}{B_1 \ell_2^3 \cos^2\theta_2 + 48 B_1 B_2 (d_1/\mu_1 + d_2/\mu_2)} , \qquad (A.15)$$

so that L is now given by

$$L = \frac{1}{1 + \dfrac{B_2 \ell_1^3 \cos^2\theta_1}{B_1 \ell_2^3 \cos^2\theta_2 + 48 B_1 B_2 (d_1/\mu_1 + d_2/\mu_2)}} \qquad (A.16$$

The internal energy change is the sum of the following terms:

1. Energy changes, U_1, due to the geometrical extension and compression of all fibres, given by

$$U_1 = \tfrac{1}{2} \int_{-b/2}^{b/2} K_1 \left[y - \frac{b}{2} (1-L)^2 \right] \phi^2 \; n_1 F(y) dy \quad ,$$

which will yield a similar expression to that found in the previous case, though we note that K_1 and L_1 now have different values. Thus

$$U_1 = \frac{\phi^2 B_1}{2\ell_1} + n_1 K_1 \; \phi^2 \left[(1-L)^2 \; \frac{b^2}{8} \right] .$$

2. Energy changes, U_2, to increase the crossing yarn amplitude.
When the threads undergo compression strains 'ΔD' as well as bending deformations, the interyarn force, v, will produce a strain energy contribution equal to half the product of v and the distance moved under this force i.e. $\frac{1}{2}v(\Delta h - \Delta D)$. Since f_1'' is defined as the excess force needed to overcome the cross yarn resistance in fabric bending we get

$$U_2 = \tfrac{1}{2}v(\Delta h - \Delta D) = \tfrac{1}{2} f_1 \, \Delta p_2 \, .$$

This leads to (from A.13)

$$U_2 = \tfrac{1}{2} n_1 K_1 \; \phi^2 \; \frac{B_2 \ell_1^3 \cos^2\theta_1}{B_1 \ell_2^3 \cos^2\theta_2 + 48 B_1 B_2 (d_1/\mu_1 + d_2/\mu_2)} \; \frac{b^2 L^2}{4} \, .$$

The total energy, U_T, is then

$$U_T = \frac{\phi^2 B_1}{2\ell_1} + n_1 K_1 \; \phi^2 \left[(1-L)^2 \; \frac{b^2}{8} \right]$$

$$+ \tfrac{1}{2} n_1 K_1 \; \phi^2 \; \frac{b^2 L^2}{4} \; \frac{B_2 \ell_1^3 \cos^2\theta_1}{B_1 \ell_2^3 \cos^2\theta_2 + 48 B_1 B_2 (d_1/\mu_1 + d_2/\mu_2)}$$

Equating the external work done with the total internal energy change we get

$$B_W = \frac{p_2 B_1}{\ell_1} + \frac{p_2\, n_1 K_1\, b^2}{4}\left[(1-L)^2 + \frac{B_2 \ell_1^3 \cos^2\theta_1}{B_1 \ell_2^3 \cos^2\theta_1 + 48 B_1 B_2 (d_1/\mu_1 + d_2/\mu_2)}\, L^2\right].$$

Substituting from (A.15) and using $K_1 = \dfrac{12 B_1/n_1}{\ell_1 h_1^2}$, in the above equation, we get

$$B_W/B_1 = \frac{1}{1+c_1}\left[1 + \frac{3b_1^2}{h_1^2}(1-L)\right],$$

or

$$B_W = \frac{B_1}{1+c_1}\left[1 + \frac{b_1^2}{h_1^2}\left\{\frac{3B_2 \ell_1^3 \cos^2\theta_1}{B_1 \ell_2^3 \cos^2\theta_2 + B_2 \ell_1^3 \cos^2\theta_1 + 48 B_1 B_2 (d_1/\mu_1 + d_2/\mu_2)}\right\}\right].$$